frontiers | Research Topics

Precision medicine approaches in radiotherapy and systemic therapy of brain metastases

Edited by
Matthias Guckenberger, Anna Berghoff and David Kaul

Published in
Frontiers in Oncology

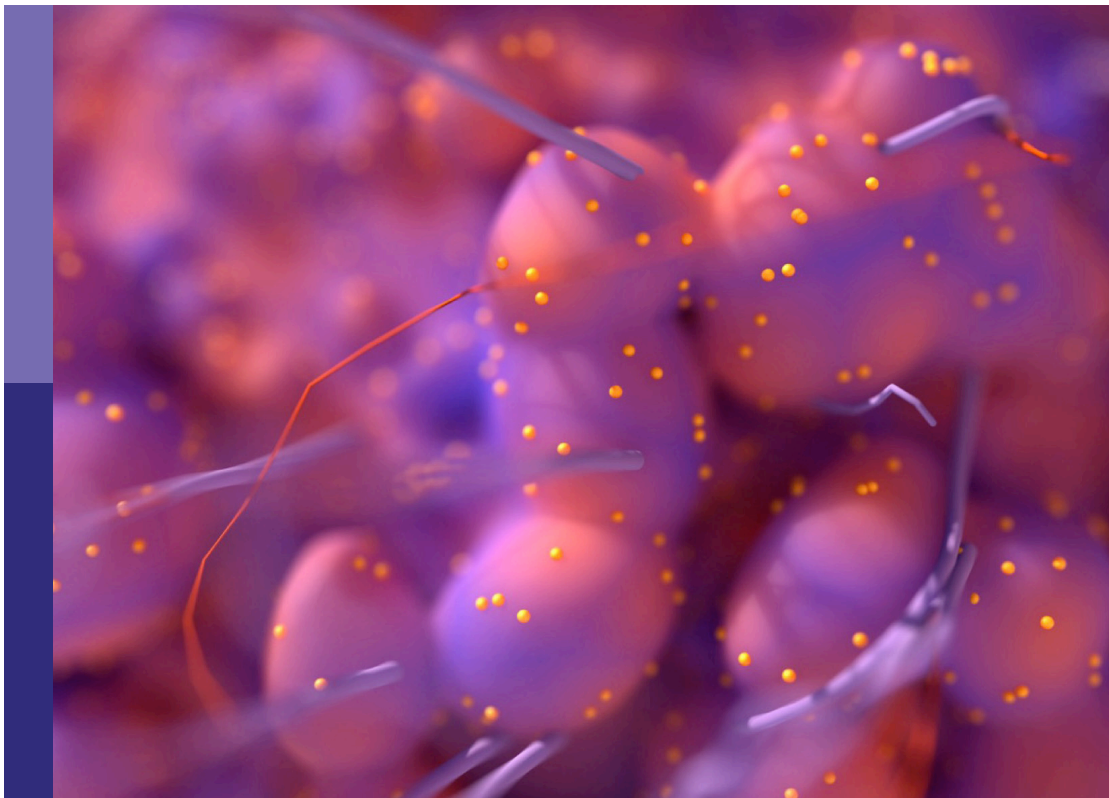

ISSN 1664-8714
ISBN 978-2-8325-2347-6
DOI 10.3389/978-2-8325-2347-6

About Frontiers

Frontiers is more than just an open access publisher of scholarly articles: it is a pioneering approach to the world of academia, radically improving the way scholarly research is managed. The grand vision of Frontiers is a world where all people have an equal opportunity to seek, share and generate knowledge. Frontiers provides immediate and permanent online open access to all its publications, but this alone is not enough to realize our grand goals.

Frontiers journal series

The Frontiers journal series is a multi-tier and interdisciplinary set of open-access, online journals, promising a paradigm shift from the current review, selection and dissemination processes in academic publishing. All Frontiers journals are driven by researchers for researchers; therefore, they constitute a service to the scholarly community. At the same time, the *Frontiers journal series* operates on a revolutionary invention, the tiered publishing system, initially addressing specific communities of scholars, and gradually climbing up to broader public understanding, thus serving the interests of the lay society, too.

Dedication to quality

Each Frontiers article is a landmark of the highest quality, thanks to genuinely collaborative interactions between authors and review editors, who include some of the world's best academicians. Research must be certified by peers before entering a stream of knowledge that may eventually reach the public - and shape society; therefore, Frontiers only applies the most rigorous and unbiased reviews. Frontiers revolutionizes research publishing by freely delivering the most outstanding research, evaluated with no bias from both the academic and social point of view. By applying the most advanced information technologies, Frontiers is catapulting scholarly publishing into a new generation.

What are Frontiers Research Topics?

Frontiers Research Topics are very popular trademarks of the *Frontiers journals series*: they are collections of at least ten articles, all centered on a particular subject. With their unique mix of varied contributions from Original Research to Review Articles, Frontiers Research Topics unify the most influential researchers, the latest key findings and historical advances in a hot research area.

Find out more on how to host your own Frontiers Research Topic or contribute to one as an author by contacting the Frontiers editorial office: frontiersin.org/about/contact

Precision medicine approaches in radiotherapy and systemic therapy of brain metastases

Topic editors

Matthias Guckenberger — University Hospital Zürich, Switzerland
Anna Berghoff — Medical University of Vienna, Austria
David Kaul — Charité University Medicine Berlin, Germany

Citation

Guckenberger, M., Berghoff, A., Kaul, D., eds. (2023). *Precision medicine approaches in radiotherapy and systemic therapy of brain metastases*. Lausanne: Frontiers Media SA. doi: 10.3389/978-2-8325-2347-6

Table of contents

frontiers | Frontiers in Oncology

TYPE Editorial
PUBLISHED 20 April 2023
DOI 10.3389/fonc.2023.1190830

OPEN ACCESS

EDITED AND REVIEWED BY
David D. Eisenstat,
Royal Children's Hospital, Australia

*CORRESPONDENCE
David Kaul
david.kaul@charite.de

SPECIALTY SECTION
This article was submitted to Neuro-Oncology and Neurosurgical Oncology, a section of the journal Frontiers in Oncology

RECEIVED 21 March 2023
ACCEPTED 17 April 2023
PUBLISHED 20 April 2023

CITATION
Kaul D, Berghoff AS and Guckenberger M (2023) Editorial: Precision medicine approaches in radiotherapy and systemic therapy of brain metastases.
Front. Oncol. 13:1190830.
doi: 10.3389/fonc.2023.1190830

Editorial: Precision medicine approaches in radiotherapy and systemic therapy of brain metastases

David Kaul[1]*, Anna S. Berghoff[2] and Matthias Guckenberger[3]

[1]Department of Radiation Oncology and Radiotherapy, Charité-Universitätsmedizin, Freie Universität Berlin, Humboldt-Universität zu Berlin and Berlin Institute of Health, Berlin, Germany, [2]Department of Medicine 1 and Comprehensive Cancer Center Vienna , Medical University of Vienna, Vienna, Austria, [3]Department of Radiation Oncology, University Hospital Zurich, University of Zurich, Zürich, Switzerland

KEYWORDS

precision medicine, brain metastases, immunotherapy, targeted therapy, radiotherapy

Editorial on the Research Topic
Precision medicine approaches in radiotherapy and systemic therapy of brain metastases

The incidence of brain metastases is on the rise, partly due to improved imaging techniques that enable more accurate detection and partly because of increased survival rates in cancer patients due to improvements in systemic therapy. As cancer care evolves, it becomes increasingly important to explore and develop novel approaches to manage brain metastases, ensuring that patients receive the most effective treatments tailored to their individual needs. In this special edition, we present nine comprehensive articles that delve into the promising and rapidly evolving field of precision medicine in the context of radiotherapy and systemic therapy of brain metastases. The continuing development and application of advanced technologies and therapies are reshaping the landscape of cancer treatment.

In the article, "*Radiosurgery for Five to Fifteen Brain Metastases: A Single Centre Experience and a Review of the Literature*" by Rogers et al. the authors examine the clinical outcomes of patients with five or more brain metastases treated with stereotactic radiosurgery (SRS). The study highlights excellent local control rates and demonstrates that overall survival following SRS for multiple brain metastases is determined by the course of the extracranial disease. This article contributes to our understanding of SRS's potential and limitations in treating carefully selected patients with multiple brain metastases.

In the article, "*Radiomic Signatures for Predicting Receptor Status in Breast Cancer Brain Metastases*," Luo et al. examine receptor discordance between primary breast cancers and brain metastases. They establish radiomic signatures using preoperative brain MRI to predict receptor status (estrogen receptor, progesterone receptor, and human epidermal growth factor receptor 2) in metastases. The study concludes that receptor conversion is

common, and radiomic signatures show potential for noninvasively predicting receptor status, which could inform therapeutic decisions.

In the article, "*Current Treatment Approaches and Global Consensus Guidelines for Brain Metastases in Melanoma*," Tan et al. review global consensus guidelines for treating melanoma brain metastases (MBM),. These guidelines provide valuable guidance for clinical decision-making in MBM treatment.

The "*Systematic literature review and meta-analysis of clinical outcomes and prognostic factors for melanoma brain metastases*" presents a systematic review and meta-analysis of clinical outcomes and prognostic factors in melanoma brain metastases (MBM) patients (Tan et al.). The analysis included 41 observational studies and 12 clinical trials on treatment outcomes, as well as 31 observational studies on prognostic factors. This study provides valuable insights into the association between patient characteristics and MBM prognosis, helping guide clinical decision-making.

In the article, "*Predictors of Lung Adenocarcinoma With Leptomeningeal Metastases: A 2022 Targeted-Therapy-Assisted molGPA Model*," Zhang et al. explore prognostic indicators of lung adenocarcinoma with leptomeningeal metastases (LM) and provide an updated graded prognostic assessment model integrated with molecular alterations (molGPA). The 2022 molGPA model demonstrates better prognostic performance than previous models, making it useful for clinical decision-making and stratification in future clinical trials

In the article, "*Radiomic Signatures for Predicting EGFR Mutation Status in Lung Cancer Brain Metastases*," the authors create a radiomic model using preoperative brain MR images from 162 patients (Zheng et al.). The best-performing model demonstrates high classification accuracy, sensitivity, and specificity. The study concludes that radiomic signatures can potentially noninvasively predict the EGFR mutation status of lung cancer brain metastases, impacting prognosis and treatment decisions.

The article, "*Clinical determinants impacting overall survival of patients with operable brain metastases from non-small cell lung cancer*," aims to improve clinical decision-making by investigating factors affecting survival in patients with resectable NSCLC brain metastases (Piffko et al.). A retrospective analysis was conducted on 264 patients, which identified several factors that impacted overall survival, such as the systemic metastatic load and the number of brain metastases (solitary vs. singular and multiple BM). The study also identified age, Karnofsky Performance Status, and gender as factors impacting survival. These findings contribute to a better understanding of the risks and course of the disease, ultimately aiding clinical decision-making in tumor boards.

The article "*The value of stereotactic biopsy of primary and recurrent brain metastases in the era of precision medicine*" investigates the diagnostic yield and safety of image-guided frame-based stereotactic biopsy (STX) in brain metastases patients (Katzendobler et al.). The retrospective study found that STX provided a definitive diagnosis in 98% of cases, with a 95% success rate in molecular genetic analyses. The procedure had a low complication rate of 2.4%, with no permanent morbidity or mortality. This study highlights STX's potential to enable precision medicine approaches in treating primary and recurrent brain metastases.

Finally, in "*What if: A Retrospective Reconstruction of Resection Cavity Stereotactic Radiosurgery to Mimic Neoadjuvant Stereotactic Radiosurgery*" examines neoadjuvant stereotactic radiosurgery (NaSRS) of brain metastases and its impact on normal brain tissue (NBT) (Acker et al.). The study analyzed hypothetical pre- and actual postoperative target volumes in 30 patients, finding that smaller tumors had a higher risk of volume increase when irradiated postoperatively. Precise delineation is crucial, as it directly affects NBT exposure, but contouring resection cavities is challenging. The article highlights the need for further research to identify patients at risk for significant volume increase, who may benefit from NaSRS. Ongoing clinical trials will further evaluate the benefits of this approach.

Collectively, these nine articles emphasize the potential of precision medicine approaches in radiotherapy and systemic therapy of brain metastases. We are moving closer to a future where personalized cancer treatment is the norm. We hope that the insights presented in this special Research Topic will inspire further research and innovation in this critical field. As the incidence of brain metastases continues to rise, it is of utmost importance that we continue to explore new treatment options and refine existing techniques to provide the best possible care for patients affected by this challenging condition. By fostering collaboration among researchers, clinicians, and the broader scientific community, we can work together to make significant strides in our ongoing battle against cancer.

Author contributions

All authors listed have made a substantial, direct, and intellectual contribution to the work and approved it for publication.

Conflict of interest

The authors declare that the research was conducted in the absence of any commercial or financial relationships that could be construed as a potential conflict of interest.

Publisher's note

frontiers | Frontiers in Oncology

MINI REVIEW
published: 05 May 2022
doi: 10.3389/fonc.2022.885472

Current Treatment Approaches and Global Consensus Guidelines for Brain Metastases in Melanoma

Xiang-Lin Tan[1†], Amy Le[2†], Fred C. Lam[3†], Emilie Scherrer[1,4], Robert G. Kerr[3], Anthony C. Lau[3], Jiali Han[5], Ruixuan Jiang[1], Scott J. Diede[1] and Irene M. Shui[1]*

[1] Merck & Co., Inc., Rahway, NJ, United States, [2] Richard M. Fairbanks School of Public Health, Indiana University, Indianapolis, IN, United States, [3] Division of Neurosurgery, Huntington Hospital, Northwell Health, Huntington, NY, United States, [4] Seagen Inc., Bothell, WA, United States, [5] Integrative Precision Health, Limited Liability Company (LLC), Carmel, IN, United States

OPEN ACCESS

Edited by:
David Kaul, Charité Universitätsmedizin Berlin, Germany

Reviewed by:
Stefano Vagge, San Martino Hospital (IRCCS), Italy
Brian Jeremy Williams, University of Louisville, United States

***Correspondence:**
Xiang-Lin Tan
xianglin.tan@merck.com

†These authors have contributed equally to this work and share first authorship

Specialty section:
This article was submitted to Neuro-Oncology and Neurosurgical Oncology, a section of the journal Frontiers in Oncology

Received: *28 February 2022*
Accepted: *08 April 2022*
Published: *05 May 2022*

Citation:
Tan X-L, Le A, Lam FC, Scherrer E, Kerr RG, Lau AC, Han J, Jiang R, Diede SJ and Shui IM (2022) Current Treatment Approaches and Global Consensus Guidelines for Brain Metastases in Melanoma. Front. Oncol. 12:885472. doi: 10.3389/fonc.2022.885472

Background: Up to 60% of melanoma patients develop melanoma brain metastases (MBM), which traditionally have a poor diagnosis. Current treatment strategies include immunotherapies (IO), targeted therapies (TT), and stereotactic radiosurgery (SRS), but there is considerable heterogeneity across worldwide consensus guidelines.

Objective: To summarize current treatments and compare worldwide guidelines for the treatment of MBM.

Methods: Review of global consensus treatment guidelines for MBM patients.

Results: Substantial evidence supported that concurrent IO or TT plus SRS improves progression-free survival (PFS) and overall survival (OS). Guidelines are inconsistent with regards to recommendations for surgical resection of MBM, since surgical resection of symptomatic lesions alleviates neurological symptoms but does not improve OS. Whole-brain radiation therapy is not recommended by all guidelines due to negative effects on neurocognition but can be offered in rare palliative scenarios.

Conclusion: Worldwide consensus guidelines consistently recommend up-front combination IO or TT with or without SRS for the treatment of MBM.

Keywords: melanoma, brain metastasis, immunotherapy, targeted therapy, treatment guidelines

1 INTRODUCTION

The global incidence of melanoma is increasing, accounting for 73% of skin cancer-related deaths (1, 2). Despite melanoma being the least common type of skin cancer, 60% of patients develop melanoma brain metastases (MBM), with a dismal median survival of 3 to 6 months (3, 4). Immunotherapy (IO), including anti-programmed cell death protein 1 (anti-PD1) and anti-cytotoxic T lymphocyte-associated protein 4 (anti-CTLA-4) therapies (5), and targeted therapy (TT) against BRAF V600 E/K mutations (BRAFi) and MEK/MAPK signaling pathways (MEKi) (6), have improved progression-free survival (PFS) and overall survival (OS) of patients with metastatic melanoma and reached median OS of up to 24.3 months (7). Delivery of precise doses of radiation

using stereotactic radiosurgery (SRS) to discrete MBM and adjuvant doses of radiation to the post-surgical resection cavity have also significantly improved local intracranial disease control (8, 9).

In this review, we conducted a targeted literature review by focusing on the current modalities for the treatment of MBM as outlined in the consensus guidelines from the European Society for Medical Oncology (ESMO) (10), European Organization for Research and Treatment of Cancer (EORTC) (11), National Comprehensive Cancer Network (NCCN) (12), Cancer Council of Australia (CCA) (13), and Japanese Dermatological Association (JDA) (14). We further offered a comprehensive comparison of the consensus guidelines for each modality.

2 METHODS

A targeted literature review for the treatment of MBM and the most recent international guidelines on the treatment of cutaneous melanoma with respect to MBM was performed. Guidelines reviewed included: 1) The National Comprehensive Cancer Network (NCCN) Clinical Practice Guidelines in Oncology, Cutaneous Melanoma, version 2.2021 (12); 2) The 2019 European Organization for Research and Treatment of Cancer (EORTC) recommendations on cutaneous melanoma diagnosis and treatment (11); 3) The European Society for Medical Oncology (ESMO) consensus conference guidelines on melanoma (10); 4) Evidence-based clinical practice guidelines for the management of MBM put forth by Cancer Council Australia (CCA) in 2020 (13); and 5) The 2019 melanoma guidelines of the Japanese Dermatological Association (14). The American Society of Clinical Oncology (ASCO) is currently preparing guidelines for the treatment of MBM but has not yet been published (15). References mentioned throughout this manuscript pertaining to the treatment of MBM were directly drawn from studies that were reviewed and referenced within the consensus guidelines themselves.

3 RESULTS

3.1 Current Modalities for the Treatment of Melanoma Brain Metastases as Outlined in the Global Consensus Guidelines

3.1.1 Role of Surgery

Surgery is recommended in the setting of large symptomatic lesions (> 3 cm diameter) presenting with mass effect, hemorrhage, or obstructive hydrocephalus. Patients with a single MBM, functional independence, limited or absent extracranial disease, should be offered surgery with palliative benefits (16, 17). MBM patients treated with immunotherapy and surgery achieve excellent local control rates (18). Similarly, patients with a single MBM treated with surgery plus whole brain radiotherapy (WBRT) have longer survival than WBRT alone (19, 20). Response to IO is associated with prolonged survival in patients who underwent resection of their MBM, while adjuvant WBRT does not (21).

3.1.2 SRS and WBRT

SRS delivers a high dose of radiation to a focused target with high three-dimensional conformality and has proven efficacy at controlling a small number (< 4) of MBM lesions (with a total cerebral tumor volume of < 5 cubic centimeters) (8, 22–24). It has been suggested that multiple lesions, failure to treat with IO or TT, poorly controlled systemic disease, and intratumoral hemorrhage are predictors of poor response to SRS (23). A phase III randomized clinical trial (RCT) showed that adjuvant SRS boost to the surgical cavity significantly lowers local recurrence but does not improve OS (25).

WBRT was traditionally used to treat patients with multiple MBMs but only affords a small increase in median survival of 3.5 months, albeit before recent systemic therapy advances (26, 27). A pooled analyses of trials comparing WBRT to WBRT plus surgery showed no significant difference in OS (28) and patients treated with WBRT had decreased neurocognitive function (29). Furthermore, a multicenter RCT comparing WBRT plus surgery with surgery alone in 215 MBM patients did not demonstrate any clinical benefit for adjuvant WBRT and therefore adjuvant WBRT is no longer offered to patients (30, 31).

3.1.3 Systemic Therapies Including IO and TT

Combination IO (anti-CTLA4 and anti-PD-1) and TT that inhibit BRAF V600 E/K and MEK (known to be mutated in approximately 40-50% of melanoma patients) are effective at treating MBM and prolonging PFS (5, 7, 32–34). The open-label, multicenter, single-arm phase II study CheckMate 204 suggested that combination IO nivolumab (nivo) plus ipilimumab (ipi) had clinically meaningful intracranial efficacy, concordant with extracranial activity in patients with at least one asymptomatic, measurable, non-irradiated BM (5). The anti-PD1 brain collaboration (ABC) trial also demonstrated clinically meaningful intracranial efficacy of combination IO nivo plus ipi (33). Similarly, the phase II multicentered COMBI-MB trial of combination TT dabrafenib plus trametinib in patients with BRAF V600 E/K mutant asymptomatic MBM demonstrated clinical safety with manageable symptoms (7). A recent systematic review and meta-analysis of combination IO, TT, and mono-agent IO in combination with radiotherapy for the treatment of MBM patients revealed that combination IO and TT had a similar intracranial response rate, while combination IO was associated with increased PFS and OS compared to mono-agent IO and combination TT (32).

3.1.4 Combination of SRS Plus IO or TT

Multiple systematic reviews and meta-analyses have demonstrated a survival benefit of combining SRS with concurrent IO or TT compared to SRS alone (9, 35–40). As such, combination IO or TT are now recommended as upfront treatments followed by SRS and/or surgical resection of MBM. When combining SRS with TT, there should be a washout period of 3 to 5 days prior to commencement of SRS (41).

3.2 Review and Comparison of Worldwide Consensus Guidelines

In the second segment of this review, we summarize and compare the most recent global consensus guidelines published by ESMO, EORTC, NCCN, CCA, and JDA (**Table 1**). Of note, Canadian guidelines were omitted because they do not discuss the treatment of MBM. Comparison of guideline recommendations are subcategorized according to treatment modalities with the understanding that all current consensus guidelines state that most MBM patients will likely require multimodal combination therapies throughout their treatment course.

3.2.1 Upfront and/or Subsequent Surgical Resection of MBM

Guidelines are inconsistent with regards to recommendations for surgical resection of MBM. The EORTC guidelines consider surgical resection as an option when SRS is not possible and that SRS is equally effective at achieving local brain control while being non-invasive, applicable to several lesions, repeatable, and provides early local control compared to surgical resection (11, 42). The NCCN (12) and CCA (13) guidelines state that patients with symptomatic lesions > 1 cm in diameter in non-eloquent cortex, resectable locations, should be offered surgical resection.

3.2.2 Use of SRS

The NCCN currently recommends 15-24 Gy SRS in a single fraction to small tumors < 3 cm (43). SRS is typically not recommended for lesions > 4 cm, which may be treated with fractionated stereotactic radiotherapy (SRT), 24-27 Gy in 3 fractions or 25-35 Gy in 5 fractions (44, 45). Adjuvant SRS at 12-20 Gy may be applied to resection cavities < 5 cm (44) with fractionated SRT for larger cavities. TT should be held for ≥ 3 days before and after fractionated SRT and for ≥ 1 day before and after SRS to avoid toxicities associated with concurrent TT and SRS/SRT treatment (41, 46–50). EORTC considers SRS to asymptomatic MBM lesions < 3 cm (solitary or up to 5 lesions) to achieve superior early local control compared to surgical resection (42). ESMO recommends SRS for the treatment of limited asymptomatic MBMs (up to 4 lesions) with a maximum diameter of 4 cm or 5-10 lesions with the largest tumor < 10 mL in volume, < 3 cm in diameter, and a total cumulative volume of ≤ 15 mL (10, 51). The Australian guidelines recommend SRS in patients with a single or a small number of lesions (52–56). All guidelines except for the JDA recommend adjuvant SRS to the post-resection cavity based on two randomized trials evaluating effects of SRS to the resection cavity of multiple types of BM (25, 57). The JDA refrained from providing strong recommendations for adjuvant SRS to the resection cavity again due a lack of phase III randomized trials comparing SRS to local brain directed therapies (14).

3.2.3 Use of WBRT

NCCN recommends considering palliative WBRT when SRS/SRT is not feasible in patients who have failed systemic therapy or in patients with signs and symptoms of leptomeningeal carcinomatosis. Hippocampal avoidance and memantine therapy should be considered to patients receiving WBRT to reduce neurocognitive toxicity (58). Adjuvant WBRT after resection or SRS/SRT is not recommended due to worsening cognitive decline following WBRT with no benefit in OS (57, 59). EORTC and EMSO guidelines recommend restricting WBRT to those few patients who have exhausted all systemic, SRS, and other local brain therapy options. All guidelines do not recommend treating patients with WBRT after surgical resection or SRS treatment for MBM.

3.2.4 Use of IO and TT

The NCCN, ESMO, EORTC, and CCA recommend upfront combination IO (nivo + ipi) as the preferred initial treatment in patients with asymptomatic MBM < 3 cm, not requiring corticosteroids and who have not received prior systemic therapies. This recommendation is based on the study reporting high intracranial response rates using nivo + ipi in patients with previously untreated asymptomatic MBM (5). Anti-PD-1 monotherapy is not recommended, and systemic corticosteroids may negatively affect the efficacy of nivo + ipi and should be avoided in MBM patients (60). For patients with BRAF V600E mutations, combination BRAFi + MEKi should be considered. Brain-directed therapy is preferred in patients with symptomatic MBM as limited evidence exists supporting the effectiveness of upfront systemic therapies for symptomatic MBM (7, 60–62). In contrast, the JDA currently provides conditional recommendations for using IO or TT for the treatment of MBM patients due to the lack of phase III clinical trials comparing the efficacy of IO, TT, SRS, or surgery for the treatment of MBM, and that the existing phase II studies are limited by selection bias and small sample size (5, 33).

4 DISCUSSION

The current iterations of consensus guidelines are limited to evidence gathered largely from relatively small, phase I and II clinical trials, retrospective case series, and observational studies (52–54, 63). CheckMate 204 was a phase II study evaluating the efficacy and safety of nivo + ipi in asymptomatic MBM patients with a relatively small sample size (n = 101 patients) and median follow-up of 14.0 months (5). Similarly, the phase II ABC study enrolled only 79 patients in 3 cohorts of patients treated with nivo or nivo+ipi, with considerable heterogeneity amongst the cohorts (33).

It is important to keep in mind when reviewing consensus practice guidelines that physicians in real-world practice may not always follow consensus guidelines. This may be due to a multitude of reasons, such as the availability of certain treatments or approval for their use by insurance providers. Studies using real-world evidence and observational data are being performed in an attempt to gain further understanding of actual treatment patterns (64). A recent study using the National Cancer Database (NCDB) of 3008 cases of MBM between 2011 to 2015 reported real-world outcomes of combination and the

TABLE 1 | Summary of published world guidelines for the treatment of melanoma brain metastases.

Treatment	NCCN Guidelines	ESMO Guidelines	EORTC Guidelines	CCA Guidelines	JDA Guidelines
Immunotherapy/ Targeted Therapy	- Upfront IO for asymptomatic, low-burden intracranial disease. - TT in patients with BRAF V600 E/K mutations.	- IO for asymptomatic patients - TT for patients with BRAF V600 E/K mutations.	- IO preferentially offered. - TT in patients with BRAF V600 E/K mutations.	- First-line in asymptomatic patients with MBM. - Efficacy of IO/TT for symptomatic lesions is low.	- IO and TT are recommended, level C evidence.
Neurosurgery	- For *symptomatic* lesions in eloquent cortex, with hemorrhage, or in brainstem. - For patients who develop MBM while on systemic IO/TT. - Consider surgery in patients with symptomatic lesions after SRS that are not responsive to steroids.	- Surgical resection of solitary lesions given level C recommendation.	- SRS and surgery are considered equally effective at local control. - Surgical debulking procedures should be reviewed critically, as there is no evidence that they improve survival.	- Surgery reserved for patients with solitary, symptomatic lesion or with oligometastatic disease without extracranial metastases.	- Limited number of studies comparing IO/TT or SRS/ surgery. - There is a need for RCTs in Japan to establish guidelines.
Stereotactic Radiosurgery	- SRS is the preferred radiation modality.	- SRS is preferred for local control prior to systemic therapies for asymptomatic patients with 1-4 lesions < 4 cm diameter or 5-10 lesions < 3 cm in diameter. - Adjuvant SRS to surgical resection cavity should be considered to decrease local recurrence. - If considering concurrent SRS with IO/TT, early treatment is preferred over late SRS as salvage.	- Upfront SRS is recommended. - Surgery is an option when SRS is not possible.	- Upfront SRS recommended for asymptomatic patients with small number of asymptomatic lesions < 3 cm in diameter. - Adjuvant SRS to surgical cavity significantly improves local recurrence.	- No phase III RCTs have been completed to compare efficacy of IO/TT vs. SRS/WBRT vs. surgery.
Whole Brain Radiotherapy	- Adjuvant WBRT is not recommended after SRS/ surgery. - Palliative WBRT is recommended only for palliative purposes when SRS is not feasible in patients with good KPS. - Hippocampal avoidance and memantine protocol should be considered to reduce neuro-cognitive toxicity.	- Not recommended due to lack of survival benefit and negative neurocognitive effects.	- WBRT should be abandoned as treatment option.	- May improve local control of SRS-treated lesions and distant lesions but has no survival benefit with negative neurocognitive effects. - Palliative WBRT may be used as last-line option in patients with multiple lesions who have failed SRS and systemic therapies.	- Lack of phase III RCTs necessary to comment on efficacy of WBRT.

IO, combination nivolumab + ipilimumab; KPS, Karnofsky Performance Score; RCT, randomized clinical trials; SRS, stereotactic radiosurgery; TT, combination dabrafenib + trametinib; WBRT, whole brain radiotherapy.

timing of IO with radiotherapy for MBM and showed longer survival in patients treated with combination IO with SRS/WBRT compared to SRS/WBRT alone and in patients receiving concurrent SRS and IO compared to non-concurrent therapy (40).

Limitations of this study included: The use of a retrospective database, precluding the ability to assess the benefit of IO given as second-line treatment since only IO given as first-line systemic therapy was recorded; And the exclusion of sociodemographic factors, disease factors, and treatment locations that could have limited a patient's access to a specific treatment modality, which could have affected their outcomes (40). Thus, the ability to reference studies using real-world data could therefore serve as complimentary information to consensus guidelines for treating physicians.

Investigators are also now exploring novel combinations of multimodal therapies in MBM patients. These ongoing trials are mostly combining triplet therapy consisting of IO and TT with other novel small molecule inhibitors (65, 66). Current ongoing trials include: EMBRAIN-MEL (NCT03898908) combining Encorafenib plus Binimetinib before SRS; RadioCoBRIM (NCT03430947) combining vemurafenib plus cobimetinib after SRS; The phase III NIBIT-M2 study (NCT02460068) comparing the chemotherapy agent fotemustine alone versus combination fotemustine plus ipi alone or combination fotemustine plus ipi and nivo; And the phase II study combining vemurafenib and combimetinib with azetolizumab (NCT03625141). Ongoing trials are also evaluating the toxicity of SRS in combination with IO or TT, as previous studies have shown statistically significant differences in radiation necrosis and brain edema among patients receiving the combination, although data are inconsistent (34).

In summary, the evidence used to compile the current versions of the worldwide consensus guidelines show promise for improving the survival of patients with MBM who receive upfront concurrent combination IO or TT with SRS. The emergence of studies using real-world evidence could serve to further compliment consensus guidelines for the treatment of MBM.

AUTHOR CONTRIBUTIONS

X-LT, AL, FL, and JH contributed to conception and design of the review and wrote portions of the manuscript. All authors contributed to manuscript critique and revision and approved the submitted version.

REFERENCES

1. Gershenwald JE, Guy GP Jr. Stemming the Rising Incidence of Melanoma: Calling Prevention to Action. *J Natl Cancer Inst* (2016) 108(1):djv381. doi: 10.1093/jnci/djv381
2. Bray F, Ferlay J, Soerjomataram I, Siegel RL, Torre LA, Jemal A. Global Cancer Statistics 2018: GLOBOCAN Estimates of Incidence and Mortality Worldwide for 36 Cancers in 185 Countries. *CA Cancer J Clin* (2018) 68 (6):394–424. doi: 10.3322/caac.21492
3. Davies MA, Liu P, McIntyre S, Kim KB, Papadopoulos N, Hwu WJ, et al. Prognostic Factors for Survival in Melanoma Patients With Brain Metastases. *Cancer* (2011) 117(8):1687–96. doi: 10.1002/cncr.25634
4. Kohler BA, Ward E, McCarthy BJ, Schymura MJ, Ries LA, Eheman C, et al. Annual Report to the Nation on the Status of Cancer, 1975-2007, Featuring Tumors of the Brain and Other Nervous System. *J Natl Cancer Inst* (2011) 103 (9):714–36. doi: 10.1093/jnci/djr077
5. Tawbi HA, Forsyth PA, Algazi A, Hamid O, Hodi FS, Moschos SJ, et al. Combined Nivolumab and Ipilimumab in Melanoma Metastatic to the Brain. *N Engl J Med* (2018) 379(8):722–30. doi: 10.1056/NEJMoa1805453
6. Schreuer M, Jansen Y, Planken S, Chevolet I, Seremet T, Kruse V, et al. Combination of Dabrafenib Plus Trametinib for BRAF and MEK Inhibitor Pretreated Patients With Advanced BRAF(V600)-mutant Melanoma: An Open-Label, Single Arm, Dual-Centre, Phase 2 Clinical Trial. *Lancet Oncol* (2017) 18(4):464–72. doi: 10.1016/S1470-2045(17)30171-7
7. Davies MA, Saiag P, Robert C, Grob JJ, Flaherty KT, Arance A, et al. Dabrafenib Plus Trametinib in Patients With BRAF(V600)-mutant Melanoma Brain Metastases (COMBI-MB): A Multicentre, Multicohort, Open-Label, Phase 2 Trial. *Lancet Oncol* (2017) 18(7):863–73. doi: 10.1016/S1470-2045(17)30429-1
8. Kelley KD, Marrero M, Knisely JP. Principles of Image-Guided Hypofractionated Stereotactic Radiosurgery for Brain Tumors. In: Sahgal A, Lo SS, Ma L, Sheehan JP, editors. *Imaged-Guided Hypofractionated Stereotactic Radiosurgery - A Practical Approach to Guide Treatment of Brain and Spine Tumors*. Boca Raton: CRC Press (2016). p. 117–27.
9. Petrelli F, De Stefani A, Trevisan F, Parati C, Inno A, Merelli B, et al. Combination of Radiotherapy and Immunotherapy for Brain Metastases: A Systematic Review and Meta-Analysis. *Crit Rev Oncol Hematol* (2019) 144:102830. doi: 10.1016/j.critrevonc.2019.102830
10. Keilholz U, Ascierto PA, Dummer R, Robert C, Lorigan P, van Akkooi A, et al. ESMO Consensus Conference Recommendations on the Management of Metastatic Melanoma: Under the Auspices of the ESMO Guidelines Committee. *Ann Oncol* (2020) 31(11):1435–48. doi: 10.1016/j.annonc.2020.07.004
11. Garbe C, Amaral T, Peris K, Hauschild A, Arenberger P, Bastholt L, et al. European Consensus-Based Interdisciplinary Guideline for Melanoma. Part 2: Treatment - Update 2019. *Eur J Cancer* (2020) 126:159–77. doi: 10.1016/j.ejca.2019.11.015
12. Swetter SM, Thompson JA, Albertini MR, Barker CA, Baumgartner J, Boland G, et al. Melanoma: Cutaneous (Version 2.2021). National Comprehensive Cancer Network (2021). Available at: https://www.nccn.org/professionals/physician_gls/pdf/cutaneous_melanoma.pdf.
13. Hong AM, Waldstein C, Shivalingam B, Carlino MS, Atkinson V, Kefford RF, et al. Management of Melanoma Brain Metastases: Evidence-based Clinical Practice Guidelines by Cancer Council Australia. *Eur J Cancer* (2021) 142:10–7. doi: 10.1016/j.ejca.2020.10.013
14. Nakamura Y, Asai J, Igaki H, Inozume T, Namikawa K, Hayashi A, et al. Japanese Dermatological Association Guidelines: Outlines of Guidelines for Cutaneous Melanoma 2019. *J Dermatol* (2020) 47(2):89–103. doi: 10.1111/1346-8138.15151
15. Seth R, Messersmith H, Kaur V, Kirkwood JM, Kudchadkar R, McQuade JL, et al. Systemic Therapy for Melanoma: Asco Guideline. *J Clin Oncol* (2020) 38 (33):3947–70. doi: 10.1200/JCO.20.00198
16. Kalkanis SN, Kondziolka D, Gaspar LE, Burri SH, Asher AL, Cobbs CS, et al. The Role of Surgical Resection in the Management of Newly Diagnosed Brain Metastases: A Systematic Review and Evidence-Based Clinical Practice Guideline. *J Neurooncol* (2010) 96(1):33–43. doi: 10.1007/s11060-009-0061-8
17. Wronski M, Arbit E. Surgical Treatment of Brain Metastases From Melanoma: A Retrospective Study of 91 Patients. *J Neurosurg* (2000) 93 (1):9–18. doi: 10.3171/jns.2000.93.1.0009
18. Lonser RR, Song DK, Klapper J, Hagan M, Auh S, Kerr PB, et al. Surgical Management of Melanoma Brain Metastases in Patients Treated With Immunotherapy. *J Neurosurg* (2011) 115(1):30–6. doi: 10.3171/2011.3.JNS091107
19. Patchell RA, Tibbs PA, Walsh JW, Dempsey RJ, Maruyama Y, Kryscio RJ, et al. A Randomized Trial of Surgery in the Treatment of Single Metastases to

the Brain. *N Engl J Med* (1990) 322(8):494–500. doi: 10.1056/NEJM199002223220802
20. Vecht CJ, Haaxma-Reiche H, Noordijk EM, Padberg GW, Voormolen JH, Hoekstra FH, et al. Treatment of Single Brain Metastasis: Radiotherapy Alone or Combined With Neurosurgery? *Ann Neurol* (1993) 33(6):583–90. doi: 10.1002/ana.410330605
21. Goyal S, Silk AW, Tian S, Mehnert J, Danish S, Ranjan S, et al. Clinical Management of Multiple Melanoma Brain Metastases: A Systematic Review. *JAMA Oncol* (2015) 1(5):668–76. doi: 10.1001/jamaoncol.2015.1206
22. Mathieu D, Kondziolka D, Cooper PB, Flickinger JC, Niranjan A, Agarwala S, et al. Gamma Knife Radiosurgery in the Management of Malignant Melanoma Brain Metastases. *Neurosurgery* (2007) 60(3):471–81; discussion 81-2. doi: 10.1227/01.NEU.0000255342.10780.52
23. Liew DN, Kano H, Kondziolka D, Mathieu D, Niranjan A, Flickinger JC, et al. Outcome Predictors of Gamma Knife Surgery for Melanoma Brain Metastases. *Clin Art J Neurosurg* (2011) 114(3):769–79. doi: 10.3171/2010.5.JNS1014
24. DiLuna ML, King JTJr., Knisely JP, Chiang VL. Prognostic Factors for Survival After Stereotactic Radiosurgery Vary With the Number of Cerebral Metastases. *Cancer* (2007) 109(1):135–45. doi: 10.1002/cncr.22367
25. Mahajan A, Ahmed S, McAleer MF, Weinberg JS, Li J, Brown P, et al. Post-Operative Stereotactic Radiosurgery Versus Observation for Completely Resected Brain Metastases: A Single-Centre, Randomised, Controlled, Phase 3 Trial. *Lancet Oncol* (2017) 18(8):1040–8. doi: 10.1016/S1470-2045(17)30414-X
26. Sampson JH, Carter JHJr., Friedman AH, Seigler HF. Demographics, Prognosis, and Therapy in 702 Patients With Brain Metastases From Malignant Melanoma. *J Neurosurg* (1998) 88(1):11–20. doi: 10.3171/jns.1998.88.1.0011
27. Fife KM, Colman MH, Stevens GN, Firth IC, Moon D, Shannon KF, et al. Determinants of Outcome in Melanoma Patients With Cerebral Metastases. *J Clin Oncol* (2004) 22(7):1293–300. doi: 10.1200/JCO.2004.08.140
28. Tsao H, Sober AJ. Melanoma Treatment Update. *Dermatol Clin* (2005) 23(2):323–33. doi: 10.1016/j.det.2004.09.005
29. Tsao MN, Xu W, Wong RK, Lloyd N, Laperriere N, Sahgal A, et al. Whole Brain Radiotherapy for the Treatment of Newly Diagnosed Multiple Brain Metastases. *Cochrane Database Syst Rev* (2018) 1:CD003869. doi: 10.1002/14651858.CD003869.pub4
30. Fogarty G, Morton RL, Vardy J, Nowak AK, Mandel C, Forder PM, et al. Whole Brain Radiotherapy After Local Treatment of Brain Metastases in Melanoma Patients–a Randomised Phase III Trial. *BMC Cancer* (2011) 11:142. doi: 10.1186/1471-2407-11-142
31. Fogarty GB, Hong A, Thompson JF. Should Patients With Melanoma Brain Metastases Receive Adjuvant Whole-Brain Radiotherapy? *Lancet Oncol* (2015) 16(5):e195–6. doi: 10.1016/S1470-2045(15)70183-X
32. Rulli E, Legramandi L, Salvati L, Mandala M. The Impact of Targeted Therapies and Immunotherapy in Melanoma Brain Metastases: A Systematic Review and Meta-Analysis. *Cancer* (2019) 125(21):3776–89. doi: 10.1002/cncr.32375
33. Long GV, Atkinson VG, Lo S, Sandhu SK, Brown M, Gonzalez M, et al. Long-Term Outcomes From the Randomized Phase II Study of Nivolumab (Nivo) or Nivo + Ipilimumab (Ipi) in Patients (Pts) With Melanoma Brain Metastases (Mets): Anti-PD1 Brain Collaboration (ABC). *Ann Oncol* (2019) 305):v534. doi: 10.1093/annonc/mdz255.001
34. Becco P, Gallo S, Poletto S, Frascione MPM, Crotto L, Zaccagna A, et al. Melanoma Brain Metastases in the Era of Target Therapies: An Overview. *Cancers (Basel)* (2020) 12(6):1640. doi: 10.3390/cancers12061640
35. Lu VM, Goyal A, Rovin RA, Lee A, McDonald KL. Concurrent Versus non-Concurrent Immune Checkpoint Inhibition With Stereotactic Radiosurgery for Metastatic Brain Disease: A Systematic Review and Meta-Analysis. *J Neurooncol* (2019) 141(1):1–12. doi: 10.1007/s11060-018-03020-y
36. Lehrer EJ, Peterson J, Brown PD, Sheehan JP, Quinones-Hinojosa A, Zaorsky NG, et al. Treatment of Brain Metastases With Stereotactic Radiosurgery and Immune Checkpoint Inhibitors: An International Meta-Analysis of Individual Patient Data. *Radiother Oncol* (2019) 130:104–12. doi: 10.1016/j.radonc.2018.08.025
37. Pin Y, Paix A, Todeschi J, Antoni D, Proust F, Noel G. Brain Metastasis Formation and Irradiation by Stereotactic Radiation Therapy Combined With Immunotherapy: A Systematic Review. *Crit Rev Oncol Hematol* (2020) 149:102923. doi: 10.1016/j.critrevonc.2020.102923
38. van Opijnen MP, Dirven L, Coremans IEM, Taphoorn MJB, Kapiteijn EHW. The Impact of Current Treatment Modalities on the Outcomes of Patients With Melanoma Brain Metastases: A Systematic Review. *Int J Cancer* (2020) 146(6):1479–89. doi: 10.1002/ijc.32696
39. Weaver BD, Goodman JR, Jensen R. Concurrent Radiosurgery and Systemic Therapies for Melanoma Brain Metastases: A Systematic Review. *Cureus* (2019) 11(11):e6147. doi: 10.7759/cureus.6147
40. Moyers JT, Chong EG, Peng J, Tsai HHC, Sufficool D, Shavlik D, et al. Real World Outcomes of Combination and Timing of Immunotherapy With Radiotherapy for Melanoma With Brain Metastases. *Cancer Med* (2021) 10(4):1201–11. doi: 10.1002/cam4.3716
41. Kroeze SG, Fritz C, Hoyer M, Lo SS, Ricardi U, Sahgal A, et al. Toxicity of Concurrent Stereotactic Radiotherapy and Targeted Therapy or Immunotherapy: A Systematic Review. *Cancer Treat Rev* (2017) 53:25–37. doi: 10.1016/j.ctrv.2016.11.013
42. Churilla TM, Chowdhury IH, Handorf E, Collette L, Collette S, Dong Y, et al. Comparison of Local Control of Brain Metastases With Stereotactic Radiosurgery vs Surgical Resection: A Secondary Analysis of a Randomized Clinical Trial. *JAMA Oncol* (2019) 5(2):243–7. doi: 10.1001/jamaoncol.2018.4610
43. Shaw E, Scott C, Souhami L, Dinapoli R, Kline R, Loeffler J, et al. Single Dose Radiosurgical Treatment of Recurrent Previously Irradiated Primary Brain Tumors and Brain Metastases: Final Report of RTOG Protocol 90-05. *Int J Radiat Oncol Biol Phys* (2000) 47(2):291–8. doi: 10.1016/S0360-3016(99)00507-6
44. Minniti G, D'Angelillo RM, Scaringi C, Trodella LE, Clarke E, Matteucci P, et al. Fractionated Stereotactic Radiosurgery for Patients With Brain Metastases. *J Neurooncol* (2014) 117(2):295–301. doi: 10.1007/s11060-014-1388-3
45. Rajakesari S, Arvold ND, Jimenez RB, Christianson LW, Horvath MC, Claus EB, et al. Local Control After Fractionated Stereotactic Radiation Therapy for Brain Metastases. *J Neurooncol* (2014) 120(2):339–46. doi: 10.1007/s11060-014-1556-5
46. Bang A, Wilhite TJ, Pike LRG, Cagney DN, Aizer AA, Taylor A, et al. Multicenter Evaluation of the Tolerability of Combined Treatment With PD-1 and CTLA-4 Immune Checkpoint Inhibitors and Palliative Radiation Therapy. *Int J Radiat Oncol Biol Phys* (2017) 98(2):344–51. doi: 10.1016/j.ijrobp.2017.02.003
47. Barker CA, Postow MA, Khan SA, Beal K, Parhar PK, Yamada Y, et al. Concurrent Radiotherapy and Ipilimumab Immunotherapy for Patients With Melanoma. *Cancer Immunol Res* (2013) 1(2):92–8. doi: 10.1158/2326-6066.CIR-13-0082
48. Anker CJ, Ribas A, Grossmann AH, Chen X, Narra KK, Akerley W, et al. Severe Liver and Skin Toxicity After Radiation and Vemurafenib in Metastatic Melanoma. *J Clin Oncol* (2013) 31(17):e283–7. doi: 10.1200/JCO.2012.44.7755
49. Peuvrel L, Ruellan AL, Thillays F, Quereux G, Brocard A, Saint-Jean M, et al. Severe Radiotherapy-Induced Extracutaneous Toxicity Under Vemurafenib. *Eur J Dermatol* (2013) 23(6):879–81. doi: 10.1684/ejd.2013.2193
50. Anker CJ, Grossmann KF, Atkins MB, Suneja G, Tarhini AA, Kirkwood JM. Avoiding Severe Toxicity From Combined BRAF Inhibitor and Radiation Treatment: Consensus Guidelines From the Eastern Cooperative Oncology Group (Ecog). *Int J Radiat Oncol Biol Phys* (2016) 95(2):632–46. doi: 10.1016/j.ijrobp.2016.01.038
51. Yamamoto M, Serizawa T, Shuto T, Akabane A, Higuchi Y, Kawagishi J, et al. Stereotactic Radiosurgery for Patients With Multiple Brain Metastases (JLGK0901): A Multi-Institutional Prospective Observational Study. *Lancet Oncol* (2014) 15(4):387–95. doi: 10.1016/S1470-2045(14)70061-0
52. Nieder C, Grosu AL, Gaspar LE. Stereotactic Radiosurgery (SRS) for Brain Metastases: A Systematic Review. *Radiat Oncol* (2014) 9:155. doi: 10.1186/1748-717X-9-155
53. Bernard ME, Wegner RE, Reineman K, Heron DE, Kirkwood J, Burton SA, et al. Linear Accelerator Based Stereotactic Radiosurgery for Melanoma Brain Metastases. *J Cancer Res Ther* (2012) 8(2):215–21. doi: 10.4103/0973-1482.98973

54. Christ SM, Mahadevan A, Floyd SR, Lam FC, Chen CC, Wong ET, et al. Stereotactic Radiosurgery for Brain Metastases From Malignant Melanoma. *Surg Neurol Int* (2015) 6(Suppl 12):S355–65. doi: 10.4103/2152-7806.163315
55. Bates JE, Youn P, Usuki KY, Walter KA, Huggins CF, Okunieff P, et al. Brain Metastasis From Melanoma: The Prognostic Value of Varying Sites of Extracranial Disease. *J Neurooncol* (2015) 125(2):411–8. doi: 10.1007/s11060-015-1932-9
56. Rades D, Sehmisch L, Huttenlocher S, Blank O, Hornung D, Terheyden P, et al. Radiosurgery Alone for 1-3 Newly-Diagnosed Brain Metastases From Melanoma: Impact of Dose on Treatment Outcomes. *Anticancer Res* (2014) 34(9):5079–82.
57. Brown PD, Ballman KV, Cerhan JH, Anderson SK, Carrero XW, Whitton AC, et al. Postoperative Stereotactic Radiosurgery Compared With Whole Brain Radiotherapy for Resected Metastatic Brain Disease (NCCTG N107C/CEC3): A Multicentre, Randomised, Controlled, Phase 3 Trial. *Lancet Oncol* (2017) 18(8):1049–60. doi: 10.1016/S1470-2045(17)30441-2
58. Brown PD, Gondi V, Pugh S, Tome WA, Wefel JS, Armstrong TS, et al. Hippocampal Avoidance During Whole-Brain Radiotherapy Plus Memantine for Patients With Brain Metastases: Phase Iii Trial Nrg Oncology Cc001. *J Clin Oncol* (2020) 38(10):1019–29. doi: 10.1200/JCO.19.02767
59. Hong AM, Fogarty GB, Dolven-Jacobsen K, Burmeister BH, Lo SN, Haydu LE, et al. Adjuvant Whole-Brain Radiation Therapy Compared With Observation After Local Treatment of Melanoma Brain Metastases: A Multicenter, Randomized Phase III Trial. *J Clin Oncol* (2019) 37(33):3132–41. doi: 10.1200/JCO.19.01414
60. Long GV, Atkinson V, Lo S, Sandhu S, Guminski AD, Brown MP, et al. Combination Nivolumab and Ipilimumab or Nivolumab Alone in Melanoma Brain Metastases: A Multicentre Randomised Phase 2 Study. *Lancet Oncol* (2018) 19(5):672–81. doi: 10.1016/S1470-2045(18)30139-6
61. Margolin K, Ernstoff MS, Hamid O, Lawrence D, McDermott D, Puzanov I, et al. Ipilimumab in Patients With Melanoma and Brain Metastases: An Open-Label, Phase 2 Trial. *Lancet Oncol* (2012) 13(5):459–65. doi: 10.1016/S1470-2045(12)70090-6
62. Dummer R, Goldinger SM, Turtschi CP, Eggmann NB, Michielin O, Mitchell L, et al. Vemurafenib in Patients With BRAF(V600) Mutation-Positive Melanoma With Symptomatic Brain Metastases: Final Results of an Open-Label Pilot Study. *Eur J Cancer* (2014) 50(3):611–21. doi: 10.1016/j.ejca.2013.11.002
63. Ahmed KA, Abuodeh YA, Echevarria MI, Arrington JA, Stallworth DG, Hogue C, et al. Clinical Outcomes of Melanoma Brain Metastases Treated With Stereotactic Radiosurgery and anti-PD-1 Therapy, anti-CTLA-4 Therapy, BRAF/MEK Inhibitors, BRAF Inhibitor, or Conventional Chemotherapy. *Ann Oncol* (2016) 27(12):2288–94. doi: 10.1093/annonc/mdw417
64. Collins R, Bowman L, Landray M, Peto R. The Magic of Randomization Versus the Myth of Real-World Evidence. *N Engl J Med* (2020) 382(7):674–8. doi: 10.1056/NEJMsb1901642
65. Tawbi H. The Standard of Care for Brain Metastases in Melanoma. *Clin Adv Hematol Oncol* (2020) 18(1):28–31.
66. Ding R, Chen L, Su Z, Xiong T, Wen Q, Peng Q, et al. Development of Immunotherapy for Brain Metastasis (Review). *Int J Oncol* (2020) 57(3):665–77. doi: 10.3892/ijo.2020.5091

Conflict of Interest: X-LT, ES, RJ, SJD, and IMS are employees of Merck & Co., Inc. JH and AL are employed by Integrative Precision Health LLC. ES was also employed by Seagen Inc.

The remaining authors declare that the research was conducted in the absence of any commercial or financial relationships that could be construed as a potential conflict of interest.

frontiers | Frontiers in Oncology

ORIGINAL RESEARCH
published: 10 May 2022
doi: 10.3389/fonc.2022.866542

Radiosurgery for Five to Fifteen Brain Metastases: A Single Centre Experience and a Review of the Literature

*Susanne J. Rogers**, *Nicoletta Lomax*, *Sara Alonso*, *Tessa Lazeroms* and *Oliver Riesterer*

Radiation Oncology Center KSA-KSB, Canton Hospital Aarau, Aarau, Switzerland

Purpose: Stereotactic radiosurgery (SRS) is now mainstream for patients with 1-4 brain metastases however the management of patients with 5 or more brain metastases remains controversial. Our aim was to evaluate the clinical outcomes of patients with 5 or more brain metastases and to compare with published series as a benchmarking exercise.

Methods: Patients with 5 or more brain metastases treated with a single isocentre dynamic conformal arc technique on a radiosurgery linac were identified from the institutional database. Endpoints were local control, distant brain failure, leptomeningeal disease and overall survival. Dosimetric data were extracted from the radiosurgery plans. Series reporting outcomes following SRS for multiple brain metastases were identified by a literature search.

Results: 36 patients, of whom 35 could be evaluated, received SRS for 5 or more brain metastases between February 2015 and October 2021. 25 patients had 5-9 brain metastases (group 1) and 10 patients had 10-15 brain metastases (group 2). The mean number of brain metastases in group 1 was 6.3 (5-9) and 12.3 (10-15) in group 2. The median cumulative irradiated volume was 4.6 cm^3 (1.25-11.01) in group 1 and 7.2 cm^3 (2.6-11.1) in group 2. Median follow-up was 12 months. At last follow-up, local control rates per BM were 100% and 99.8% as compared with a median of 87% at 1 year in published series. Distant brain failure was 36% and 50% at a median interval of 5.2 months and 7.4 months after SRS in groups 1 and 2 respectively and brain metastasis velocity at 1 year was similar in both groups (9.7 and 11). 8/25 patients received further SRS and 7/35 patients received whole brain radiotherapy. Median overall survival was 10 months in group 1 and 15.7 months in group 2, which compares well with the 7.5 months derived from the literature. There was one neurological death in group 2, leptomeningeal disease was rare (2/35) and there were no cases of radionecrosis.

Conclusion: With careful patient selection, overall survival following SRS for multiple brain metastases is determined by the course of the extracranial disease. SRS is an efficacious and safe modality that can achieve intracranial disease control and should be offered to patients with 5 or more brain metastases and a constellation of good prognostic factors.

Keywords: radiosurgery, brain, metastasis, multiple, single isocenter, LINAC

OPEN ACCESS

Edited by:
David Kaul,
Charité Universitätsmedizin Berlin, Germany

Reviewed by:
Güliz Acker,
Charité University Medicine Berlin, Germany
Ilinca Popp,
University of Freiburg Medical Center, Germany
Alexander Muacevic,
Ludwig Maximilian University of Munich, Germany

****Correspondence:***
Susanne J. Rogers
susanne.rogers@ksa.ch;
orcid.org/0000-0003-0094-1890

Specialty section:
This article was submitted to Neuro-Oncology and Neurosurgical Oncology, a section of the journal Frontiers in Oncology

Received: *31 January 2022*
Accepted: *07 March 2022*
Published: *10 May 2022*

Citation:
Rogers SJ, Lomax N, Alonso S, Lazeroms T and Riesterer O (2022) Radiosurgery for Five to Fifteen Brain Metastases: A Single Centre Experience and a Review of the Literature. Front. Oncol. 12:866542. doi: 10.3389/fonc.2022.866542

INTRODUCTION

The treatment landscape for patients with brain metastases has transformed in the past 15 years. A nihilistic approach used to prevail due to the associated mean survival of 3-4 months (1). Patients mostly presented with a poor performance status due to large, symptomatic brain metastases and were treated with whole brain radiotherapy (WBRT). WBRT can achieve symptomatic relief but without significant tumour control and cause of death in such patients is frequently neurological (2). A positive correlation between radiotherapy dose, local control rate and overall survival in patients with brain metastases has been established (3) and stereotactic radiosurgery (SRS), which is high dose irradiation to small target volumes, can achieve long lasting local control of brain metastases with minimal toxicity in patients eligible for this approach. The mean and maximum biologically equivalent doses in brain metastases with SRS are 3 and 5 times greater respectively than with 10 x 3Gy WBRT (4) and by achieving intracranial disease control and avoiding a neurological cause of death, can even increase survival as compared with WBRT (5, 6).

With earlier detection of small brain metastases through increased access to magnetic resonance (MR) imaging, the development of disease-specific prognostic indices, identification of druggable molecular targets and widespread adoption of immunotherapy, the prognosis for subgroups of patients with brain metastases and controlled extracranial disease has increased dramatically. Overall survival of up to four years in patients with more than four brain metastases from EGFR- and ALK-mutated non-small cell lung cancer following radiosurgery has been reported (7). Consequently, the management of brain metastases in patients with a better prognosis should be individualized and intensified in patients with a constellation of positive prognostic factors.

Radiosurgery has developed from a time-consuming, labor-intensive therapy only viable for patients with very few brain metastases to a practically manageable option for patients with multiple brain metastases (MBM). The definition of multiplicity is currently unresolved and, according to the National Comprehensive Cancer Network (NCCN), extends to 'all patients who would profit from radiosurgery as compared with whole brain radiotherapy' (8). Historically, patients were highly selected for brain radiosurgery due to the limited access to radiosurgery platforms. Three or four brain metastases are, or at least were, generally the upper limit for radiosurgery in many centers (9). This is partly due to the lengthy duration of sequential treatment of MBM, the time-intensive quality assurance and constraints by healthcare systems. Furthermore, the radiosurgery community was slow to adopt radiosurgery for MBM due to safety concerns. The potential toxicity from the cumulative irradiated volume when treating MBM was uncertain, and it was argued that the integral dose to the brain was likely to be as high as with WBRT but this has been disproven (10). Publication of the large, multicentre cohort JLGK0901 study, which reported that overall survival and most secondary endpoints following radiosurgery for 5-10 brain metastases were not inferior to 2-4 brain metastases (11), has been practice changing. The same group also reported that clinical outcomes for patients with 10-15 brain metastases were equivalent to patients with 2-9 brain metastases when treated with radiosurgery (12). The number of patients with MBM referred to our centre for radiosurgery has steadily increased in recent years. The optimal therapy for five or more brain metastases is still controversial (13) and represents the focus of this study. The purpose of this work was to evaluate the clinical outcomes of our cohort of patients, to discuss the technique and to provide a systematic overview of the current literature.

METHODS

Inclusion Criteria

The prospectively-maintained institutional database was searched for consecutive patients who received radiosurgery to five or more intact brain metastases in a single treatment course between 1st December 2015 and 1st November 2021. Ethics approval was obtained (EKNZ 2019-01705) and patients who, at the time of treatment, declined general consent to participate in future research were not included. All patients were presented at a multidisciplinary neuro-oncology tumour board where a recommendation for SRS was made.

Treatment Planning Technique

A CT with contiguous 0.6mm slices (14) was performed in a customized radiosurgery mask (Brainlab, Germany) and a 1.5 T T1-Gad MPR planning MRI scan were obtained on the same day. The CT and MRI were fused rigidly and then again with deformable registration to correct any distortion in the MRI. Following autosegmentation of the organs at risk (Brainlab Elements), the contrast-enhancing brain metastases were contoured and a 1mm planning target volume (PTV) margin was added to each, unless they were located in the brainstem when no PTV margin was added. For metastases more than 4cm off-axis and of volume <0.07 cm^3 (equivalent to a diameter of approximately 5 mm), a 1.5 mm or sometimes 2mm margin was applied to correct for any rotational inaccuracy.

The prescription dose was 20 Gray (Gy) in a single fraction to 98–99% of the PTV (15), with a maximum dose between 125 and 143% (equivalent to prescribing to the 70–80% isodose surface (%IDS) when normalized to the maximum point dose). The structure 'brain minus GTV' was created and if more than 10 cm^3 of this 'organ at risk' (OAR) received 10 Gy per metastasis, the dose was reduced to 30 Gy in 5 fractions, allowing 20 cm^3=V20Gy, using the same prescription isodose. Metastases greater than 2cm in diameter or located in eloquent cortex were also treated with hypofractionated stereotactic radiotherapy (hfSRT). In the brainstem, small metastases were treated with a single fraction of 18 Gy. Treatment plans were generated using Elements Multimets v1.5 and v2.0 (Brainlab, Germany).

Treatment Delivery

Treatment was delivered with non-coplanar dynamic conformal arcs (DCA) on a Truebeam STx linear accelerator (linac) with Novalis Radiosurgery platform (Brainlab/Varian) with high

definition MLC leaves (2.5 mm) and a 6 degrees of freedom (DoF) couch. 4mg daily prophylactic dexamethasone for 3 days was prescribed for metastases with a cumulative volume in excess of 1 cm^3.

An accurate patient set-up and treatment delivery was ensured using the Brainlab stereoscopic Exactrac kV x-ray 6D image-guided radiotherapy system. Before delivering each DCA, the stereoscopic radiographic images were matched to the reference digital radiographs reconstructed from the planning CT data set. Before delivery of the first arc, translational and rotational corrections were applied using the 6DoF couch. Verification images were taken before each further arc and corrections applied for translational shifts greater than 0.5mm and rotational shifts greater than 0.5 degrees.

Follow-up MRIs were performed every 3-months after radiosurgery and time to local recurrence, nodular leptomeningeal recurrence, new brain metastases and radionecrosis were calculated from the date of last radiosurgery. Patient follow-up was censored at death or last contact up to 31st October 2021.

Statistical Analysis

Kaplan–Meier analysis was utilized to calculate the actuarial local control rate and overall survival rates, otherwise descriptive statistics were applied. Patients were censored at death for the local control analysis.

Literature Review

Terms for the literature search in Pubmed with no time limit and up to 31st October 2021 were "radiosurgery", "metastasis", "brain" and "multiple". Original reports published in English, French or German of patients who received radiosurgery for 2 or more brain metastases were included if sufficient data regarding outcomes of patients with 5 or more brain metastases were available. Dosimetric evaluations without clinical data were excluded, as were reviews of the technical or clinical issues. Reports pertaining mainly to quality of life, health economics, toxicity and non-SRS therapies were also excluded. No filters, limits or automation were used. No assumptions were made as to missing data, which are presented as 'not reported' (NR). The review was performed following the PRISMA 2020 guidelines however a formal meta-analysis was beyond the scope of this work.

RESULTS

Radiosurgery for 5 or more brain metastases was delivered to 37 patients between February 2017 and October 2021. 5-9 brain metastases were treated in 26/37 (70%) (group 1) and 10 or more brain metastases were irradiated in 11/37 patients (30%) (group 2). One patient in group 1 moved abroad for further treatment and was lost to follow-up and one patient in group 2 was not included in the final analysis as only one of the five hypofractionated stereotactic radiotherapy fractions could be delivered, thus 25 and 10 patients were evaluated in groups 1 and 2 respectively. All patients were in recursive partitioning analysis (RPA) group 2 as none had a single metastasis and all patients had a minimum Karnofsky Performance Status of 70%. Median patient follow-up in group 1 was 12.1 months and in group 2 was 15.6 months.

Patient demographics are shown in **Table 1**. Patients in groups 1 (5-9 BM) and 2 (10-15 BM) were similar in terms of age and performance status. Two thirds of each group had non-small cell lung cancer but driver mutations were rare (**Table 1**). On average, patients in group 2 had twice as many BMs as those in group 1 (mean 12.3 vs 6.3). More patients in group 2 had a synchronous diagnosis of BM (within 4 weeks of the primary tumour, often as part of tumor staging), and thus a shorter mean interval to diagnosis of the BMs (median 0.7, mean 10.9 months) than patients in group 1 (median 3.9, mean 18 months). No patients in group 2 had had prior WBRT, whereas 2/25 (8%) patients in group 1 had previously received therapeutic WBRT. More than two thirds of patients received concomitant systemic therapy as summarized in **Table 1**. With regard to dose prescription, 5 of 25 patients (20%) in group 1 received a combination of single fraction and hfSRT in the same treatment course and in group 2, 30% (3 of 10 patients) required this combined prescription approach.

Table 2 represents the dosimetric features of the radiosurgery plans for multiple brain metastases. The brain metastases were small with a cumulative total volume of 4.6 cm^3 in group 1 and 7.2 cm^3 in group 2 respectively. The plan quality as measured by the conformity and gradient indices were comparable in the two groups.

With regard to clinical outcomes, local control was evaluated per lesion and per patient. At a median follow-up of 12.1 and 15.6 months, the local control rates at last follow-up approximated 100% in both groups (**Figure 1** per patient and **Table 3** per lesion). Metabolic activity was detected in two initially larger metastases on FET-PET CT scan 1 year after hfSRT as discussed below. There were no reported toxicities according to CTCAE v5.0. Median overall survival was 10 and 15.9 months in groups 1 and 2 respectively (**Figure 2**), which exceeds that reported in the literature to date. 17 publications were included in the literature review (**Figure 3**). 10/17 described outcomes following SRS for patients with five or more brain metastases and seven publications with patients with four or more brain metastases were included, as the cut-off for the definition of MBM is arbitrary (**Table 4**). Only two series used a linac to deliver SRS (25, 30). Considering all patients and the data provided, the median number of brain metastases irradiated per patient was 7 and the median cumulative tumour volume per patient was 5.7cm^3. The median local control rate at 1 year was 87% and the median overall survival was 7.6 months.

DISCUSSION

Numerous comparative planning studies of radiosurgery for MBM have been published, however there are fewer reports of clinical outcomes of patients treated with 5 or more brain metastases, and very few with a linac (25, 31). This observation prompted us to evaluate our cohort of patients and to benchmark these real-world data from routine clinical practice against the literature.

TABLE 1 | Patient demographics.

Patient Characteristics	Group 1 (5-9 BM)	Group 2 (10-15 BM)
Number of patients	25	10
Gender M:F	14: 11	3: 7
Age (yrs) mean (range)	65.4 (50-80)	62.5 (51-69)
Mean Karnofsky Performance Status (%), mean (range)	86.5 (70-100)	88.3 (80-90)
Adenocarcinoma of the lung: other	17: 8	7: 3
-Targetable TK mutation Y:N	2: 23 (8%)	2:8 (20%)
Mean number of BMs per patient (range)	6.3 (5-9)	12.3 (10-15)
No. of patients with a ds-GPA score for the primary	19/25	10/10
Median ds-GPA (range)	1.5 (0-2.5)	1.5 (1-2.5)
Prior irradiation of other BM Y: N	5: 20 (20%)	1: 9 (10%)
-SRT/SRS	3/5	1/1
-WBRT	2/5	
Synchronous: metachronous BM	16: 9 (64%)	8:2 (80%)
Time to BM from diagnosis of primary in months median (range)	3.9 (0-187.5)	0.7 (0-95.5)
Extracranial metastases Y:N	20:5 (80%)	10:0 (100%)
Synchronous systemic treatment Y:N	10:15 (66.7%)	8:2 (80%)
-Chemotherapy	3/10	2/8
-Immunotherapy	2/10	0/8
-Immunochemotherapy	2/10	4/8
-Tyrosine kinase inhibitor	3/10	2/8
Symptomatic BM Y: N	1:24 (4%)	2:8 (20%)
No. of patients with combined SRS/hfSRT: single fraction SRS only prescribed in same treatment course	5:20 (20%)	3:7 (30%)

BM, brain metastasis; SRS, stereotactic radiosurgery; hfSRT, hypofractionated stereotactic radiotherapy.

TABLE 2 | Dosimetric features of SRS plans for multiple metastases.

Plan Characteristics	Group 1 (5-9 BM)	Group 2 (10-15 BM)
Median GTV per metastasis, cm^3 (range)	0.2 (0.06-1.47)	0.32 (0.04-0.56)
Median PTV per metastasis, cm^3 (range)	0.9 (0.20-3.08)	0.6 (0.22-0.98)
Cumulative total PTV per patient, cm^3 Median (range)	4.6 (1.25-11.01)	7.2 (2.6-11.1)
Mean number of isocentres per patient (range)	2.3 (1-4)	3.0 (2-4)
Mean distance of metastasis from isocentre, cm (range)	2.9 (1.72-3.88)	3.2 (3.08-3.88)
Mean inverse Paddick Index per BM (range)	1.3 (1.15-1.54)	1.5 (1.41-1.74)
Mean Gradient Index per BM (range)	3.8 (2.54-4.88)	4.0 (3.47-5.3)
Mean number of arcs per isocentre (range)	7.8 (3-10)	8.8 (4-10)
Mean number of monitor units per Gray (range)	279.6 (212-539)	318.9 (169-577)

BM, brain metastasis.

The local control rates per patient and per lesion in excess of 90% at 12 months in both groups confirm accurate irradiation of the small target volumes and reflect the greater efficacy of SRS for small metastases (32). One patient with 13 BMs had local progression of 1 brain metastasis after initial hfSRT. 11 brain metastases were small and could be treated with a single fraction, but two were located in the eloquent motor cortex. As the patient was symptomatic with focal seizures affecting his dominant arm and the PTV volume was 3.98 cm^3, these two metastases were treated in a separate volume with hfSRT to 30 Gy in 5 fractions. After 10.4 months, an MRI scan was reported to show enlargement following an initial good partial response and thus possible tumour progression of the largest metastasis. FET-PET imaging confirmed metabolic activity of vital tumour cells, rather than radionecrosis, in the two metastases treated with hfSRT as well as a third metastasis. In the context of extracranial progressive disease and to minimise the risk of radionecrosis, salvage WBRT with hippocampal avoidance was performed. Neurological death was reported in one patient in group 2 who succumbed during a generalized epileptic seizure 16 months after SRS for MBM whilst hospitalized and receiving best supportive care for extracranial disease progression. In the other 34 patients, extracranial disease progression was the cause of death.

As early as 2000, Suzuki et al. reported good safety and local control data but a mean survival of only 11 weeks for 24 patients treated with SRS for more than 10 brain metastases. Early reports emphasised the lack of difference in OS as compared with patients treated with SRS for more or fewer than 4 brain metastases (26). At a median follow-up of 12 months, 50% of all 35 patients with 5 or more brain metastases in this series are alive (approximately 50% of each group). The prolonged median overall survival of up to 16 months in our series demonstrates

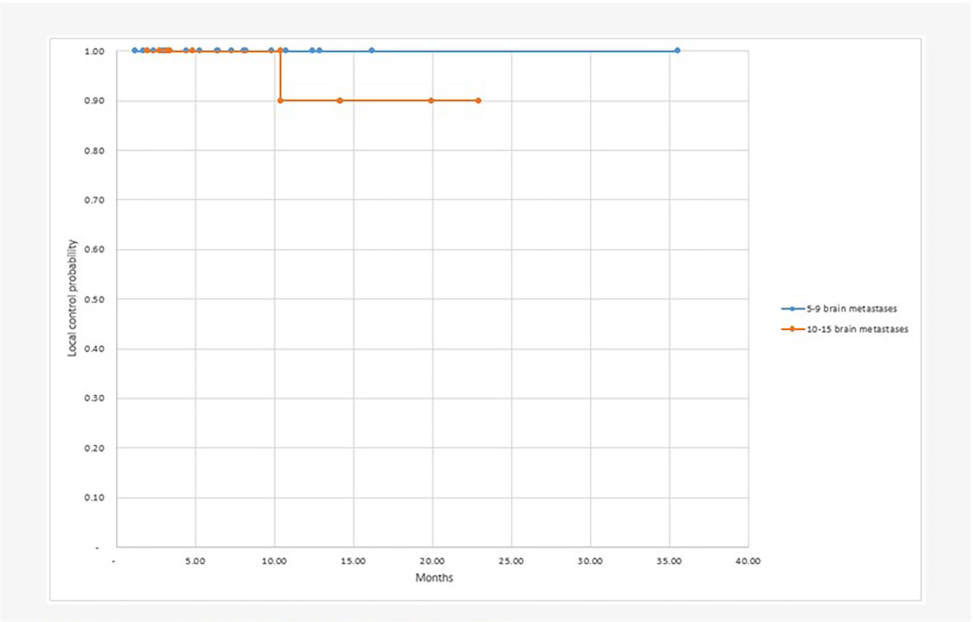

Months	0	5	10	15	20
Number at risk group 1	25	14	9	3	1
Number at risk group 2	10	6	4	3	2

FIGURE 1 | Median local control after radiosurgery for 5 or more brain metastases: Group 1 with 5-9 brain metastases (100% local control at 35 months follow-up) and group 2 with 10-15 brain metastases (90% local control at 23 months follow-up).

TABLE 3 | Clinical outcomes following SRS.

Clinical outcome	Group 1 (5-9 BM)	Group 2 (10-15 BM)
Median follow-up (range) in months	12.1 (0.6-37.5)	15.6 (3.8-24)
Local failure at last follow-up (per BM)	0/159 (0%)	2/123 (0.02%)
Distant brain failure (new BM) Y:N	9:16 (36%)	5:5 (50%)
Time to distant brain failure in months median (range)	5.2 (2-24)	7.4 (2-22.5)
Brain metastasis velocity (no. of new BM/year)		
-at first distant brain failure	9.7	11
-at time of last follow-up	1.9	2.7
Incidence of leptomeningeal relapse	1:24 (4%)	1:9 (10%)
Brain irradiation at DBF Y:N	9:16 (36%)	5:5 (50%)
-hfSRT/SRS	7/9 (1*/7) (78%)	1*/5 (20%)
-WBRT	2/9 (22%)	5/5 (100%)
Extracranial disease progression Y:N	15:10 (60%)	7:3 (70%)
Therapy at extracranial disease progression (several possible)	15/15 (100%)	3/7 (30%)
-SBRT	2/15	1/3
-Surgery	1/15	0/3
-Chemotherapy	0/15	1/3
-Tyrosine kinase inhibitor	7/15	1/3
-Immunotherapy	5/15	0/3
-Best supportive care		1/3
Median overall survival (range) in months	10.0 (0.6-35.9)	15.7 (3.8-24)
Deceased at last follow-up	14/25 (56%)	5/10 (50%)
Neurological cause of death (no. of patients)	0/25	1/10

*NR, not reached; BM, brain metastasis; DBF, distant brain failure; hfSRT, hypofractionated stereotactic radiotherapy; *SRS at second DBF; WBRT at third DBF.*

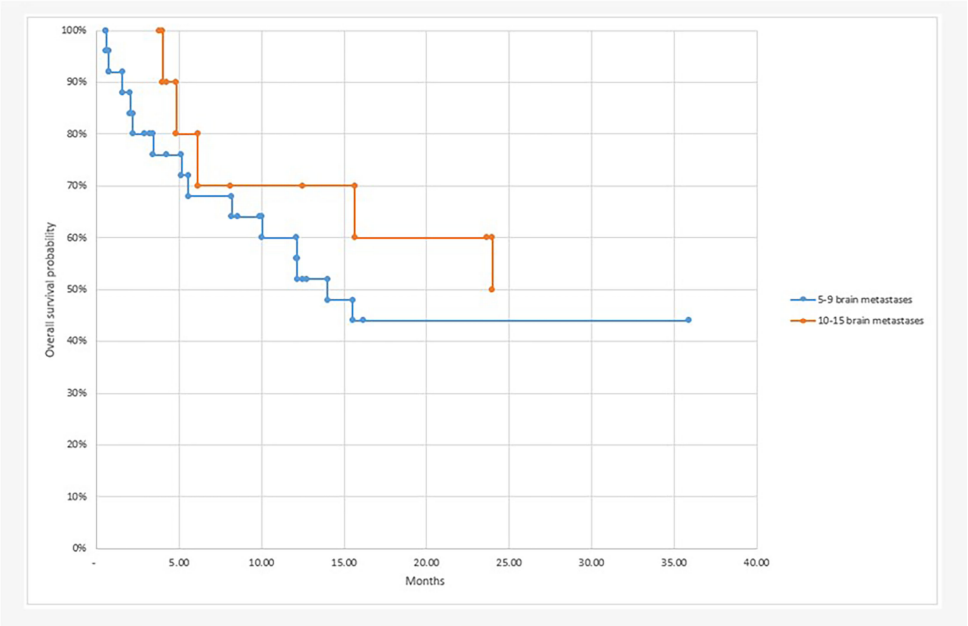

Months	0	5	10	15	20
Number at risk group 1	25	14	9	3	1
Number at risk group 2	10	6	4	3	2

FIGURE 2 | Median overall survival after radiosurgery: 10 months in the 5-9 brain metastases group vs 15.7 months in the 10-15 brain metastases group.

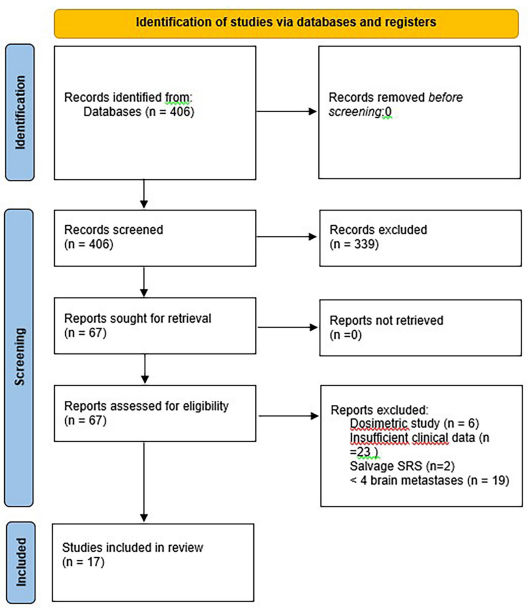

FIGURE 3 | Flow diagram representing the number of records identified and reasons for exclusion.

TABLE 4 | Summary of the literature pertaining to clinical outcomes after radiosurgery for four or more brain metastases.

	No. of		Platform	Median no. of BM (range)	Median follow-up (mths)	Median total treatment volume per patient (cm^3) (range)	PTV per metastasis (cm^3) Mean, (range)	Prescribed dose (Gy) Mean (range)	1 yr LC (%)	DBF 1yr (%) Med. time to DBF (mths)	Median OS (mths)	Criteria/ Comments
	BM	pts										
Nam et al., 2005 (16)	≥4 BM	46	Gamma knife	Mean 4.24 (127)	13.3	Mean 8.38 (0.87-104)	1.92	17.9 (12-30)	69.5	20.9	5.4	
Bhatnagar et al., 2006 (17)	≥4	205	Gamma knife	5 (4-18)	Mean 8	6.8 (0.6-51)	NR	16	71	43 9	8	46% SRS in combination with WBRT 38% SRS as salvage after WBRT
Kim et al., 2008 (18)	≥10	26	Gamma knife	16.6 (10-37)	NA	10.9 (1.0-42.2)	NR	15(9-23)	79.5% @ 6 mths	26.9 6 mths	7.8	
Chang et al., 2010 (19)	6-10 11-15 >15	58 17 33	Gamma knife	NR	10.7 12.3 8	NR	NR	NR	83 92 89	11 8 6 (p=0.028)	10 13 8	
Lee et al., 2011 (20)	4-14	36	Gamma knife	7 (4-14)	4.5	1.2 (0.002-12.6)	NR	17.8 (12-22)	84.2 @ 9 mths	22.2 4	9.1	Median KPS 90 80.6% no prior WBRT 70% dose if WBRT < 2 yrs
Grandhi et al., 2012 (21)	≥10	61	Gamma knife		4	4.86 (0.14 -40.21)	0.64 (0.01–2.87)	16	48.	77.6 3	4.5	77% KPS 90-100 37.7% no prior WBRT
Mohammadi et al., 2012 (22)	≥5	170	Gamma knife	6 (5-20)	6.2	3.2 (0.2-37.2)	Max. diameter 1.8 (0.5-5.1)	NR	97	40 (crude) 2.1	6.7	SRS as salvage in 110/170 (65%) patients
Rava et al., 2013 (23)	≥10	53	Gamma knife	11 (10-34)	NR	NR	NR	16.6	86.8	90 3	<10BM: 6.8 >10BM: 5.8	KPS >70, 36% no prior WBRT PTV = GTV + 1-2mm
Salvetti et al., 2013 (24)	5-15 5-9	96 10-15	Gamma knife	7 (5-15)	4.1	6.12 (0.42-57.83)	0.26 (0.007-46.54)	20 (14-36.4)	84.8	41	4.8 3.4(NS)	All histologies except SCLC and CUP, KPS>70, 53% no prior WBRT
Yamamoto et al., 2014 (11)	5-10	208	Gamma knife	6	12	3.54 (NR-13.90)	Max. diameter 1.62 (0.08-2.97)	<4$cm^3$22 >4$cm^3$20	93.5	64	10.8	Max 3cm diam/ 10cm^3, cumulative tumor vol. <15cm^3, KPS>70, no prior WBRT
Frakes et al., 2015 (25)	≥5	28	Linac + Exactrac		6.3	3.7 (0.6-16.9)	0.34 (0.01-12.5)	24 (15-24)		57.1% @med 3 mths (1-15)	7.6 from SRS	Exclusively melanoma patients
Greto et al., 2016 (26)	>4 BM	11	Gamma knife	NR	7.2	NR	Mean PTV 0.39 (0.006-1.86)	20.3 (11-24)	95	3	72.4% @1yr	
Knoll et al., 2016 (27)	>4 BM	70	Gamma knife or Cyberknife	NR	NR	1.8 cm^3	NR	NR	96.8 @ 6 mths	NR	8.5 (4.4-12.9)	
Yamamoto et al., 2019 (12)	2-9 >10	467 467	Gamma knife	NR	6.1 (1.2-11.8)	Mean 10.4 (0.06-115.3) 9.8 (0.15-81.4)	Mean of largest tumour 5.8 (0.04-57.8) 5.3 (0.03-65)	20.9 (10-25) 21.1 (12-25)	Timepoint? 92 96.2		7.1 6.9	
Hamel-Perreault	5-9 >10	81 22	Gamma knife	7 (5-19)	13 (1-35)	2.0 (0.06-28.0)	1.1 (0.02-16)	20 (16-25)	79% at 6 months	53% at 6 months	6 (1-58)	

(Continued)

TABLE 4 | Continued

	No. of		Platform	Median no. of BM (range)	Median follow-up (mths)	Median total treatment volume per patient (cm^3) (range)	PTV per metastasis (cm^3) Mean, (range)	Prescribed dose (Gy) Mean (range)	1 yr LC (%)	DBF 1yr (%) Med. time to DBF (mths)	Median OS (mths)	Criteria/ Comments
	BM	pts										
et al., 2019 (28)												
Susko et al., 2020 (29)	≥- 10	143	Gamma knife	13 (11-17)	7.4 (2.7-15.9)	4.1 (2-9.9)	NR	19 (18-19)	96.8% (primary) 83.6% (salvage)	80.2 (primary 80.8 (salvage)	11.7 (primary) 7.4 (salvage)	
Alongi 2021 (30)	2-22	172	2.5mm MLC Linac SI-VMAT	4 (2-22)	20	5.7 (0.3–74.3)	0.2 (0.08–24.4)	mean 9 (4–25) 1 x15 to-5 x 6	86.7	80.6	12 (3-33)	Single isocentre
KSA series 2022	5-9 10-15	25 10	2.5mm MLC Linac + Exactrac SI-DCA	NR	12.1 15.6	4.6 (1.25-11.01) 7.2 (2.6-11.1)	0.5(14.04) 0.2(3.98)	20 (18-29) 1 fr 1 x 18 to 5 x 6	100 90	36% 50% 5.2 7.4	10 (0.6-35.9) 15.7 (3.8-24)	All histologies except SCLC (50% adeno NSCLC) KPS >80, 6% prior WBRT

Pts, patients; fr, fraction; NR, not reported.

appropriate identification of patients with MBM likely to benefit from radiosurgery. Patient selection is often levelled as a criticism of single centre series, however is necessary in the setting of SRS for MBM to personalize therapy and to optimize use of resources. The management of such patients requires particular consideration of their prognosis due to extracranial as well as the intracranial tumour situation, with for example differentiation of visceral from non-visceral metastases (17). The disease-specific graded prognostic assessment (ds-GPA) scores in groups 1 and 2 were low (median 1.5) as more than four brain metastases receives a score of zero, furthermore most patients had extracranial disease and driver mutations were infrequent in these small patient groups. Sperduto et al. determined a median survival of 12 months with a ds-GPA score of 1.5-2 in patients with adenocarcinoma of the lung, which is in the order of the median 10-16 months in this study. Several patients are alive with an overall survival of 24-35.9 months, well in excess of that predicted from their ds-GPA scores. Nagtegaal et al. found a correlation between actual and predicted overall survival according to ds-GPA score in a cohort of over 350 patients with 0-10 brain metastases (33), except for a worse than predicted OS in the subgroup of patients with adenocarcinoma of the lung and a ds-GPA score of 2.5-4.0. Recently, the ds-GPA could not be validated in a cohort of patients with melanoma, putatively due to the effects of immunotherapy and targeted therapies (34). This group suggested a novel approach to predictive scoring using a combination of tumour volume, timing of onset and any systemic therapies, which reflects the continual personalization of therapy for patients with brain metastases (34).

It has been suggested that the number of brain metastases is a surrogate for the disease burden, rather than being prognostic per se (27) however brain metastases velocity (BMV), that is to say the number of new brain metastases developing per year, is predictive of outcome (35). A statistically longer interval to new brain metastases for patients with >2 BMs relative to patients with >15 BMs at SRS has been shown (35). Time to distant brain failure was similar in groups 1 and 2 in our cohort, 5.2 vs 7.2 months respectively, however we used different cut-offs of 5-9 BMs and >10 BMs. The BMV at one year was similar in group 2 (11) to group 1 (9.7) and both would be classified as intermediate risk (35), however at last follow up, BMV was higher in the group with more than 10 initial BMs (2.7 vs 1.9). It is likely that the BMV and the irradiated volume are most predictive in combination. Technically, it is highly feasible to repeat courses of SRS, as we did for 57% of patients with subsequent new brain metastases, to effectively postpone WBRT (36). Generally, due to the spatial distribution of multiple small BMs, little consideration needs to be paid to the previous dose volume histograms (DVH), unless a metastasis is in close proximity to an organ at risk or to a previously irradiated metastasis due to the increased risk of radionecrosis associated with salvage re-irradiation (37). A contraindication to repeat SRS to new brain metastases would be leptomeningeal disease however, which may develop more frequently in patients with a higher number of brain metastases (38) (2/35, 5.7%, in our series) as these patients benefit from WBRT.

The acceptance of SRS as a safe technique for MBM prompted in silico comparisons of radiosurgery plans with multiple isocentres generated with conventional techniques (Gammaknife, Elekta) against linac-based volumetric arc radiation therapy (VMAT) as competing technologies (39). Due to the different beam geometry, greater low dose spill with VMAT was shown and the reporting of the gradient index (GI), in addition to the conformity index (CI), was recommended to compare dose to normal brain. The treatment planning software used in this study generates the GI as well as the inverse Paddick conformity index (PI) (40). **Table 2** shows that the CIs generated by the SI-DCA plans were similar to those achieved with a Gamma knife (Elekta, Sweden), as reported by Hazard et al. (15).

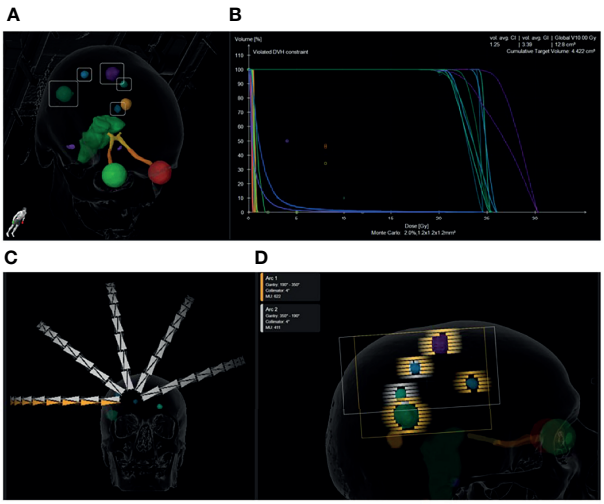

FIGURE 4 | Graphical representation of a single isocentre dynamic conformal arc plan prescribed to 1 x 20 Gy for a patient with 7 brain metastases from non-small cell lung cancer. Five metastases were treated with this plan. The 6th and 7th were located inferiorly and were irradiated with 1 x 20 Gy in a second plan to maintain the distance of the PTVs from the isocentre below 5 cm. 3D view of the location and size of the metastases **(A)**. Dose volume histogram showing >99% coverage of the PTVs with 100% dose and minimal dose to the organs at risk. The cumulative PTV volume was 4.4cm^3 and the cumulative volume of brain receiving 10 Gy is 12.8cm^3. The mean conformity index for each PTV was 1.25 and the mean gradient index for each PTV was 3.39 **(B)**. 10 dynamic conformal arcs (5 duplicated non-coplanar arcs) were used to achieve the desired dose distribution **(C)**. 2.5mm MLC leaves were used to conform to the spherical metastases. Arc 1 (orange) treated 4 brain metastases along its path and Arc 2 (white) treated three on the return trajectory **(D)**.

In the case of MBM, if metastases are located close together, the dose GI (DGI) is inversely related to the distance between metastases and is affected by the accumulation of dose between metastases (41).

Although it is suggested that an ideal GI would be under 3 for a single lesion, as the PTV volume falls below a size of 0.5cm^3, larger GI values must be expected. This is shown in a theoretical analysis of the dose spillage based on PTV surface area and volume and based on clinical data (42). **Table 2** shows GIs at the higher end of the range (3.8 in group 1 and 4.0 in group 2) which reflect that in the case of SRS for MBM, the PTV is typically very small and that the GI is increased due to close proximity of the metastases. However, importantly, it also shows that plan quality was not inferior for 10-15 brain metastases as compared with 5-9 brain metastases

Whereas SRS for MBM is technically feasible with multiple isocentres, the onerous treatment planning, quality assurance and the duration of therapy with irradiation of sequential targets impeded the wider adoption of the technique. SRS for MBM has been facilitated by the development of single isocentre (SI) techniques (43, 41), which are now available as time and resource-saving automated treatment planning software for the synchronous treatment of two or more BM (44). SI-VMAT plans have been compared head to head in dosimetric studies with plans generated with multi-isocentre VMAT (45, 46), multi-isocentre Gamma knife (39), multi-isocentre robotic radiosurgery (Cyberknife, Accuray) (47, 48), and with the SI-DCA technique used in our centre (**Figure 4**) and have been deemed clinically equivalent (49). SI-VMAT plans can be optimized to improve dosimetric parameters at the expense of number of arcs and MUs (50). A series of SI-VMAT plans for more than five brain metastases generated with 5mm MLCs reported comparatively poor GIs of 5.0 -5.6 (51). According to Ohira et al, optimization of the collimator angle (52) can achieve better sparing of healthy brain, although additional jaw tracking did not yield a benefit (53). The better GIs achieved with the DCA than with VMAT stem from its development as an extension of radiosurgery with conical collimators, but come at the cost of conformity in the case of non-spherical targets (54). We therefore prefer DCA for small brain metastases but instead use a more VMAT-like solution (Cranial SRS, Elements, Brainlab) for surgical cavities or elliptical lesions at the cost of a single isocentre. A clinician blinded to treatment technique did not find any significant difference in quality between plans generated with SI-VMAT (Hyperarc, Varian) and with RayStation for Cyberknife (16), reinforcing the notion that radiosurgery is platform independent as long as a high quality is achieved. Reviews of the technical aspects of SRS for MBM are available (55, 56) and guidelines for SRS for MBM with a linac (57) and with gamma knife (58) were published in 2019.

In addition to the choice between dynamic conformal arc or VMAT planning techniques, the width of the multileaf collimator (MLC) is a further variable to be considered. Use of a 2.5mm MLC as compared with a 5mm MLC for SI-VMAT results in significantly better CIs and GIs (52), although this can be somewhat offset by the addition of more VMAT arcs to 5mm MLC plans (59). This also applies to the DCA technique and is one of the reasons why we have grouped metastases and used more than one isocentre (**Figure 4D**) to ensure coverage by the high definition 2.5mm MLCs in the central 8cm of the field, rather than by the 5mm MLCs at the periphery. A major reason underlying the use of more than one isocentre in our patients to date has been concern about increasing rotational uncertainty with increasing distance from the isocentre and risk of compromise in coverage (7). Use of a head frame for SI-VMAT to reduce rotational uncertainties has been reported (60), however frameless linac-based SRS is more usual, and inaccuracies within 1mm for targets in phantoms within 6cm of the isocentre have been documented (61). An alternative approach is to increase the PTV margin with increasing distance from the isocentre to account for any uncertainties. However, a recently published series did not find that local failure correlated with increasing distance of the target from the isocentre using an image-guided frameless approach with patient positioning in 6DoF, a uniform 1mm PTV margin and a median distance to isocentre of 4.7cm (0.2-10) (62). A third reason for using more than one isocentre in our patients is that the SI technique could not combine different fractionation schedules. As mentioned above, a DCA plan is preferred for intact metastases and an hfSRT VMAT-like plan for surgical

cavities or metastases near organs at risk such as the brainstem and chiasma. A further advantage of 2-3 SI plans is that different groups of brain metastases can be irradiated on different days, to spare normal brain through spatial fractionation (63). Whilst whole brain radiotherapy with hippocampal avoidance has been developed to reduce neurocognitive decline following the irradiation of MBM, the best way to minimise dose and thus protect the hippocampus (7) and all other functional areas of uninvolved normal brain, is through radiosurgery (64), even for more than 10 BMs (29). In one series, one third of patients had cognitive dysfunction before SRS (65) and such patients require efficient therapy without additional neurocognitive toxicity.

It is well established that the side effects of radiosurgery increase with the volume of a brain metastasis, hence the recommendation for resection or a dose reduction according to diameter (RTOG) or hypofractionation to minimise the risks of radionecrosis. In the setting of MBM, the irradiated volume will increase as the number of brain metastases increases. The metrics are being elucidated in parallel with the adoption of the technique, but current practice is to apply the $10cm^2$ V10Gy or $8cm^3$ V12Gy constraint to each metastasis as if treating a single metastasis (66). At present the dose is usually reduced according to the diameter of the largest metastasis (55) but is not known if the traditional RTOG constraints apply in the context of MBM and a review as to the possible approaches to dose prescription for adjacent metastases has recently been published (67). The low rates of radionecrosis here, according to contrast-enhanced MRI, are likely due to the small lesion size and use of hypofractionation in up to 30% of cases.

The Japanese JLGK0901 study showed no difference in cumulative complication incidence for patients with 5-10 BMs as compared with 2-4 BMs or a single BM (68) with a total cumulative volume of 15 cm^3 (11, 68). It has become widely recognized that cumulative volume is more important than the number of metastases, however there is no current consensus as to maximum safe volume and a cut-off of $25cm^3$ is routinely used by another group (58). Volume not only plays a role in toxicity but also prognosis, as a cut-off of 7 cm^3 irradiated volume was associated with a difference in overall survival of 20 vs 7 months in a series of patients with breast cancer (69). Tumor volume $>10cm^3$ but not number of BMs has been associated with worse OS (12, 70) and a PTV <7.1 cm^3 was the only significant prognostic factor for survival (64.1 vs 39.5% 1 year survival) in the series reported by Alongi et al. (30). When choosing a cumulative volume cut-off from the literature, it is important to consider the technique employed. For example, we have adopted an upper limit of 7 cm^3 cumulative GTV as, with a 1mm margin to PTV, this equates to approximately 15 cm^3, the cumulative irradiated volume recommended by Yamamoto et al. In our experience, this limit is more often reached in patients treated with SRS for fewer, larger symptomatic metastases than in patients with the numerous low volume metastases presented here. Of note, patients in group 2 had a median cumulative PTV of 7.2 cm^3 and a maximum total PTV of 11.1 cm^3.

In 2018, a survey of radiosurgery practitioners reported that 77% of respondents would offer SRS alone for 7 brain metastases under 1 cm diameter with extracranial disease control, 46% for 10 brain metastases, 26% for 15 brain metastases (71). The volume of brain metastases was deemed more important than the number and performance status was also a vital selection parameter. Nam et al. found recursive partitioning analysis (RPA) score (72) to be more important than multiplicity as did Salvetti et al, and all our patients had a Karnofsky Performance Index between 80 and 100% and an RPA of II. Regression analysis to compare groups 1 and 2 was not performed as the lack of events (0% local failure group 1, 0.02% local failure group 2, no reported toxicity) meant this analysis was unlikely to yield any data of significance. In 2021, a survey of the German Radiation Oncology Society, including but not exclusively radiosurgery practitioners, found that WBRT is still the most common modality used for 4-10 brain metastases, with SRS offered by a third according to performance status and number of metastases (73). These surveys highlight the current controversy regarding the optimal management of 5 or more BMs outside brain tumour centers with high volume of patients and the tendency of radiation oncologists to offer WBRT as compared with neurosurgeons practicing radiosurgery (58). Practice may change with the future publication of the current trials randomizing WBRT against SRS (74), however accrual is challenging as SRS is usually the patient's preference and is often available off trial.

The main strength of this series is homogeneity: patient selection by one senior radiation oncologist led to very similar patient demographics in the two groups apart from the number of brain metastases. The delineation of organs at risk was standardized by automatic segmentation and target contouring by two experienced radiation oncologists minimized interobserver variability (data not shown). Predominantly automated treatment planning by two senior physicists contributed to the high quality plans. An internal guideline was followed to ensure consistent procedure, however the plan was individualized for each patient according to the distance of the brain metastases from the isocentre, the treatment prescription, fractionation and proximity to organs at risk. The main weakness is the limited number of patients, however most series originating outside Japan are of similar size. The median overall survival of 10 months for patients with 5-9 BMs is consistent with Yamamoto et al. (12) and Nichol et al. (75), and the median survival of in our small group of patients with 10 or more BMs exceeds that reported to date.

CONCLUSION

Our data are consistent with the literature, which shows non-inferior intracranial outcomes for radiosurgery for 5 or more small volume brain metastases as compared with 1-4 brain metastases. Extracranial disease progression is the most common cause of death, even in patients with more than 10 brain metastases. Due to its high efficacy and low toxicity, SRS can be a cost-effective therapy for MBM and can be offered to patients with a good performance status and small volume intracranial disease with future therapeutic options for any extracranial disease. In view of the literature corroborating cumulative tumour volume being more prognostic than the number of metastases, prognostic scores should

continue to be developed to optimize patient selection for this therapeutic modality.

DATA AVAILABILITY STATEMENT

The raw data supporting the conclusions of this article will be made available by the authors, without undue reservation.

ETHICS STATEMENT

The studies involving human participants were reviewed and approved by Ethikkommission Nordwest- und Zentralschweiz. Written informed consent for participation was not required for this study in accordance with the national legislation and the institutional requirements.

AUTHOR CONTRIBUTIONS

All authors contributed to study conception and design. Material preparation, data collection and analysis were performed by SR, NL, SA, TL, and OR. The first draft of the manuscript was written by SR and all authors commented on previous versions of the manuscript. All authors read and approved the final manuscript.

REFERENCES

1. Patchell RA, Tibbs PA, Walsh JW, Dempsey RJ, Maruyama Y, Kryscio RJ, et al. A Randomized Trial of Surgery in the Treatment of Single Metastases to the Brain. *N Engl J Med* (1990) 322(8):494–500. doi: 10.1056/NEJM199002223220802
2. Mulvenna P, Nankivell M, Barton R, Faivre-Finn C, Wilson P, McColl E, et al. Dexamethasone and Supportive Care With or Without Whole Brain Radiotherapy in Treating Patients With Non-Small Cell Lung Cancer With Brain Metastases Unsuitable for Resection or Stereotactic Radiotherapy (QUARTZ): Results From a Phase 3, Non-Inferiority, Randomised Trial. *Lancet* (2016) 388(10055):2004–14. doi: 10.1016/S0140-6736(16)30825-X
3. Amsbaugh MJ, Yusuf MB, Gaskins J, Dragun AE, Dunlap N, Guan T, et al. A Dose-Volume Response Model for Brain Metastases Treated With Frameless Single-Fraction Robotic Radiosurgery: Seeking to Better Predict Response to Treatment. *Technol Cancer Res Treat* (2017) 16(3):344–51. doi: 10.1177/1533034616685025
4. Xue J, Kubicek GJ, Grimm J, LaCouture T, Chen Y, Goldman HW, et al. Biological Implications of Whole-Brain Radiotherapy Versus Stereotactic Radiosurgery of Multiple Brain Metastases. *J Neurosurg* (2014) 121 (Suppl):60–8. doi: 10.3171/2014.7.GKS141229
5. Park SH, Hwang SK, Kang DH, Lee SH, Park J, Hwang JH, et al. Gamma Knife Radiosurgery for Multiple Brain Metastases From Lung Cancer. *J Clin Neurosci* (2009) 16(5):626–9. doi: 10.1016/j.jocn.2008.08.003
6. El Shafie RA, Celik A, Weber D, Schmitt D, Lang K, Konig L, et al. A Matched-Pair Analysis Comparing Stereotactic Radiosurgery With Whole-Brain Radiotherapy for Patients With Multiple Brain Metastases. *J Neurooncol* (2020) 147(3):607–18. doi: 10.1007/s11060-020-03447-2
7. Robin TP, Camidge DR, Stuhr K, Nath SK, Breeze RE, Pacheco JM, et al. Excellent Outcomes With Radiosurgery for Multiple Brain Metastases in ALK and EGFR Driven Non-Small Cell Lung Cancer. *J Thorac Oncol* (2018) 13 (5):715–20. doi: 10.1016/j.jtho.2017.12.006
8. Guidelines, N.C.P. *Central Nervous System Cancers V2.2021* (2021). Available at: https://www.nccn.org/login?ReturnURL=https://www.nccn.org/professionals/physician_gls/pdf/cns.pdf.
9. Khalsa SS, Chinn M, Krucoff M, Sherman JH. The Role of Stereotactic Radiosurgery for Multiple Brain Metastases in Stable Systemic Disease: A Review of the Literature. *Acta Neurochir (Wien)* (2013) 155(7):1321–7; discussion 1327-8. doi: 10.1007/s00701-013-1701-5
10. Yamamoto M, Ide M, Nishio S, Urakawa Y. Gamma Knife Radiosurgery for Numerous Brain Metastases: Is This a Safe Treatment? *Int J Radiat Oncol Biol Phys* (2002) 53(5):1279–83. doi: 10.1016/S0360-3016(02)02855-9
11. Yamamoto M, Kawabe T, Sato Y, Higuchi Y, Nariai T, Watanabe S, et al. Stereotactic Radiosurgery for Patients With Multiple Brain Metastases: A Case-Matched Study Comparing Treatment Results for Patients With 2-9 Versus 10 or More Tumors. *J Neurosurg* (2014) 121(Suppl):16–25. doi: 10.3171/2014.8.GKS141421
12. Yamamoto M, Higuchi Y, Sato Y, Aiyama H, Kasuya H, Barfod BE, et al. Stereotactic Radiosurgery for Patients With 10 or More Brain Metastases. *Prog Neurol Surg* (2019) 34:110–24. doi: 10.1159/000493056
13. Kraft J, Zindler J, Minniti G, Guckenberger M, Andratschke N. Stereotactic Radiosurgery for Multiple Brain Metastases. *Curr Treat Options Neurol* (2019) 21(2):6. doi: 10.1007/s11940-019-0548-3
14. Thrower SL, Al Feghali KA, Luo D, Paddick I, Hou P, Briere T, et al. The Effect of Slice Thickness on Contours of Brain Metastases for Stereotactic Radiosurgery. *Adv Radiat Oncol* (2021) 6(4):100708. doi: 10.1016/j.adro.2021.100708
15. Hazard LJ, Wang B, Skidmore TB, Chern SS, Salter BJ, Jensen RL, et al. Conformity of LINAC-Based Stereotactic Radiosurgery Using Dynamic Conformal Arcs and Micro-Multileaf Collimator. *Int J Radiat Oncol Biol Phys* (2009) 73(2):562–70. doi: 10.1016/j.ijrobp.2008.04.026
16. Kadoya N, Abe Y, Kajikawa T, Ito K, Yamamoto T, Umezawa R, et al. Automated Noncoplanar Treatment Planning Strategy in Stereotactic Radiosurgery of Multiple Cranial Metastases: HyperArc and CyberKnife Dose Distributions. *Med Dosim* (2019) 44(4):394–400. doi: 10.1016/j.meddos.2019.02.004
17. Bhatnagar AK, Flickinger JC, Kondziolka D, Lunsford LD. Stereotactic Radiosurgery for Four or More Intracranial Metastases. *Int J Radiat Oncol Biol Phys* (2006) 64(3):898–903. doi: 10.1016/j.ijrobp.2005.08.035
18. Kim CH, Im YS, Nam DH, Park K, Kim JH, Lee JI, et al. Gamma Knife Radiosurgery for Ten or More Brain Metastases. *J Korean Neurosurg Soc* (2008) 44(6):358–63. doi: 10.3340/jkns.2008.44.6.358
19. Chang WS, Kim HY, Chang JW, Park YG, Chang JH. Analysis of Radiosurgical Results in Patients With Brain Metastases According to the Number of Brain Lesions: Is Stereotactic Radiosurgery Effective for Multiple Brain Metastases? *J Neurosurg* (2010) 113 (Suppl):73–8. doi: 10.3171/2010.8.GKS10994
20. Lee CK, Lee SR, Cho JM, Yang KA, Kim SH. Therapeutic Effect of Gamma Knife Radiosurgery for Multiple Brain Metastases. *J Korean Neurosurg Soc* (2011) 50(3):179–84. doi: 10.3340/jkns.2011.50.3.179
21. Grandhi R, Kondziolka D, Panczykowski D, Monaco EA 3rd, Kano Niranjan HA. Stereotactic Radiosurgery Using the Leksell Gamma Knife Perfexion Unit in the Management of Patients With 10 or More Brain Metastases. *J Neurosurg* (2012) 117(2):237–45. doi: 10.3171/2012.4.JNS11870
22. Mohammadi AM, Recinos PF, Barnett GH, Weil RJ, Vogelbaum MA, Chao ST, et al. Role of Gamma Knife Surgery in Patients With 5 or More Brain Metastases. *J Neurosurg* (2012) 117(Suppl):5–12. doi: 10.3171/2012.8.GKS12983
23. Rava P, Leonard K, Sioshansi S, Curran B, Wazer DE, Cosgrove GR, et al. Survival Among Patients With 10 or More Brain Metastases Treated With Stereotactic Radiosurgery. *J Neurosurg* (2013) 119(2):457–62. doi: 10.3171/2013.4.JNS121751
24. Salvetti DJ, Nagaraja TG, McNeill IT, Xu Z, Sheehan J. Gamma Knife Surgery for the Treatment of 5 to 15 Metastases to the Brain: Clinical Article. *J Neurosurg* (2013) 118(6):1250–7. doi: 10.3171/2013.2.JNS121213

25. Frakes JM, Figura NB, Ahmed KA, Juan TH, Patel N, Latifi K, et al. Potential Role for LINAC-Based Stereotactic Radiosurgery for the Treatment of 5 or More Radioresistant Melanoma Brain Metastases. *J Neurosurg* (2015) 123 (5):1261–7. doi: 10.3171/2014.12.JNS141919
26. Greto D, Scoccianti S, Compagnucci A, Arilli C, Casati M, Francolini G, et al. Gamma Knife Radiosurgery in the Management of Single and Multiple Brain Metastases. *Clin Neurol Neurosurg* (2016) 141:43–7. doi: 10.1016/j.clineuro.2015.12.009
27. Knoll MA, Oermann EK, Yang AI, Paydar I, Steinberger J, Collins B, et al. Survival of Patients With Multiple Intracranial Metastases Treated With Stereotactic Radiosurgery: Does the Number of Tumors Matter? *Am J Clin Oncol* (2018) 41(5):425–31. doi: 10.1097/COC.0000000000000299
28. Hamel-Perreault E, Mathieu D, Masson-Cote L. Factors Influencing the Outcome of Stereotactic Radiosurgery in Patients With Five or More Brain Metastases. *Curr Oncol* (2019) 26(1):e64–9. doi: 10.3747/co.25.4244
29. Susko MS, Garcia MA, Ma L, Nakamura JL, Raleigh DR, Fogh S, et al. Stereotactic Radiosurgery to More Than 10 Brain Metastases: Evidence to Support the Role of Radiosurgery for Ideal Hippocampal Sparing in the Treatment of Multiple Brain Metastases. *World Neurosurg* (2020) 135:e174-e180. doi: 10.1016/j.wneu.2019.11.089
30. Alongi F, Nicosia L, Figlia V, Giaj-Levra N, Cuccia F, Mazzola R, et al. Long-Term Disease Outcome and Volume-Based Decision Strategy in a Large Cohort of Multiple Brain Metastases Treated With a Mono-Isocentric Linac-Based Stereotactic Radiosurgery Technique. *Clin Transl Oncol* (2021) 23 (8):1561–70. doi: 10.1007/s12094-020-02550-0
31. Ruggieri R, Naccarato S, Mazzola R, Ricchetti F, Corradini S, Fiorentino A, et al. Linac-Based VMAT Radiosurgery for Multiple Brain Lesions: Comparison Between a Conventional Multi-Isocenter Approach and a New Dedicated Mono-Isocenter Technique. *Radiat Oncol* (2018) 13(1):38. doi: 10.1186/s13014-018-0985-2
32. Abuodeh Y, Ahmed KA, Naghavi AO, Venkat PS, Sarangkasiri S, Johnstone PAS, et al. Postoperative Stereotactic Radiosurgery Using 5-Gy X 5 Sessions in the Management of Brain Metastases. *World Neurosurg* (2016) 90:58–65. doi: 10.1016/j.wneu.2016.02.007
33. Nagtegaal SHJ, Claes A, Suijkerbuijk KPM, Schramel F, SnijdersbT. J, Verhoeff JJC, et al. Comparing Survival Predicted by the Diagnosis-Specific Graded Prognostic Assessment (DS-GPA) to Actual Survival in Patients With 1-10 Brain Metastases Treated With Stereotactic Radiosurgery. *Radiother Oncol* (2019) 138:173–9. doi: 10.1016/j.radonc.2019.06.033
34. Schaule J, Kroeze SGC, Blanck O, Stera S, Kahl KH, Roeder F, et al. Predicting Survival in Melanoma Patients Treated With Concurrent Targeted- or Immunotherapy and Stereotactic Radiotherapy: Melanoma Brain Metastases Prognostic Score. *Radiat Oncol* (2020) 15(1):135. doi: 10.1186/s13014-020-01708-y
35. Farris M, McTyre ER, Cramer CK, Hughes R, Randolph DM 2nd, Ayala-Peacock DN, et al. Brain Metastasis Velocity: A Novel Prognostic Metric Predictive of Overall Survival and Freedom From Whole-Brain Radiation Therapy After Distant Brain Failure Following Upfront Radiosurgery Alone. *Int J Radiat Oncol Biol Phys* (2017) 98(1):131–41. doi: 10.1016/j.ijrobp.2017.01.201
36. Fritz C, Borsky K, Stark LS, Tanadini-Lang S, Kroeze SGC, Krayenbuhl J, et al. Repeated Courses of Radiosurgery for New Brain Metastases to Defer Whole Brain Radiotherapy: Feasibility and Outcome With Validation of the New Prognostic Metric Brain Metastasis Velocity. *Front Oncol* (2018) 8:551. doi: 10.3389/fonc.2018.00551
37. McKay WH, McTyre ER, Okoukoni C, Alphonse-Sullivan NK, Ruiz J, Munley MT, et al. Repeat Stereotactic Radiosurgery as Salvage Therapy for Locally Recurrent Brain Metastases Previously Treated With Radiosurgery. *J Neurosurg* (2017) 127(1):148–56. doi: 10.3171/2016.5.JNS153051
38. Huang AJ, Huang KE, Page BR, Ayala-Peacock DN, Lucas JTJr., Lesser GJ, et al. Risk Factors for Leptomeningeal Carcinomatosis in Patients With Brain Metastases Who Have Previously Undergone Stereotactic Radiosurgery. *J Neurooncol* (2014) 120(1):163–9. doi: 10.1007/s11060-014-1539-6
39. McDonald D, Schuler J, Takacs I, Peng J, Jenrette J, Vanek K, et al. Comparison of Radiation Dose Spillage From the Gamma Knife Perfexion With That From Volumetric Modulated Arc Radiosurgery During Treatment of Multiple Brain Metastases in a Single Fraction. *J Neurosurg* (2014) 121 (Suppl):51–9. doi: 10.3171/2014.7.GKS141358
40. Paddick I. A Simple Scoring Ratio to Index the Conformity of Radiosurgical Treatment Plans. Technical Note. *J Neurosurg* (2000) 93(Suppl 3):219–22. doi: 10.3171/jns.2000.93.supplement_3.0219
41. Lau SK, et al. Frameless Single-Isocenter Intensity Modulated Stereotactic Radiosurgery for Simultaneous Treatment of Multiple Intracranial Metastases. *Transl Cancer Res* (2014) 3(4):383–90. doi: 10.3978/j.issn.2218-676X.2014.07.01
42. Zhao B, Jin JY, Wen N, Huang Y, Siddiqui MS, Chetty IJ, et al. Prescription to 50-75% Isodose Line may be Optimum for Linear Accelerator Based Radiosurgery of Cranial Lesions. *J Radiosurg SBRT* (2014) 3(2):139–47.
43. Huang Y, Huang KE, Page BR, Ayala-Peacock DN, Lucas JTJr., Lesser GJ, et al. Radiosurgery of Multiple Brain Metastases With Single-Isocenter Dynamic Conformal Arcs (SIDCA). *Radiother Oncol* (2014) 112(1):128–32. doi: 10.1016/j.radonc.2014.05.009
44. Parikh NR, Kundu P, Levin-Epstein R, Chang EM, Agazaryan N, Hegde JV, et al. Time-Driven Activity-Based Costing Comparison of Stereotactic Radiosurgery to Multiple Brain Lesions Using Single-Isocenter Versus Multiple-Isocenter Technique. *Int J Radiat Oncol Biol Phys* (2020) 108 (4):999–1007. doi: 10.1016/j.ijrobp.2020.06.035
45. Ohira S, Ueda Y, Akino Y, Hashimoto M, Masaoka A, Hirata T, et al. HyperArc VMAT Planning for Single and Multiple Brain Metastases Stereotactic Radiosurgery: A New Treatment Planning Approach. *Radiat Oncol* (2018) 13(1):13. doi: 10.1186/s13014-017-0948-z
46. Clark GM, Popple RA, Young PE, Fiveash JB. Feasibility of Single-Isocenter Volumetric Modulated Arc Radiosurgery for Treatment of Multiple Brain Metastases. *Int J Radiat Oncol Biol Phys* (2010) 76(1):296–302. doi: 10.1016/j.ijrobp.2009.05.029
47. Slosarek K, Bekman B, Wendykier J, Grzadziel A, Fogliata A, Cozzi L, et al. In Silico Assessment of the Dosimetric Quality of a Novel, Automated Radiation Treatment Planning Strategy for Linac-Based Radiosurgery of Multiple Brain Metastases and a Comparison With Robotic Methods. *Radiat Oncol* (2018) 13 (1):41. doi: 10.1186/s13014-018-0997-y
48. Ruggieri R, Naccarato S, Mazzola R, Ricchetti F, Corradini S, Fiorentino A, et al. Linac-Based Radiosurgery for Multiple Brain Metastases: Comparison Between Two Mono-Isocenter Techniques With Multiple non-Coplanar Arcs. *Radiother Oncol* (2019) 132:70–8. doi: 10.1016/j.radonc.2018.11.014
49. Narayanasamy G, Stathakis S, Gutierrez AN, Pappas E, Crownover R, Floyd JR2nd, et al. A Systematic Analysis of 2 Monoisocentric Techniques for the Treatment of Multiple Brain Metastases. *Technol Cancer Res Treat* (2017) 16 (5):639–44. doi: 10.1177/1533034616666998
50. Morrison J, Hood R, Yin FF, Salama JK, Kirkpatrick J, Adamson J, et al. Is a Single Isocenter Sufficient for Volumetric Modulated Arc Therapy Radiosurgery When Multiple Itracranial Metastases are Spatially Dispersed? *Med Dosim* (2016) 41(4):285–9. doi: 10.1016/j.meddos.2016.06.007
51. El Shafie RA, Tonndorf-Martini E, Schmitt D, Celik A, Weber D, Lang K, et al. Single-Isocenter Volumetric Modulated Arc Therapy vs. CyberKnife M6 for the Stereotactic Radiosurgery of Multiple Brain Metastases. *Front Oncol* (2020) 10:568. doi: 10.3389/fonc.2020.00568
52. Ohira S, Ueda Y, Kanayama N, Isono M, Inui S, Komiyama R, et al. Impact of Multileaf Collimator Width on Dose Distribution in HyperArc Fractionated Stereotactic Irradiation for Multiple (-) Brain Metastases. *Anticancer Res* (2021) 41(6):3153–9. doi: 10.21873/anticanres.15101
53. Pudsey LMM, Cutajar D, Wallace A, Saba A, Schmidt L, Bece A, et al. The Use of Collimator Angle Optimization and Jaw Tracking for VMAT-Based Single-Isocenter Multiple-Target Stereotactic Radiosurgery for Up to Six Targets in the Varian Eclipse Treatment Planning System. *J Appl Clin Med Phys* (2021) 22(9):171–82. doi: 10.1002/acm2.13360
54. Hofmaier J, Bodensohn R, Garny S, Hadi I, Fleischmann DF, Eder M, et al. Single Isocenter Stereotactic Radiosurgery for Patients With Multiple Brain Metastases: Dosimetric Comparison of VMAT and a Dedicated DCAT Planning Tool. *Radiat Oncol* (2019) 14(1):103. doi: 10.1186/s13014-019-1315-z
55. Sahgal A, Ruschin M, Ma L, Verbakel W, Larson D, Brown PD, et al. Stereotactic Radiosurgery Alone for Multiple Brain Metastases? A Review of Clinical and Technical Issues. *Neuro Oncol* (2017) 19(suppl_2):ii2–ii15. doi: 10.1093/neuonc/nox001
56. Skourou C, Hickey D, Rock L, Houston P, Sturt P, O'Sullivan S, et al. Treatment of Multiple Intracranial Metastases in Radiation Oncology: A

Contemporary Review of Available Technologies. *BJR Open* (2021) 3 (1):20210035. doi: 10.1259/bjro.20210035
57. Hartgerink D, Swinnen A, Roberge D, Nichol A, Zygmanski P, Yin FF, et al. LINAC Based Stereotactic Radiosurgery for Multiple Brain Metastases: Guidance for Clinical Implementation. *Acta Oncol* (2019) 58(9):1275–82. doi: 10.1080/0284186X.2019.1633016
58. Niranjan A, Monaco E, Flickinger J, Lunsford LD. Guidelines for Multiple Brain Metastases Radiosurgery. *Prog Neurol Surg* (2019) 34:100–9. doi: 10.1159/000493055
59. Abisheva Z, Floyd SR, Salama JK, Kirkpatrick J, Yin FF, Moravan MJ, et al. The Effect of MLC Leaf Width in Single-Isocenter Multi-Target Radiosurgery With Volumetric Modulated Arc Therapy. *J Radiosurg SBRT* (2019) 6(2):131–8.
60. Ahn KH, Yenice KM, Koshy M, Slavin KV, Aydogan B. Frame-Based Radiosurgery of Multiple Metastases Using Single-Isocenter Volumetric Modulated Arc Therapy Technique. *J Appl Clin Med Phys* (2019) 20(8):21–8. doi: 10.1002/acm2.12672
61. Calvo-Ortega JF, Pozo M, Moragues S, Casals J. Targeting Accuracy of Single-Isocenter Intensity-Modulated Radiosurgery for Multiple Lesions. *Med Dosim* (2017) 42(2):104–10. doi: 10.1016/j.meddos.2017.01.006
62. Kraft J, van Timmeren JE, Mayinger M, Frei S, Borsky K, Stark LS, et al. Distance to Isocenter is Not Associated With an Increased Risk for Local Failure in LINAC-Based Single-Isocenter SRS or SRT for Multiple Brain Metastases. *Radiother Oncol* (2021) 159:168–75. doi: 10.1016/j.radonc.2021.03.022
63. Kelly DA. Treatment of Multiple Brain Metastases With a Divide-and-Conquer Spatial Fractionation Radiosurgery Approach. *Med Hypotheses* (2014) 83(4):425–8. doi: 10.1016/j.mehy.2014.04.024
64. Brown PD, Ballman KV, Cerhan JH, Anderson SK, Carrero XW, Whitton AC, et al. Postoperative Stereotactic Radiosurgery Compared With Whole Brain Radiotherapy for Resected Metastatic Brain Disease (NCCTG N107C/CEC.3): A Multicentre, Randomised, Controlled, Phase 3 Trial. *Lancet Oncol* (2017) 18 (8):1049–60. doi: 10.1016/S1470-2045(17)30441-2
65. Schimmel WCM, Gehring K, Hanssens PEJ, Sitskoorn MM. Cognitive Functioning and Predictors Thereof in Patients With 1-10 Brain Metastases Selected for Stereotactic Radiosurgery. *J Neurooncol* (2019) 145(2):265–76. doi: 10.1007/s11060-019-03292-y
66. Milano MT, Grimm J, Niemierko A, Soltys SG, Moiseenko V, Redmond KJ, et al. Single- and Multifraction Stereotactic Radiosurgery Dose/Volume Tolerances of the Brain. *Int J Radiat Oncol Biol Phys* (2021) 110(1):68–86. doi: 10.1016/j.ijrobp.2020.08.013
67. Di Rito A, Chaikh A, Troussier I, Darmon I, Thariat J. Radiosurgery and Stereotactic Irradiation of Multiple and Contiguous Brain Metastases: A Practical Proposal of Dose Prescription Methods and a Literature Review. *Cancer Radiother* (2021) 25(1):92–102. doi: 10.1016/j.canrad.2020.06.031
68. Yamamoto M, Serizawa T, Higuchi Y, Sato Y, Kawagishi J, Yamanaka K, et al. A Multi-Institutional Prospective Observational Study of Stereotactic Radiosurgery for Patients With Multiple Brain Metastases (JLGK0901 Study Update): Irradiation-Related Complications and Long-Term Maintenance of Mini-Mental State Examination Scores. *Int J Radiat Oncol Biol Phys* (2017) 99 (1):31–40. doi: 10.1016/j.ijrobp.2017.04.037
69. Mix M, Elmarzouky R, O'Connor T, Plunkett R, Prasad D, et al. Clinical Outcomes in Patients With Brain Metastases From Breast Cancer Treated With Single-Session Radiosurgery or Whole Brain Radiotherapy. *J Neurosurg* (2016) 125(Suppl 1):26–30. doi: 10.3171/2016.7.GKS161541
70. Routman DM, Bian SX, Diao K, Liu JL, Yu C, Ye J, et al. The Growing Importance of Lesion Volume as a Prognostic Factor in Patients With Multiple Brain Metastases Treated With Stereotactic Radiosurgery. *Cancer Med* (2018) 7(3):757–64. doi: 10.1002/cam4.1352
71. Dutta SW, Sheehan JP, Niranjan A, Lunsford LD, Trifiletti DM. Evolution in the Role of Stereotactic Radiosurgery in Patients With Multiple Brain Metastases: An International Survey. *J Clin Neurosci* (2018) 57:6–12. doi: 10.1016/j.jocn.2018.08.029
72. Gaspar L, Scott C, Rotman M, Asbell S, Phillips T, Wasserman T, et al. Recursive Partitioning Analysis (RPA) of Prognostic Factors in Three Radiation Therapy Oncology Group (RTOG) Brain Metastases Trials. *Int J Radiat Oncol Biol Phys* (1997) 37(4):745–51. doi: 10.1016/S0360-3016(96)00619-0
73. Kraft J, Mayinger M ., Willmann J, Brown M, Tanadini-Lang S, Wilke L, et al. Management of Multiple Brain Metastases: A Patterns of Care Survey Within the German Society for Radiation Oncology. *J Neurooncol* (2021) 152(2):395–404. doi: 10.1007/s11060-021-03714-w
74. Soike MH, Hughes TR, Farris M, McTyre ER, Cramer CK, Bourland JD, et al. Does Stereotactic Radiosurgery Have a Role in the Management of Patients Presenting With 4 or More Brain Metastases? *Neurosurgery* (2019) 84(3):558–66. doi: 10.1093/neuros/nyy216
75. Nichol A, Ma R, Hsu F, Gondara L, Carolan H, Olson R, et al. Volumetric Radiosurgery for 1 to 10 Brain Metastases: A Multicenter, Single-Arm, Phase 2 Study. *Int J Radiat Oncol Biol Phys* (2016) 94(2):312–21. doi: 10.1016/j.ijrobp.2015.10.017

Conflict of Interest: SR has received Speaker's Honoraria from Brainlab.

The remaining authors declare that the research was conducted in the absence of any commercial or financial relationships that could be construed as a potential conflict of interest.

Publisher's Note: All claims expressed in this article are solely those of the authors and do not necessarily represent those of their affiliated organizations, or those of the publisher, the editors and the reviewers. Any product that may be evaluated in this article, or claim that may be made by its manufacturer, is not guaranteed or endorsed by the publisher.

frontiers | Frontiers in Oncology

ORIGINAL RESEARCH
published: 06 June 2022
doi: 10.3389/fonc.2022.878388

Radiomic Signatures for Predicting Receptor Status in Breast Cancer Brain Metastases

Xiao Luo[1,2†], Hui Xie[1,2†], Yadi Yang[1,2], Cheng Zhang[1,2], Yijun Zhang[1,3], Yue Li[1,4], Qiuxia Yang[1,2], Deling Wang[1,2], Yingwei Luo[1,2], Zhijun Mai[1,2], Chuanmiao Xie[1,2‡] and Shaohan Yin[1,2*‡]*

[1] State Key Laboratory of Oncology in South China, Collaborative Innovation Center for Cancer Medicine, Sun Yat-sen University Cancer Center, Guangzhou, China, [2] Department of Radiology, Sun Yat-Sen University Cancer Center, Guangzhou, China, [3] Department of Pathology, Sun Yat-Sen University Cancer Center, Guangzhou, China, [4] Department of Molecular Diagnostics, Sun Yat-Sen University Cancer Center, Guangzhou, China

OPEN ACCESS

Edited by:
David Kaul,
Charité Universitätsmedizin Berlin, Germany

Reviewed by:
Paul Windisch,
Kantonsspital Winterthur, Switzerland
Erica Shen,
University of Connecticut, United States

***Correspondence:**
Shaohan Yin
yinshh@sysucc.org.cn
Chuanmiao Xie
xiechm@sysucc.org.cn

[†]These authors have contributed equally to this work and share first authorship

[‡]These authors have contributed equally to this work and share last authorship

Specialty section:
This article was submitted to Neuro-Oncology and Neurosurgical Oncology, a section of the journal Frontiers in Oncology

Received: 18 February 2022
Accepted: 12 May 2022
Published: 06 June 2022

Citation:
Luo X, Xie H, Yang Y, Zhang C, Zhang Y, Li Y, Yang Q, Wang D, Luo Y, Mai Z, Xie C and Yin S (2022) Radiomic Signatures for Predicting Receptor Status in Breast Cancer Brain Metastases. Front. Oncol. 12:878388. doi: 10.3389/fonc.2022.878388

Backgrounds: A significant proportion of breast cancer patients showed receptor discordance between primary cancers and breast cancer brain metastases (BCBM), which significantly affected therapeutic decision-making. But it was not always feasible to obtain BCBM tissues. The aim of the present study was to analyze the receptor status of primary breast cancer and matched brain metastases and establish radiomic signatures to predict the receptor status of BCBM.

Methods: The receptor status of 80 matched primary breast cancers and resected brain metastases were retrospectively analyzed. Radiomic features were extracted using preoperative brain MRI (contrast-enhanced T1-weighted imaging, T2-weighted imaging, T2 fluid-attenuated inversion recovery, and combinations of these sequences) collected from 68 patients (45 and 23 for training and test sets, respectively) with BCBM excision. Using least absolute shrinkage selection operator and logistic regression model, the machine learning-based radiomic signatures were constructed to predict the estrogen receptor (ER), progesterone receptor (PR), and human epidermal growth factor receptor 2 (HER2) status of BCBM.

Results: Discordance between the primary cancer and BCBM was found in 51.3% of patients, with 27.5%, 27.5%, and 5.0% discordance for ER, PR, and HER2, respectively. Loss of receptor expression was more common (33.8%) than gain (18.8%). The radiomic signatures built using combination sequences had the best performance in the training and test sets. The combination model yielded AUCs of 0.89, 0.88, and 0.87, classification sensitivities of 71.4%, 90%, and 87.5%, specificities of 81.2%, 76.9%, and 71.4%, and accuracies of 78.3%, 82.6%, and 82.6% for ER, PR, and HER2, respectively, in the test set.

Conclusions: Receptor conversion in BCBM was common, and radiomic signatures show potential for noninvasively predicting BCBM receptor status.

Keywords: breast neoplasms, receptor, brain neoplasms, radiomics, magnetic resonance imaging

INTRODUCTION

Breast cancer is the most prevalent cancer worldwide (1) and the second-most likely solid malignancy to spread to the brain (2). Breast cancer produces highly heterogeneous tumors that are classified into clinically relevant subtypes based on the status of the estrogen receptor (ER), progesterone receptor (PR), human epidermal growth factor receptor 2 (HER2) and Ki67. Discordance in receptor status between primary breast tumors and metastatic disease has been increasingly reported (3–9). Such transformation can significantly impact treatment strategies, responses to therapy, and patient outcomes (6, 8, 10–14). Growing evidence suggests that it is good clinical practice to biopsy distant metastases to assess receptor status whenever possible; such assessments are recommended in American Society of Clinical Oncology and the joint European Association of Neuro-Oncology – European Society for Medical Oncology guidelines (15, 16). Clinical data have shown that the incidence of breast cancer brain metastases (BCBM) is increasing due to advances in systemic therapy and central nervous system imaging (2). In patients with extracranial disease that is under effective control, the development of new-onset or progressive brain metastases poses a clinical challenge due to the difficulties in identifying BCBM genetic status or receptor expression. Radiologists can depict the distribution, number, size, and morphological characteristics of brain metastases using MRI but cannot confirm the molecular alterations. Obtaining BCBM materials by biopsy or resection may not be practical or feasible depending on the patient's performance status. Additionally, the risks of neurosurgery, sampling bias, and the fact that the procedure does not always provide an accurate account of the intrinsic intertumor and intratumor heterogeneity must be considered (3, 5, 9).These issues emphasize the need to develop an innovative approach for deriving metastasis biomarkers. Radiomics is an emerging technology that extracts high-dimensional features from images to mine the potential biological characteristics of tumors (17). Although several studies have applied radiomics to predict epidermal growth factor receptor (EGFR) or B-Raf proto-oncogene (BRAF) mutations in brain metastases (18–22), radiomic signatures associated with BCBM receptor status have not been reported.

Therefore, this study aimed to investigate receptor status in primary breast cancer and paired resected brain metastases and establish radiomic signatures to predict the ER, PR, and HER2 status of BCBM using preoperative brain MRI. We hypothesized that differential receptor expression between primary breast cancers and their brain metastases could be captured by radiomic signatures.

MATERIALS AND METHODS

Patients

This retrospective single-center analysis included patients with breast cancer who consecutively underwent brain metastasis surgical resection at the Sun Yat-sen University Cancer Center between July 12, 2013 and September 19, 2021. The inclusion criteria were patients who: (a) had a primary breast tumor confirmed by biopsy or postoperative pathology; (b) had been diagnosed with BCBM; and (c) underwent brain metastasis surgical resection. For the receptor analysis, patients who did not have complete pathology data for the matched primary breast tumor and brain metastasis were excluded. For the radiomic analysis, patients who did not have complete pathology data for the brain metastasis and brain MRI were excluded (**Figure 1**). There were no limitations on patient gender and age. Clinical data were acquired from electronic medical records. Patients who were eventually enrolled were randomly assigned to the training and test sets (2:1), and there was no overlap patient between two sets.

This study was approved by the institutional review boards (No. B2021-198-01) of our center, and informed consent was exempted.

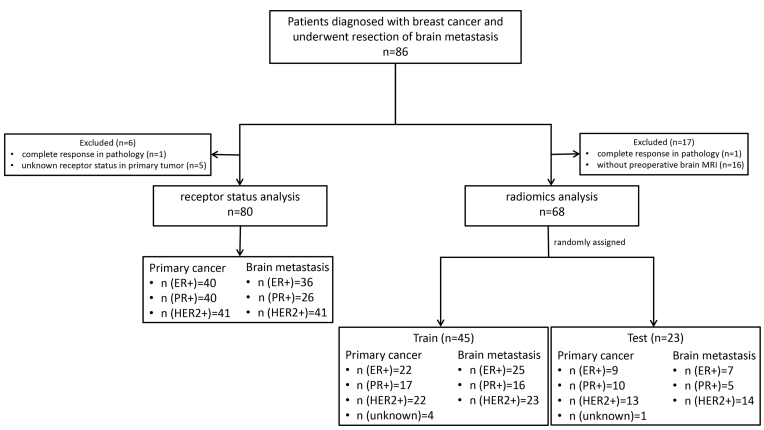

FIGURE 1 | The flowchart of participants. ER, estrogen receptor; P, progesterone receptor; HER2, human epidermal growth factor receptor 2.

ER, PR, and HER2 Status

Given that treatment selection can induce changes in receptor expression (6, 13), the ER, PR, and HER2 status of the primary tumor was determined from the pathology results after surgery for patients who did not receive neoadjuvant therapy. Puncture results were analyzed for patients who received neoadjuvant therapy or did not undergo surgery. Brain metastasis receptor status was assessed using surgical histopathology. ER and PR positive were defined as > 1% of tumor cell nuclei staining positively with any intensity. The histology and immunohistochemistry status of the breast cancer and matched metastases were analyzed by a pathologist with 8 years of experience according to the World Health Organization criteria (23). HER2 positive was defined as HER2 membrane staining score 3+ by immunohistochemistry or 2+ with fluorescence *in-situ* hybridization or HER2 amplification interpreted *via* next-generation sequencing technology by a molecular diagnostician with 4 years of experience. Hormone receptor (HR) status positive was defined as ER or PR positive.

Image Acquisition

Sixty-eight eligible patients underwent brain MRI with 1.5-T (8 patients) or 3.0-T (60 patients) scanners. Contrast-enhanced T1-weighted imaging (T1CE), T2-weighted imaging (T2WI) and T2 fluid-attenuated inversion recovery (T2-FLAIR) were collected for feature extraction. The imaging parameters are provided in the **Supplementary Materials**. The MRI examination closest to surgery was selected. For patients with multiple brain metastases, only the lesions matched with the surgical pathology were included in the radiomic analysis.

Image Segmentation and Radiomic Feature Extraction and Selection

The radiomic analysis was processed as shown in **Figure 2**. Paired brain metastases imaged in the above three sequences were manually contoured around the lesions on the axial view by a junior radiologist with four years of experience using ITK-SNAP (version 3.6; www.itksnap.org). The region of interest avoided hemorrhagic, edematous, necrotic, and cystic areas. These segmentations were reviewed by a senior neuroradiologist with 12 years of experience and refined if necessary.

Radiomic features were extracted using PyRadiomics, an open-source Python package for the extraction of radiomic features from medical images (http://www.radiomics.io/pyradiomics.html). This radiomic quantification platform enables the standardization of both image processing and feature definitions (24). The gray value discretization was conducted with a fixed bin width of 25. Because MRI scanners with different field strengths were used, the intensity range of the images was normalized between 0 and 100 as a default set by the platform. We performed resampling with a pixel spacing of (3, 3, 3). The descriptions and feature explanations can be found on the PyRadiomics website. The parameter settings for feature extraction and image preprocessing details are provided as a.py file and a.yaml file in the **Supplementary Materials**.

The interclass correlation coefficient (ICC) was used to assess the stability of each feature. Ten patients were randomly selected from the cohort and segmented again by the same radiologist for the stability evaluation. Intraobserver stability was calculated for each feature (**Supplementary Figure 1**). Stable radiomic features were defined as ICCs > 0.9. An initial selection was performed by deleting collinear strongly correlated variables detected using Pearson's correlation, for which the cutoff value was 0.95. A univariate analysis was performed for each feature, and features with $P < 0.05$ were considered for selection. Marginally significant features were selected using the least absolute shrinkage and selection operator (LASSO) and logistic regression model, which performed variable selection and regularization to enhance the prediction accuracy and interpretability of the statistical model. All features with non-zero coefficients were selected in this step. Finally, backward elimination was selectively performed to reduce the number of features included in the final set (**Supplementary Table 1**).

The radiomic model performance was internally tested using an independent test cohort. The discrimination performance of the established model was quantified using the receiver operating characteristic curve (ROC) and the area under the curve (AUC).

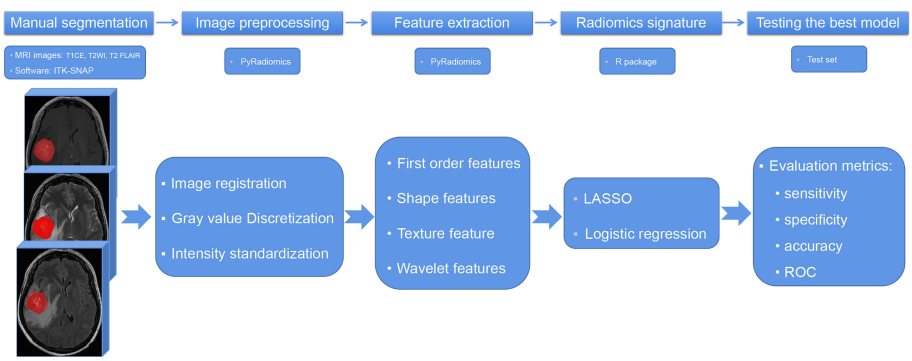

FIGURE 2 | The flowchart of radiomic analysis. T1CE, contrast-enhanced T1-weighted imaging; T2WI, T2-weighted imaging; T2 FLAIR, T2 fluid-attenuated inversion recovery; LASSO, least absolute shrinkage selection operator; ROC, receiver operating characteristic curve.

Statistical Analysis

Statistical analyses were performed using R software version 4.0.2 (http://www.r-project.org/). The frequency of receptor expression in the primary cancers and BCBM was calculated and compared using McNemar's test. Percentages of conversion were calculated for the whole receptors, and for each receptor. We used the following R packages: irr (version 0.84.1) for calculating ICCs; caret (version 6.0–86) for Pearson's correlation analyses; glmnet (version 4.0–2) for LASSO logistic regression; rms (version 6.0–1) for logistic regression; and pROC (version 1.17) for ROC and AUC. The classification performance of the radiomic model was evaluated by the AUC, sensitivity, specificity, and accuracy. All statistical tests were two-sided, and $P < 0.05$ was considered statistically significant.

RESULTS

Patient Characteristics

As shown in **Figure 1**, 86 patients with BCBM were enrolled. Six patients were excluded due to complete response revealed by postoperative pathology (n = 1) or unknown primary breast cancer receptor status (n = 5). Eighty patients with matched primary tumor and brain metastases were included in the receptor conversion analysis. For the radiomic feature extraction, 18 patients were excluded due to complete response (n = 1) or lacking preoperative brain MRI (n = 17). Thus, 68 patients were included in the BCBM receptor status prediction. The mean interval between MRI scanning and resection was 13.5 days (range, 3–34 days).

All patients were women with unilateral breast cancer who underwent a single metastasis excision. The mean age at the initial breast cancer diagnosis was 44 ± 9 years (range, 23–63 years) in both the receptor and radiomic analyses. Of the known primary tumor types, most (> 95%) were invasive ductal carcinoma (**Table 1**).

Receptor Status

The ER, PR, and HER2 conversion rates are summarized in **Figure 3A**. Among 80 paired samples, 50% (40/80), 45% (36/80), and 51% (41/80) of patients had ER-positive, PR-positive, and HER2-positive primary tumors, respectively, whereas in the corresponding BCBM these values were 45% (36/80), 33% (26/80), and 51% (41/80). The overall discordance between the primary cancer and the metastases was 51.3% (41/80), with conversion rates of 27.5% (22/80) for ER, 27.5% (22/80) for PR, and 5% (4/80) for HER2. HER2 was less likely to show discordance than ER or PR (both odds ratio [OR] = 0.139, 95% confidence interval [CI]: 0.045–0.425). The conversion from positive to negative (33.8%, 27/80) occurred significantly more often than from negative to positive (18.8%, 15/80) (OR = 2.208, 95% CI: 1.066–4.572). Patients with PR-positive had a higher rate of receptor discordance than patients with PR-negative (44.4% vs 13.6%, OR = 5.067, 95% CI: 1.715–14.969). A similar trend was seen for ER conversion, but the difference was not statistically significant (32.5% vs 22.5%, OR = 1.658, 95% CI: 0.614–4.482). No significant difference in discordance was detected between

TABLE 1 | Study patient characteristics.

Characteristics	Receptor status analysis	Radiomics analysis	
		Training	Test
Number of Patients	80	45	23
Age [a] (mean ± SD, years)	44 ± 9	44 ± 9	43 ± 9
Primary tumor grade (n, %)			
IDC I	3 (3.8)	1 (2.2)	1 (4.3)
IDC II	25 (31.3)	12 (26.7)	9 (39.1)
IDC III	28 (35.0)	18 (40.0)	5 (21.7)
Special type	3 (3.8)	1 (2.2)[b]	1 (4.3)[c]
Unknown	20 (25.0)	1 (2.2)	7 (30.4)
Interval between the MRI and the BCBM resection (mean ± SD, days)	NA	15 ± 7	11 ± 7
Excised brain metastases			
Size [d] (mean ± SD, mm)	40 ± 13	40 ± 13	45 ± 13
Location (cerebrum, n, %)	56 (70.0)	31 (68.9)	19 (82.6)
Breast cancer family history			
Yes	0	0	0
No	80 (100)	45 (100)	23 (100)
Menopausal status [e]			
Premenopausal	67 (83.8)	37 (82.2)	19 (82.6)
Postmenopausal	12 (16.2)	7 (15.6)	4 (17.3)

[a]at initial diagnosis of breast cancer; [b]mucinous carcinoma; [c]metaplastic carcinoma; [d]maximum diameter at axial section; [e]a patient underwent hysterectomy before breast cancer diagnosis included in the receptor status analysis and training group; SD, standard deviation; IDC, invasive ductal carcinoma; MRI, magnetic resonance imaging; BCBM, breast cancer brain metastases; NA, not applicable.

patients with HER2 positive and negative (4.9% vs 5.1%, OR = 0.949, 95% CI: 0.127–7.087). Subtype changes between the primary breast cancer and BCBM are illustrated in **Figure 3B**. The HR-negative/HER2-positive subtype was the most common in both primary tumors (25%, 20/80) and BCBM (33%, 26/80). The total subtype discordance was 51% (41/80). Of the discordant cases, higher conversion rates were observed in patients with HR-negative/HER2-positive (6%, 5/80), HR-positive/HER2-negative (6%, 5/80), and triple-positive (5%, 4/80).

Feature Selection and Radiomic Signature Construction

For each MRI sequence and receptor, we built radiomic signatures using the training set and evaluated their classification performance in the test set. We extracted 1,470 radiomic features from each sequence, comprising 14 shape features, 288 first-order features, 352 gray-level co-occurrence matrix features, 224 gray-level dependence matrix features, 256 gray-level run-length matrix features, 256 gray-level size-zone matrix features, and 80 neighboring gray-tone difference matrix features (**Supplementary Table 1**).

The number of radiomic features selected to differentiate the ER, PR, and HER2 status was reduced to nine, eight, and six, respectively, from the combination sequences to build the radiomic model. **Table 2** lists the significant features for differentiating receptor status in the combination sequence model. Most selected features for the ER and PR were from T2 FLAIR (5/9 and 3/6), and most features for HER2 were from T2WI (6/8).

Prediction Performance

Prediction performance details are provided in **Table 3** and **Figures 3C**, **4**. Overall, the combination sequences achieved the best AUC for each receptor in the training and test sets, with AUCs of 0.89, 0.88, and 0.87, classification sensitivities of 71.4%, 90%, and 87.5%, specificities of 81.2%, 76.9%, and 71.4%, and accuracies of 78.3%, 82.6%, and 82.6% in the test set for ER, PR, and HER2, respectively. However, the AUCs were not significantly different between the combination sequences and the single sequences in the test (all $P > 0.05$).

For 63 patients (41 and 22 in training and test sets, respectively) with available receptor status for matched primary breast cancer and BCBM, an overall conversion rate of 57% (36/63) was observed, with discordances of 27% (17/63) for ER, 27% (17/63) for PR, and 3% (2/63) for HER2. Overall, radiomic signatures achieved a BCBM classification accuracy of 85% in the test set (**Figure 3C**). The total discordance between breast cancer and the paired BCBM was 64% (14/22), with discordances of 32% (7/22) for ER, 25% (8/22) for PR, and 5% (1/22) for HER2. The overall classification accuracy of the radiomic model for discordant cases was 76% (11/14; 3 for ER, 7 for PR, and 1 for HER2).

DISCUSSION

In this retrospective study, we analyzed the ER, PR, and HER2 status of matched primary breast cancers and resected BCBM. The overall discordance rate between the primary cancer and the metastasis receptor status was 51.3%; the individual rates were 27.5% for ER, 27.5% for PR, and 5% for HER2. Conversion from positive to negative occurred more frequently than negative to positive, significantly so for PR. Given that this phenomenon may impact therapeutic decision-making and the barriers to BCBM material collection in clinical practice, we developed radiomic signatures based on preoperative brain MRI to predict the ER, PR, and HER2 status of BCBM. Integrative radiomic features predicted BCBM receptor status with AUCs of 0.89, 0.88, and 0.87 for ER, PR, and HER2, respectively. The integrative signatures correctly identified 76% of cases with discordance between the primary breast cancer and BCBM in

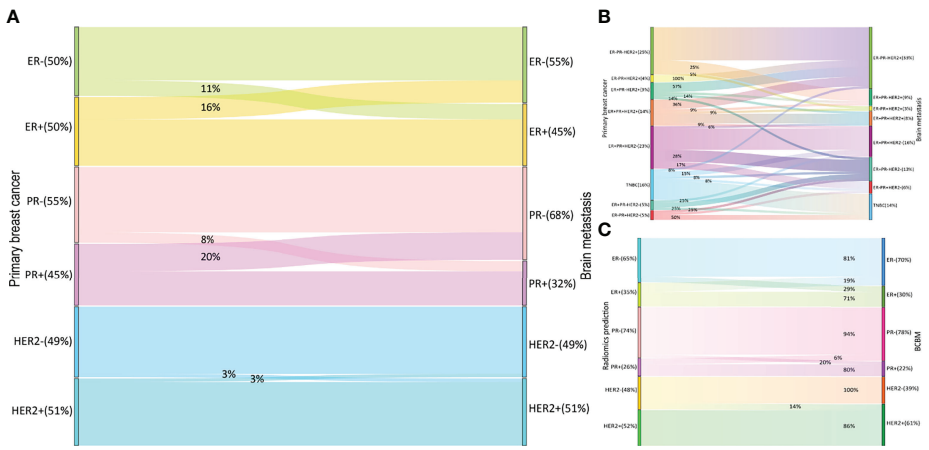

FIGURE 3 | Receptor switch in BCBM and radiomics predicting receptor status in the test set. Receptor **(A)** and subtype **(B)** switch in BCBM; the prediction results for BCBM **(C)** BCBM, breast cancer brain metastases; ER, estrogen receptor; PR, progesterone receptor; HER2, human epidermal growth factor receptor 2.

TABLE 2 | Radiomic features to differentiate receptor status in combination model.

Receptor	Sequence	Feature category	Features
ER			
	T1CE	NGTDM	Busyness
	T1CE	GLDM	Dependence variance
	T2WI	GLSZM	Small area low gray level emphasis
	T2WI	First-order statistics	Maximum
	T2 FLAIR	GLCM	Cluster prominence
	T2 FLAIR	GLCM	Inverse variance
	T2 FLAIR	GLCM	Informational measure of correlation 1
	T2 FLAIR	GLRLM	Long run high gray level emphasis
	T2 FLAIR	GLCM	Cluster shade
PR			
	T1CE	GLDM	Dependence non uniformity normalized
	T2WI	GLCM	Informational measure of correlation 1
	T2WI	NGTDM	Contrast
	T2WI	GLDM	Dependence variance
	T2WI	GLSZM	Low gray level zone emphasis
	T2WI	GLRLM	Run length non uniformity
	T2WI	GLDM	Dependence variance
	T2 FLAIR	GLCM	Informational measure of correlation 1
HER2			
	T1CE	GLDM	Large dependence high gray level emphasis
	T1CE	First-order statistics	Skewness
	T2WI	GLSZM	Zone variance
	T2 FLAIR	GLCM	Inverse variance
	T2 FLAIR	First-order statistics	Mean
	T2 FLAIR	GLDM	Dependence variance

T1CE, contrast-enhanced T1-weighted imaging; T2-FLAIR, T2 fluid-attenuated inversion recovery; T2WI, T2-weighted imaging; ER, estrogen receptor, PR, progesterone receptor, HER2, human epidermal growth factor receptor 2; NGTDM, neighboring gray tone difference matrix; GLDM, gray level dependence matrix; GLSZM, gray level size zone matrix; GLCM, gray level co-occurrence matrix; GLRLM, gray level run length matrix.

the test set. Our findings support that breast cancer is a highly heterogeneous disease, highlighting the importance of reassessing BCBM receptor status to guide systemic therapy. The radiomics could potentially provide a noninvasive imaging biomarker for evaluating BCBM receptor phenotypes.

A recent meta-analysis detected a 42.6% overall receptor discordance between the primary breast cancer and BCBM, with 17.0% for ER, 23.0% for PR, and 12.0% for HER2 (25). Another systematic review reported a 22% total receptor discordance (9). The total conversion rate in this study was higher at 51.3%, but we found a lower HER2 discordance rate of 5%. Loss of receptor expression was more common (33.8%) than gain (18.84%), which was consistent with previous reports (3, 5, 13, 25). Breast cancer subtypes impact the BCBM incidence, kinetics, and prognosis (26); however, data on BCBM subtype switch are limited. Our analysis showed a tendency toward HR-negative/HER2-positive and ER-positive/PR-negative/HER2-negative subtypes and a trend away from the HR-positive/HER2-negative and triple-positive subtypes from the primary tumor to the BCBM (**Figure 3B**). These findings differ from Alexander et al. (9), in which the trend was toward triple-negative and HER2-positive subtypes and away from ER-positive/HER2-positive subtypes.

In the case of receptor loss, patients may suffer from therapy response failure at the cost of related toxicity. Alternatively, patients may miss an opportunity to receive effective treatments due to a lack of knowledge about receptor gain in metastases. Both circumstances could impact patient survival (13). Guidelines recommend retesting receptor status for metastases (15, 16); however, given the challenges in routinely obtaining intracranial tissue, BCBM are underrepresented. Minimally invasive techniques for evaluating circulating cell-free tumor DNA in the cerebrospinal fluid have been developed (27), but there is inadequate evidence supporting the utility of this technique as a reliable alternative to biopsies for determining BCBM receptor status.

Radiomic analysis enables noninvasive assessments of tumor status and relevant molecular information. Limited studies have reported promising results for differentiating brain metastasis molecular status using radiomics (19–22). Shofty et al. applied a machine-learning method to predict BRAF mutation in brain metastases using brain MRI in 53 patients with surgical resection from melanoma, achieving a mean accuracy of 79%, mean sensitivity of 72%, and AUC of 0.78 (20). However, the study did not include an independent test set to assess the performance, which could result in overfitting. A study evaluated EGFR mutation status in 99 brain metastases from 51 patients with lung cancer, resulting in an AUC, accuracy, sensitivity, and specificity of 0.73, 78.6%, 81.3%, and 76.9%, respectively (21). However, extracting features from multiple lesions within a patient could generate overlapping features. Another study by Wang et al. extracted features from T1CE, T2-FLAIR, T2WI and diffusion-weighted imaging (DWI) to extract features from 52 patients with lung adenocarcinoma (22). The radiomic signature of T2-FLAIR yielded an excellent AUC of 0.987, a classification accuracy of 99.1%, sensitivity of

TABLE 3 | The radiomic performance of predicting receptor status in BCBM using different sequences.

Receptor	Training					Test				
	Sensitivity (%, 95% CI)	Specificity (%, 95% CI)	Accuracy (%, 95% CI)	AUC (95% CI)	*P* [a]	Sensitivity (%, 95% CI)	Specificity (%, 95% CI)	Accuracy (%, 95% CI)	AUC (95% CI)	*P* [a]
ER										
T1CE	84.0 (69.6, 98.4)	65.0 (44.1,85.9)	75.6 (74.8, 764)	0.76 (0.61, 0.90)	0.003*	71.4 (29.0,96.3)	62.5 (35.4, 84.8)	65.2 (42.7, 83.6)	0.75 (0.45, 1.0)	0.258
T2WI	84.0 (69.6, 98.4)	90.0 (76.9, 100.0)	86.7 (86.2, 87.2)	0.91 (0.83, 0.99)	0.133	100.0 (59.0, 100.0)	56.2 (29.9, 80.2)	69.6 (47.1, 86.8)	0.83 (0.66, 1.0)	0.398
T2 FLAIR	80.0 (64.3,95.7)	95.0 (85.4, 100.0)	86.7 (86.2, 87.2)	0.93 (0.85,1.0)	0.230	57.1 (18.4, 90.1)	93.80 (69.8, 99.8)	82.6 (61.2, 95.0)	0.88 (0.75, 1.0)	0.903
Combination	100.0 (100.0, 100.0)	90.0 (76.9, 1.00)	95.6 (95.4, 95.7)	0.96 (0.91, 1.0)		71.4 (29.0, 96.3)	81.2 (54.4, 96.0)	78.3 (56.3,92.5)	0.89 (0.76, 1.0)	
PR										
T1CE	81.8 (59.0, 100.0)	64.7 (48.6, 80.8)	68.9 (68.0, 69.8)	0.76 (0.60, 0.91)	0.036*	60.0 (26.2, 87.8)	76.9 (46.2, 95.0)	69.6 (47.1, 86.8)	0.77 (0.57, 0.97)	0.422
T2WI	90.9 (73.9, 100.0)	82.4 (69.5, 95.2)	84.4 (83.9, 85.0)	0.93 (0.85, 1.0)	0.850	70.0 (34.8, 93.3)	84.6 (54.6, 98.1)	78.3 (56.3, 92.5)	0.85 (0.67, 1.0)	0.259
T2 FLAIR	63.6 (35.2, 92.1)	85.3 (73.4, 97.2)	80.0 (79.3, 80.7)	0.75 (0.59, 0.91)	0.020*	40.0 (12.2, 73.8)	92.3 (64.0, 99.8)	69.6 (47.1, 86.8)	0.78 (0.59, 0.98)	0.444
Combination	100.0 (100.0, 100.0)	79.4 (65.8, 93.0)	84,4 (83.9, 85.0)	0.93 (0.86, 1.0)		90.0 (55.5, 99.7)	76.9 (46.2, 95.0)	82.6 (61.2, 95.0)	0.88 (0.72, 1.0)	
HER2										
T1CE	85.7 (70.7, 100.0)	66.7 (47.8,85.5)	75.6 (74.8, 76.4)	0.77 (0.63, 0.91)	0.014*	56.2 (29.9, 80.2)	71.4 (29.0, 96.3)	60.9 (38.5, 80.3)	0.78 (0.58, 0.97)	0.295
T2WI	66.7 (46.5, 86.8)	79.2 (62.9, 95.4)	73.3 (72.5, 74.2)	0.75 (0.61, 0.90)	0.008*	56.2 (29.9, 80.2)	100.0 (59.0, 100.0)	69.6 (47.1, 86.8)	0.80 (0.62, 0.99)	0.510
T2 FLAIR	100.0 (100.0, 100.0)	83.3 (68.4, 98.2)	91.1 (90.8, 91.5)	0.94 (0.86, 1.0)	0.563	87.5 (61.7, 98.4)	57.1 (18.4,90.1)	78.3 (56.3, 92.5)	0.79 (0.57, 1.0)	0.192
Combination	100.0 (100.0, 100.0)	87.5 (74.3, 100.0)	93.3 (93.1, 93.6)	0.96 (0.90, 1.0)		87.5 (61.7, 98.4)	71.4 (29.0, 96.3)	82.6 (61.2, 95.0)	0.87 (0.71, 1.0)	

[a]*the AUC of T1CE, T2WI and T2 FLAIR compared with the combination of that three sequences, respectively; *, statistically significant; BCBM, breast cancer brain metastases; AUC, area under the curve; CI, confidence interval; ER, estrogen receptor; PR, progesterone receptor; HER2, human epidermal growth factor receptor 2; T1CE, contrast-enhanced T1-weighted imaging; T2-FLAIR, T2 fluid-attenuated inversion recovery; T2WI, T2-weighted imaging.*

100%, and specificity of 98.0% in the validation cohort. However, the EGFR mutation status in that study were evaluated in lung cancer tissues, which may result in inauthentic performance due to discordance between primary lung cancer and brain metastases, which is reportedly up to 26.5% (21, 28).

To our knowledge, radiomics for predicting BCBM receptor status has not been published yet. As we evaluated the receptor status in resected brain materials, our model may be more accurate than those deriving receptor status from primary cancers. We found that significant radiomic features selected from multiple sequences seemed to generate a superior AUC compared with single sequence, which is in line with Park et al. (21), who reported that features selected from the integration of T1CE and diffusion tensor images improved EGFR mutation status differentiation in brain metastases from lung cancer. For single sequence applied to predict ER and HER2 status, we found that the radiomic signature of T2-FLAIR had the best performance, consistent with Wang et al. (22), who found that T2-FLAIR yielded better EGFR mutation discrimination than TICE, T2WI, and DWI. For PR, radiomic signatures extracted from T2WI had the best performance. Our results indicate that single sequence have different predictive values for different receptors. Furthermore, more second-order features than first-order statistics were included, suggesting that multiparametric high-throughput characteristics enable a more accurate assessment.

There are several limitations to this study. First, this is a retrospective single-center design, which may create selection bias. The model performance should be validated using a larger prospective multi-center dataset. Nonetheless, this is a primary study to explore the feasibility of classifying BCBM receptor expression using radiomics. In patients with limited brain metastases, local therapy such as surgical resection or radiotherapy is the gold standard, but the systemic treatment is often continued (16, 29). Using our models, this could lead to a local therapy but also, in some patients, to a change in systemic therapies because of a modification of the receptor status. Besides, there are clinical reasons for the resection which could introduce a bias. Second, the sample size is not big enough because these samples are not easy to come by in clinical practice. Third, as the prediction performance of our model is not perfect, more novel techniques such as deep learning or functional MRI imaging should be investigated to extract features in future study. However, using an open-source Python package to extract features may improve reproducibility. In addition, conventional MRI sequences have wider adaptability in clinical practices. Due to the limitations of current radiomic technology, brain metastases tissue, obtained by biopsy or excision, is still necessary if it is practical and feasible. Third, we did not assess therapeutic regimen changes and their impact on patient outcomes because that was not within the study scope.

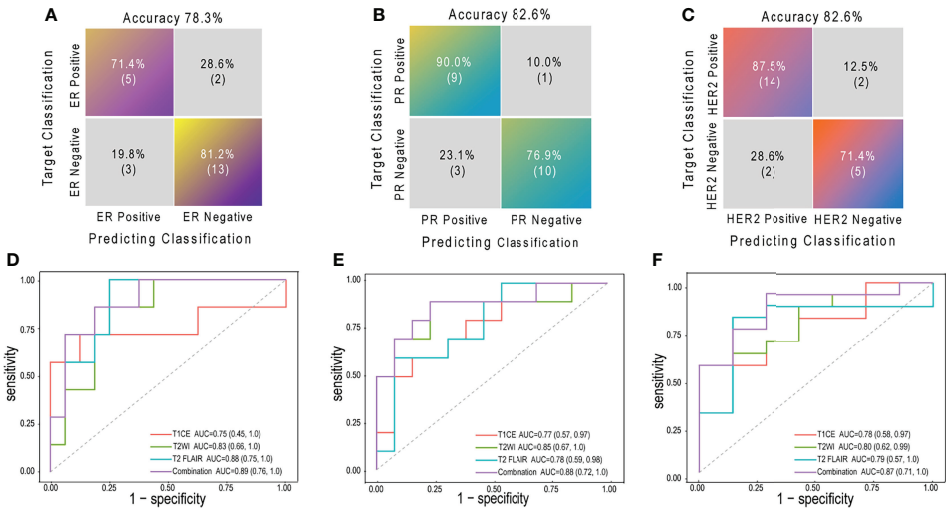

FIGURE 4 | The confusion matrices and ROCs of combination radiomic signatures in test set. Confusion matrices for ER **(A)**, PR **(B)** and HER2 **(C)**; ROCs for ER **(D)**, PR **(E)** and HER2 **(F)** ROC, receiver operating characteristic curve; ER, estrogen receptor; PR, progesterone receptor; HER2, human epidermal growth factor receptor 2; AUC, area under the curve; T1CE, contrast-enhanced T1-weighted imaging; T2WI, T2-weighted imaging; T2 FLAIR, T2 fluid-attenuated inversion recovery; combination, combination features of three sequences above.

CONCLUSION

In conclusion, receptor conversion was common in BCBM, and reappraising receptor status is necessary in clinical practice. Our multiparametric radiomic model can noninvasively predict the receptor status for BCBM, which will facilitate improved patient care and outcomes.

DATA AVAILABILITY STATEMENT

The original contributions presented in the study are included in the article/**Supplementary Material**. Further inquiries can be directed to the corresponding authors.

ETHICS STATEMENT

The studies involving human participants were reviewed and approved by the institutional review board of Sun Yat-sen University Cancer Center. Written informed consent for participation was not required for this study in accordance with the national legislation and the institutional requirements.

AUTHOR CONTRIBUTIONS

XL, XHX, CX, and SY contributed to conception and design of the study. YY, YZ, YueL, QY, and DW organized the database. CZ, YingL, and ZM performed the statistical analysis. XL and HX wrote the first draft of the manuscript. YY and SY wrote sections of the manuscript. All authors contributed to manuscript revision, read, and approved the submitted version.

SUPPLEMENTARY MATERIAL

The Supplementary Material for this article can be found online at: https://www.frontiersin.org/articles/10.3389/fonc.2022.878388/full#supplementary-material

REFERENCES

1. Sung H, Ferlay J, Siegel RL, Laversanne M, Soerjomataram I, Jemal A, et al. Global Cancer Statistics 2020: Globocan Estimates of Incidence and Mortality Worldwide for 36 Cancers in 185 Countries. *CA Cancer J Clin* (2021) 71 (3):209–49. doi: 10.3322/caac.21660
2. Achrol AS, Rennert RC, Anders C, Soffietti R, Ahluwalia MS, Nayak L, et al. Brain Metastases. *Nat Rev Dis Primers* (2019) 5(1):5. doi: 10.1038/s41572-018-0055-y
3. Yeung C, Hilton J, Clemons M, Mazzarello S, Hutton B, Haggar F, et al. Estrogen, Progesterone, and Her2/Neu Receptor Discordance Between Primary and Metastatic Breast Tumours-A Review. *Cancer Metastasis Rev* (2016) 35(3):427–37. doi: 10.1007/s10555-016-9631-3
4. Priedigkeit N, Hartmaier RJ, Chen Y, Vareslija D, Basudan A, Watters RJ, et al. Intrinsic Subtype Switching and Acquired Erbb2/Her2 Amplifications and Mutations in Breast Cancer Brain Metastases. *JAMA Oncol* (2017) 3 (5):666–71. doi: 10.1001/jamaoncol.2016.5630
5. Timmer M, Werner JM, Rohn G, Ortmann M, Blau T, Cramer C, et al. Discordance and Conversion Rates of Progesterone-, Estrogen-, and Her2/Neu-Receptor Status in Primary Breast Cancer and Brain Metastasis Mainly Triggered by Hormone Therapy. *Anticancer Res* (2017) 37(9):4859–65. doi: 10.21873/anticanres.11894

6. Pedrosa R, Mustafa DA, Soffietti R, Kros JM. Breast Cancer Brain Metastasis: Molecular Mechanisms and Directions for Treatment. *Neuro Oncol* (2018) 20 (11):1439–49. doi: 10.1093/neuonc/noy044
7. Hulsbergen AFC, Claes A, Kavouridis VK, Ansaripour A, Nogarede C, Hughes ME, et al. Subtype Switching in Breast Cancer Brain Metastases: A Multicenter Analysis. *Neuro Oncol* (2020) 22(8):1173–81. doi: 10.1093/neuonc/noaa013
8. Sperduto PW, Mesko S, Li J, Cagney D, Aizer A, Lin NU, et al. Estrogen/Progesterone Receptor and Her2 Discordance Between Primary Tumor and Brain Metastases in Breast Cancer and Its Effect on Treatment and Survival. *Neuro Oncol* (2020) 22(9):1359–67. doi: 10.1093/neuonc/noaa025
9. Morgan AJ, Giannoudis A, Palmieri C. The Genomic Landscape of Breast Cancer Brain Metastases: A Systematic Review. *Lancet Oncol* (2021) 22(1):e7–e17. doi: 10.1016/S1470-2045(20)30556-8
10. Hanley BP, Walsh SM, O'Leary DP, MacNally SP, Power C, Farrell M, et al. The Significance of Receptor Status Discordance Between Breast Cancer Primary and Brain Metastasis. *Breast J* (2018) 24(4):683–5. doi: 10.1111/tbj.13028
11. Xiao W, Li X, Yang A, Chen B, Zheng S, Zhang G, et al. Analysis of Prognostic Factors Affecting the Brain Metastases Free Survival and Survival After Brain Metastases in Breast Cancer. *Front Oncol* (2020) 10:431. doi: 10.3389/fonc.2020.00431
12. Yang Z, Li N, Li X, Lei L, Wang X. The Prognostic Impact of Hormonal Receptor and Her-2 Expression Discordance in Metastatic Breast Cancer Patients. *Onco Targets Ther* (2020) 13:853–63. doi: 10.2147/OTT.S231493
13. Yi ZB, Yu P, Zhang S, Wang WN, Han YQ, Ouyang QC, et al. Profile and Outcome of Receptor Conversion in Breast Cancer Metastases: A Nation-Wide Multicenter Epidemiological Study. *Int J Cancer* (2021) 148(3):692–701. doi: 10.1002/ijc.33227
14. Zhao W, Sun L, Dong G, Wang X, Jia Y, Tong Z. Receptor Conversion Impacts Outcomes of Different Molecular Subtypes of Primary Breast Cancer. *Ther Adv Med Oncol* (2021) 13:17588359211012982. doi: 10.1177/17588359211012982
15. Van Poznak C, Somerfield MR, Bast RC, Cristofanilli M, Goetz MP, Gonzalez-Angulo AM, et al. Use of Biomarkers to Guide Decisions on Systemic Therapy for Women With Metastatic Breast Cancer: American Society of Clinical Oncology Clinical Practice Guideline. *J Clin Oncol* (2015) 33(24):2695–704. doi: 10.1200/JCO.2015.61.1459
16. Le Rhun E, Guckenberger M, Smits M, Dummer R, Bachelot T, Sahm F, et al. Eano-Esmo Clinical Practice Guidelines for Diagnosis, Treatment and Follow-Up of Patients With Brain Metastasis From Solid Tumours. *Ann Oncol* (2021) 32(11):1332–47. doi: 10.1016/j.annonc.2021.07.016
17. Lambin P, Rios-Velazquez E, Leijenaar R, Carvalho S, van Stiphout RG, Granton P, et al. Radiomics: Extracting More Information From Medical Images Using Advanced Feature Analysis. *Eur J Cancer* (2012) 48(4):441–6. doi: 10.1016/j.ejca.2011.11.036
18. Ahn SJ, Kwon H, Yang JJ, Park M, Cha YJ, Suh SH, et al. Contrast-Enhanced T1-Weighted Image Radiomics of Brain Metastases May Predict Egfr Mutation Status in Primary Lung Cancer. *Sci Rep* (2020) 10(1):8905. doi: 10.1038/s41598-020-65470-7
19. Chen BT, Jin T, Ye N, Mambetsariev I, Daniel E, Wang T, et al. Radiomic Prediction of Mutation Status Based on Mr Imaging of Lung Cancer Brain Metastases. *Magn Reson Imaging* (2020) 69:49–56. doi: 10.1016/j.mri.2020.03.002
20. Shofty B, Artzi M, Shtrozberg S, Fanizzi C, DiMeco F, Haim O, et al. Virtual Biopsy Using Mri Radiomics for Prediction of Braf Status in Melanoma Brain Metastasis. *Sci Rep* (2020) 10(1):6623. doi: 10.1038/s41598-020-63821-y
21. Park YW, An C, Lee J, Han K, Choi D, Ahn SS, et al. Diffusion Tensor and Postcontrast T1-Weighted Imaging Radiomics to Differentiate the Epidermal Growth Factor Receptor Mutation Status of Brain Metastases From Non-Small Cell Lung Cancer. *Neuroradiology* (2021) 63(3):343–52. doi: 10.1007/s00234-020-02529-2
22. Wang G, Wang B, Wang Z, Li W, Xiu J, Liu Z, et al. Radiomics Signature of Brain Metastasis: Prediction of Egfr Mutation Status. *Eur Radiol* (2021) 31 (7):4538–47. doi: 10.1007/s00330-020-07614-x
23. WHO Classification Of Tumours Editorial Board. *Breast Tumours. 5th ed.* Lyon: IARC Press (2019).
24. van Griethuysen JJM, Fedorov A, Parmar C, Hosny A, Aucoin N, Narayan V, et al. Computational Radiomics System to Decode the Radiographic Phenotype. *Cancer Res* (2017) 77(21):e104–e7. doi: 10.1158/0008-5472.CAN-17-0339
25. Kotecha R, Tonse R, Rubens M, McDermott MW, Odia Y, Appel H, et al. Systematic Review and Meta-Analysis of Breast Cancer Brain Metastasis and Primary Tumor Receptor Expression Discordance. *Neurooncol Adv* (2021) 3 (1):vdab010. doi: 10.1093/noajnl/vdab010
26. Darlix A, Louvel G, Fraisse J, Jacot W, Brain E, Debled M, et al. Impact of Breast Cancer Molecular Subtypes on the Incidence, Kinetics and Prognosis of Central Nervous System Metastases in a Large Multicentre Real-Life Cohort. *Br J Cancer* (2019) 121(12):991–1000. doi: 10.1038/s41416-019-0619-y
27. De Mattos-Arruda L, Ng CKY, Piscuoglio S, Gonzalez-Cao M, Lim RS, De Filippo MR, et al. Genetic Heterogeneity and Actionable Mutations in Her2-Positive Primary Breast Cancers and Their Brain Metastases. *Oncotarget* (2018) 9(29):20617–30. doi: 10.18632/oncotarget.25041
28. Rau KM, Chen HK, Shiu LY, Chao TL, Lo YP, Wang CC, et al. Discordance of Mutation Statuses of Epidermal Growth Factor Receptor and K-Ras Between Primary Adenocarcinoma of Lung and Brain Metastasis. *Int J Mol Sci* (2016) 17(4):524. doi: 10.3390/ijms17040524
29. Chao ST, De Salles A, Hayashi M, Levivier M, Ma L, Martinez R, et al. Stereotactic Radiosurgery in the Management of Limited (1-4) Brain Metasteses: Systematic Review and International Stereotactic Radiosurgery Society Practice Guideline. *Neurosurgery* (2018) 83(3):345–53. doi: 10.1093/neuros/nyx522

Conflict of Interest: The authors declare that the research was conducted in the absence of any commercial or financial relationships that could be construed as a potential conflict of interest.

frontiers | Frontiers in Oncology

ORIGINAL RESEARCH
published: 10 June 2022
doi: 10.3389/fonc.2022.903851

Predictors of Lung Adenocarcinoma With Leptomeningeal Metastases: A 2022 Targeted-Therapy-Assisted molGPA Model

Milan Zhang[1†], Jiayi Tong[2†], Weifeng Ma[1], Chongliang Luo[3], Huiqin Liu[1], Yushu Jiang[1], Lingzhi Qin[1], Xiaojuan Wang[1], Lipin Yuan[1], Jiewen Zhang[1], Fuhua Peng[4], Yong Chen[2], Wei Li[1] and Ying Jiang[4*]*

[1] Department of Neurology, Henan Joint International Research Laboratory of Accurate Diagnosis, Treatment, Research and Development, Henan Provincial People's Hospital, People's Hospital of Zhengzhou University, Zhengzhou, China,
[2] Department of Biostatistics, Epidemiology and Informatics, University of Pennsylvania, Philadelphia, PA, United States,
[3] Division of Public Health Sciences, Washington University School of Medicine in St. Louis, St Louis, MO, United States,
[4] Department of Neurology, The Third Affiliated Hospital of Sun Yat-sen University, Guangzhou, China

Objective: To explore prognostic indicators of lung adenocarcinoma with leptomeningeal metastases (LM) and provide an updated graded prognostic assessment model integrated with molecular alterations (molGPA).

Methods: A cohort of 162 patients was enrolled from 202 patients with lung adenocarcinoma and LM. By randomly splitting data into the training (80%) and validation (20%) sets, the Cox regression and random survival forest methods were used on the training set to identify statistically significant variables and construct a prognostic model. The C-index of the model was calculated and compared with that of previous molGPA models.

Results: The Cox regression and random forest models both identified four variables, which included KPS, LANO neurological assessment, TKI therapy line, and controlled primary tumor, as statistically significant predictors. A novel targeted-therapy-assisted molGPA model (2022) using the above four prognostic factors was developed to predict LM of lung adenocarcinoma. The C-indices of this prognostic model in the training and validation sets were higher than those of the lung-molGPA (2017) and molGPA (2019) models.

Conclusions: The 2022 molGPA model, a substantial update of previous molGPA models with better prediction performance, may be useful in clinical decision making and stratification of future clinical trials.

Keywords: leptomeningeal metastases, lung adenocarcinoma, molGPA model, overall survival, targeted therapy

OPEN ACCESS

Edited by:
David Kaul,
Charité Universitätsmedizin Berlin, Germany

Reviewed by:
David Wasilewski,
Spanish National Cancer Research Center (CNIO), Spain
Ariane Steindl,
Medical University of Vienna, Austria

***Correspondence:**
Wei Li
liwei71@126.com
Ying Jiang
jiangy9@mail.sysu.edu.cn

†These authors have contributed equally to this work

Specialty section:
This article was submitted to Neuro-Oncology and Neurosurgical Oncology, a section of the journal Frontiers in Oncology

Received: *24 March 2022*
Accepted: *17 May 2022*
Published: *10 June 2022*

Citation:
Zhang M, Tong J, Ma W, Luo C, Liu H, Jiang Y, Qin L, Wang X, Yuan L, Zhang J, Peng F, Chen Y, Li W and Jiang Y (2022) Predictors of Lung Adenocarcinoma With Leptomeningeal Metastases: A 2022 Targeted-Therapy-Assisted molGPA Model. Front. Oncol. 12:903851. doi: 10.3389/fonc.2022.903851

INTRODUCTION

Leptomeningeal metastases (LM) refers to the seeding of tumor cells within the subarachnoid space and leptomeninges. It occurs in up to 10% of adult patients with solid tumors, especially melanoma, breast cancer, and non-small cell lung cancer (NSCLC) (1, 2). The incidence of LM as a devastating complication of NSCLC is increasing, especially in patients with targeted molecule-driven mutations (3, 4). Lung adenocarcinoma, which is the main component of NSCLC, is more likely to develop LM. Molecular targeted therapy has shown antitumor activity in central nervous system metastases, with median overall survival ranging from 1 to 3 months for historical treatments and 3 to 11 months for new treatments (4, 5). Therefore, patients with lung adenocarcinoma have a greater risk of developing sequelae of advanced diseases in the future, such as brain metastasis (BM) and LM. These trends, coupled with the wide application of magnetic resonance imaging (MRI), indicate that an increasing number of patients will be diagnosed with LM in the next few years.

Some existing studies have focused on predicting the occurrence of heterogeneous BM. The Radiation Therapy Oncology Group (RTOG) database was used to generate the recursive partitioning analysis (RPA) classes which were modified in 2012 (modified RPA) (6–8). RPA is a prognostic index that is divided into three classes based on age, Karnofsky performance status (KPS), control of primary tumor, and extracranial metastases (ECM). The graded prognostic assessment (GPA) index was developed in 2007 and revised in 2017 to form a lung-molGPA model using age, KPS, ECM, number of BM, and gene status to define four disease classes, with median survival ranging from 3.0 to 14.8 months (9–12). In 2019, another molGPA model was developed to predict LM using factors, such as KPS, ECM, and gene status (13).

In both the lung-molGPA (2017) and molGPA (2019) models, gene mutation status was identified as a significant prognostic factor (11, 12). From a clinical perspective, gene mutation status, which indicates molecular-targeted therapy, also has a significant impact on the treatment of EM and LM. However, the efficacy of third-generation targeted drugs has led to revolutionary development compared to first- or second-generation targeted therapeutic approaches (2–5, 14, 15). According to the BLOOM and AURA studies (5, 14, 15), the third-generation epidermal growth factor receptor (*EGFR*)-tyrosine kinase inhibitor (TKI) resulted in a significantly improved median overall survival (OS) of 11.0-18.8 months compared to even higher doses of first- or second-generation *EGFR* TKIs with a median OS of 3.1-6.2 months (2). The differences in efficacy between generations of targeted therapy may affect the prediction efficiency of the molGPA models. Therefore, in this study, we compared the effects of gene mutation status and targeted therapy on survival, and developed a novel 2022 lung-molGPA for the patients of lung adenocarcinoma with LM.

To the best of our knowledge, no studies have been conducted to predict the survival of lung adenocarcinoma with LM using targeted therapy; moreover, the use of machine learning methods, such as random forests, is lacking. Therefore, this study aimed to fill this research gap and study the role of targeted therapy in the prediction of lung adenocarcinoma with LM using both conventional molGPA and random forest models.

METHODS

Study Design and Samples

The study was conducted in accordance with the principles of the Declaration of Helsinki, and the protocol was approved by the Medical Ethics Committee of Henan Provincial People's Hospital (approval number: 2017-28). All study participants provided written informed consent for the research and publication.

We collected data from 202 lung adenocarcinoma patients with LM, enrolled between April 2017 and January 2022, at Henan Provincial People's Hospital, Zhengzhou, China. The inclusion criteria were as follows: (i) ≥ 18 years; (ii) diagnosis of lung adenocarcinoma confirmed by histopathology; and (iii) LM diagnosis ascertained according to the NCCN guidelines and the European Association of Neuro-Oncology-European Society for Medical Oncology (EANO-ESMO) guidelines (16). According to the Leptomeningeal Assessment in Neuro-Oncology (LANO) neurological assessment in LM (**Supplement Table 1**) (17), all patients underwent complete work up, including standardized neurological examination, brain and spine MRI, CSF analysis, during hospitalization. Patients with insufficient clinical information (n=29) or missing follow-up data (n=11) were excluded. Finally, 162 patients were included in the study cohort and randomly assigned to the training (80%, n = 130) and validation (20%, n = 32) sets (**Figure 1**).

Baseline clinicopathological characteristics of each patient were obtained from their medical records; they included age, sex, smoking status, ECM, controlled primary tumor, clinical presentations, KPS, gene profiles of *EGFR* mutation and *ALK* alteration, ThinPrep cytologic test (TCT), and brain and spine MRI. Treatments including TKI therapy, chemotherapy, bevacizumab, surgery, radiotherapy, intrathecal chemotherapy, and immune checkpoint inhibitors were included in the study. Controlled primary tumor was defined as remission or stable disease, without any clinical, radiologic, or laboratory findings suggestive of tumor progression at 2 months (6, 7, 18). The overall survival (OS) was defined as the time from diagnosis of LM to death.

Statistical Analysis

Missing values were imputed for variables with small missing proportion. Continuous variables, that is, CSF white blood cells, protein, and glucose, were transformed by taking the logarithm. Other continuous variables were categorized based on clinical reasoning and statistical methods. KPS status was divided into 3 groups: < 60 (high-risk group), 60-70 (moderate-risk group), and 80-100 (low-risk group). Age was dichotomized using a 65-year cutoff. Univariate Cox models were performed on the training set (n = 130), covering baseline characteristics, clinical symptoms, brain and spinal MRI, CSF analysis and treatment, to identify statistically significant variables. With significant variables in

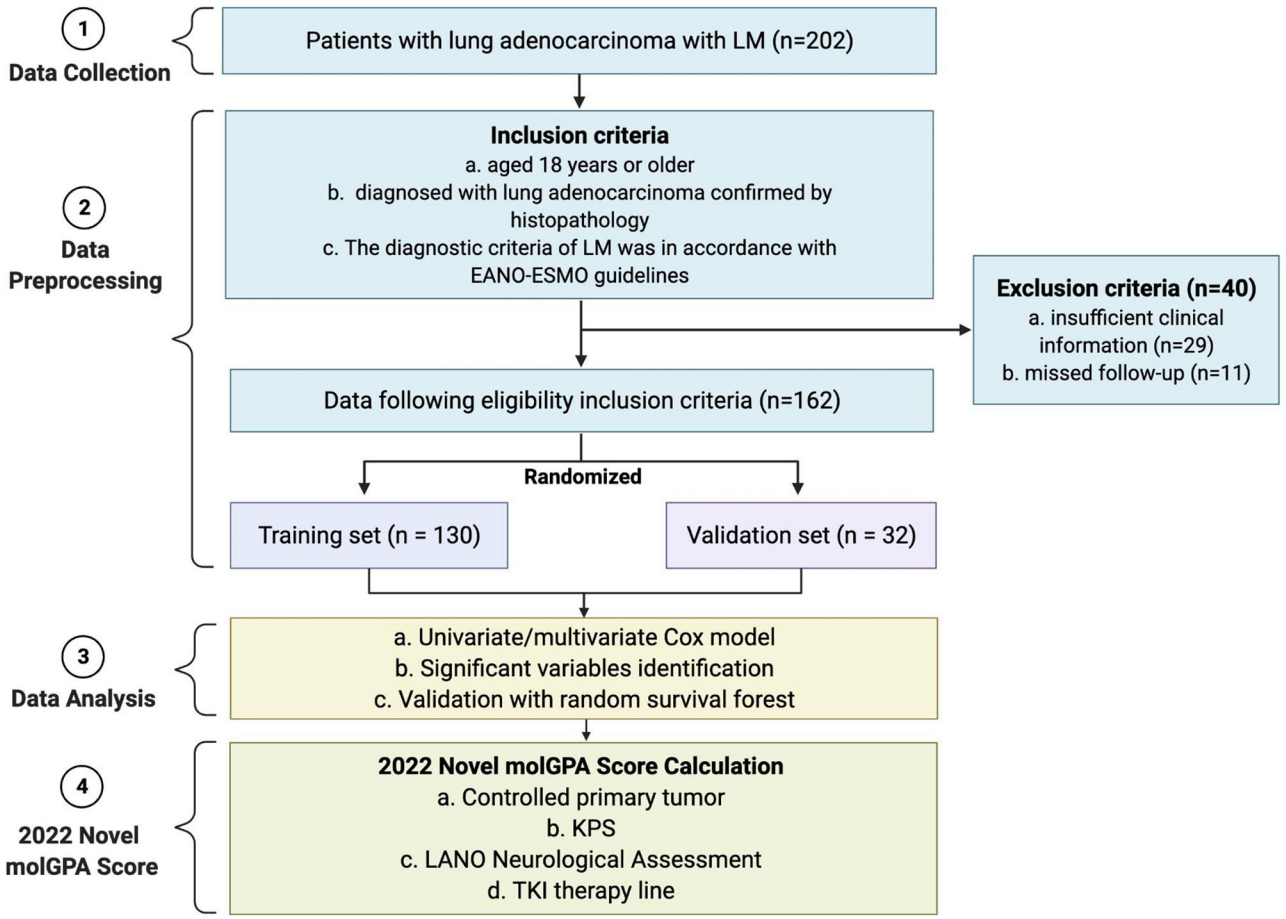

FIGURE 1 | Flow diagram of the enrollment of patients with lung adenocarcinoma with LM, and pipeline of data analysis to get the 2022 molGPA score. LM, leptomeningeal metastases; EANO-ESMO, European Association of Neuro-Oncology-European Society for Medical Oncology. KPS, Karnofsky performance status; LANO, Leptomeningeal Assessment in Neuro-Oncology; TKI, tyrosine kinase inhibitor; GPA, Graded Prognostic Assessment.

the univariate analysis, a multivariate Cox model was fitted to the training set to select significant predictors to construct the prognostic model.

We further utilized the random survival forest method to validate the selected predictors using the Cox model. In addition to the clinical prediction because of the high variance bias trade-of capability, Random survival forests (19, 20) method is also usually used to select the most important variables that are linked with the time-to-event outcome (i.e., OS). Given these advantages of random survival forests, we first utilized all variables in the model to identify those with positive importance values. With the top variables, we performed the random survival forest method again to select significant variables, and compared them with those from the Cox model. Furthermore, the C-index of the prognostic model constructed using the top variables was calculated.

We constructed a novel molGPA model (2022) using statistically significant variables. The model was then used to predict the OS of LM with lung adenocarcinoma cancer. The C-index of the prognostic model was calculated and compared with the lung-molGPA (2017, **Supplemental Table 2**) and molGPA (2019) models (**Supplemental Table 3**) by taking the average of the C-index values from the randomly split training and validation sets 100 times. Missing values were imputed for variables with small missing proportion using R package *mice* with default settings (e.g., the number of multiple imputations is 5) (21). All analyses were conducted in R software using the *mice* package (21) for multiple imputation, *survival* package (22) for Cox model and C-index, and the *randomForestSRC* package (19, 20) for random forest. The R code for analysis is available on the Github Page: https://github.com/Penncil/A-2022-Targeted-therapy-assisted-molGPA-.

RESULTS

Clinicopathological Characteristics of the Patients

The baseline clinical characteristics of patients in the training and validation cohorts are presented in **Table 1**. There were no

TABLE 1 | Demographic and clinical characteristics of the 162 lung adenocarcinoma patients with LM.

Characteristic	Patients, No. (%)		*p*-value
	Training set (n = 130)	Validation Set (n = 32)	
Age			0.30
≤65	90 (69.2)	25 (78.1)	
>65	40 (30.8)	7 (21.9)	
Sex			0.54
Male	57 (43.8)	16 (50.0)	
Female	73 (56.2)	16 (50.0)	
Smoke			0.89
No	95 (73.1)	23 (71.9)	
Yes	35 (26.9)	9 (28.1)	
Median time diagnosis to LM (median, range)	10 (0, 120)	6 (0, 100)	0.52
Clinical symptoms			
Headache	97 (74.6)	21 (65.7)	0.34
Abnormal levels of consciousness and behavior	35 (26.9)	7 (21.9)	0.55
Cognitive impairment	25 (19.2)	4 (12.5)	0.33
Epilepsy	26 (20.0)	9 (28.1)	0.36
Cranial neuropathies	41 (31.5)	12 (37.5)	0.54
Spinal neuropathies	13 (10.0)	2 (6.3)	0.46
KPS at diagnosis of LM			0.11
<60	50 (38.5)	7 (21.9)	
60-70	42 (32.3)	13 (40.6)	
80-100	38 (29.2)	12 (37.5)	
Gene status*			0.11
EGFR/ALK mutation	103 (79.2)	25 (78.1)	
Wild type	13 (10.0)	6 (18.8)	
Unknown	14 (10.8)	1 (3.1)	
LANO neurological assessment			0.44
≥6	34 (26.2)	7 (21.9)	
3-5	22 (16.9)	5 (15.6)	
≤2	74 (56.9)	20 (62.5)	
Extracranial metastases			0.52
No	16 (12.3)	4 (12.5)	
Yes	114 (87.7)	28 (87.5)	
Brain metastasis			0.65
No	51 (39.2)	14 (43.8)	
Yes	79 (60.8)	18 (56.5)	
Controlled primary tumor			0.33
No	82 (63.1)	23 (71.9)	
Yes	48 (36.9)	9 (28.1)	
Thinprep cytologic test*			0.54
Positive	99 (76.2)	18 (56.2)	
Negative/Unknown	31 (23.8)	14 (43.8)	
Brain and spinal MRI*			0.46
Positive	117 (90.0)	30 (93.8)	
Negative	13 (10.0)	2 (6.2)	
TKI therapy line			0.15
≤2nd	45 (34.6)	13 (40.6)	
3rd	58 (44.6)	12 (37.5)	
Treatments before LM			
TKIs	77 (59.3)	15 (46.9)	0.22
Chemotherapy	60 (46.2)	14 (43.8)	0.81
Bevacizumab	13 (10.0)	3 (9.4)	0.92
Without treatments	37 (28.5)	16 (50.5)	0.54
Treatments for LM			
TKIs	103 (79.2)	24 (75.0)	0.40
Chemotherapy	66 (50.7)	19 (59.4)	0.39
Bevacizumab	38 (29.2)	7 (21.9)	0.12
Operation	20 (15.4)	8 (25.0)	0.26
Radiotherapy	24 (18.5)	4 (12.5)	0.39
Intrathecal chemotherapy	22 (16.9)	3 (9.4)	0.23
Immunotherapy	5 (3.8)	2 (6.3)	0.61

*LM, leptomeningeal metastases; KPS, Karnofsky performance status; EGFR, epidermal growth factor receptor; ALK, anaplastic lymphoma kinase; TKI, tyrosine kinase inhibitor; LANO, Leptomeningeal Assessment in Neuro-Oncology; ECM, extracranial metastases; BM, brain metastasis; MRI, magnetic resonance imaging. *Missing values: gene mutation status (11.1% missing), thinprep cytologic test (29.6% missing), brain and spinal MRI (2.4 % missing).*

significant differences in sex, age, smoking status, clinical symptoms, KPS, gene mutation status, LANO neurological assessment, ECM, BM, controlled primary tumor, TCT, and brain or spinal MRI between the training and validation sets. The median time from NSCLC to LM diagnosis was 10 (range: 0-120) months and 6 (range: 0-100) months in the two cohorts, respectively. Missing values of gene mutation status (11.1% missing), lumbar puncture pressure (29.6% missing), CSF white blood cells (29.6% missing), protein (29.6% missing), and glucose (29.6% missing) were imputed.

Treatment

As shown in **Table 1**, prior to LM diagnosis, 77/130 and 15/32 patients had undergone TKI therapy, 60/130 and 14/32 patients received cytotoxic chemotherapy, and 37/132 and 16/32 patients initially diagnosed with LM did not receive any treatment in the two cohorts, respectively.

EGFR/*ALK* alterations were detected in of 103/132 and of 25/32 patients in the two cohorts, respectively. Among those who received *EGFR*-TKI or *ALK*-TKI therapy after LM diagnosis, some patients (45/103 and 13/25) received first- or second-generation TKIs (gefitinib, erlotinib, icotinib, afatinib, crizotinib, alectinib, and ceritinib), while other patients (58/103 and 12/25) received third-generation TKIs (osimertinib and lorlatinib).

Survival Analysis *via* Cox Regression Model

As shown in **Table 2**, the univariate Cox proportional hazard regression models showed that age, KPS, controlled primary tumor, gene mutation status, CSF chloride, LANO neurological assessment, and TKI therapy line were significantly associated with OS (all with $p < 0.05$). There was no significant correlation between ECM, BM, MRI, and CSF white blood cells, protein

TABLE 2 | Univariate and multivariate Cox regression analysis of overall survival of the training set.

Variables	Model			
	Univariate analysis		Multivariate analysis	
	HR (95% CI)	*p* value	HR (95% CI)	*p* value
Age, year				
>65	1 [Reference]		1 [Reference]	
≤65	0.63 (0.41, 0.96)	0.03	0.96 (0.60, 1.53)	0.88
Sex				
Male	1 [Reference]			
Female	0.88 (0.59, 1.32)	0.53		
KPS				
<60 (reference level)	1 [Reference]		1 [Reference]	
60-70	0.39 (0.25, 0.63)	<0.01		
80-100	0.21 (0.12, 0.36)	<0.01	0.47 (0.22, 1.00)	<0.05
Concurrent BM				
No	1 [Reference]			
Yes	0.92 (0.61, 1.38)	0.67		
Number of BM				
	0.97 (0.88, 1.06)	0.46		
Concurrent ECM				
No	1 [Reference]			
Yes	1.26 (0.70, 2.26)	0.44		
Controlled primary tumor				
No	1 [Reference]		1 [Reference]	
Yes	0.55 (0.36, 0.84)	0.01	0.66 (0.40, 1.06)	0.09
Mutation status				
No mutation	1 [Reference]		1 [Reference]	
EGFR/ALK mutation	0.45 (0.27, 0.77)	<0.01	2.05 (0.73, 5.77)	0.26
LANO neurological assessment				
	1.13 (1.10, 1.17)	<0.01	1.12 (1.06, 1.17)	<0.01
CSF analysis				
Chloride	0.97 (0.95, 1.00)	0.05		
Thinprep cytologic test	1.00 (0.99, 1.01)	0.08		
Brain and spinal MRI				
Negative	1 [Reference]			
Positive	1.04 (0.54, 2.01)	0.91		
TKI therapy line				
No therapy	1 [Reference]			
1^{st} or 2^{nd}	0.52 (0.30, 0.90)	<0.01		
3^{rd}	0.31 (0.18, 0.54)	<0.01	0.24 (0.08, 0.71)	0.01

LM, leptomeningeal metastases; KPS, Karnofsky performance status; EGFR, epidermal growth factor receptor; ALK, anaplastic lymphoma kinase; TKI, tyrosine kinase inhibitor; LANO, Leptomeningeal Assessment in Neuro-Oncology; ECM, extracranial metastases; BM, brain metastasis; MRI, magnetic resonance imaging.

levels, glucose levels and OS (p > 0.05). With the significant variables identified by the univariate Cox model, we further fitted the multivariate Cox model and found that KPS (HR = 0.47, 95% CI [0.22, 1.00], p=0.046), LANO neurological assessment (HR = 1.12, 95% CI [1.06, 1.17], p < 0.001), and TKI therapy (HR = 0.24, 95% CI [0.08, 0.71], p = 0.01) were significantly associated with OS in patients with LM. Controlled primary tumors may be a significant factor for OS (HR = 0.66, 95% CI [0.40, 1.06], p = 0.09), with a p-value at the boundary. However, gene mutation status was not statistically significant in the multivariate Cox model (p = 0.26). Considering the correlation between gene mutation status and TKI therapy line (3, 4), we fitted the multivariate Cox model again by including the gene mutation status only (**Supplemental Table 4**). The results showed that the p-value of the gene mutation status was 0.07.

Random Survival Forest Model

A random survival forest model for predicting survival of patients with lung adenocarcinoma with LM was fitted to validate the results of the Cox model. As shown in **Figure 2**, candidate predictor variables were ranked according to their importance in terms of prognostic accuracy. Among these variables, the top four variables, which included KPS, LANO neurological assessment, TKI therapy line, and controlled primary tumor with p-values less than 0.05, were consistent with those identified by the multivariate Cox proportional hazard regression model.

Establishment and Internal Validation of the 2022 molGPA Model

By selecting statistically significant variables with the multivariate Cox and random forest models, we developed a novel molGPA model (2022) for LM of lung adenocarcinoma cancer using four parameters: controlled primary tumor, KPS, LANO neurological assessment, and TKI therapy line (**Table 3**). Factors with larger effect sizes were given a maximum score of 1.0, including KPS from 80 to 100 (HR, 0.47 vs KPS < 60), LANO neurological assessment ≤2 (HR, 1.12) and 3rd-TKI therapy line (HR, 0.42 vs no TKI therapy), with higher scores corresponding to better prognosis. The controlled primary tumor had a smaller effect size (HR, 0.66), with a maximum score of 0.5. The model had a maximum score of 3.5; the higher the score, the lower the risk was. The targeted-therapy-assisted molGPA score was calculated for each patient and categorized into three groups: molGPA 0 (group 1, high risk), 0.5-1.0 (group 2, mediate risk), and ≥ 1.5 (group 3, low risk). For all the patients, the median OS for the three subgroups was 1.01 (95% CI [0.09, 3.58]), 1.45 (95% CI [0.24, 12.09]), and 8.02 (95% CI [0.98, 38.13]) months, respectively. The Kaplan-Meier curve for predicting the OS probability of the study population is shown in **Figure 3**, which demonstrates significant separation among the three groups.

TABLE 3 | The scoring criteria of the 2022 novel molGPA.

Prognostic Factor	2022 Novel molGPA Scoring Criteria		
	0	0.5	1
Controlled primary tumor	No	Yes	NA
KPS	<60	60-70	80-100
LANO neurological assessment	≥6	3-5	≤2
TKI therapy line	No	1st and 2nd	3rd

GPA, graded prognostic assessment; KPS, Karnofsky performance status; LANO, Leptomeningeal Assessment in Neuro-Oncology; TKI, tyrosine kinase inhibitor.

Model Evaluation

The previously reported lung-molGPA model (2017) (12) and molGPA model for LM (2019) (13) were tested in all patients. The C-index was calculated among the three models by taking the average of the C-index values from 100 randomly split training and validation sets. For each split, molGPA scores and concordance values were calculated. The higher the C-index, the better the survival time predicted by the model. The concordance results are shown in **Table 4**, where the average C-index of this model on the training set was 0.710 (95% CI [0.69, 0.73]), which is 7.00% higher than that of the

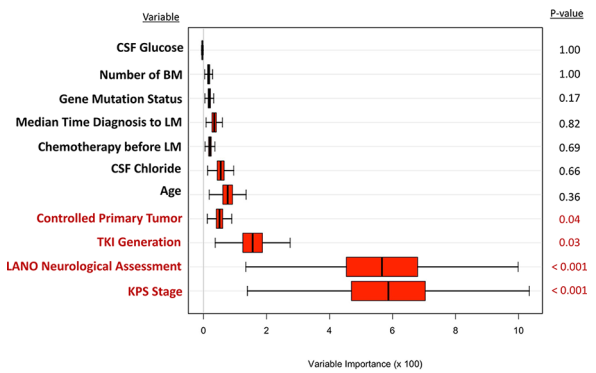

FIGURE 2 | The random forest model for predicting survival of lung adenocarcinoma with LM. LM, leptomeningeal metastases; KPS, Karnofsky performance status; LANO, Leptomeningeal Assessment in Neuro-Oncology; TKI, tyrosine kinase inhibitor; CSF, cerebrospinal fluid; GPA, Graded Prognostic Assessment.

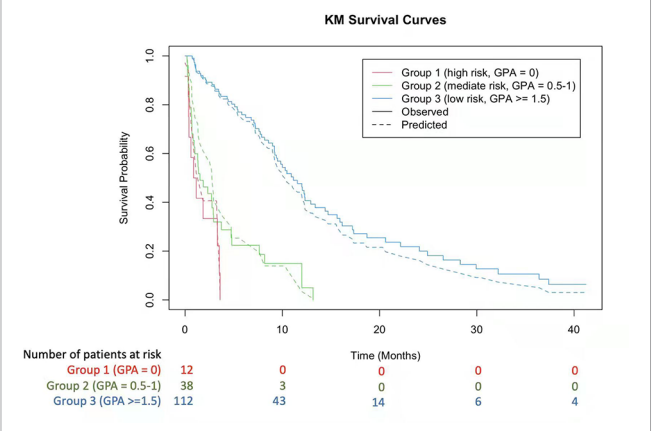

FIGURE 3 | Kaplan-Meier Curves Showing Survival using the 2022 molGPA for lung adenocarcinoma with LM. GPA, Graded Prognostic Assessment.

TABLE 4 | Concordance results of three GPA models.

Models	Training set (95% CI)	Validation Set (95% CI)
Lung-molGPA (2017)	0.66 (0.64, 0.69)	0.66 (0.56, 0.76)
MolGPA for LM (2019)	0.67 (0.65, 0.70)	0.67 (0.58, 0.77)
Novel molGPA (2022)	0.71 (0.69, 0.73)	0.71 (0.63,0.80)

LM, leptomeningeal metastases; GPA, graded prognostic assessment.

lung-molGPA (2017) and 5.5% higher than that of molGPA (2019) models. The C-index of the model on the validation set was 0.714 (95% CI [0.63, 0.80]), which was 8.3% higher than that of the lung-molGPA (2017) and 5.9% higher than that of the molGPA (2019) models.

We also calculated the C-indices of the random survival-forest-derived prognostic model. The C-index for the training set (80% of the cohort) was 0.722 (95% CI [0.69, 0.74]), and 0.714 (95% CI [0.60, 0.84]) for the validation set (20% of the cohort). The C-index of the training set was slightly larger (1.7%) than that of the Cox-based prognostic model. This is because the prognostic model with the random survival forest method included all variables listed in **Figure 2** rather than only the top four variables. The C-indices of the validation set of these two prognostic models (i.e., Cox-based and random-survival-forest-based) were the same (i.e., C-index = 0.714).

DISCUSSION

To the best of our knowledge, this is the first attempt to construct a 2022 targeted-therapy-assisted molGPA for LM of lung adenocarcinoma using a multivariate Cox proportional hazard regression model and the random survival forest method. The molGPA model considered the following four variables: controlled primary tumor, KPS, LANO neurological assessment, and TKI therapy line. According to the molGPA model scores, patients were divided into three groups: 0 for high-risk, 0.5-1.0 for immediate high-risk, and ≥ 1.5 for low-risk. In both the training and validation sets, patients with an LM molGPA score ≥ 1.5 (low risk) were more likely to have a better OS than the other two groups. The C-index values of the proposed prognostic model for the training and validation sets were higher than those of the lung-molGPA (2017) and molGPA (2019) models (12, 13).

Our 2022 target-therapy-assisted molGPA for LM has several advantages. First, TKI therapy was used instead of gene mutations. The recent revolution in the treatment of patients with prognostic biomarkers has resulted in significant improvements in survival outcomes. As earlier mentioned, molecular markers were included as important factors in the lung-molGPA (2017) and molGPA (2019) models, and had been validated by several studies for its prognostic value in real-world cohorts (12, 13, 23, 24). However, in this study, gene mutation status was not statistically significant in the multivariate Cox model. Considering the correlation between gene mutation status and TKI therapy line, we fitted the multivariate Cox model again by including the gene mutation status only (**Supplemental Table 4**). The results showed a boundary p-value = 0.07 for the gene mutation status was 0.07, which suggested the possible prognostic value of mutated status in real-life cohorts. We further found that the TKI therapy line was a significant positive prognostic factor for LM, identified by the multivariate Cox and random forest models. The efficacy of first-generation *EGFR*-TKIs for *EGFR*+ NSCLC remains poor because of low CSF penetration (25, 26). Although second-generation *EGFR*-TKIs, such as afatinib, can partially penetrate the blood-brain barrier, they exhibit no obvious advantages as treatment for LM (27). Osimertinib, an irreversible third-generation *EGFR* TKI, is highly effective in both untreated and previously treated patients with *EGFR*-mutant NSCLC, according to several encouraging international clinical trials (13–15, 28). For *ALK*+ NSCLC, lorlatinib is a novel, highly potent, brain-penetrant, third-generation *ALK* TKI with broad-spectrum potency against most known resistance mutations that can develop during treatment with existing first- and second-generation *ALK* TKIs; its efficacy is significant in BM and LM (29). Guttmann DM (30) also proposed that lung-molGPA is the critical first step in accurately defining the prognosis of patients with gene mutations; however, it also highlights the need for a prognostic index incorporating the utilization and timing of targeted therapy. Therefore, we considered that the TKI therapy line could be used as a significant positive prognostic factor in the prediction of LM.

The second advantage of our proposed molGPA is the use of the LANO assessment, a significant factor commonly used in clinical practice, which has never been considered by other prediction models. The LANO scorecard was formed by the Response Assessment in Neuro-Oncology (RANO) Leptomeningeal Metastasis Working Group, an international multidisciplinary group with the goal of improving response criteria and defining endpoints for neuro-oncology trials (17, 31). Although the LANO neurological assessment in LM has not yet been validated, the LANO scorecard generated a proposal for the response assessment in LM and has been widely used in international randomized clinical trials, including the BLOOM and AURA studies (5, 14, 15, 31, 32). Patients with LM from lung adenocarcinoma are treated in different departments, including neurology, oncology, and respiratory medicine. The LANO assessment (**Supplemental Table 1**) is a standardized assessment for neurological examination in the prediction model and is easily utilized by neurologists, oncologists, nurses, and physician assistants.

Third, KPS and controlled primary tumors, two clinically important significant prognostic factors, were considered in our molGPA model. Patients with a KPS score of 80-100 had better OS than those with KPS of 60-70 and KPS < 60. KPS was significantly associated with survival and was included in all the prediction models for BM and LM (6–10, 12, 13). A controlled primary tumor, requiring the estimation of control of systemic disease, was included in the RPA and basic score for BM (BSBM) models (6, 7, 18). In the study, controlled primary tumor had a p-value of 0.09 in the multivariate Cox model while a boundary p-value between 0.05 and 0.1 indicates weak evidence or a trend (33, 34). On the other hand, it was confirmed that in the full set data using random forest model, controlled primary tumor is significant with p=0.04. Because of

the above two reasons, we considered controlled primary tumor as a significant factor and incorporated it into the proposed 2022 molGPA model. The controlled primary tumor was assigned a maximum of 0.5, based on its HR and statistical significance in the molGPA model for LM. Extracranial metastases were included in the Lung-molGPA (2017) and molGPA (2019) models (12, 13). However, in this study, extracranial metastases showed no statistical significance in Cox proportional hazard regression model and random forest analysis, which may be related to sample bias, requiring further analysis and verification of a larger sample of patients.

Our study had several limitations. First, it was a retrospective study from a single center and single ethnic population, which led to incompleteness of some variables. For example, forty-eight patients did not undergo lumbar puncture and had no available information on variables such as protein and white blood cells. However, the sensitivity analysis showed that excluding variables with missing data did not change our conclusions. Second, third-generation TKIs contain different *EGFR*- and *ALK-related* drugs, which may affect the prognostic effect of the TKI therapy line. Third, this study evaluated only lung cancer, not other solid cancers, such as melanoma and breast cancer, which are also common in LM. We intend to validate the 2022 molGPA model for LM with lung cancer and extend the model to other solid tumors in the further study.

CONCLUSIONS

We developed a novel targeted-therapy-assisted 2022 molGPA model for predicting LM in lung adenocarcinoma by incorporating a TKI therapy line in addition to a controlled primary tumor, KPS, and LANO neurological assessment. The 2022 molGPA model has a better prediction performance and is a substantial update of previous molGPA models (11, 12). The 2022 molGPA model provides a user-friendly tool for estimating survival of lung adenocarcinoma patients with LM and may be useful in clinical decision-making and stratification of future clinical trials.

DATA AVAILABILITY STATEMENT

The datasets presented in this study can be found in online repositories. The names of the repository/repositories and accession number(s) can be found below: The git repository of this study pertinent code is at https://github.com/Penncil/2022_molGPA.

ETHICS STATEMENT

The studies involving human participants were reviewed and approved by The medical ethics committee at the Henan Provincial People's Hospital (ethics number: 2017-28). The patients/participants provided their written informed consent to participate in this study.

AUTHOR CONTRIBUTIONS

WL, YJ, JZ, FP and YC contributed to the conception and design of this study. WM, MZ, HL, YJ, LQ, XW and LY collected and organized the data. JT, CL, YC and MZ analyzed the data. MZ, JT, YJ, CL and WL drafted the manuscript. All the authors read and approved the final manuscript. All authors contributed to the article and approved the submitted version.

FUNDING

This work was supported by grant to WL from the Medical Science and Technology Project of Henan Province (NO. SBGJ2018077). The funder had no role in study design, data collection and analysis, decision to publish, or preparation of the manuscript.

ACKNOWLEDGMENTS

The icons in **Figure 1** are made by Pixel perfect from www.flaticon.com. The authors thank all patients for their participation and also thank Ziguang Xu, Xinya Gao, and Yingying Shi for their excellent technical support in gene detection and CSF cytology.

SUPPLEMENTARY MATERIAL

The Supplementary Material for this article can be found online at: https://www.frontiersin.org/articles/10.3389/fonc.2022.903851/full#supplementary-material

REFERENCES

1. Le Rhun E, Preusser M, van den Bent M, Andratschke N, Weller M. How We Treat Patients With Leptomeningeal Metastases. *ESMO Open* (2019) 4: e000507. doi: 1136/esmoopen-2019-000507
2. Thakkar JP, Kumthekar P, Dixit KS, Stupp R, Lukas RV. Leptomeningeal Metastasis From Solid Tumors. *J Neurol Sci* (2020) 411:116706. doi: 10.1016/j.jns.2020.116706
3. Kuiper JL, Hendriks LE, van der Wekken AJ, de Langen AJ, Bahce I, Thunnissen E, et al. Treatment and Survival of Patients With *EGFR*-Mutated Non-Small Cell Lung Cancer and Leptomeningeal Metastasis: A Retrospective Cohort Analysis. *Lung Cancer* (2015) 89:255–61. doi: 10.1016/j.lungcan.2015.05.023
4. Cheng H, Perez-Soler R. Leptomeningeal Metastases in Non-Small-Cell Lung Cancer. *Lancet Oncol* (2018) 19:e43–55. doi: 10.1016/S1470-2045(17)30689-7

5. Yang JCH, Kim SW, Kim DW, Lee JS, Cho BC, Ahn JS, et al. Osimertinib in Patients With Epidermal Growth Factor Receptor Mutation-Positive Non-Small-Cell Lung Cancer and Leptomeningeal Metastases: The BLOOM Study. *J Clin Oncol* (2020) 38(6):538–47. doi: 10.1200/JCO.19.00457
6. Gaspar L, Scott C, Rotman M, Asbell S, Phillips T, Wasserman T, et al. Recursive Partitioning Analysis (RPA) of Prognostic Factors in Three Radiation Therapy Oncology Group (RTOG) Brain Metastases Trials. *Int J Radiat Oncol Biol Phys* (1997) 37:745–51. doi: 10.1016/S0360-3016(96)00619-0
7. Videtic GM, Adelstein DJ, Mekhail TM, Rice TW, Stevens GH, Lee SY, et al. Validation of the RTOG Recursive Partitioning Analysis (RPA) Classification for Small-Cell Lung Cancer-Only Brain Metastases. *Int J Radiat Oncol Biol Phys* (2007) 67(1):240–3. doi: 10.1016/j.ijrobp.2006.08.019
8. Yamamoto M, Kawabe T, Higuchi Y, Sato Y, Barfod BE, Kasuya H, et al. Validity of Three Recently Proposed Prognostic Grading Indexes for Breast Cancer Patients With Radiosurgically Treated Brain Metastases. *Int J Radiat Oncol Biol Phys* (2012) 84:1110–5. doi: 10.1016/j.ijrobp.2012.02.040
9. Sperduto PW, Berkey B, Gaspar LE, Mehta M, Curran W. A New Prognostic Index and Comparison to Three Other Indices for Patients With Brain Metastases: An Analysis of 1,960 Patients in the RTOG Database. *Int J Radiat Oncol Biol Phys* (2008) 70(2):510–4. doi: 10.1016/j.ijrobp.2007.06.074
10. Sperduto PW, Chao ST, Sneed PK, Luo X, Suh J, Roberge D, et al. Diagnosis-Specific Prognostic Factors, Indexes, and Treatment Outcomes for Patients With Newly Diagnosed Brain Metastases: A Multi-Institutional Analysis of 4,259 Patients. *Int J Radiat Oncol Biol Phys* (2010) 77:655–61. doi: 10.1016/j.ijrobp.2009.08.025
11. Sun CX, Li T, Zheng X, Cai JF, Meng XL, Yang HJ, et al. Recursive Partitioning Analysis Classification and Graded Prognostic Assessment for Non-Small Cell Lung Cancer Patients With Brain Metastasis: A Retrospective Cohort Study. *Chin J Cancer Res* (2011) 23:177–82. doi: 10.1007/s11670-011-0177-1
12. Sperduto PW, Yang TJ, Beal K, Pan H, Brown PD, Bangdiwala A, et al. Estimating Survival in Patients With Lung Cancer and Brain Metastases: An Update of the Graded Prognostic Assessment for Lung Cancer Using Molecular Markers (Lung-molGPA). *JAMA Oncol* (2016) 3(6):827. doi: 10.1001/jamaoncol.2016.3834
13. Yin K, Li YS, Zheng MM, Jiang BY, Li WF, Yang JJ, et al. A Molecular Graded Prognostic Assessment (molGPA) Model Specific for Estimating Survival in Lung Cancer Patients With Leptomeningeal Metastases. *Lung Cancer* (2019) 131:134–8. doi: 10.1016/j.lungcan.2019.03.015
14. Wu YL, Ahn MJ, Garassino MC, Han JY, Katakami N, Kim HR, et al. CNS Efficacy of Osimertinib in Patients With T790M-Positive Advanced Non-Small-Cell Lung Cancer: Data From a Randomized Phase III Trial (AURA3). *J Clin Oncol* (2018) 36(26):2702–9. doi: 10.1200/JCO.2018.77.9363
15. Goss G, Tsai CM, Shepherd FA, Bazhenova L, Lee JS, Chang GC, et al. Osimertinib for Pretreated *EGFR* Thr790Met-Positive Advanced Non-Small-Cell Lung Cancer (AURA2): A Multicentre, Open-Label, Single-Arm, Phase 2 Study. *Lancet Oncol* (2016) 17(12):1643–52. doi: 10.1016/S1470-2045(16)30508-3
16. Le Rhun E, Weller M, Brandsma D, Van den Bent M, de Azambuja E, Henriksson R, et al. EANO-ESMO Clinical Practice Guidelines for Diagnosis, Treatment and Follow-Up of Patients With Leptomeningeal Metastasis From Solid Tumours. *Ann Oncol* (2017) 28:iv84–99. doi: 10.1093/annonc/mdx221
17. Chamberlain M, Junck L, Soffietti R, Rudà R, Raizer J. Leptomeningeal Metastases: A RANO Proposal for Response Criteria. *Neuro-oncology* (2017) 19(4):484–92. doi: 10.1093/neuonc/now183
18. Lorenzoni J, Devriendt D, Massager N, David P, Ruíz S, Vanderlinden B, et al. Radiosurgery for Treatment of Brain Metastases: Estimation of Patient Eligibility Using Three Stratification Systems. *Int J Radiat Oncol Biol Phys* (2004) 60:218–24. doi: 10.1016/j.ijrobp.2004.02.017
19. Ishwaran H, Kogalur UB, Blackstone EH, et al. Random Survival Forests. *Ann Appl Stat* (2008) 2(3):841–60. doi: 10.1214/08-AOAS169
20. Ishwaran H, Kogalur UB. Fast Unified Random Forests for Survival, Regression, and Classification (RF-SRC), R Package Version 2.13.0. (2021).
21. Buuren SV, Groothuis-Oudshoorn K. MICE: Multivariate Imputation by Chained Equations in R. *J Stat Softw* (2011) 45(3):1–67. doi: 10.18637/jss.v045.i03
22. Therneau T. A Package for Survival Analysis in R. R Package Version 3. (2021) 2–12.
23. Steindl A, Schlieter F, Klikovits T, Leber E, Gatterbauer B, Frischer JM, et al. Prognostic Assessment in Patients With Newly Diagnosed Small Cell Lung Cancer Brain Metastases: Results From a Real-Life Cohort. *J Neurooncol* (2019) 145(1):85–95. doi: 10.1007/s11060-019-03269-x
24. Nieder C, Hintz M, Oehlke O, Bilger A, Grosu AL. Validation of the Graded Prognostic Assessment for Lung Cancer With Brain Metastases Using Molecular Markers (lung-molGPA). *Radiat Oncol* (2017) 12(1):107. doi: 10.1186/s13014-017-0844-6
25. Nosaki K, Yamanaka T, Hamada A, Shiraishi Y, Harada T, Himeji D, et al. Erlotinib for Non-Small Cell Lung Cancer With Leptomeningeal Metastases: A Phase II Study (LOGIK1101). *Oncologist* (2020) 25(12):e1869–78. doi: 10.1634/theoncologist.2020-0640
26. Togashi Y, Masago K, Masuda S, Mizuno T, Fukudo M, Ikemi Y, et al. Cerebrospinal Fluid Concentration of Gefitinib and Erlotinib in Patients With Non-Small Cell Lung Cancer. *Cancer Chemother Pharmacol* (2012) 70 (3):399–405. doi: 10.1007/s00280-012-1929-4
27. Tamiya A, Tamiya M, Nishihara T, Shiroyama T, Nakao K, Tsuji T, et al. Cerebrospinal Fluid Penetration Rate and Efficacy of Afatinib in Patients With *EGFR* Mutation-Positive Non-Small Cell Lung Cancer With Leptomeningeal Carcinomatosis: A Multicenter Prospective Study. *Anticancer Res* (2017) 37 (8):4177–82. doi: 10.21873/anticanres.11806
28. Popat S. Osimertinib as First-Line Treatment in *EGFR*-Mutated Non-Small-Cell Lung Cancer. *N Engl J Med* (2018) 378(2):192. doi: 10.1056/NEJMe1714580
29. Solomon BJ, Besse B, Bauer TM, Felip E, Soo RA, Camidge DR, et al. Lorlatinib in Patients With ALK-Positive Non-Small-Cell Lung Cancer: Results From a Global Phase 2 Study. *Lancet Oncol* (2018) 19(12):1654–67. doi: 10.1016/S1470-2045(18)30649-1
30. Guttmann DM, Berman AT. Brain Metastases in Lung Cancer With Targetable Mutations: Should We Allow Targeted Treatment in Prognostic Indices? *JAMA Oncol* (2018) 4(3):421–2. doi: 10.1001/jamaoncol.2016.7022
31. Huang RY, Wen PY. Response Assessment in Neuro-Oncology Criteria and Clinical Endpoints. *Magn Reson Imaging Clin N Am* (2016) 24(4):705–18. doi: 10.1016/j.mric.2016.06.003
32. Chamberlain M, Soffietti R, Raizer J, Rudà R, Brandsma D, Boogerd W, et al. Leptomeningeal Metastasis: A Response Assessment in Neuro-Oncology Critical Review of Endpoints and Response Criteria of Published Randomized Clinical Trials. *Neuro Oncol* (2014) 16(9):1176. doi: 10.1093/neuonc/nou089
33. Ganesh H, Cave V. P-Values, P-Values Everywhere! *New Z Vet J* (2018) 66 (2):55–6. doi: 10.1080/00480169.2018.1415604
34. Thiese MS, Ronna B, Ott U, value interpretations P. And Considerations. *J Thorac Dis* (2016) 8(9):E928. doi: 10.21037/jtd.2016.08.16

Conflict of Interest: The authors declare that the research was conducted in the absence of any commercial or financial relationships that could be construed as a potential conflict of interest.

Publisher's Note: All claims expressed in this article are solely those of the authors and do not necessarily represent those of their affiliated organizations, or those of the publisher, the editors and the reviewers. Any product that may be evaluated in this article, or claim that may be made by its manufacturer, is not guaranteed or endorsed by the publisher.

frontiers | Frontiers in Oncology

ORIGINAL RESEARCH
published: 14 July 2022
doi: 10.3389/fonc.2022.931812

Radiomic Signatures for Predicting *EGFR* Mutation Status in Lung Cancer Brain Metastases

Lie Zheng[1,2†], *Hui Xie*[1,2†], *Xiao Luo*[1,2], *Yadi Yang*[1,2], *Yijun Zhang*[1,3], *Yue Li*[1,4], *Shaohan Yin*[1,2], *Hui Li*[1,2*‡] *and Chuanmiao Xie*[1,2*‡]

[1] State Key Laboratory of Oncology in South China, Collaborative Innovation Center for Cancer Medicine, Sun Yat-sen University Cancer Center, Guangzhou, China, [2] Department of Radiology, Sun Yat-Sen University Cancer Center, Guangzhou, China, [3] Department of Pathology, Sun Yat-Sen University Cancer Center, Guangzhou, China, [4] Department of Molecular Diagnostics, Sun Yat-Sen University Cancer Center, Guangzhou, China

OPEN ACCESS

Edited by:
David Kaul,
Charité Universitätsmedizin Berlin, Germany

Reviewed by:
Duo Hong,
China Medical University, China
Lin Lu,
Columbia University, United States

***Correspondence:**
Chuanmiao Xie
xiechm@sysucc.org.cn
Hui Li
lihui@sysucc.org.cn

†These authors contributed equally to this work and share first authorship

‡These authors contributed equally to this work and share last authorship

Specialty section:
This article was submitted to Neuro-Oncology and Neurosurgical Oncology, a section of the journal Frontiers in Oncology

Received: 29 April 2022
Accepted: 17 June 2022
Published: 14 July 2022

Citation:
Zheng L, Xie H, Luo X, Yang Y, Zhang Y, Li Y, Yin S, Li H and Xie C (2022) Radiomic Signatures for Predicting EGFR Mutation Status in Lung Cancer Brain Metastases. Front. Oncol. 12:931812. doi: 10.3389/fonc.2022.931812

Background: Lung cancer is the most common primary tumor metastasizing to the brain. A significant proportion of lung cancer patients show epidermal growth factor receptor (*EGFR*) mutation status discordance between the primary cancer and the corresponding brain metastases, which can affect prognosis and therapeutic decision-making. However, it is not always feasible to obtain brain metastases samples. The aim of this study was to establish a radiomic model to predict the *EGFR* mutation status of lung cancer brain metastases.

Methods: Data from 162 patients with resected brain metastases originating from lung cancer (70 with mutant *EGFR*, 92 with wild-type *EGFR*) were retrospectively analyzed. Radiomic features were extracted using preoperative brain magnetic resonance (MR) images (contrast-enhanced T1-weighted imaging, T1CE; T2-weighted imaging, T2WI; T2 fluid-attenuated inversion recovery, T2 FLAIR; and combinations of these sequences), to establish machine learning-based models for predicting the *EGFR* status of excised brain metastases (108 metastases for training and 54 metastases for testing). The least absolute shrinkage selection operator was used to select informative features; radiomics models were built with logistic regression of the training cohort, and model performance was evaluated using an independent test set.

Results: The best-performing model was a combination of 10 features selected from multiple sequences (two from T1CE, five from T2WI, and three from T2 FLAIR) in both the training and test sets, resulting in classification area under the curve, accuracy, sensitivity, and specificity values of 0.85 and 0.81, 77.8% and 75.9%, 83.7% and 73.1%, and 73.8% and 78.6%, respectively.

Conclusions: Radiomic signatures integrating multi-sequence MR images have the potential to noninvasively predict the *EGFR* mutation status of lung cancer brain metastases.

Keywords: epidermal growth factor receptor (EGFR), lung cancer, brain neoplasms, radiomics, magnetic resonance imaging

INTRODUCTION

Lung cancer patients frequently develop brain metastases (BMs), and these patients account for 51% of all BM patients (1). Epidermal growth factor receptor (*EGFR*) mutations are detected in 10%–60% of all non-small cell lung cancer (NSCLC) patients (2), and are associated with poor survival (3). Ligand binding to EGFR leads to receptor tyrosine kinase activation and mediates cell proliferation and invasion (4). Previous studies have shown that EGFR tyrosine kinase inhibitor treatment improves survival in patients with advanced NSCLC and sensitive *EGFR* mutations (5, 6). Thus, the determination of *EGFR* mutation status is critical for prognosis and treatment.

Discordance in *EGFR* status between primary lung tumors and BMs has been increasingly reported (7–9), indicating that it is not completely accurate to determine the *EGFR* status of BMs based on the status of the primary tumor. Therefore, molecular diagnostic tests are now recommended by clinical guidelines, to determine the eligibility of patients with advanced NSCLC for targeted therapies (10, 11). However, barriers remain to defining the *EGFR* status of BMs. First, magnetic resonance imaging (MRI) is the preferred method for BM screening, diagnosis, response evaluation, and follow-up, as radiologists can use it to depict the distribution and morphological characteristics of the BMs. However, MRI cannot be used to determine the molecular status of the BM. Second, obtaining BM materials by biopsy or resection may not be feasible depending on the patient's status. Additionally, the risks of neurosurgery, sampling bias, and the fact that the procedure does not always provide an accurate account of the intrinsic intertumor and intratumor heterogeneity must be considered. These issues emphasize the need to develop an innovative approach for deriving biomarkers of metastasis. Radiomics is an emerging technology that extracts high-dimensional features from images to mine the potential biological characteristics of tumors. Studies have evaluated the relationship of radiomics features with the isocitrate dehydrogenase gene status of gliomas (12) or the *BRAF* gene status of melanoma BMs (13). Although several studies have applied radiomics to identify *EGFR* mutations in either BMs or primary lung cancers using brain MRI, the study populations were relatively small, especially for patients with *EGFR* mutations, or the *EGFR* mutation status of the BMs was determined based on the primary tumor status, rather than samples obtained from the BMs (14–23).

Therefore, the aim of this study was to establish a radiomic model *via* machine learning to predict the *EGFR* status of BMs confirmed by postoperative histopathology, using preoperative brain MRI sequences. We hypothesized that differential *EGFR* expression levels in BMs could be captured by radiomic signatures.

MATERIALS AND METHODS

Study Patients

This retrospective single-center study included patients with lung cancer who consecutively underwent BM surgical resection at Sun Yat-sen University Cancer Center from July 8, 2014, to July 6, 2021. Patients were included if they: (a) had primary lung cancer confirmed by biopsy or postoperative pathology, (b) had been diagnosed with BM, and (c) underwent surgical resection of the BM. Patients were excluded if they: (a) did not have complete pathology data for the BM, (b) did not receive an *EGFR* test for the excised BM, (c) did not undergo preoperative brain MRI, or (d) underwent brain radiotherapy during preoperative brain MRI and BM resection (**Figure 1**). There were no limitations on the number or size of the BMs. Clinical data (e.g., age, sex, and history of smoking) were acquired from the electronic medical records. This study was approved by the Institutional Review Board (No. B2021-198-01) of our center, and the requirement for informed consent was waived.

Pathological Diagnosis and *EGFR* Testing

Histopathological sections of the primary lung cancer and the corresponding metastases were reviewed and classified according to the World Health Organization criteria by a pathologist with 8 years of experience (Y.J.Z.) (24). The mutation status in exons 18 to 21 of the *EGFR* gene was assessed using amplification-refractory mutation detection system–polymerase chain reaction or next-generation sequencing technology (25). The results were interpreted by a molecular diagnostician with 5 years of experience (Y.L.).

Image Acquisition

Patients underwent brain MRI with 1.5-T or 3.0-T scanners produced by different manufacturers. Contrast-enhanced T1-weighted imaging (T1CE), T2-weighted imaging (T2WI), and T2 fluid-attenuated inversion recovery (T2-FLAIR) data were collected for feature extraction. For the T1CE sequence, the three-dimensional acquisition was routinely performed in the sagittal plane according to our department protocols. The scanner details and typical imaging parameters of the three targeted sequences are provided in the **Supplementary Material 1**. The MRI examination performed closest to brain surgery was selected. For patients with multiple BMs, only the lesions that matched both the surgical pathology and *EGFR* testing results were included in the radiomic analysis. To accurately assess the genetic status of the BMs, patients

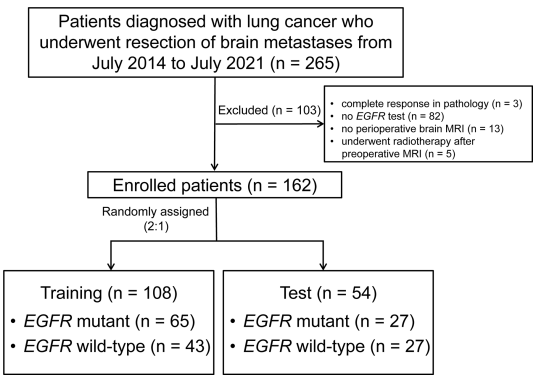

FIGURE 1 | The participant recruitment process MRI, magnetic resonance imaging; *EGFR*, epidermal growth factor receptor.

were excluded if more than two BMs were removed simultaneously and their *EGFR* testing results did not match.

Image Segmentation

Radiomic analysis was performed as shown in **Figure 2**. Paired BMs imaged in the above three sequences were manually contoured around the lesions on a slice-by-slice basis in the axial view by a junior radiologist (L.X.) with 4 years of experience using ITK-SNAP (version 3.6; www.itksnap.org). The segmented regions of interest were confirmed by a senior neuroradiologist with 12 years of experience (Y.S.H.) and refined if necessary. To accurately match postoperative *EGFR* status with BMs in MR images, only the resected lesions were segmented for feature extraction.

Radiomic Feature Extraction and Selection

Radiomic signatures were extracted using PyRadiomics, an open-source Python package for the extraction of radiomic features from medical images (http://www.radiomics.io/pyradiomics.html). This radiomic quantification platform enables the standardization of both image processing and feature definitions. Gray value discretization was performed with a fixed bin width of 25. Because MRI scanners with different field strengths were used, the intensity range of the images was normalized between 0 and 100 as a default set by the platform. We performed resampling with a pixel spacing of (3, 3, 3). The descriptions and feature explanations can be found on the PyRadiomics website. The parameter settings for image preprocessing and the feature extraction details are provided in **Supplementary Table S1**.

To obtain stable radiomic features for modeling and to evaluate the variability of these signatures, we randomly selected 40 patients from the cohort and their brain tumors were independently segmented by two radiologists (L.X. and Y.S.H.). The interclass correlation coefficient (ICC) was used to assess the stability of each feature. Intraobserver stability was calculated for each feature (**Supplementary Figure S1**). Stable radiomic features were defined as ICC values > 0.7. An initial selection was performed by deleting collinear strongly correlated variables detected using Pearson's correlation analysis, for which the cut-off correlation coefficient value was 0.95. Univariate analysis was performed for each feature, and features with $P < 0.05$ were considered for selection. Marginally significant features were selected using the least absolute shrinkage and selection operator (LASSO) and a logistic regression model, which performed variable selection and regularization to enhance the prediction accuracy and interpretability of the statistical model. All features with non-zero coefficients were selected in this step. Finally, backward elimination was selectively performed to reduce the number of features included in the final set (**Supplementary Table S1**). The performance of the radiomic model was tested internally using an independent test cohort.

Statistical Analysis

Patient characteristics were compared using a chi-square test for categorical variables, an independent Student's t test for normally distributed continuous variables, and a Mann–Whitney U test for continuous variables without a normal distribution. The *EGFR* expression status in the primary cancers and BMs was calculated and compared using a Wilcoxon signed ranks test. We used the following R packages: irr (version 0.84.1) for calculating ICCs; caret (version 6.0–86) for Pearson's correlation analyses; glmnet (version 4.0–2) for LASSO logistic regression analysis; rms (version 6.0–1) for logistic regression analysis; and pROC (version 1.17) for receiver operating characteristic curve (ROC) and area under the curve (AUC) analyses. The discrimination performance of the established model was quantified using ROC and AUC values, sensitivity, specificity, and accuracy. All statistical tests were two-sided, and a *P*-value < 0.05 was considered statistically significant. Statistical analyses were performed using R software version 4.0.2 (http://www.r-project.org/).

RESULTS

Patient Characteristics

As shown in **Figure 1**, 265 patients with lung cancer BMs were enrolled in the study. One hundred and three patients were

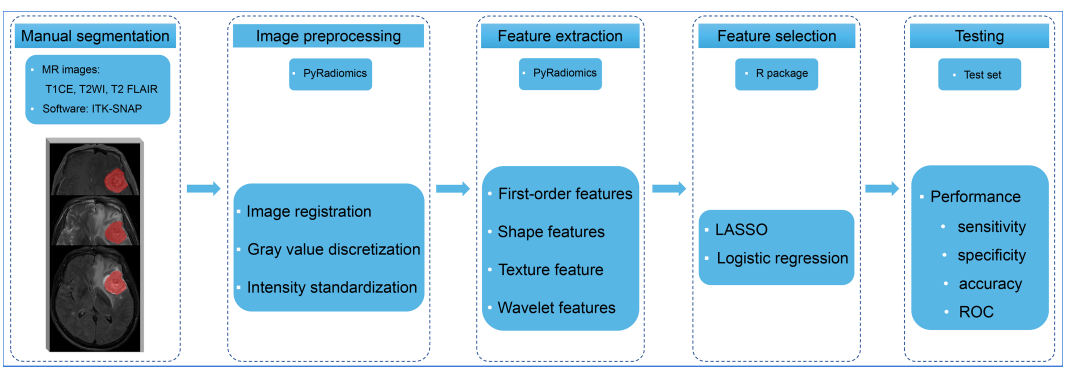

FIGURE 2 | The radiomics analysis workflow Multiple-sequence MR images were selected and manually contoured. The radiomic features were extracted and selected from processed images to build models to predict the *EGFR* status of brain metastases. The performance of the models was evaluated using an independent test set. T1CE, contrast-enhanced T1-weighted imaging; T2WI, T2-weighted imaging; T2 FLAIR, T2 fluid-attenuated inversion recovery; LASSO, least absolute shrinkage and selection operator; ROC, receiver operating characteristic curve.

excluded due to a complete response revealed by postoperative pathology (n = 3), the absence of *EGFR* gene testing (n = 82), a lack of preoperative brain MRI (n = 13), or having undergone brain radiotherapy after preoperative MRI (n = 5). Thus, 162 patients were finally included.

All patients had a single BM removed. The median interval between MRI scanning and resection was 6 days (range, 0–75 days). Of the 162 patients (age, 57 ± 9 years [range, 22–74 years]; 97 [59.9%] males), 62 (38.2%) had a history of smoking, 133 (82.1%) were diagnosed with adenocarcinoma, 95 (58.6%) had a single BM, and 11 patients (6.8%) had more than 10 lesions. The distributions of patient and lesion characteristics in the training and test sets are provided in **Table 1**. There were no significant differences in baseline characteristics between the training and test sets.

Resected BM Characteristics

The targeted lesions had a mean diameter of 39 ± 14 mm (range, 13–76 mm), and most of them were located in the cerebrum (85%), followed by the cerebellum (17%). Cysts and hemorrhages were observed in 84% and 30% of the BMs, respectively.

Of the 162 resected BMs used for radiomics analysis, 70 (43.2%) were positive for an *EGFR* mutation and 92 (56.8%) were negative. The frequency of *EGFR* mutations was higher in patients with adenocarcinoma than in those with non-adenocarcinoma (adenocarcinoma vs. non-adenocarcinoma, 48.1% vs. 18.5%, $P = 0.023$). *EGFR* mutations were present at a significantly higher frequency in females than in males (64.6% vs. 28.9%, $P < 0.001$). None of the females had a history of smoking; thus, we analyzed the *EGFR* status in males and found a higher incidence of *EGFR* mutations in males with a history of smoking than those without (42.9% vs. 21.0%, $P = 0.022$). Of the patients with *EGFR* mutations, 42 had mutations in exon 19 (60.0%); 21 (30.0%) had mutations in exon 21; and 7 (10.0%) had rare mutations in exon 18 (including three with G719X missense mutations and one with an S768I-V769L compound mutation), an insertion mutation in exon 20 (S768I), and compound mutations in exons 20 (T790M) and 21 (L858R).

Of the 265 patients initially included in the study, the *EGFR* mutation status of 52 patients was available for both the primary lung cancer and the corresponding BMs. An *EGFR* mutation was detected in 18 lung cancers and 24 BMs. Of the patients who had *EGFR* mutation-positive primary tumors, two (11.1%) had different mutations in the metastatic tumors. In one patient, there was a change from compound mutations in exons 18 and 21 to a mutation in exon 18, and in another patient, there was a change from a mutation in exon 21 to compound mutations in exons 18 and 21. No patients that were positive for an *EGFR* mutation in the primary tumor showed a loss of the mutation in the BM. Of the 34 patients who had *EGFR* mutation-negative primary tumors, 6 (17.6%) developed a new *EGFR* mutation in the metastatic tumor (two with deletion mutations in exon 19, three with missense

TABLE 1 | Patient and brain metastasis characteristics.

Characteristics	Training	Test	*P*
No. of patients	108	54	
No. of male patients	67 (62)	30 (56)	0.428
Average age (years)	57 ± 9	54 ± 10	0.427
No. of smokers	58 (54)	25 (46)	0.374
Histology			0.246
adenocarcinoma	86 (80)	47 (87)	
non-adenocarcinoma	22 (20)	7 (13)	
No. of brain metastases			0.354
1	61 (56)	34 (63)	
2	18 (17)	10 (19)	
3	10 (9)	4 (7)	
4-10	12 (11)	2 (4)	
>10	7 (6)	4 (7)	
Excised brain metastases			
EGFR status			
mutation in exon			
18	2 (2)	2 (4)	0.333
19	28 (26)	14 (26)	
20	2 (2)	0	
21	10 (9)	11 (20)	
20 & 21	1(1)	0	
wild-type	65 (60)	27 (50)	
Size (mm)	40 ± 14	39 ± 13	0.577
Location			0.086
cerebrum	91 (84)	46 (85)	
cerebellum	14 (13)	8 (15)	
brainstem	1 (1)	0	
lateral ventricle	2 (2)	0	
Cyst present	92 (85)	44 (81)	0.545
Hemorrhage present	34 (31)	15 (28)	0.629
Median time between the MRI and the resection (days)	6	6	0.404

Data represent the number, number (%), or mean (standard deviation); EGFR, epidermal growth factor receptor, MRI, magnetic resonance imaging.

mutations in exon 21, and one with co-current mutations in exons 20 and 21). We defined discordance as a conversion of mutation status from mutant to wild-type or vice versa or a change from one type of *EGFR* mutation to a different type. Thus, *EGFR* mutation status showed an overall discordance rate of 15.4% (Wilcoxon signed ranks test, $P = 0.461$) between the primary cancer and the corresponding BMs. The *EGFR* mutation status distributions are presented in **Figure 3**.

Feature Selection and Radiomic Signature Construction

From each sequence, we extracted 1,470 radiomic features, comprising 14 shape features, 288 first-order features, 352 gray-level co-occurrence matrix features, 224 gray-level dependence matrix features, 256 gray-level run-length matrix features, 256 gray-level size-zone matrix features, and 80 neighboring gray-tone difference matrix features. Through a series of methods for selection (e.g., ICC, Pearson's correlation, univariate analysis, LASSO, and backward elimination; **Supplementary Table S1**), the number of radiomic features selected to differentiate the *EGFR* mutation status was reduced to four, eight, four, and ten for T1CE, T2WI, T2 FLAIR, and combined sequences, respectively, to build the radiomic models. Half of the features in the combined model were from T2WI (5/10). **Table 2** lists the significant features used to differentiate *EGFR* mutation status in the various sequence models.

Prediction Performance

For each MRI sequence, we built radiomic signatures using the training set and evaluated their classification performance in the test set. The prediction performance details are provided in **Table 3** , **Figures 4**, **5**.

Overall, the combination sequences achieved the best AUC in both the training and test sets, with AUCs of 0.85 and 0.81, classification sensitivities of 83.7% and 73.1%, specificities of 73.8% and 75.9%, and accuracies of 77.8% and 75.9%, respectively. The AUCs were significantly different between the combination sequences and the single sequences in the training set (all $P < 0.05$), but showed no difference in the test set ($P = 0.164$–0.216). For single sequences, each sequence appeared to have a similar performance in the training and test sets, with AUC ranges of 0.69–0.76 and 0.72–0.74; classification sensitivities of 62.8%–81.4% and 69.2%–80.8%; specificities of 56.9%–69.2% and 60.7%–71.4%; and accuracies of 66.7%–68.5% and 70.4%–74.1%. The T2WI model achieved a higher AUC than the T1CE or T2 FLAIR model. **Figure 4A** illustrates the confusion matrix of the classification results obtained using the combined model in the test set. **Figures 4B**, **5** show the ROC curves and the decision curve analysis for the classification of *EGFR* mutations in all models.

DISCUSSION

In this proof-of-concept study, we extracted radiomic features from multiple MRI sequence images (T1CE, T2WI, and T2 FLAIR) of excised BMs originating from lung cancer and used these features to build machine-learning models for the classification of *EGFR* mutation status in BMs. Compared with a single sequence, the combination model, which extracted 10 key features from three sequences, achieved higher overall identification performance, yielding an AUC value of 0.81 in the independent test set. Additionally, the rate of discordance of *EGFR* mutation status between primary lung tumors and paired BMs was 15.4% in the 52 patients who underwent *EGFR* gene testing in both the primary tumor and the BM. Our findings indicate that the proposed radiomics signatures based on brain MRI can distinguish between mutant and wild-type *EGFR* in BMs, and the switch in *EGFR* status observed between the

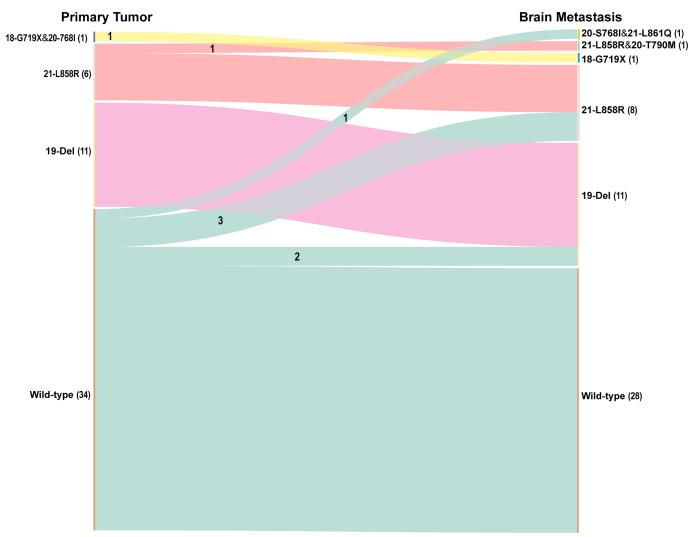

FIGURE 3 | The *EGFR* mutation status distributions of primary lung cancers and paired metastases Overall, the *EGFR* status showed a discordance rate of 15.4% between the primary cancer and the matched brain metastases. The number of patients is provided in parentheses. *EGFR*, epidermal growth factor receptor.

TABLE 2 | Radiomic features used to differentiate *EGFR* mutation status in various sequences.

Sequences	Sequence	Feature category	Features
Combination			
	T1CE	Original shape	Flatness
	T1CE	Wavelet.HHH GLCM	Cluster shade
	T1CE	Square GLSZM	Low gray-level zone Emphasis
	T2WI	GLSZM	Low gray-level zone Emphasis
	T2WI	Wavelet.LHL GLCM	Correlation
	T2WI	Wavelet.HHH GLCM	Imc 2
	T2WI	Square root first order	Skewness
	T2WI	Exponential GLCM	Correlation
	T2 FLAIR	Wavelet.HLH GLSZM	Gray-level variance
	T2 FLAIR	Exponential first order	Interquartile range
Single			
	T1CE	Original shape	Flatness
	T1CE	First order	Median
	T1CE	GLCM	Cluster shade
	T1CE	GLSZM	Low gray-level zone Emphasis
	T2WI	Original shape	Elongation
	T2WI	GLSZM	Low gray-level zone Emphasis
	T2WI	Wavelet.LLH first order	10^{th} Percentile
	T2WI	Wavelet.LHL GLCM	Correlation
	T2WI	Wavelet.HHH GLCM	Imc 2
	T2WI	Square root first order	Skewness
	T2WI	Exponential GLCM	Correlation
	T2WI	Exponential GLSZM	Low gray-level zone Emphasis
	T2 FLAIR	GLCM	Correlation
	T2 FLAIR	Exponential first order	Interquartile range
	T2 FLAIR	Wavelet.HLH GLSZM	Gray-level variance
	T2 FLAIR	Gradient first order	Minimum

EGFR, epidermal growth factor receptor; T1CE, contrast-enhanced T1-weighted imaging; T2WI, T2-weighted imaging; T2-FLAIR, T2 fluid-attenuated inversion recovery; GLCM, gray-level co-occurrence matrix; GLSZM, gray-level size zone matrix.

primary tumor and the BMs also indicates the importance of considering that the *EGFR* gene mutation status may differ between the metastases and the primary tumor.

New molecular agents targeting specific pathways have been developed and key molecules in tumor growth and progression have been identified. A typical example of such a target is the *EGFR* gene, which is an indicator of targeted treatment, an independent predictor of the treatment response, and a predictor of outcomes (26–28). Given the inconsistencies in target gene expression between primary tumors and their distant metastases, molecular diagnostic testing is now recommended for metastases in patients with advanced NSCLC whenever possible, to determine their eligibility for targeted therapies. Such assessments are recommended by the

TABLE 3 | The performance of radiomics in predicting *EGFR* mutation status in various sequences.

Sequences	Sensitivity (95% CI)	Specificity (95% CI)	Accuracy (95% CI)	AUC (95% CI)	*P* [a]
Training					
Combination	83.7 (72.7, 94.8)	73.8 (63.2, 84.5)	77.8 (77.5, 78.1)	0.85 (0.78, 0.92)	
T1CE	81.4 (69.8, 93.0)	56.9 (44.9, 69.0)	66.7 (66.3, 67.1)	0.74 (0.65, 0.84)	0.011*
T2WI	74.4 (61.4, 87.5)	65.6 (53.0, 76.2)	68.5 (68.1, 68.9)	0.76 (0.66, 0.85)	0.017*
T2 FLAIR	62.8 (48.3, 77.2)	69.2 (58.0, 80.5)	66.7 (66.3, 67.1)	0.69 (0.59, 0.79)	0.001*
Test					
Combination	73.1 (56.0, 90.1)	78.6 (63.4, 93.8)	75.9 (75.3, 76.6)	0.81 (0.70, 0.93)	
T1CE	69.2 (51.5,87.0)	71.4 (54.7, 88.2)	70.4 (69.6, 71.1)	0.72 (0.58, 0.86)	0.216
T2WI	80.8 (65.6, 95.9)	67.9 (50.6, 85.2)	74.1 (73.4, 74.8)	0.74 (0.61, 0.88)	0.182
T2 FLAIR	80.8 (65.6, 95.9)	60.7 (42.6, 78.8)	70.4 (69.6, 71.1)	0.72 (0.58, 0.86)	0.164

*EGFR, epidermal growth factor receptor; AUC, area under the curve; CI, confidence interval; T1CE, contrast-enhanced T1-weighted imaging; T2-FLAIR, T2 fluid-attenuated inversion recovery; T2WI, T2-weighted imaging; [a], the AUC of T1CE, T2WI, and T2 FLAIR compared with the combination of the three sequences; *, statistically significant.*

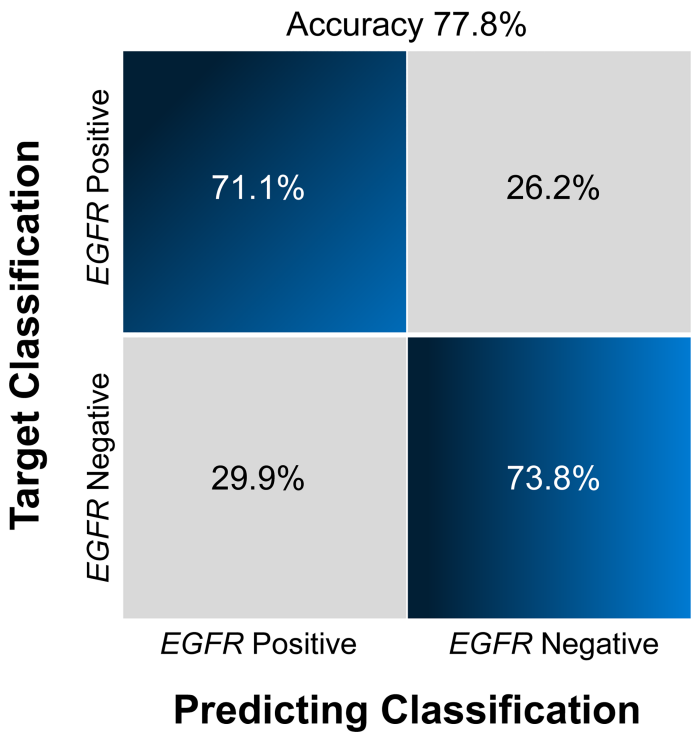

FIGURE 4 | Confusion matrix **(A)** and ROCs **(B)** for the classification of *EGFR* mutation status in the test set The confusion matrix was generated using a combined model. The combined model appeared to achieve a higher AUC than any individual sequence, but the differences were not statistically significant. *EGFR*, epidermal growth factor receptor; ROC, receiver operating characteristics curve; AUC, area under the curve; T1CE, contrast-enhanced T1-weighted imaging; T2-FLAIR, T2 fluid-attenuated inversion recovery; T2WI, T2-weighted imaging; combination, combined model extracting features from the three sequences.

American Society of Clinical Oncology (29) and the European Association of Neuro-Oncology-European Society for Medical Oncology (10). Currently, however, it is not always practical to obtain a specimen of the BM by biopsy or surgery.

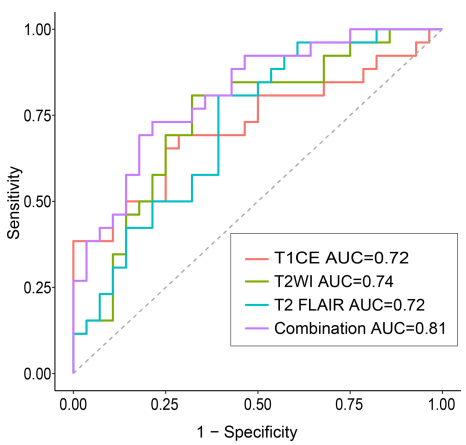

FIGURE 5 | The decision curve analyses of various models The best decision benefit was observed with the combined model. T1CE, contrast-enhanced T1-weighted imaging; T2-FLAIR, T2 fluid-attenuated inversion recovery; T2WI, T2-weighted imaging; combination, combined model extracting features from three sequences.

Therefore, several studies have used radiomics models to noninvasively predict the *EGFR* mutation status of lung cancer or BMs using brain MRI (15, 21). Ahn et al. extracted features from T1CE of 61 patients comprising 210 BMs with a size > 5 mm, and used several machine-learning algorithms to predict the *EGFR* gene mutation status of primary lung cancer, reaching an accuracy of 86.7% (AUC, 0.868) (15). In a similar study, Chen et al. built a model based on radiomic features generated by T1CE and T2 FLAIR (110 patients with 452 lesions, of whom 75 were *EGFR* positive) and clinical data using random forest classifiers, to classify *EGFR*, anaplastic lymphoma kinase, and Kirsten rat sarcoma virus gene mutation status in primary lung tumors and generated AUC values of 0.91, 0.92, and 0.99, respectively (21). However, both of these previous studies assumed an identical molecular profile in the BMs, thus overlooking possible discordances in *EGFR* mutation status between the lung cancer and the BMs. Additionally, there was no separate test set to validate the model performance, which may have led to overfitting.

Limited efforts have been focused on radiomics signatures to detect *EGFR* mutation status in BMs. Wang et al. analyzed four sequences (T1CE, T2WI, T2 FLAIR, and diffusion tensor images [DWI]) collected from 52 lung adenocarcinoma patients (28 with mutant *EGFR*, 24 with wild-type *EGFR*) (23). Although they concluded that the radiomics signature of T2 FLAIR achieved an AUC of 0.871, an accuracy of 0.845, a sensitivity of 0.901, and a specificity of 0.891 for discriminating *EGFR* mutation status

using an independent testing data set, they also assumed that *EGFR* expression was consistent between the metastatic tumor and the primary tumor, which may not be accurate as discussed above. Haim et al. applied a deep-learning approach, using a ResNet-50 convolutional neural network, to predict *EGFR* mutation status in NSCLC BMs based on the *EGFR* testing results from resected BMs (20). However, they used data from a small cohort of 59 patients, of which only 16 patients were *EGFR*-positive. Moreover, they cropped regions of interest of the mid-tumor region and ± two slices for each patient. Such areas may be not sufficient to represent the entire tumor and may miss the three-dimensional features of the tumor. In contrast to previous studies, we enrolled, to the best of our knowledge, the largest reported study population of patients who underwent resection of their lung cancer BMs, to propose a radiomics signature based on multiple sequences of brain MRI. Moreover, despite adenocarcinomas showing the highest *EGFR* mutation rate among all histological cancer types, we included all patients with lung cancer, unlike other studies that exclusively selected patients with NSCLC or adenocarcinoma. Furthermore, we evaluated the *EGFR* mutation status in resected brain samples, which may better reflect the real mutation status. In addition, we used an open-source tool, Pyradiomics, for radiomics feature extraction, which may have improved the reproducibility of the feature extraction process.

We also found that the combination of features from multiple sequences had better classification performance than a single sequence, which was consistent with the study of Park et al. (18). Compared to single sequence, they reported that features extracted from the integration of T1CE and diffusion tensor images improved the capacity to determine the *EGFR* mutation status of BMs derived from lung cancer. Of the 10 features analyzed in our study, the biggest contribution came from T2WI. Furthermore, more second-order features than first-order features were selected, implying that multiparametric high-throughput characteristics enable a more accurate assessment than single parameters. Of the single sequences used to predict *EGFR* status, we found that the radiomic signatures of T2WI had the best performance. This differs from the result reported by Wang et al. (23), who found that T2-FLAIR yielded better *EGFR* mutation discrimination than TICE, T2WI, and DWI. Our results indicate that multiple sequences have higher predictive value than single sequences for the determination of *EGFR* mutation status.

Another finding in our study was that the discordance rate between the primary tumors and the corresponding BMs reached 15.4%. These results were comparable to those of previous studies that have reported heterogeneity in *EGFR* mutations between primary tumors and BMs, with variability rates ranging from 12% to 33% (8, 9, 30). Discordance between primary and metastatic tumors may be explained by clonal selection and intratumor heterogeneity (31). Clonal selection during the multistep metastatic process, combined with the potential effects of the tumor microenvironment and/or the treatment, may explain the discordance observed in metachronous metastases. Moreover, cancer is a highly heterogeneous disease, and polyclonal cell lines may exist with various *EGFR* statuses. Finally, the effect of different techniques on discordance cannot be excluded (32). Notably, two rare mutations were found in our study. A male patient with adenocarcinoma had both a deletion in exon 19 and an L858R missense mutation in exon 21 in the primary tumor, but the mutation in exon 21 was lost in the BM. Another adenocarcinoma in a female patient was found to have an S768I insertion in exon 20 and a G719X missense mutation in exon 18, but, similarly, the insertion was lost in the BM. The mechanism responsible for these changes will be investigated in future studies. We did not observe any *EGFR*-positive primary tumors that switched to an *EGFR*-negative form in BMs. Our data suggest that gaining *EGFR* mutations or switching *EGFR* subtypes may be more frequent than the complete loss of *EFGR* mutations when the primary tumors metastasize to the brain (negative to positive vs. positive to negative, 17.6% vs. 0%, Yates' continuity correction, $P = 0.567$; change mutation type vs. positive to negative, 11.1% vs. 0%, Fisher's exact test, $P = 0.486$), but these differences did not reach statistical significance, possibly due to the small number of samples.

This study has several limitations. First, this was a retrospective single-center design, which may have created selection bias. The performance of the model should be validated using a larger prospective multi-center dataset. Nonetheless, this is the largest reported cohort exploring the feasibility of classifying *EGFR* expression in BMs based on radiomics. Second, as in most previous studies, a region of interest was delineated for the entire metastasis. We did not analyze the subregional features of the tumor, e.g., the areas with enhancement, necrosis, hemorrhage, or edema. Third, more novel techniques such as deep learning or functional MRI were not applied to extract features. However, using an open-source Python package to extract features may have improved the reproducibility. In addition, conventional MRI sequences have wider adaptability in clinical practice. Finally, we did not distinguish between mutation subtypes, e.g., common vs. rare or sensitive vs. resistant mutations, given the limited number of samples with rare and resistant mutations.

CONCLUSIONS

We demonstrated that it is feasible to apply a multi-sequence radiomic model to noninvasively predict the *EGFR* mutation status of lung cancer BMs. Moreover, the discordance observed between the primary tumors and the BMs indicates that *EGFR* alterations in metastases should be considered when a molecular targeted treatment is to be implemented.

DATA AVAILABILITY STATEMENT

The raw data supporting the conclusions of this article will be made available by the authors, without undue reservation.

ETHICS STATEMENT

The studies involving human participants were reviewed and approved by Institutional Review Board of Sun Yat-Sen

University Cancer Center, approval No. B2021-198-01. Written informed consent for participation was not required for this study in accordance with the national legislation and the institutional requirements.

AUTHOR CONTRIBUTIONS

Conceptualization: LZ, HX, XL, HL, CX. Literature search: XL. Study design: LZ, HX, XL, HL. Data curation: HX, XL, YZ, YL. Software: HX, XL. Supervision: HL, CX. Visualization: LZ, HX, XL. Writing – original draft: LZ. Editing: HX, XL. Review & approval: all authors

SUPPLEMENTARY MATERIAL

The Supplementary Material for this article can be found online at: https://www.frontiersin.org/articles/10.3389/fonc.2022.931812/full#supplementary-material

REFERENCES

1. Lamba N, Wen PY, Aizer AA. Epidemiology of Brain Metastases and Leptomeningeal Disease. *Neuro-Oncology* (2021) 23(9):1447–56. doi: 10.1093/neuonc/noab101
2. Midha A, Dearden S, McCormack R. EGFR Mutation Incidence in Non-Small-Cell Lung Cancer of Adenocarcinoma Histology: A Systematic Review and Global Map by Ethnicity (Mutmapii). *Am J Cancer Res* (2015) 5(9):2892–911.
3. Selvaggi G, Novello S, Torri V, Leonardo E, De Giuli P, Borasio P, et al. Epidermal Growth Factor Receptor Overexpression Correlates With a Poor Prognosis in Completely Resected Non-Small-Cell Lung Cancer. *Ann Oncol* (2004) 15(1):28–32. doi: 10.1093/annonc/mdh011
4. Levantini E, Maroni G, Del Re M, Tenen DG. EGFR Signaling Pathway as Therapeutic Target in Human Cancers. *Semin Cancer Biol* (2022) 12:S1044–579X(22)00096-7. doi: 10.1016/j.semcancer
5. Kris MG, Natale RB, Herbst RS, Lynch TJ, Prager D, Belani CP, et al. Efficacy of Gefitinib, an Inhibitor of the Epidermal Growth Factor Receptor Tyrosine Kinase, in Symptomatic Patients With Non-Small Cell Lung Cancer - A Randomized Trial. *JAMA-Journal Am Med Assoc* (2003) 290(16):2149–58. doi: 10.1001/jama.290.16.2149
6. Perez-Soler R, Chachoua A, Hammond LA, Rowinsky EK, Huberman M, Karp D, et al. Determinants of Tumor Response and Survival With Erlotinib in Patients With Non-Small-Cell Lung Cancer. *J Clin Oncol* (2004) 22 (16):3238–47. doi: 10.1200/jco.2004.11.057
7. Gow CH, Chang YL, Hsu YC, Tsai MF, Wu CT, Yu CJ, et al. Comparison of Epidermal Growth Factor Receptor Mutations Between Primary and Corresponding Metastatic Tumors in Tyrosine Kinase Inhibitor-Naive Non-Small-Cell Lung Cancer. *Ann Oncol* (2009) 20(4):696–702. doi: 10.1093/annonc/mdn679
8. Lee CC, Soon YY, Tan CL, Koh WY, Leong CN, Tey JCS, et al. Discordance of Epidermal Growth Factor Receptor Mutation Between Primary Lung Tumor and Paired Distant Metastases in Non-Small Cell Lung Cancer: A Systematic Review and Meta-Analysis. *PLoS One* (2019) 14(6):e0218414. doi: 10.1371/journal.pone.0218414
9. Daniele L, Cassoni P, Bacillo E, Cappia S, Righi L, Volante M, et al. Epidermal Growth Factor Receptor Gene in Primary Tumor and Metastatic Sites From Non-Small Cell Lung Cancer. *J Thorac Oncol* (2009) 4(6):684–8. doi: 10.1097/JTO.0b013e3181a52359
10. Le Rhun E, Guckenberger M, Smits M, Dummer R, Bachelot T, Sahm F, et al. EANO-ESMO Clinical Practice Guidelines for Diagnosis, Treatment and Follow-Up of Patients With Brain Metastasis From Solid Tumours. *Ann Oncol* (2021) 32(11):1332–47. doi: 10.1016/j.annonc.2021.07.016
11. Burel-Vandenbos F, Ambrosetti D, Coutts M, Pedeutour F. Egfr Mutation Status in Brain Metastases of Non-Small Cell Lung Carcinoma. *J Neuro-Oncol* (2013) 111(1):1–10. doi: 10.1007/s11060-012-0990-5
12. Choi KS, Choi SH, Jeong B. Prediction of Idh Genotype in Gliomas With Dynamic Susceptibility Contrast Perfusion MR Imaging Using an Explainable Recurrent Neural Network. *Neuro-Oncology* (2019) 21(9):1197–209. doi: 10.1093/neuonc/noz095
13. Meissner A-K, Gutsche R, Galldiks N, Kocher M, Juenger ST, Eich M-L, et al. Radiomics for the Noninvasive Prediction of the BRAF Mutation Status in Patients With Melanoma Brain Metastases. *Neuro-Oncology* (2021) 22: noab294. doi: 10.1093/neuonc/noab294
14. Zhu H, Song Y, Huang Z, Zhang L, Chen Y, Tao G, et al. Accurate Prediction of Epidermal Growth Factor Receptor Mutation Status in Early-Stage Lung Adenocarcinoma, Using Radiomics and Clinical Features. *Asia-Pacific J Clin Oncol* (2022). doi: 10.1111/ajco.13641
15. Ahn SJ, Kwon H, Yang J-J, Park M, Cha YJ, Suh SH, et al. Contrast-Enhanced T1-Weighted Image Radiomics of Brain Metastases May Predict EGFR Mutation Status in Primary Lung Cancer. *Sci Rep* (2020) 10(1):8905. doi: 10.1038/s41598-020-65470-7
16. Li S, Luo T, Ding C, Huang Q, Guan Z, Zhang H. Detailed Identification of Epidermal Growth Factor Receptor Mutations in Lung Adenocarcinoma: Combining Radiomics With Machine Learning. *Med Phys* (2020) 47(8):3458–66. doi: 10.1002/mp.14238
17. Jia T, Xiong J, Li X, Ma J, Ren Y, Xu Z, et al. Detecting Epidermal Growth Factor Receptor Mutation Status in Patients With Lung Adenocarcinoma Using Radiomics and Random Forest. *J Thorac Oncol* (2017) 12(11):S1860–S. doi: 10.1016/j.jtho.2017.09.581
18. Park YW, An C, Lee J, Han K, Choi D, Ahn SS, et al. Diffusion Tensor and Postcontrast T1-Weighted Imaging Radiomics to Differentiate the Epidermal Growth Factor Receptor Mutation Status of Brain Metastases From Non-Small Cell Lung Cancer. *Neuroradiology* (2021) 63(3):343–52. doi: 10.1007/s00234-020-02529-2
19. Jia T-Y, Xiong J-F, Li X-Y, Yu W, Xu Z-Y, Cai X-W, et al. Identifying EGFR Mutations in Lung Adenocarcinoma by Noninvasive Imaging Using Radiomics Features and Random Forest Modeling. *Eur Radiol* (2019) 29 (9):4742–50. doi: 10.1007/s00330-019-06024-y
20. Haim O, Abramov S, Shofty B, Fanizzi C, DiMeco F, Avisdris N, et al. Predicting EGFR Mutation Status by a Deep Learning Approach in Patients With Non-Small Cell Lung Cancer Brain Metastases. *J Neuro-Oncol* (2022) 157(1):63–9. doi: 10.1007/s11060-022-03946-4
21. Chen BT, Jin T, Ye N, Mambetsariev I, Daniel E, Wang T, et al. Radiomic Prediction of Mutation Status Based on MR Imaging of Lung Cancer Brain Metastases. *Magnetic Resonance Imaging* (2020) 69:49–56. doi: 10.1016/j.mri.2020.03.002
22. Li S, Ding C, Zhang H, Song J, Wu L. Radiomics for the Prediction of EGFR Mutation Subtypes in Non-Small Cell Lung Cancer. *Med Phys* (2019) 46 (10):4545–52. doi: 10.1002/mp.13747
23. Wang G, Wang B, Wang Z, Li W, Xiu J, Liu Z, et al. Radiomics Signature of Brain Metastasis: Prediction of EGFR Mutation Status. *Eur Radiol* (2021) 31 (7):4538–47. doi: 10.1007/s00330-020-07614-x
24. WHO Classification of Tumours Editorial Board. *WHO Classification of Tumours*. Lyon: International Agency for Research on Cancer Press (2021).
25. Mosele F, Remon J, Mateo J, Westphalen CB, Barlesi F, Lolkema MP, et al. Recommendations for the Use of Next-Generation Sequencing (NGS) for Patients With Metastatic Cancers: A Report From the ESMO Precision Medicine Working Group. *Ann Oncol* (2020) 31(11):1491–505. doi: 10.1016/j.annonc.2020.07.014
26. Waqar SN, Govindan R. Adjuvant Therapy With EGFR Tyrosine Kinase Inhibitors: Tempering Great Expectations With Realism. *J Clin Oncol* (2021) 39(7):697–700. doi: 10.1200/JCO.20.03297
27. Singh R, Lehrer EJ, Ko S, Peterson J, Lou Y, Porter AB, et al. Brain Metastases From Non-Small Cell Lung Cancer With EGFR or Alk Mutations: A Systematic Review and Meta-Analysis of Multidisciplinary Approaches. *Radiother Oncol* (2020) 144:165–79. doi: 10.1016/j.radonc.2019.11.010
28. Meador CB, Sequist LV, Piotrowska Z. Targeting EGFR Exon 20 Insertions in Non-Small Cell Lung Cancer: Recent Advances and Clinical Updates. *Cancer Discovery* (2021) 11(9):2145–57. doi: 10.1158/2159-8290.CD-21-0226

29. Van Poznak C, Somerfield MR, Bast RC, Cristofanilli M, Goetz MP, Gonzalez-Angulo AM, et al. Use of Biomarkers to Guide Decisions on Systemic Therapy for Women With Metastatic Breast Cancer: American Society of Clinical Oncology Clinical Practice Guideline. *J Clin Oncol* (2015) 33(24):2695–704. doi: 10.1200/JCO.2015.61.1459
30. Bozzetti C, Tiseo M, Lagrasta C, Nizzoli R, Guai A, Leonardi F, et al. Comparison Between Epidermal Growth Factor Receptor (EGFR) Gene Expression in Primary Non-Small Cell Lung Cancer (NSCLC) and in Fine-Needle Aspirates From Distant Metastatic Sites. *J Thorac Oncol* (2008) 3 (1):18–22. doi: 10.1097/JTO.0b013e31815e8ba2
31. Turajlic S, Sottoriva A, Graham T, Swanton C. Resolving Genetic Heterogeneity in Cancer. *Nat Rev Genet* (2019) 20(7):404–16. doi: 10.1038/s41576-019-0114-6
32. Imyanitov EN, Iyevleva AG, Levchenko EV. Molecular Testing and Targeted Therapy for Non-Small Cell Lung Cancer: Current Status and Perspectives. *Crit Rev Oncol Hematol* (2021) 157:103194. doi: 10.1016/j.critrevonc.2020.103194

Conflict of Interest: The authors declare that the research was conducted in the absence of any commercial or financial relationships that could be construed as a potential conflict of interest.

frontiers | Frontiers in Oncology

TYPE Original Research
PUBLISHED 20 October 2022
DOI 10.3389/fonc.2022.951805

OPEN ACCESS

EDITED BY
Anna Berghoff,
Medical University of Vienna, Austria

REVIEWED BY
David Wasilewski,
Charité University Medicine Berlin, Germany
Güliz Acker,
Charité University Medicine Berlin, Germany

*CORRESPONDENCE
Malte Mohme
m.mohme@uke.de

†These authors have contributed equally to this work

SPECIALTY SECTION
This article was submitted to Neuro-Oncology and Neurosurgical Oncology, a section of the journal Frontiers in Oncology

RECEIVED 24 May 2022
ACCEPTED 22 September 2022
PUBLISHED 20 October 2022

CITATION
Piffko A, Asey B, Dührsen L, Ristow I, Salamon J, Wikman H, Maire CL, Lamszus K, Westphal M, Sauvigny T and Mohme M (2022) Clinical determinants impacting overall survival of patients with operable brain metastases from non-small cell lung cancer.
Front. Oncol. 12:951805.
doi: 10.3389/fonc.2022.951805

Clinical determinants impacting overall survival of patients with operable brain metastases from non-small cell lung cancer

Andras Piffko[1,2,3], Benedikt Asey[1], Lasse Dührsen[1], Inka Ristow[4], Johannes Salamon[4], Harriet Wikman[5], Cecile L. Maire[1], Katrin Lamszus[1], Manfred Westphal[1], Thomas Sauvigny[1†] and Malte Mohme[1*†]

[1]Department of Neurosurgery, University Medical Center Hamburg-Eppendorf, Hamburg, Germany, [2]Department of Radiation and Cellular Oncology, University of Chicago, Chicago, IL, United States, [3]The Ludwig Center for Metastasis Research, University of Chicago, Chicago, IL, United States, [4]Department of Diagnostic and Interventional Radiology and Nuclear Medicine, University Medical Center Hamburg-Eppendorf, Hamburg, Germany, [5]Department of Tumor Biology, University Medical Center Hamburg-Eppendorf, Hamburg, Germany

Non-small cell lung cancer (NSCLC) is currently the leading cause of cancer-related death worldwide, and the incidence of brain metastases (BM) in NSCLC patients is continuously increasing. The recent improvements of systemic treatment in NSCLC necessitate continuous updates on prognostic subgroups and factors determining overall survival (OS). In order to improve clinical decision-making in tumor boards, we investigated the clinical determinants affecting survival in patients with resectable NSCLC BM. A retrospective analysis was conducted of NSCLC patients with surgically resectable BM treated in our institution between 01/2015 and 12/2020. The relevant clinical factors affecting survival identified by univariate analysis were included in a multivariate logistic regression model. Overall, 264 patients were identified, with a mean age of 62.39 ± 9.98 years at the initial diagnosis of NSCLC BM and OS of 23.22 ± 1.71 months. The factors that significantly affected OS from the time of primary tumor diagnosis included the systemic metastatic load (median: 28.40 ± 4.82 vs. 40.93 ± 11.18 months, p = 0.021) as well as a number of BM <2 (median: 17.20 ± 2.52 vs. 32.53 ± 3.35 months, p = 0.014). When adjusted for survival time after neurosurgical intervention, a significant survival benefit was found in patients <60 years (median 16.13 ± 3.85 vs. 9.20 ± 1.39 months, p = 0.011) and, among others, patients without any concurrent systemic metastases at time of NSCLC BM diagnosis. Our data shows that the number of BM (singular/solitary), the Karnofsky Performance Status, gender, and age but not localization (infra-/supratentorial), mass-edema index or time to BM occurrence impact OS, and postsurgical survival in NSCLC BM patients. Additionally, our study shows that patients in

10.3389/fonc.2022.951805

prognostically favorable clinical subgroups an OS, which differs significantly from current statements in literature. The described clinically relevant factors may improve the understanding of the risks and the course of this disease and Faid future clinical decision making in tumor boards.

KEYWORDS

NSCLC, metastasis, brain metastasis, survival, resectable, surgery

Introduction

Non–small cell lung cancer (NSCLC) is the leading cause of death in cancer patients (1.3 million/year) worldwide, accounting for 25% of all cancer-related deaths (1). Despite significant improvements in treatment, especially within the field of immuno-oncology (2–4), NSCLC mortality remains extremely high and the overall 5-year survival rates rarely exceed 15% (1, 5). Approximately 40% of patients with stage III NSCLC will develop brain metastases (BM) (6). The incidence of brain metastases continues to rise, partly as a result of improved extracranial disease control and subsequently prolonged survival (7, 8), partly due to other factors, such as more readily available and increasingly accurate diagnostic procedures, which facilitate an earlier and a more frequent diagnosis of intracranial disease. In clinical practice, the occurrence of BM at the initial diagnosis (ID) or during the treatment course of NSCLC has been associated with a reduction of the quality of life, and, more importantly, with a dismal disease course and poor prognosis. In addition, BM may lead to neurological impairments by affecting both cognitive and sensory functions and thus further diminish the quality of life (9, 10). However, due to the high degree of heterogeneity in metastatic dissemination, the timing of BM occurrence, and various clinical determinants, such as gender, age, systemic tumor dissemination, and clinical factors that impact overall survival (OS), reliable data on the differences in the disease course for patients undergoing neurosurgical resection are scarce. To improve future treatment strategies and tumor board decision-making processes, a better understanding of the risk stratification for patients with NSCLC BM patients is urgently needed. Therefore, the aim of our study was to analyze clinical determinants affecting patient survival after ID, as well as survival after neurosurgical resection.

Results

Study cohort

We identified 264 patients who were treated for brain metastatic NSCLC in our institution between 01/2015 and 12/2020. The mean age at the ID of NSCLC was 61.54 ± 10.06 years (range 33–83 years). The male-to-female ratio was 1:1.18. The median time to BM development was 10.98 ± 20.62 months, thus accounting for the mean age at the neurosurgical intervention of 62.39 ± 9.98 years. In total, 61.38% (n=151/246) of patients were diagnosed with synchronous NSCLC BM at our institution without a prior NSCLC diagnosis and were thus termed "BM at ID." Of these 151 patients, 81 (53.64%) showed an additional synchronous metastatic disease of other organs. The average number of brain metastases was 1.93 ± 0.136, and the mean size of the largest observed BM lesion was 12.93 ± 1.51 cm^3. The majority of the patients primarily underwent surgery with the goal of total resection [96.06% (n = 244/256)]. Partial resection was performed in 1.56% (n = 4/256) of cases and tissue biopsies in 3.12% (n = 8/256). The median OS from the time of the primary tumor diagnosis was 15.00 ± 2.27 months. Postoperative complications affected 26/264 patients (9.85%). A total of 10 (3.78%) complications included postoperative hemorrhages at the resection site, three (1.13%) patients suffered from postoperative CSF fistulas, eight (3.03%) received antibiotics for postoperative wound infections, four (1.51%) developed hydrocephalus, and postoperative cerebral infarctions were found in one (0.38%) patient with surgical complications.

The histological subtype classification of the BM tissue was available in 84.09% (n=222/264) of cases. The most common NSCLC histological diagnoses based on the analysis of the BM tissue were comprised of adenocarcinomas (n=183/222, 82.43%) followed by squamous cell (n=21/222, 9.46%) and

neuroendocrine carcinomas (n=11/222, 4.95%) and not-otherwise-specified (NOS) histology (n=7/222, 3.15%). A single intracerebral metastasis was observed in two-thirds of patients (67.4%, n=159/236), while 11.9% (n=28/236) and 20.8% of patients (n=49/236) patients presented with two or three and more intracerebral tumor manifestations, respectively. Information about the mutation status of the primary NSCLC was available in n=66/264 cases (25.0%). The most commonly observed driver mutations of the primary tumor affected *TP53* [n=9/66 (13.64%)] and *KRAS* [n=9/66 (13.64%)], followed by *EGFR* [n=7/36 (10.61%)]. Programmed cell death 1 ligand 1 (PD-L1) expression was analyzed in 44/264 (16.67%) of primary tumor samples, and the mean PD-L1 expression was graded 45.35% in tumor cells (range 0%–90%) and 3.26% on infiltrating immune cells (range 0%–20%).

The mutational analysis information of the BM tissue was available in n=92/264 (34.85%) of all cases in the analyzed time period. The most observed driver mutation, similar to our observation in the primary tumor, affected *TP53*, detected in 25.0% (n=23/92) of cases, followed by *KRAS* (16.30%, n=15/92) and *EGFR* (9.78%, n=9/92). Other druggable mutations such as *ALK* [n=1/92 (2.78%)] and *ROS* [n=2/92 (2.78%)] were rare in the observed patient cohort. PD-L1 expression in the BM tissue was analyzed in n=74/264 (28.03%) of cases, and the mean PD-L1 expression was graded 36.88% in tumor cells (range 0%–90%) and 4.01% on infiltrating immune cells (range 0%–20%)

In total, 48.5% of patients (n=128/264) received no NSCLC-specific treatment before the neurosurgical intervention [n=23/151, (15.2%) patients within the "BM at ID" group had been diagnosed with NSCLC less than 4 weeks before the identification of brain metastases and had thus just begun first treatment chemotherapy cycles]. Information about preoperative adjuvant treatments was available in 159/264 patients (60.22%). Of these patients, n=133/159 (83.65%) received chemotherapy (CTX). As expected, the most commonly prescribed chemotherapeutics—applied in n=126/133 cases (94.74%)—were platinum based (containing either cisplatinum or carboplatinum). Information about the postoperative radiotherapy of BM was available in n=159/264 (60.23%) of cases. Out of 159 cases, 45 (28.30%) received whole-brain radiotherapy (WBRT) and n=8/159 (5.03%) received no postoperative radiation treatment, while the remaining 109 cases underwent fractionated stereotactic brain radiotherapy (SBRT) or gamma knife radio surgery (GKRS), with the additional treatment of non-resected lesions in cases deemed necessary. The most commonly applied cumulative dose in SBRT was 35 Gy in seven fractions (25/109 cases), while the most commonly applied fractionation regiment in WBRT consisted of 10 × 3 Gy [30 Gy cumulative dose, 23/45 cases (51.11%)].

We scored the patient cohort according to the Karnofsky Performance Status (KPS) and included the values in our analyses at three distinct points in time: 1) pre-operative (mean 76.25 ± 16.65) 2) postoperative (mean 80.85 ± 18.33), and 3) the last documented score available (mean 29.15 ± 38.39) (Table 1). Further, detailed clinical information is displayed in Table 1.

Clinical determinants for overall survival

Overall, 97 of 255 patients (38.04%) were younger than 60 years at the time of neurosurgical intervention. The comparison of OS between patients aged over versus under 60 years (Figure 1A) indicated a survival benefit of younger patients without quite reaching statistical significance in this cohort [p = 0.072, log-rank (Mantel–Cox) test]. A similar trend of a potential survival benefit was observed with female sex (n=133/251, 52.98%); however, as above, the difference did not prove statistically significant [Figure 1B, p = 0.123, log-rank (Mantel–Cox) test]. The systemic metastatic load at time of initial BM diagnosis was evaluated by comparing a singular BM status (one BM lesion, with concurrent systemic metastases) to a solitary BM status (one BM lesion, without further systemic metastases). In total, 67% (n=68/120) of patients presented with solitary BM status. As expected, the lack of additional systemic metastases in solitary BM patients correlated with a significant survival benefit when contrasted with the singular BM group (Figure 1C, median: 28.40 ± 4.82 vs. 40.93 ± 11.18 months respectively, p = 0.021, log-rank (Mantel–Cox) test). We dichotomized based on the supra-/infratentorial localization of the singular BM lesion (or localization of the largest lesion in case of multiple BM); however, we did not observe a significant effect on OS [Figure 1D, p = 0.696, log-rank (Mantel–Cox) test]. The total number of BM did, however, significantly affect the OS of the patient cohort, benefitting patients affected by <2 BM at the time of diagnosis, irrespective of the occurrence of additional systemic metastases [Figure 1E, median: 17.20 ± 2.52 vs. 32.53 ± 3.35 months, p = 0.014, log-rank (Mantel–Cox) test].

The mass-edema index (MEI), calculated as size of contrast-enhanced area in T1-weighted MRI/the size of peritumoral brain edema (PTB) in T2/flair-weighted MRI, did not affect OS [Figure 1F, p = 0.381, log-rank (Mantel–Cox) test].

The cut-off value for high KPS was set at 70%. This analysis showed that the preoperatively high KPS scores do not confer a significant survival benefit [Figure 1G, p = 0.173, log-rank (Mantel–Cox) test]; however, a postoperatively scored KPS of 70% or higher does [Figure 1H, median 9.47 ± 0.94, vs. 30.43 ± 2.76, p < 0.001, log-rank (Mantel–Cox) test].

Clinical determinants for survival time after brain surgery

We adjusted for the duration of survival after neurosurgical intervention and observed a significance in the previously suggested survival benefit of patients aged 60 years or younger

10.3389/fonc.2022.951805

TABLE 1 Clinical information of patient cohort.

	N (%)	Mean	Std. dev.
Age at ID	**255/264 (96.60)**	61.54	10.06
Age at surgery	**258/264 (94.73)**	62.39	9.98
Female gender	**143/264 (54.17)**		
Time to BM development (months)	**246/264 (93.18)**	10.98	20.62
BM at ID	**151/264 (61.38)**		
KPS pre-op	**253/264 (95.83)**	76.25	16.65
KPS post-op	**246/264 (93.18)**	80.85	18.33
KPS last documented	**235/264 (89.02)**	29.15	38.39
Histology	**222/264 (84.09)**		
Adeno	183/222 (82.43)		
Squamous cell	21/222 (9.46)		
Neuro-endocrine	11/222 (4.95)		
NOS	7/222 (3.15)		
Initial T status	**201/264 (76.14)**		
T1	47/201 (23.38)		
T2	59/201 (29.35)		
T3	41/201 (20.40)		
T4	55/201 (27.36)		
Initial N status	**200/264 (75.75)**		
N0	69/200 (34.50)		
N1	31/200 (15.50)		
N2	56/200 (28.00)		
N3	45/200 (27.50)		
Initial M status	**224/264 (94.95)**		
M0	61/264 (27.23)		
M1	164/264 (73.21)		
Mets at NSCLC ID (other than BM)	**100/264 (37.88)**		
Liver	12/100 (12.00)		
Lung	29/100 (29.00)		
Bone	22/100 (22.00)		
Adrenal Gland	29/100 (29.00)		
Other	8/100 (8.00)		
BM count	**236/264 (89.39)**		
1	159/236 (67.37)		
2	28/236 (11.86)		
≥3	49/236 (20.76)		
BM localization (largest lesion)	**225/264 (85.22)**		
Supratentorial	181/225 (80.44)		
Infratentorial	44/225 (19.56)		
Primary tumor mutational status	**66/264 (25.00)**		
KRAS	9/66 (13.64)		
EGFR	7/66 (10.61)		
MET	3/66 (4.55)		
BRAF	0/66 (0)		
ALK	1/66 (1.52)		
ROS	1/66 (1.52)		
FGFR3	4/66 (6.06)		
PIK3CA	2/66 (3.03)		

(Continued)

TABLE 1 Continued

	N (%)	Mean	Std. dev.
TP53	9/66 (13.64)		
BM mutational status	**92/264 (34.85)**		
KRAS	15/92 (16.30)		
EGFR	9/92 (9.78)		
MET	1/92 (1.09)		
BRAF	2/92 (2.17)		
ALK	1/92 (1.09)		
ROS	2/92 (2.17)		
FGFR3	2/92 (2.17)		
PIKC3A	3/92 (3.26)		
TP53	23/92 (25.00)		
Treatment after NSCLC diagnosis	**159/264 (60.23)**		
CTX after NSCLC diagnosis	**133/264 (83.65)**		
RT after BM diagnosis	**159/264 (60.23)**		
WBRT	8/159 (5.03)		
SBRT / GKS	109/159 (71.24)		
ICB	**46/264 (17.42)**		
Type of operative approach	**256/264 (97.00)**		
Total resection	244/256 (96.06)		
Partial resection	4/256 (1.56)		
Biopsy	8/256 (3.12)		
Known positive smoking status	**133/264 (50.37)**		
Seizures	**67/264 (25.38)**		
Meningeosis carcinomatosa	**8/264 (3.03)**		
Follow up time	**261/264 (98.86)**	22.56	26.86

KPS, Karnofsky Performance Status; NOS, not otherwise specified; NSCLC, non-small cell lung cancer; ID, initial diagnosis; BM, brain metastasis; CTX, chemotherapy; RT, radiation therapy; WBRT, whole brain radiotherapy; SBRT, stereotactic body radiation; GKS, gamma knife surgery; ICB, immune checkpoint blockade.

[Figure 2A, median 16.13 ± 3.85 vs. 9.20 ± 1.39 months, p = 0.036, log-rank (Mantel–Cox) test]. The adjusted OS was 11.47 ± 0.95 months. A statistically significant difference between survival rates after brain surgery was again not reached between male and female patients, with a trend pointing toward a survival benefit of female patients [Figure 2B, p = 0.165, log-rank (Mantel–Cox) test]. In addition, no survival benefit was seen in patients diagnosed with BM less than 2 months after the NSCLC diagnosis [Figure 2C, p = 0.597, log-rank (Mantel–Cox) test].

Despite the observed statistically significant OS benefit of patients affected with fewer than two BM, we did not find the same effect on the survival time after neurosurgical intervention [Figure 2D, p = 0.108, log-rank (Mantel–Cox) test]. When comparing the size of solitary BM as seen in the volumetric measurements of contrast-enhanced areas in T1-weighted magnetic resonance imaging (MRI), we observed a trend toward an improved survival of patients with tumors <7 cm^3 [Figure 2E, p = 0.097, log-rank (Mantel–Cox) test].

To further delineate the effects of the systemic metastatic status on OS, patients were stratified according to their systemic and intracranial metastatic load at the time of BM diagnosis. We stratified the patients into three groups; singular brain metastasis with concurrent systemic metastases, solitary brain metastasis (no concurrent systemic metastases), and multiple brainmetastases and observed a significant survival benefit inpatients with solitary BM status [Figure 2F, median: 8.47 ± 1.71, 22.03 ± 7.29 and 9.20 ± 2.81 months, respectively, p=0.018, log-rank (Mantel–Cox) test].

A supra- vs. infratentorial localization of BM had no effect on survival again after neurosurgical [Figure 2G, p = 0.912, log-rank (Mantel–Cox) test], neither did the comparison between mass-edema indices <1 and >1 [Figure 2H, p = 0.998, log-rank (Mantel–Cox) test].

We compared the groups of patients diagnosed with BM at NSCLC diagnosis, patients who previously received systemic chemotherapy (CT) for their underlying NSCLC disease (labeled “after CT”), and patients who received any combination of immune checkpoint blockade (ICB) and chemotherapeutics prior to their BM diagnosis (labeled “after IT”) and saw a slight trend toward a survival benefit of patients that previously received a combination of CT and ICB [Figure 2I, median 9.80 ± 1.87 vs. 22.73 ± 7.09 vs. 10.87 ± 2.34 months,

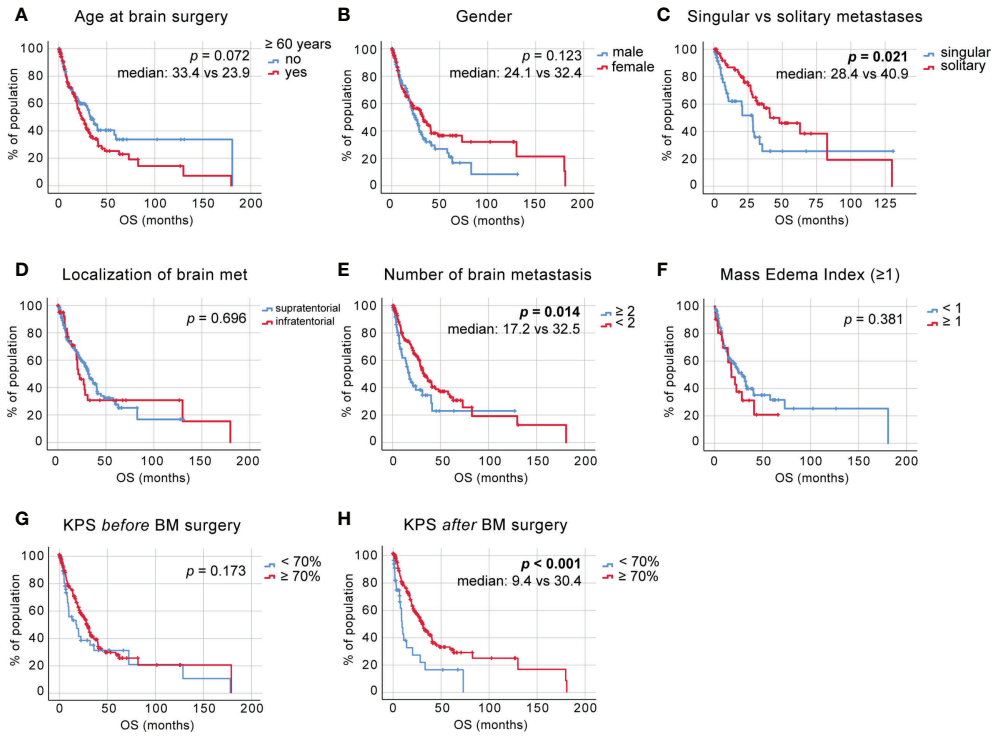

FIGURE 1
Overall survival (OS) in non-small cell lung cancer (NSCLC) brain metastases (BM) patients **(A)** Kaplan–Meier survival analysis of OS from the time point of initial diagnosis in patients <60 and >60 years of age, **(B)** in male vs. female patients, **(C)** in patients with a singular vs. solitary BM status, **(D)** depending on BM localization, **(E)** depending on the number of BM, **(F)** depending on the mass-edema index (MEI), **(G)** depending on the preoperative Karnofsky Performance Status (KPS) score, and **(H)** depending on the KPS score at discharge.

respectively, p = 0.285, log-rank (Mantel–Cox) test], which we will follow up in further studies.

We again scored our patients according to the KPS and analyzed survival post-BM resection. This analysis showed that patients with a KPS of >70 at initial diagnosis show significantly improved postoperative survival [Figure 2J, median 7.57 ± 1.66 vs. 12.5 ± 1.57 months, p = 0.003, log-rank (Mantel–Cox) test]. The increase in survival also became apparent when comparing KPS scores at discharge [Figure 2K, median 7.60 ± 3.24 vs. 12.23 ± 1.63 months, p = 0.010, log-rank (Mantel–Cox) test]. In addition, KPS changes due to the surgical intervention demonstrated to also have a significant impact on survival from the time point of BM surgery [Figure 2L, median 7.60 ± 3.41 and 12.23 ± 1.96, respectively, p = 0.030].

Clinically favorable patient population

To further dissect the effects of these clinical determinants on the survival probabilities of specific patient groups after surgical intervention, we incorporated relevant findings from the univariate analyses into a multivariate analysis. Significant factors affecting postoperative survival are shown in Table 2 and were incorporated in a Cox regression analysis. This includes 1) the presence of solitary vs. multiple BM (HR 1.034, 95% CI 0.316 – 0.819, p = 0.005) and 2) pre-operative KPS (HR 0.981, 95% CI 0.967 – 0.996, p = 0.011) as well as age (HR 1.034, 95% CI 1.009 – 1.059, p = 0.007). Stratification of the patient cohort by singular or solitary BM status showed a significant survival benefit of patients with solitary BM in Cox regression analysis [Figure 3A, HR =0.608, CI 0.386 - 0.958, p = 0.032].

Further, we classified the patient cohort into a favorable outcome group (solitary BM, age <60 years) and an unfavorable outcome group (singular and multiple BM, age >60 years) and performed Cox regression analysis, which demonstrated significantly increased survival after BM surgery in patients aged 60 years and younger with a solitary BM status (no concurrent systemic metastases) [Figure 3B, HR 0.172, CI 0.070 – 0.423, p <0.001].

Discussion

In this large single-center retrospective analysis of NSCLC BM patients, we aimed to understand the effects of the most common clinical determinants on patient survival after the initial diagnosis and neurosurgical intervention. The study cohort contained 264

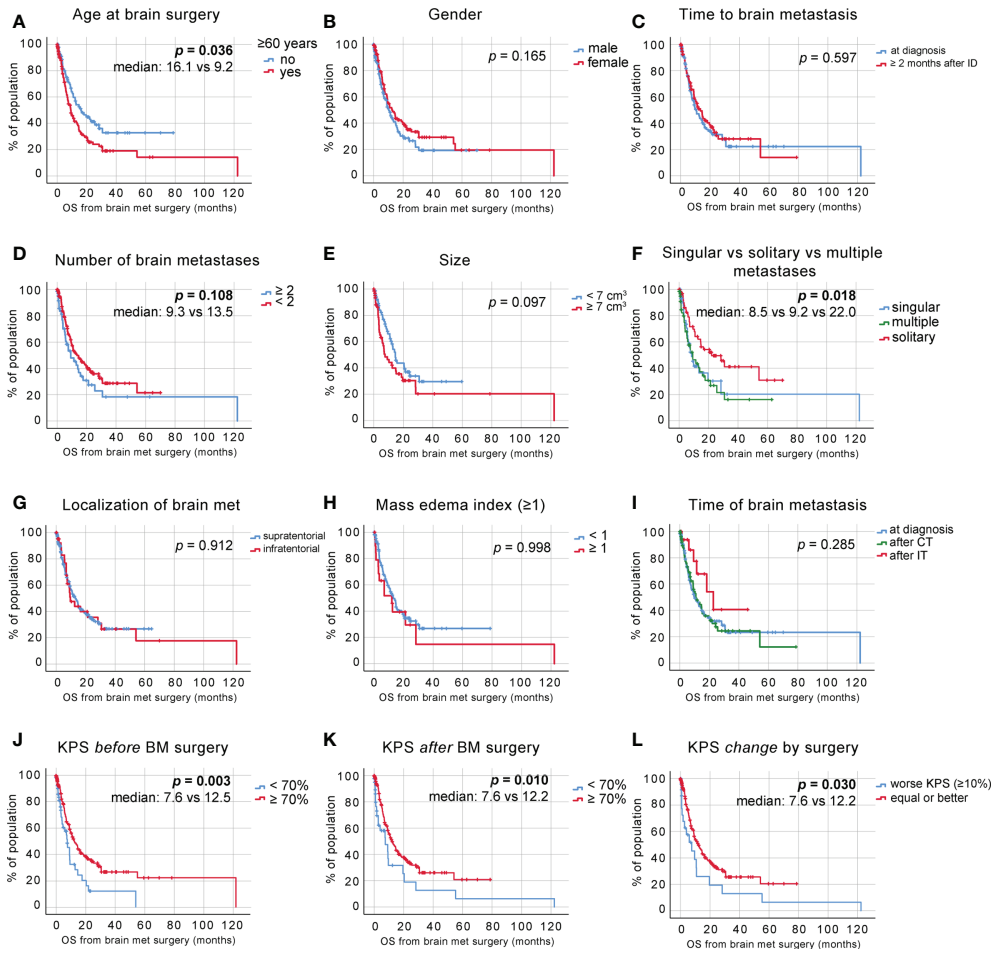

FIGURE 2
OS postneurosurgical intervention. **(A)** Kaplan–Meier survival analysis postneurosurgical intervention in patients <60 and >60 years of age, **(B)** in male vs. female patients, **(C)** depending on the time to BM diagnosis, **(D)** depending on the number of BM, **(E)** depending on the size of BM, **(F)** in patients with singular vs. solitary vs. multiple BM status, **(G)** depending on BM localization, **(H)** depending on the MEI, **(I)** depending on postdiagnosis treatment (at diagnosis—no treatment pre-non-small cell lung cancer (NSCLC) BM diagnosis, after CT—chemotherapy treatment pre-NSCLC BM diagnosis, and after immunotherapy (IT)— immune checkpoint blockade treatment pre-NSCLC BM diagnosis), **(J)** depending on the preoperative KPS score, **(K)** depending on the KPS score at discharge, and **(L)** depending on the KPS score change due to surgical intervention.

patients, with similar clinical characteristics as had previously been reported for the patients affected by this disease (11–13). The median OS of the herein-reported patient cohort was 15.0 ± 2.27 months, which was thus higher than the 377 retrospectively analyzed patients by Jünger et al. (median OS 14.1 months, 95% CI 12.2 – 15.8) (12), or 126 NSCLC patients analyzed by Fabi et al. (median OS 12 months, CI 9.0 – 16.0) (13). The reasons for this apparent increase in OS are manifold and may include, among others, improvements in surgical and imaging techniques and targeted molecular therapies as well as recent technological developments in radiotherapy. Intriguingly, the presented cohort consisted of 54.17% female patients, despite a distinctively higher prevalence of NSCLC diagnoses in male patients within the German population [for example, 34.690/53.500 (64.84%) of NSCLC patients in 2016 were men (14)]. Accordingly, most studies with comparable patient populations have reported a higher incidence of the male gender [54.9% in the study by Jünger and colleagues (12) and 52.4% in the study by Smith et al. (15)]. A possible explanation was sought in the predominance of adenocarcinomas identified in our patient cohort (82.43%) as these are generally more commonly found—and steadily increasing—in female patients (14); however, similar disseminations of histological diagnoses could be observed in the aforementioned studies [78.4% and 82.0%, respectively, (12, 15)]. Thus, additional factors might have contributed to the predominance of female patients that will be interesting to evaluate in future studies.

The rise of SBRT as first-line postoperative treatment modality has enabled the localized treatment of multiple intracerebral lesions and, partly owing to concerns about

10.3389/fonc.2022.951805

TABLE 2 Clinical determinants for overall survival and survival after surgery.

Clinical determinants for overall survival	Univariate (Log Rank) p-value	COX regression HR, 95%CI, p-value
Age (<60 years)	$p = 0.072$	
Female gender	$p = 0.123$	
Solitary BM status	$\mathbf{p = 0.021}$*	0.509, 0.316 – 0.819, p = 0.005
BM localization	$p = 0.696$	
Mass-edema index	$p = 0.381$	
KPS pre-op	$p = 0.173$	
KPS post-op	**p < 0.001***	0.980, 0.968 – 0.992, p = 0.001
Clinical determinants for survival after surgery		
Age (<60 years)	$\mathbf{p = 0.036}$*	1.034, 1.009 – 1.059, p = 0.007
Female gender	$p = 0.165$	
BM at NSCLC ID	$p = 0.597$	
<2 BM	$p = 0.108$	
Size (<7cm^3)	$p = 0.097$	
Solitary BM status	$\mathbf{p = 0.032}$*	1.034, 0.316 – 0.819, p = 0.005
BM localization	$p = 0.912$	
Mass-edema index	$p = 0.998$	
Previous treatment	$p = 0.285$	
KPS pre-op	$\mathbf{p = 0.003}$*	0.981, 0.967 – 0.996, p = 0.011

*included in COX regression.
BM, brain metastases; KPS, Karnofsky Performance Status; NSCLC, non-small cell lung cancer; ID, initial diagnosis.

cognitive decline in patients receiving WBRT, has been recommended for patients with one-to-four lesions in the American Society of Radiation Oncology (ASTRO) guidelines since 2012 (16). More recently, further technological improvements have enabled the expansion of stereotactic radiosurgery (SRS) indications to include patients with up to 10 BM lesions and multiple clinical trials exploring the efficacy of SRS in patients with >20 BM are currently ongoing (17, 18), thus enabling a more targeted and localized control of brain metastatic disease for an increasing number of patients. Moreover, despite suffering from inconsistent response rates in cerebral metastases, recent targeted therapies such as ICB have undoubtedly enabled a more personalized treatment approach in oncological patients. In our analysis, we saw that a treatment with a combination of chemotherapeutics and ICB seemed to favor longer survival without quite reaching statistical significance and thus has to be analyzed in a larger cohort in the near future. A recent study by Rounis etal. (19) focused specifically on a subgroup of patients who received PD-1/PD-L1 inhibitors as treatment for NSCLC BM and found that specific clinical parameters, such as age <70 years, prior CNS radiation, and the synchronous appearance of BM, significantly affected

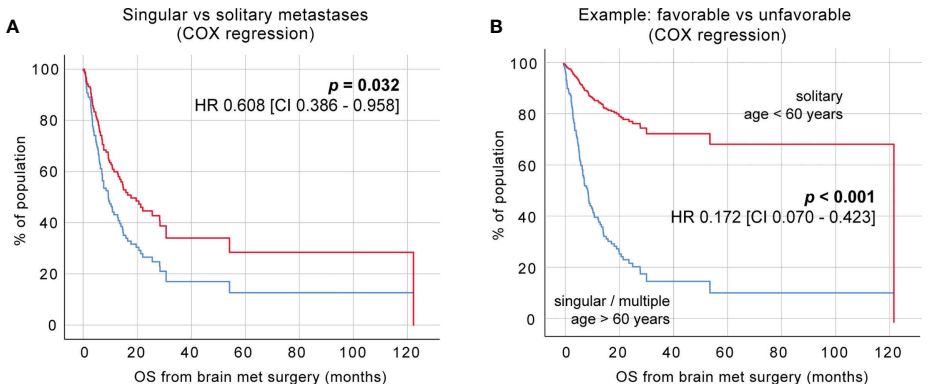

FIGURE 3
Identification of favorable clinical subgroups. **(A)** Cox regression of a singular vs. solitary BM status. **(B)** Cox regression of favorable vs. unfavorable patient groups.

ICB disease control. However, it is important to point out that this study was focused on the patients who received ICB as monotherapy, as opposed to the patients included in our cohort, who received any combination of CT and ICB.

Our findings suggest that the most significant factors affecting OS are 1) a lack of additional systemic metastases ("solitary BM lesion") and 2) the number of BM lesions at the time of BM diagnosis. The stratification of patients into singular BM with concurrent systemic metastases, solitary BM without systemic affection, or multiple metastases at the time of BM surgery has shown a significant difference with an almost threefold increase in survival post neurosurgical intervention in patients with a solitary BM status (median 8.5 vs. 9.2 vs. 22.0 months, respectively, Figure 2F). This discernible effect of the number of metastatic lesions on OS underlines the idea that oligometastatic disease—as proposed by Samuel Hellman and Ralph Weichselbaum in their seminal paper in 1995 (20)—might represent a different spectrum of metastatic disease than widespread disease and should, in this case, be considered amenable to a curative therapeutic strategy (20, 21). The paradigm shift necessary to distinguish oligometastasized patients from those with widespread, multifocal disease could help identify clinically favorable subgroups and enhance our understanding of personalized treatment strategies. Purely by focusing on factors positively correlated with OS, we were able to identify patients with clinically favorable features (solitary BM, age <60 years) with a mean OS of 53.82 months, which is noteworthy since it extends the scope of patient survival far beyond the mean values currently discussed for BM patients in the literature. Nevertheless, more focused studies are needed to identify these patient groups and understand the nature and extent of cerebral oligometastatic disease. A positive outlook is provided by the studies of oligometastatic disease affecting other organs, such as a recent study by Pitroda etal. (22), in which the authors performed an integrative analysis of 134 patients affected by one-to-three liver metastases and were able to identify three groups with a 10-year OS rate of 94%, 45%, and 19%, respectively (22).

Additionally, to the number of metastases, when adjusted for survival after neurosurgical intervention, we identified age <60 years as a predictor of significantly increased patient survival after analyzing multiple age cut-off values. Interestingly, this survival difference only delineated as a significant predictor after adjusting the survival for values after neurosurgical intervention as opposed to the survival time after initial BM diagnosis. Few of the aforementioned studies adjusted for this distinction; thus, it would be interesting to evaluate whether and how the survival benefit perceived in younger patients is connected with neurosurgical interventions. In line with the positive effects of younger age on the survival of NSCLC BM patients, the overall disease status exemplified by higher KPS values also showed an expected positive effect on OS as well as survival post-BM surgery. Intriguingly, when comparing the OS values, we found that the preoperative KPS did not show a significant effect ($p = 0.173$, Figure 1G), whereas a postoperative KPS >70% did show a significant OS benefit (median 9.4 vs. 30.4, $p < 0.001$). When comparing the impact of KPS on survival post-BM resection, we found that both pre- and postop KPS scores >70% showed significantly increased survival (Figures 2K–M). This finding is important because it signifies the effect of BM surgery on the course of the disease—a postoperative decrease in the KPS score significantly impacts the course of disease with an overall reduction of survival.

Over 80% of the brain metastatic lesions were classified as adenocarcinomas, followed by squamous cells, with similar numbers recently reported (12). The rate and dissemination of genetic mutations was inconsistent between primary tumors and matched BM lesions, as exemplified by the difference in mutations affecting *TP53* (13.64% in primary tumor vs. 25.00% in BM) or *KRAS* (13.64% in primary tumor vs. 16.30% in BM). Apart from the possibility of technological disparities (as analyses were, in some cases, conducted in separate centers), this disparity correlates with the recent reports of altered genetic mutations observed in whole exome sequencing between 86 primary lung cancers and their matched BM (23). Surprisingly, the rate of *EGFR*-mutated lung cancers in our cohort was 9.78%, while comparable studies (15) reported 22.2% and 13.6% (12), respectively. Furthermore, mutations in *KRAS* have been reported as the most common genetic mutations in NSCLC, with mutation rates of approximately 30% (17), yet they were surpassed by the rate of *TP53* mutations in our observations.

A significant limitation of this study is the lack of the availability of the mutational status in the majority (65.15%) of patient cases. This may partly be due to the length of the observational period starting in 2015, as the rate of molecular analyses has significantly increased in the past years and could also represent a lack of accessible patient information, as the molecular analyses in our center are, in many cases, initiated by the departments continuing the treatment after neurosurgical resection (oncology and radiotherapy) and might not be readily accessible. Comparable studies (12) similarly reported the mutational status in 37.7% of cases. Nevertheless, a trend in survival benefit after neurosurgical resection was revealed in patients receiving ICB + CTX combination treatment and median OS reached 36.1 months in this group. Additional additional analyses of this subcohort will be further addressed in our future studies. Another limitation of our study is the lack of consistent follow-up information after patient discharge. Despite our efforts to incorporate every piece of available data, in our university hospital setting, patients are discharged early after neurosurgical intervention and the majority of postoperative radiotherapy and oncologic treatments are continued in ambulatory settings. The data from these institutions are not routinely made available to us.

As opposed to a study by Spanberger et al. (24), who described a significant survival benefit in patients with smaller peritumoral brain edema, in our cohort, we did not identify

peritumoral brain edema as a significant factor on OS and survival after neurosurgical intervention. However, this may be, in part, due to the difference in the measurement and grading of PTB as well as interobserver bias. A recent study by Berghoff and colleagues showed a positive correlation between the extent of peritumoral brain edema and the density of $CD8^+$ tumor-infiltrating lymphocytes (TILs) associated with favorable median OS times. However, one might argue that the increase in OS in this study cohort was mainly driven by the number of TILs rather than the extent of edema, as outlined in the significant correlation between the survival prognosis and the immunoscore (25). Importantly, this study analyzed BM from multiple primary tumors with the highest TIL infiltration observed in melanoma and renal cancer.

Taken together, our study highlights the importance of understanding the clinical course in NSCLC patients with BM for risk stratification and clinical decision-making in the era of interdisciplinary tumor boards. With improved surgical techniques and the introduction of intraoperative neuromonitoring or neuronavigation, the overall morbidity of BM resection has decreased over the past decades (10). Together with significant advances in targeted- and immuno-oncological treatment options, as well as improved radiotherapy protocols, patients diagnosed with NSCLC BM represent a patient population whose survival may significantly benefit from the use of aggressive multimodal therapy, even in the cerebrally metastatic—and especially so in the oligometastatic - stage.

Methods

Patient characteristics and study cohort

The electronic patient database was queried for patients aged 18 years or older who underwent surgery in our institution for NSCLC BM during the period 01/2014–12/2020. Key demographic and clinical parameters were identified, and the course of disease as well as follow-up screenings were extracted from the external physician's letters where appropriate. The disease stage at the initial diagnosis was stratified according to the 7th edition of the UICC TNM classification. The smoking status was stratified according to the packages of cigarettes or equivalent tobacco products per day and years smoked (pack years, py).

Histological results were obtained from biopsies and surgically resected tumor tissues and examined regularly by the senior physicians of the departments of pathology and neuropathology at the University Medical Center Hamburg-Eppendorf. Patients with differing histological diagnoses were excluded from analysis. The mutational analyses and PD-L1 expression of primary tumor tissues were conducted in the department of pathology or extracted from external reports.

The period between the primary tumor diagnosis and BM was calculated from the date of the histological diagnosis of the primary tumor (either in our institution or from the external physician's letters) until the date of the histological diagnosis of BM. OS was calculated from the time of the histological diagnosis of the primary NSCLC tumor or the histological diagnosis of BM to the date of death or last follow-up, extracted from the external physician's letters where applicable.

A team of experienced neurosurgeons performed all surgeries and intraoperative navigation. Additional supportive techniques (i.e., neuromonitoring) were applied in the cases deemed necessary by the primary surgeon. Postoperative treatment decisions as well as decisions about follow-up screenings and procedures were reached within an interdisciplinary institutional tumor board, involving board-certified neurosurgeons, medical oncologists, radiation oncologists, and neuroradiologists.

Data analysis was performed on anonymized data sets. The study was conducted in accordance with the ethical guidelines of the Helsinki Declaration and the Hamburger Hospital Act.

MRI and volumetry

The size, number, and extent of intracranial tumors were assessed in three-dimensional reconstructions of coronal, axial, and sagittal planes and measured in cm^3 using Brainlab software (Version 4.0.0.159, Brainlab AG, Munich, Germany) in presurgical MRI scans [pre- and postcontrast T1-weighted sequences, T2-weighted sequences, and/or fluid attenuated inversion recovery (FLAIR) sequences]. For this, the regions of interest (ROIs) were contoured semimanually around contrast-enhanced regions in each slice of T1-weighted MRI images and PTB was identified as obvious perifocal hyperintensity using the same method in T2-weighted or FLAIR images. The MEI was measured from the tumor border and calculated by dividing the size of the tumor in T1-weighted images and the size of edema in T2-weighted images. The localization of BM was stratified into 1) supra-/infratentorial, 2) main cerebral lobe affected (frontal, parietal, temporal, occipital, cerebellar, and other), 3) depth from the cortex (0 = in direct contact with dura mater cerebri, 1 = less than 1 cm below cortex, 2 = >1 cm below cortex). In the case of multiple intracerebral lesions, the MEI and localization of the largest lesion were used for survival stratification.

Statistical analysis

Statistical analysis was performed using SPSS Statistics Version 25 (IBM, Armonk, NY, USA). Metric data are presented with means and standard deviations (Table 1). Kaplan–Meier estimates were used as a non-parametric statistic to calculate survivals depending on patient characteristics (Figures 1 and 2; Table 2). The survival distributions were compared using the log-rank test. Median survival times, 95% confidence intervals, and patients at risk were provided for

Kaplan–Meier estimates. Subsequently, significant patient characteristics were tested for multicollinearity using a Pearson correlation matrix and variance inflation factors. For Cox regression analysis (Table 2), significant patient characteristics were selected according to the results of collinearity analysis. Survival curves were calculated and plotted from Cox proportional hazards (Figure 3). Additionally, hazard ratios and the corresponding 95% confidence intervals are provided. Patients lost to follow-up or still alive at the end of the observation period were censored in statistical survival analysis. P-values lower than 0.05 were considered statistically significant and stratified as $p < 0.05$ (*), $p < 0.01$ (**), and $p < 0.001$ (***). All statistical analyses were reviewed by an experienced statistician from the Institute of Medical Biometry and Epidemiology, University Medical Center Hamburg Eppendorf.

Data availability statement

The anonymized data sets are available on reasonable request. Requests to access the datasets should be directed to a.piffko@uke.de.

Ethics statement

The studies involving human participants were reviewed and approved by Hamburg ethics committee. Written informed consent for participation was not required for this study in accordance with the national legislation and the institutional requirements.

Author contributions

Conceptualization: AP, TS, and MM. Methodology: AP and TS. Software: AP and TS. Data curation: AP, BA, and IR. Formal analysis: AP, TS, and MM. Investigation: AP, BA, IR, and CM. Resources: LD, MW, KL, HW, and JS. Writing—original draft preparation: AP, MM, and TS. Writing—review and editing: CM, LD, HW, IR, and JS. Visualization: AP and TS. Funding acquisition: MW, KL, HW, and JS. All authors contributed to the article and approved the submitted version.

Funding

The work was supported by the Bender Stiftung, Sander Stiftung (to HW and MM), and the Erich and Gertrud Roggenbuck Stiftung (to MM).

Acknowledgments

The authors would like to thank Linda Krause, PhD, from the Institute of Medical Biometry and Epidemiology, University Medical Center Hamburg-Eppendorf for her close revision and support for this work.

Conflict of interest

The authors declare that the research was conducted in the absence of any commercial or financial relationships that could be construed as a potential conflict of interest.

Publisher's note

Supplementary material

The Supplementary Material for this article can be found online at: https://www.frontiersin.org/articles/10.3389/fonc.2022.951805/full#supplementary-material

SUPPLEMENTARY TABLE 1
Patient no. at risk (including censored events) for 0, 50, 100, 150 and 200 months after BM diagnosis for

SUPPLEMENTARY TABLE 2
Patient no. at risk (including censored events) for 0, 20, 40, 60, 80, 100 and 120 months after BM surgery for Figure 2.

References

1. Siegel RL, Miller KD, Fuchs HE, Jemal A. Cancer statistics 2021. *CA: A Cancer J Clin* (2021) 71(1):7–335. doi: 10.3322/caac.21654

2. Borghaei H, Paz-Ares L, Horn L, Spigel DR, Steins M, E Ready N, et al. Nivolumab versus docetaxel in advanced nonsquamous non–Small-Cell lung cancer. *N Engl J Med* (2015) 373(17):1627–39. doi: 10.1056/nejmoa1507643

3. Mok TSK, Wu Y-L, Kudaba I, Kowalski DM, Cho BC, Turna HZ, et al. "Pembrolizumab versus chemotherapy for previously untreated, PD-L1-Expressing, locally advanced or metastatic non-Small-Cell lung cancer (KEYNOTE-042): A randomised, open-label, controlled, phase 3 trial." *Lancet (London England)* (2019) 393(10183):1819–30. doi: 10.1016/S0140-6736(18)32409-7

4. Garassino MC, Gadgeel S, Esteban E, Felip E, Speranza G, Domine M, et al. Patient-reported outcomes following pembrolizumab or placebo plus pemetrexed and platinum in patients with previously untreated, metastatic, non-squamous non-Small-Cell lung cancer (KEYNOTE-189): A multicentre, double-blind, randomised, placebo-controlled. *Lancet Oncol* (2020) 21(3):387–97. doi: 10.1016/S1470-2045(19)30801-0

5. Duma N, Santana-Davila R, Molina JR. Non–small cell lung cancer: Epidemiology, screening, diagnosis, and treatment. *Mayo Clin. Proc* (2019) 94(8) :1623–40. doi: 10.1016/j.mayocp.2019.01.013

6. Rybarczyk-Kasiuchnicz A, Ramlau R, Stencel K. Treatment of brain metastases of non-small cell lung carcinoma. *Int J Mol Sci* (2021) 22(2):593. doi: 10.3390/ijms22020593

7. Nayak L, Lee EQ, Wen PY. Epidemiology of brain metastases. *Curr Oncol Rep* (2012) 14(1):48–545. doi: 10.1007/s11912-011-0203-y

8. Moravan MJ, Fecci PE, Anders CK, Clarke JM, Salama AKS, Adamson JD, et al. Current multidisciplinary management of brain metastases. *Cancer* (2020) 126(7):1390–406. doi: 10.1002/cncr.32714

9. Mitchell DK, Kwon HJ, Kubica PA, Huff WX, O'Regan R, Dey M. Brain metastases: An update on the multi-disciplinary approach of clinical management. *Nature Reviews Clinical Oncology* (2020) 68(1): 69–85. doi: 10.1016/j.neuchi.2021.04.001

10. Proescholdt MA, Schödel P, Doenitz C, Pukrop T, Höhne J, Schmidt NO, et al. The management of brain metastases–systematic review of neurosurgical aspects. *Cancers* (2021) 13(7): 1616. doi: 10.3390/CANCERS13071616

11. Walker MS, Wong W, Ravelo A, Miller PJE, Schwartzberg LS. Effect of brain metastasis on patient-reported outcomes in advanced NSCLC treated in real-world community oncology settings. *Clin Lung Cancer* (2018) 19(2):139–475. doi: 10.1016/j.cllc.2017.10.003

12. Jünger ST, Schödel P, Ruess D, Ruge M, Brand JS, Wittersheim M, et al. Timing of development of symptomatic brain metastases from non-small cell lung cancer: Impact on symptoms, treatment, and survival in the era of molecular treatments. *Cancers* (2020) 12(12):1–10. doi: 10.3390/cancers12123618

13. Fabi A, Felici A, Metro G, Mirri A, Bria E, Telera S, et al. Brain metastases from solid tumors: Disease outcome according to type of treatment and therapeutic resources of the treating center. *J Exp Clin Cancer Res* (2011) 30(1):10. doi: 10.1186/1756-9966-30-10

14. Barnes B. *Bericht zum Krebsgeschehen in Deutschland 2016*. Zentrum für Krebsregisterdaten im Robert Koch-Institut (Hrsg). Berlin (2016).

15. Smith DR, Bian Y, Wu C-C, Saraf A, Tai C-H, Nanda T, et al. Natural history, clinical course and predictors of interval time from initial diagnosis to development of subsequent NSCLC brain metastases. *J Neuro-Oncol* (2013) 143:145–55. doi: 10.1007/s11060-019-03149-4

16. Tsao MN, Rades D, Wirth A, Lo SS, Danielson BL, Gaspar LE, et al. Radiotherapeutic and surgical management for newly diagnosed brain Metastasis (Es): An American society for radiation oncology evidence-based guideline. *Pract Radiat Oncol* (2012) 2(3):210. doi: 10.1016/J.PRRO.2011.12.004

17. Suh JH, Kotecha R, Chao ST, Ahluwalia MS, Sahgal A, Chang EL. Current approaches to the management of brain metastases. *Nat Rev Clin Oncol* (2020) 17:279–99. doi: 10.1038/s41571-019-0320-3

18. Yamamoto M, Serizawa T, Shuto T, Akabane A, Higuchi Y, Kawagishi J, et al. Stereotactic radiosurgery for patients with multiple brain metastases (JLGK0901): A multi-institutional prospective observational study." *Lancet Oncol* (2014) 15(4):387–95. doi: 10.1016/S1470-2045(14)70061-0

19. Rounis K, Skribek M, Makrakis D, De Petris L, Agelaki S, Ekman S, et al. Correlation of clinical parameters with intracranial outcome in non-small cell lung cancer patients with brain metastases treated with pd-1/Pd-L1 inhibitors as monotherapy. *Cancers* (2021) 13(7): 1562. doi: 10.3390/cancers13071562

20. Weichselbaum RR, Hellmann S. Oligometastases. *J Clin Oncol* (1995) 13 (1):8–105. doi: 10.1200/JCO.1995.13.1.8

21. Weichselbaum RR. The 46th David a. karnofsky memorial award lecture: Oligometastasis — from conception to treatment. *J Clin Oncol* (2018) 36(32):3240–50. doi: 10.1200/JCO.18.00847

22. Pitroda SP, Khodarev NN, Huang L, Uppal A, Wightman SC, Ganai S, et al. Integrated molecular subtyping defines a curable oligometastatic state in colorectal liver metastasis. *Nat Commun* (2018) 9(1): 1793. doi: 10.1038/s41467-018-04278-6

23. Brastianos PK, Carter SL, Santagata S, P. Cahill D, Taylor-Weiner A, . Jones RT, et al. Genomic characterization of brain metastases reveals branched evolution and potential therapeutic targets. *Cancer Discov* (2015) 5(11):1164–775. doi: 10.1158/2159-8290.cd-15-0369

24. Spanberger T, Berghoff AS, Dinhof C, Ilhan-Mutlu Aysegül, Magerle M, Hutterer M, et al. Extent of peritumoral brain edema correlates with prognosis, tumoral growth pattern, HIF1a expression and angiogenic activity in patients with single brain metastases. *Clin Exp Metastasis* (2013) 30(4):357–68. doi: 10.1007/s10585-012-9542-9

25. Berghoff AS, Fuchs E, Ricken G, Mlecnik B, Bindea G, Spanberger T, et al. Density of tumor-infiltrating lymphocytes correlates with extent of brain edema and overall survival time in patients with brain metastases. *OncoImmunology* (2016) 5(1):e1057388. doi: 10.1080/2162402X.2015.1057388

frontiers | Frontiers in Oncology

TYPE Systematic Review
PUBLISHED 08 December 2022
DOI 10.3389/fonc.2022.1025664

OPEN ACCESS

EDITED BY
David Kaul,
Charité Universitätsmedizin Berlin, Germany

REVIEWED BY
David Wasilewski,
Charité University Medicine Berlin, Germany
Wendy Sherman,
Mayo Clinic Florida, United States

*CORRESPONDENCE
Xiang-Lin Tan
xianglin.tan@merck.com

†These authors have contributed equally to this work

SPECIALTY SECTION
This article was submitted to Neuro-Oncology and Neurosurgical Oncology, a section of the journal Frontiers in Oncology

RECEIVED 23 August 2022
ACCEPTED 24 November 2022
PUBLISHED 08 December 2022

CITATION
Tan X-L, Le A, Scherrer E, Tang H, Kiehl N, Han J, Jiang R, Diede SJ and Shui IM (2022) Systematic literature review and meta-analysis of clinical outcomes and prognostic factors for melanoma brain metastases. *Front. Oncol.* 12:1025664. doi: 10.3389/fonc.2022.1025664

Systematic literature review and meta-analysis of clinical outcomes and prognostic factors for melanoma brain metastases

Xiang-Lin Tan[1*†], Amy Le[2†], Emilie Scherrer[1,3], Huilin Tang[4], Nick Kiehl[2], Jiali Han[4], Ruixuan Jiang[1], Scott J. Diede[1] and Irene M. Shui[1]

[1]Merck & Co., Inc., Rahway, NJ, United States, [2]Department of Epidemiology, Richard M. Fairbanks School of Public Health, Indiana University, Indianapolis, IN, United States, [3]Seagen Inc., Bothell, WA, United States, [4]Integrative Precision Health, LLC, Carmel, IN, United States

Background: More than 60% of all stage IV melanoma patients develop brain metastases, while melanoma brain metastases (MBM) is historically difficult to treat with poor prognosis.

Objectives: To summarize clinical outcomes and prognostic factors in MBM patients.

Methods: A systematic review with meta-analysis was conducted, and a literature search for relevant studies was performed on November 1, 2020. Weighted average of median overall survival (OS) was calculated by treatments. The random-effects model in conducting meta-analyses was applied.

Results: A total of 41 observational studies and 12 clinical trials with our clinical outcomes of interest, and 31 observational studies addressing prognostic factors were selected. The most common treatments for MBM were immunotherapy (IO), MAP kinase inhibitor (MAPKi), stereotactic radiosurgery (SRS), SRS+MAPKi, and SRS+IO, with median OS from treatment start of 7.2, 8.6, 7.3, 7.3, and 14.1 months, respectively. Improved OS was observed for IO and SRS with the addition of IO and/or MAPKi, compared to no IO and SRS alone, respectively. Several prognostic factors were found to be significantly associated with OS in MBM.

Conclusion: This study summarizes pertinent information regarding clinical outcomes and the association between patient characteristics and MBM prognosis.

KEYWORDS

melanoma, brain metastasis, immunotherapy, targeted therapy, radiosurgery, prognostic factors, outcomes

Introduction

Brain metastasis is a frequent and grave complication of melanoma (1). The median overall survival (OS) of patients with melanoma brain metastases (MBM) has historically been approximately 4 months after diagnosis. Recent studies have shown that immune checkpoint inhibitors targeting the programmed cell death protein 1 (PD1) and cytotoxic T-lymphocyte associated protein 4 (CTLA-4) pathways as well as novel small-molecule tyrosine kinase inhibitors targeting BRAF driver mutations, can improve survival in MBM (2). Margolin et al. reported a phase II trial investigating the activity of ipilimumab in MBM patients and showed that it was safe and resulted in tumor regression in some patients (3). Long et al. studied dabrafenib in BRAF mutated MBM in a phase II clinical trial, and demonstrated activity against brain metastases in MBM patients with or without prior local treatment (4). The treatment of MBM has thus shifted significantly in recent years, creating a growing body of research on novel targeted therapies in MBM in the realm of clinical oncology. However, there is still a lack of understanding of the efficacy of newer therapies for patients with MBM.

It has been suggested that patients who present with larger, symptomatic metastases are at higher risk for poorer performance status and worse prognosis, providing a strong rationale for early detection and treatment of MBM (5). An institutional database study of patients with melanoma enrolled on clinical trials from 1986 to 2004 by Davies et al. found that 330 developed MBM and prognostic factors for OS were earlier diagnosis, increased number of MBM, leptomeningeal involvement, and development of MBM after systemic therapy for extracranial metastatic disease (6). Nevertheless, prognostic factors for OS in MBM patients are not well defined.

To address these gaps in the research literature, there is a need to summarize the clinical outcomes and prognostic factors in patients with MBM at diagnosis or who develop MBM during the course of treatment. We performed a systematic review and meta-analysis to examine clinical outcomes, including OS and progression-free survival (PFS), and prognostic factors for patients with MBM, focusing on the most recent research.

Patients and methods

Study design and search strategy

This study was performed in accordance with the Preferred Reporting Items for Systematic Reviews and Meta-Analysis (PRISMA) guidelines. Relevant studies with full text articles published in English in the last five years were searched in the databases: EMBASE, MEDLINE, Cochrane Register of Controlled Trials, and Cochrane Review on November 1, 2020. Search terms included "melanoma", "brain metastasis" or "cerebral metastasis", and related terms (e.g. metastases), along with an epidemiology studies filter to include the eligible study designs (Tables S1–S4). Eligible studies were identified and selected according to the following eligibility criteria: 1) Studies published from November 1, 2015 to November 1, 2020; 2) study population are adult patients (>18 years) with melanoma who develop or present with at least one brain metastases; 3) reported clinical outcomes (OS, PFS) or prognostic factors for OS in MBM patients; 4) study designs included prospective and retrospective cohort studies, case-controls, cross-sectional studies, controlled or uncontrolled longitudinal studies; 5) no minimum sample sizes were required. Exclusion criteria included that the study was not published in English language, that the study was in animals or laboratory setting only, did not fall within the date range (published before November 1, 2015), had a duplicate study population, or if the relevant intervention (treatment) or outcomes of interest (OS, PFS, HR) were not available. Two reviewers independently selected studies according to the inclusion and exclusion criteria and extracted data, with a third independent reviewer available to address any discrepancies and perform a quality check. Bibliographies from review articles were reviewed thoroughly to identify relevant additional studies and trial results.

Data extraction

The clinical outcomes of interest for this study were OS and PFS. We extracted median OS/PFS (in months) and the hazard ratios (HR) for OS/PFS along with 95% confidence intervals (CI). Some studies reported OS/PFS from date of diagnosis of MBM (time between diagnosis of brain metastases and death or last follow up), while others reported OS/PFS from start of treatment (time from the first treatment start date to the time of death or last follow-up). We also extracted the HR and 95% CI for each prognostic factor for OS in MBM patients, including age, sex, biomarkers, performance status, intracranial and extracranial disease status, and mutation status.

Data analysis

The weighted average (by sample size) was calculated for the median months of OS by treatments. For studies that presented Kaplan-Meier (K-M) survival data without reporting HR, we used a previously published methodology for estimating HR from time-to-event analyses (7). Meta-HR for OS with corresponding 95% CIs were calculated for clinical outcomes and prognostic factors using random-effects models. Cochrane's Q test and the I^2 statistic were used to assess heterogeneity

between studies, with a *P*-value < 0.05 for Cochrane's Q test and I^2 > 50% considered cut-offs for significant heterogeneity (8, 9). The results from the meta-analysis are presented graphically as forest plots. Publication bias was assessed by contour-enhanced funnel plots of standard error against the effect estimate. All statistical analyses were performed using STATA (Version 14; Stata Corp., College Station, TX).

For clinical outcomes of observational studies, multiple studies were reported with clear information on treatment assignments for stereotactic radiosurgery (SRS) alone, MAP kinase inhibitor (MAPKi, which includes BRAFi [BRAF inhibitor] and/or MEKi [MEK inhibitor] and is used in patients with a BRAF mutation), SRS+IO, SRS+MAPKi, and SRS+MAPKi+IO. Therefore, we grouped those studies together, and performed meta-analyses for treatment comparisons by separating for those with OS from start of treatment and those with OS from date of diagnosis. However, if one study reported separate results for anti-PD1 and anti-CTLA-4 using a common reference group, these results were not grouped into a single IO group, but instead were reported separately in the summary tables.

For prognostic factors of MBM, the studies with similar definitions were grouped and meta-analysis was performed to summarize their association with OS in MBM patients. However, due to variable cut-off values and different reference groups chosen in some studies, we were not able to perform meta-analysis on all studies.

Results

Study selection

Our PRISMA study protocol is presented schematically in Figure 1. For clinical outcomes, 134 full-text articles of observational studies were screened, and 93 articles were excluded (19 due to duplication of the same population, 6 had no treatment reported, and 68 had no outcomes of interest). Ten full-text articles of clinical trials were included, and two additional clinical trials were identified from ClinicalTrials.gov. Finally, 41 observational studies and 12 clinical trials with our clinical outcomes of interest (OS and/or PFS) were included. For prognostic factors among MBM, 52 full-text articles were screened, and 21 were excluded (5 due to no clear MBM information, and 16 due to no HR). Thirty-one full-text papers for prognostic factors were included in the final analysis.

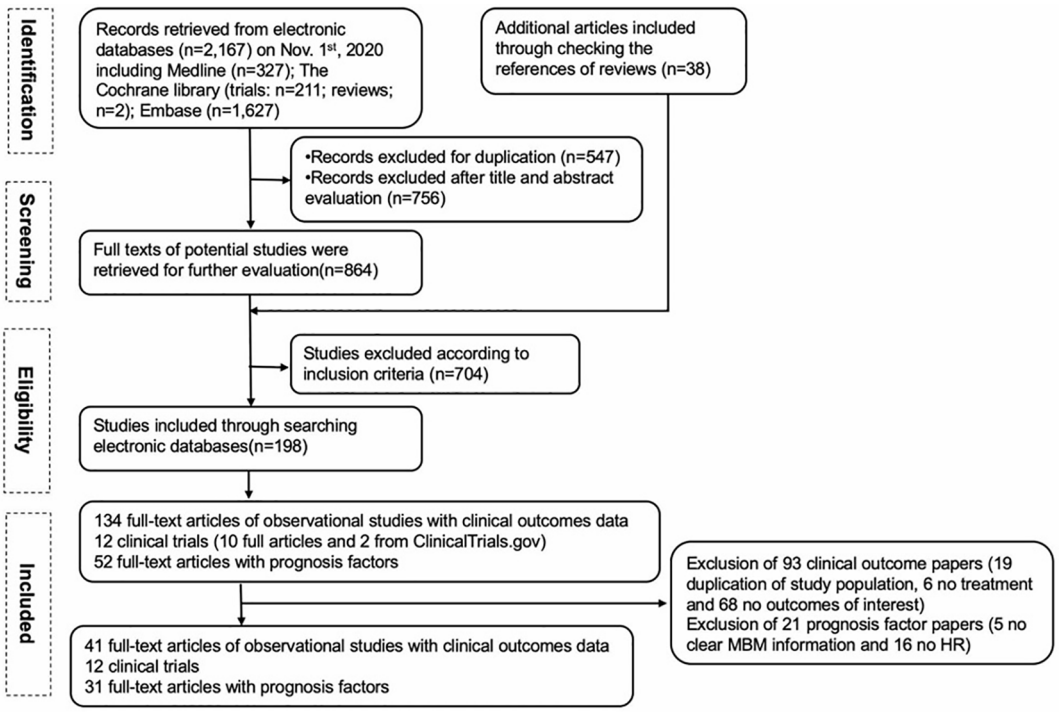

FIGURE 1
The study flow chart.

OS reported in observational studies

We present the clinical outcomes from 41 observational studies in which median OS or HR for OS were available to extract, ordered either from start of treatment (29 studies) or from date of diagnosis (12 studies) (Supporting Information, Tables S5, S6) (10–50). The median OS averaged across studies utilizing the same treatment combinations is also shown in Table 1, ranging from 7.2-14.8 months from start of treatment and 6.2-16.6 months from date of diagnosis. For SRS+IO, the weighted average median OS was 14.1 months from start of treatment, and 16.6 months from date of diagnosis.

TABLE 1 Weighted average median overall survival (OS) in months by treatment.

Treatment	OS from Start of Treatment		OS from Data of Diagnosis	
	Number of studies	Median OS	Number of studies	Median OS
IO	4	7.2	4	14.6
MAPKi	3	8.6	2	13.7
SRS+ IO + MAPKi	1	14.8	0	N/A
SRS + IO	5	14.1	4	16.6
SRS + MAPKi	1	7.3	1	7.0
SRS	5	7.3	2	11.6
WBRT	0	N/A	4	6.2

IO, immunotherapy; MAPKi, MAP kinase inhibitor; OS, Overall survival; SRS, stereotactic radiosurgery; WBRT, whole brain radiation therapy.

Meta-analysis by treatment for OS in observational studies

Meta-analysis by treatment for OS were summarized in Table 2, and forest plots were provided in Figures S1-S6. The significant benefit of IO on OS from start of treatment was observed by the comparison of SRS+IO *vs.* SRS alone (n = 8), with meta-HR of 0.48 (95% CI, 0.32-0.73). SRS compared to whole brain radiation therapy (WBRT) had a meta-HR of 0.55 (95% CI, 0.31-0.98) based on analysis of 2 studies (19, 20). Non-significant improvement of OS was observed for SRS+IO +MAPKi *vs.* SRS alone (meta-HR 0.40; 95% CI, 0.05-3.63; n=2), MAPKi *vs.* no MAPKi (meta-HR, 0.82; 95% CI, 0.46-1.46; n=3), and SRS+MAPKi *vs.* SRS alone (meta-HR, 0.71; 95% CI, 0.35-1.44; n=5) (11–13, 15, 16, 20–22).

Meta-analysis results by treatment for OS from date of diagnosis showed similar results. For the OS from date of diagnosis, treatment with SRS+IO *vs.* SRS alone had meta-HR of 0.34 (95% CI, 0.15-0.81; n=3) (Table 2, Figure S2), and IO alone *vs.* no IO had a meta-HR of 0.62 (95% CI, 0.45-0.86; n=4) (Table 2, Figure S6) (39, 41, 42). For MAPKi vs. no MAPKi, meta-analysis showed meta-HR of 0.45 (95% CI, 0.28-0.73; n=2) (43, 50). However, no significant improvement OS from date of diagnosis was observed for SRS *vs.* WBRT or for SRS+MAPKi vs. SRS alone (39–42, 50).

PFS reported in observational studies

Ten selected observational studies contained data on PFS, which ranged from 2-20.3 months from start of treatment or from 3.4-19 months from date of diagnosis (Table S7). Of the 10 studies, 9 also contained OS data, while one study by Robin et al. only included PFS data (51). PFS results were generally consistent with OS results, for example the study by Minniti

TABLE 2 Meta-analysis by treatment for overall survival (OS) in observational studies.

Treatment	Reference	Number of studies	Meta-HR (95% CI)
OS from Start of Treatment			
MAPKi	No MAPKi	3	0.82 (0.46-1.46)
SRS + IO	SRS alone	8	0.48 (0.32-0.73)
SRS + MAPKi	SRS alone	5	0.71 (0.35-1.44)
SRS + IO + MAPKi	SRS alone	2	0.40 (0.05-3.63)
SRS	WBRT	2	0.55 (0.31-0.98)
OS from Date of Diagnosis			
IO	No IO	4	0.62 (0.45-0.86)
MAPKi	No MAPKi	2	0.45 (0.28-0.73)
SRS + IO	SRS alone	3	0.34 (0.15-0.81)
SRS + MAPKi	SRS alone	3	0.58 (0.33-1.03)
SRS	WBRT	3	0.78 (0.37-1.65)

IO, immunotherapy; MAPKi, MAP kinase inhibitor; Meta-HR, Meta-analysis hazard ratio; OS, Overall survival; SRS, stereotactic radiosurgery; WBRT, whole brain radiation therapy.

et. al., 2019 that showed improved OS with SRS+IO found median PFS of 19 months from date of diagnosis of MBM (31).

OS reported in clinical trials

The median OS and HR for OS results in 12 identified clinical trials are summarized in Table S8 (52–63). Eleven clinical trials reported median OS ranging from 2.5 months (in patients who received only WBRT) to OS not reached (NR) in patients who received IO. However, comparison between trials was difficult given the different interventions being tested, the different patient populations (e.g. symptomatic vs. asymptomatic, previously treated vs. untreated, etc), and the relatively small numbers of patients in most trials (8 of the 12 trials had 25 patients or less in a study arm).

Prognostic factors for OS in patients with MBM

The HRs for each prognostic factor extracted from 31 observational studies are summarized in Table S9, meta-HR are summarized in Table 3, and forest plots provided in Figures S7–S15 (1, 27, 47, 48, 50, 64–89). Meta-analysis suggested elevated lactate dehydrogenase (LDH) levels, male gender, BRAF wild-type, increased number of intracranial metastases, presence of active extracranial metastases, lower Karnofsky Performance Scale (KPS), and larger MBM volume were significantly associated with worse prognosis in patients with MBM.

In particular, five studies showed increased LDH was associated with shorter survival (meta-HR, 1.66; 95% CI, 1.19-2.30). Five studies tested for an association between gender and OS and found decreased OS with male gender compared to female gender (meta-HR, 1.38; 95% CI, 1.10-1.74; n=5). Nine studies showed improved outcomes with BRAF mutation compared to BRAF wildtype (meta-HR, 0.66; 95% CI, 0.52-0.83; n=9). Nine studies assessed whether higher burden of MBM was associated with OS. In general, the data supported that more abundant intracranial metastases are associated with decreased OS. Among studies that had a reference group of 1 MBM compared to higher numbers, patients with 2 to 4 or 5 metastases had a meta-HR of 1.41 (95% CI, 1.11-1.80; n=5), and patients with more than 4 or 5 metastases had a meta-HR of 2.27 (95% CI, 2.08-2.48; n=6). Eight studies demonstrated worse survival outcomes with active extracranial disease compared to controlled disease (meta-HR, 1.86; 95% CI, 1.35-2.56). Decreased KPS (worse performance status) was associated with worse prognosis based on the results of thirteen studies, and the meta-HR was 2.73 (95% CI, 1.72-4.33; n=4), 4.23 (95% CI, 1.28-13.95; n=2), or 3.18 (95% CI, 2.02-5.00; n=2), using (≤70 *vs.* >70), (≤80 *vs.* >80), or (≤90 *vs.* >90) as cutoff points, respectively. Compared to those with KPS 90-100, those with KPS of ≤ 70 had a meta-HR of 2.70 (95% CI, 1.80-4.06; n=2). Larger total intracranial tumor volume was found to be associated with worse survival (meta-HR = 1.02; 95% CI, 1.01-1.03; n=2). Presence of leptomeningeal disease and advanced age trended towards association with worse prognosis, however the meta-HRs were non-significant.

Discussion

Overall, evidence from observational studies suggest that SRS with addition of IO or IO plus MAPKi may improve

TABLE 3 Meta-analysis hazard ratios (Meta-HR) for prognostic factors of overall survival (OS) among patients with MBM.

Prognostic Factor	Comparison Group	Number of studies	Meta-HR (95% CI)
LDH	High *vs.* Normal	5	1.66 (1.19-2.30)
Sex	Male *vs.* Female	5	1.38 (1.10-1.74)
BRAF	Mutated *vs.* Wild-type	9	0.66 (0.52-0.83)
Intracranial metastases	≥ 4/5 MBM *vs.* 1 MBM	6	2.27 (2.08-2.48)
Extracranial metastases	Active *vs.* Controlled	8	1.86 (1.35-2.56)
KPS	≤70 *vs.* >70	4	2.73 (1.72-4.33)
	≤70 *vs.* >90-100	2	2.70 (1.80-4.06)
	> 80 *vs.* ≤80	2	4.23 (1.28-13.95)
	≥90 *vs.* <90	2	3.18 (2.02-5.00)
Brain metastases volume	Larger *vs.* smaller	2	1.02 (1.01-1.03)
Leptomeningeal disease	Present *vs.* Absent	2	2.36 (0.99-5.62)
Age	Continuous	7	1.01 (1.00-1.02)
	≥ 65 *vs.* <65 years	2	1.07 (0.72-1.57)

KPS, Karnofsky Performance Scale; LDH, lactate dehydrogenase; MBM, melanoma brain metastases; Meta-HR, Meta-analysis hazard ratio.

survival outcomes in patients with MBM, compared to SRS alone. When averaged across studies utilizing the same treatment combinations, SRS+ IO had an improved median OS in months from start of treatment of approximately 14.1 months based on 5 studies. Treatment with combined SRS+IO +MAPKi was also promising with one study showing a median OS of 14.8 months. Meta-analyses provided support for the benefit from SRS+IO compared to SRS alone (12, 15). Further meta-analysis for studies that measured OS from date of diagnosis also showed that IO and SRS+IO had significantly improved OS compared to no IO and SRS alone, respectively.

A recent meta-analysis of MBM patients by Tawbi et al. (90) included 13 trials, of which 3 were randomized controlled trials, 9 were single-arm studies, and 1 was a non-randomized comparative study. They calculated median OS through a meta-analysis of K-M curves for selected interventions including IO or TT or as a weighted average of median OS. They observed that median OS was longer with nivolumab plus ipilimumab (28.3 months; 95% CI = 19.7-31.9) than with the other interventions including IO monotherapy or TT (range 5.7-11.8 months), based on pooled K-M curves. Similar OS benefit was also observed with nivolumab plus ipilimumab when the weighted average of the median was used (median OS 29.2 months) compared with the other interventions. This analysis suggested a clinical advantage with this treatment combination, but the heterogeneity of the data with respect to prior therapies (many patients received prior surgery, RT, systemic therapy, IO, or TT) and patient characteristics contributed uncertainty to the analysis.

Studies included in both the Tawbi et al. meta-analysis and our systematic review were a randomized trial by Long et al., 2018 and single-arm studies by McArthur et al., 2017, Davies et al., 2017, Kluger et al., 2019, and Tawbi et al., 2018 (52, 58–60, 62). However, in our analysis, prolonged median OS with IO was not demonstrated to the extent seen in the meta-analysis by Tawbi et al. In our study, average median OS from start of treatment was 7.2 months, 14.1 months, and 14.8 months for IO alone, SRS+IO, and SRS+IO+MAPKi, respectively. This may have been due to the heterogeneity of study populations, with inclusion of patients in the observational studies who had received a variety of prior treatments. Selection bias is also a limitation as healthier patients may be more likely to be selected for combination therapy such as SRS+IO or nivolumab +ipilimumab, and patients that undergo SRS generally have a limited number of brain metastases compared to patients that undergo WBRT or are not recommended for any radiation. It is worth noting that there may be unaccounted-for differences in patients who participated in clinical trials compared to those who did not (91). Given the variable patient populations and interventions, meta-analysis was not performed on the 12 clinical trials identified in our systematic review. More clinical trial data is needed for MBM patients in order to determine the most beneficial interventions.

In addition, our results suggest that elevated LDH levels, male gender, BRAF wild-type, more-numerous intracranial metastases, larger total MBM volume, presence of active extracranial metastases, and lower KPS scores may be prognostic for reduced OS in patients with MBM. While it is not unexpected that worse performance status and higher burden of disease were associated with reduced OS, some of the other associations are less clear. It is possible that an unknown confounding factor or biomarker is related to the association between gender and reduced OS. Limitations for this analysis included heterogeneity in participants, interventions, and outcomes studied (variable definitions in some studies related to the cutoff values and reference groups for some prognostic factors). A limitation of the OS meta-analysis results is that many studies defined date of diagnosis as the start date for OS calculation, rather than defining the start date as the day of treatment start, leading to more variability. Overall, this population is difficult to study given most of the data available is from retrospective reports or small clinical trials. Many of the meta-analyses performed included only a small number of studies. Since immunotherapy was not the primary focus, additional prognostic biomarkers such a neutrophil-lymphocyte ratio and PD-L1 were not included in this review. We have stayed abreast of the new literature on this specific topic after the date of our search execution. However, no major studies fell into our inclusion criteria.

In conclusion, although MBM is known to be associated with poor survival, evidence from our systematic review and meta-analysis of observational studies indicates that IO or combination IO and MAPKi therapy with SRS may lead to improved outcomes compared to patients treated without these therapies. A better understanding of prognostic factors may help clinicians with treatment planning, outcome assessment, and planning of support measures for individual MBM patients. Larger, randomized clinical trials would help to further elucidate the most effective therapy combinations to meet the needs of this understudied population.

Data availability statement

The raw data supporting the conclusions of this article will be made available by the authors, without undue reservation.

Author contributions

Study design, X-LT, ES, JH, and IS. Data collection, HT, NK, and JH. Data analysis, HT and JH. Manuscript writing, X-LT,

AL, and JH. Manuscript review and approval, X-LT, AL, ES, HT, NK, JH, RJ, SD, and IS. All authors contributed to the article and approved the submitted version.

Conflict of interest

X-LT, ES, RJ, SD, and IS are employed by Merck & Co., Inc. JH, HT, and AL are employed by Integrative Precision Health LLC.

The authors declare that this study received funding from Merck & Co., Inc., Rahway, NJ, USA. The funder had the following involvement with the study: study design, collection, analysis, interpretation of data, the writing of this article and the decision to submit it for publication.

Publisher's note

Supplementary material

The Supplementary Material for this article can be found online at: https://www.frontiersin.org/articles/10.3389/fonc.2022.1025664/full#supplementary-material

References

1. Kavouridis VK, Harary M, Hulsbergen AFC, Lo YT, Reardon DA, Aizer AA, et al. Survival and prognostic factors in surgically treated brain metastases. *J Neuro-Oncol* (2019) 143(2):359–67. doi: 10.1007/s11060-019-03171-6

2. Dodson C, Smith DA, Richards TJ, Devita RR, Hoimes CJ, Ramaiya NH. Systemic therapies for melanoma brain metastases: A primer for radiologists. *J Comput Assist Tomogr.* (2020) 44(3):346–55. doi: 10.1097/RCT.0000000000001006

3. Margolin K, Ernstoff MS, Hamid O, Lawrence D, McDermott D, Puzanov I, et al. Ipilimumab in patients with melanoma and brain metastases: An open-label, phase 2 trial. *Lancet Oncol* (2012) 13(5):459–65. doi: 10.1016/S1470-2045(12)70090-6

4. Long GV, Trefzer U, Davies MA, Kefford RF, Ascierto PA, Chapman PB, et al. Dabrafenib in patients with Val600Glu or Val600Lys BRAF-mutant melanoma metastatic to the brain (BREAK-MB): A multicentre, open-label, phase 2 trial. *Lancet Oncol* (2012) 13(11):1087–95. doi: 10.1016/S1470-2045(12)70431-X

5. Raizer JJ, Hwu WJ, Panageas KS, Wilton A, Baldwin DE, Bailey E, et al. Brain and leptomeningeal metastases from cutaneous melanoma: Survival outcomes based on clinical features. *Neuro Oncol* (2008) 10(2):199–207. doi: 10.1215/15228517-2007-058

6. Davies MA, Liu P, McIntyre S, Kim KB, Papadopoulos N, Hwu WJ, et al. Prognostic factors for survival in melanoma patients with brain metastases. *Cancer* (2011) 117(8):1687–96. doi: 10.1002/cncr.25634

7. Tierney JF, Stewart LA, Ghersi D, Burdett S, Sydes MR. Practical methods for incorporating summary time-to-event data into meta-analysis. *Trials.* (2007) 8:16. doi: 10.1186/1745-6215-8-16

8. Higgins JP, Thompson SG, Deeks JJ, Altman DG. Measuring inconsistency in meta-analyses. *BMJ.* (2003) 327(7414):557–60. doi: 10.1136/bmj.327.7414.557

9. Pereira TV, Patsopoulos NA, Salanti G, Ioannidis JP. Critical interpretation of cochran's q test depends on power and prior assumptions about heterogeneity. *Res Synth Methods* (2010) 1(2):149–61. doi: 10.1002/jrsm.13

10. Acharya S, Mahmood M, Mullen D, Yang D, Tsien CI, Huang J, et al. Distant intracranial failure in melanoma brain metastases treated with stereotactic radiosurgery in the era of immunotherapy and targeted agents. *Adv Radiat Oncol* (2017) 2(4):572–80. doi: 10.1016/j.adro.2017.07.003

11. An Y, Jiang W, Kim BYS, Qian JM, Tang C, Fang P, et al. Stereotactic radiosurgery of early melanoma brain metastases after initiation of anti-CTLA-4 treatment is associated with improved intracranial control. *Radiotherapy Oncol* (2017) 125(1):80–8. doi: 10.1016/j.radonc.2017.08.009

12. Carron R, Gaudy-Marqueste C, Amatore F, Padovani L, Malissen N, Balossier A, et al. Stereotactic radiosurgery combined with anti-PD1 for the management of melanoma brain metastases: A retrospective study of safety and efficacy. *Eur J Cancer* (2020) 135:52–61. doi: 10.1016/j.ejca.2020.04.028

13. Choong ES, Lo S, Drummond M, Fogarty GB, Menzies AM, Guminski A, et al. Survival of patients with melanoma brain metastasis treated with stereotactic radiosurgery and active systemic drug therapies. *Eur J Cancer* (2017) 75:169–78. doi: 10.1016/j.ejca.2017.01.007

14. Diao K, Bian SX, Routman DM, Yu C, Ye JC, Wagle NA, et al. Stereotactic radiosurgery and ipilimumab for patients with melanoma brain metastases: Clinical outcomes and toxicity. *J Neuro-Oncol* (2018) 139(2):421–9. doi: 10.1007/s11060-018-2880-y

15. Gaudy-Marqueste C, Dussouil AS, Carron R, Troin L, Malissen N, Loundou A, et al. Survival of melanoma patients treated with targeted therapy and immunotherapy after systematic upfront control of brain metastases by radiosurgery. *Eur J Cancer* (2017) 84:44–54. doi: 10.1016/j.ejca.2017.07.017

16. Kaidar-Person O, Zagar TM, Deal A, Moschos SJ, Ewend MG, Sasaki-Adams D, et al. The incidence of radiation necrosis following stereotactic radiotherapy for melanoma brain metastases: The potential impact of immunotherapy. *Anti-Cancer Drugs* (2017) 28(6):669–75. doi: 10.1097/CAD.0000000000000497

17. Matsunaga S, Shuto T, Yamamoto M, Yomo S, Kondoh T, Kobayashi T, et al. Gamma knife radiosurgery for metastatic brain tumors from malignant melanomas: A Japanese multi-institutional cooperative and retrospective cohort study (JLGK1501). *Stereotactic Funct Neurosurgery* (2018) 96(3):162–71. doi: 10.1159/000489948

18. Minniti G, Paolini S, D'Andrea G, Lanzetta G, Cicone F, Confaloni V, et al. Outcomes of postoperative stereotactic radiosurgery to the resection cavity versus stereotactic radiosurgery alone for melanoma brain metastases. *J Neurooncol* (2017) 132(3):455–62. doi: 10.1007/s11060-017-2394-z

19. Rauschenberg R, Bruns J, Brütting J, Daubner D, Lohaus F, Zimmer L, et al. Impact of radiation, systemic therapy and treatment sequencing on survival of patients with melanoma brain metastases. *Eur J Cancer.* (2019) 110:11–20. doi: 10.1016/j.ejca.2018.12.023

20. Bhatia A, Birger M, Veeraraghavan H, Um H, Tixier F, McKenney AS, et al. MRI Radiomic features are associated with survival in melanoma brain metastases treated with immune checkpoint inhibitors. *Neuro-Oncol* (2019) 21(12):1578–86. doi: 10.1093/neuonc/noz141

21. Gorka E, Fabó D, Gézsi A, Czirbesz K, Fedorcsák I, Liszkay G. Dabrafenib therapy in 30 patients with melanoma metastatic to the brain: A single-centre controlled retrospective study in Hungary. *Pathol Oncol Res* (2018) 24(2):401–6. doi: 10.1007/s12253-017-0256-9

22. Iorgulescu JB, Harary M, Zogg CK, Ligon KL, Reardon DA, Hodi FS, et al. Improved risk-adjusted survival for melanoma brain metastases in the era of checkpoint blockade immunotherapies: Results from a national cohort. *Cancer Immunol Res* (2018) 6(9):1039–45. doi: 10.1158/2326-6066.CIR-18-0067

23. Ahmed KA, Abuodeh YA, Echevarria MI, Arrington JA, Stallworth DG, Hogue C, et al. Clinical outcomes of melanoma brain metastases treated with stereotactic radiosurgery and anti-PD-1 therapy, anti-CTLA-4 therapy, BRAF/MEK inhibitors, BRAF inhibitor, or conventional chemotherapy. *Ann Oncol* (2016) 27(12):2288–94. doi: 10.1093/annonc/mdw417

24. De La Fuente M, Beal K, Carvajal R, Kaley TJ. Whole-brain radiotherapy in patients with brain metastases from melanoma. *CNS Oncol* (2015) 3(6):401–6. doi: 10.2217/cns.14.40

25. Drago JZ, Lawrence D, Livingstone E, Zimmer L, Chen T, Giobbie-Hurder A, et al. Clinical experience with combination BRAF/MEK inhibitors for melanoma with brain metastases: A real-life multicenter study. *Melanoma Res* (2019) 29 (1):65–9. doi: 10.1097/CMR.0000000000000527

26. Frakes JM, Figura NB, Ahmed KA, Juan TH, Patel N, Latifi K, et al. Potential role for LINAC-based stereotactic radiosurgery for the treatment of 5 or more radioresistant melanoma brain metastases. *J Neurosurgery* (2015) 123(5):1261–7. doi: 10.3171/2014.12.JNS141919

27. Geukes Foppen MH, Boogerd W, Blank CU, van Thienen JV, Haanen JB, Brandsma D. Clinical and radiological response of BRAF inhibition and MEK inhibition in patients with brain metastases from BRAF-mutated melanoma. *Melanoma Res* (2018) 28(2):126–33. doi: 10.1097/CMR.0000000000000429

28. Le Rhun E, Wolpert F, Fialek M, Devos P, Andratschke N, Reyns N, et al. Response assessment and outcome of combining immunotherapy and radiosurgery for brain metastasis from malignant melanoma. *ESMO Open* (2020) 5(4):e000763. doi: 10.1136/esmoopen-2020-000763

29. Knispel S, Stang A, Zimmer L, Lax H, Gutzmer R, Heinzerling L, et al. Impact of a preceding radiotherapy on the outcome of immune checkpoint inhibition in metastatic melanoma: A multicenter retrospective cohort study of the DeCOG. *J ImmunoTherapy Cancer* (2020) 8(1):e000395. doi: 10.1136/jitc-2019-000395

30. McHugh FA, Kow CY, Falkov A, Heppner P, Law A, Bok A, et al. Metastatic melanoma: Surgical treatment of brain metastases – analysis of 110 patients. *J Clin Neurosci* (2020) 73:144–9. doi: 10.1016/j.jocn.2019.12.063

31. Minniti G, Anzellini D, Reverberi C, Cappellini GCA, Marchetti L, Bianciardi F, et al. Stereotactic radiosurgery combined with nivolumab or ipilimumab for patients with melanoma brain metastases: Evaluation of brain control and toxicity. *J ImmunoTherapy Cancer* (2019) 7(1):102. doi: 10.1186/s40425-019-0588-y

32. Tetu P, Allayous C, Oriano B, Dalle S, Mortier L, Leccia MT, et al. Impact of radiotherapy administered simultaneously with systemic treatment in patients with melanoma brain metastases within MelBase, a French multicentric prospective cohort. *Eur J Cancer* (2019) 112:38–46. doi: 10.1016/j.ejca.2019.02.009

33. Pomeranz Krummel DA, Nasti TH, Izar B, Press RH, Xu M, Lowder L, et al. Impact of sequencing radiation therapy and immune checkpoint inhibitors in the treatment of melanoma brain metastases. *Int J Radiat Oncol Biol Physics* (2020) 108 (1):157–63. doi: 10.1016/j.ijrobp.2020.01.043

34. Rahman R, Cortes A, Niemierko A, Oh KS, Flaherty KT, Lawrence DP, et al. The impact of timing of immunotherapy with cranial irradiation in melanoma patients with brain metastases: intracranial progression, survival and toxicity. *J Neuro-Oncol* (2018) 138(2):299–306. doi: 10.1007/s11060-018-2795-7

35. Schmidberger H, Rapp M, Ebersberger A, Hey-Koch S, Loquai C, Grabbe S, et al. Long-term survival of patients after ipilimumab and hypofractionated brain radiotherapy for brain metastases of malignant melanoma: sequence matters. *Strahlentherapie und Onkologie* (2018) 194(12):1144–51. doi: 10.1007/s00066-018-1356-5

36. Skrepnik T, Sundararajan S, Cui H, Stea B. Improved time to disease progression in the brain in patients with melanoma brain metastases treated with concurrent delivery of radiosurgery and ipilimumab. *Oncoimmunology* (2017) 6(3):e1283461. doi: 10.1080/2162402X.2017.1283461

37. Stera S, Balermpas P, Blanck O, Wolff R, Wurster S, Baumann R, et al. Stereotactic radiosurgery combined with immune checkpoint inhibitors or kinase inhibitors for patients with multiple brain metastases of malignant melanoma. *Melanoma Res* (2019) 29(2):187–95. doi: 10.1097/CMR.0000000000000542

38. Yusuf MB, Amsbaugh MJ, Burton E, Chesney J, Woo S. Peri-SRS administration of immune checkpoint therapy for melanoma metastatic to the brain: Investigating efficacy and the effects of relative treatment timing on lesion response. *World Neurosurg* (2017) 100:632–40.e4. doi: 10.1016/j.wneu.2017.01.101

39. Amaral T, Tampouri I, Eigentler T, Keim U, Klumpp B, Heinrich V, et al. Immunotherapy plus surgery/radiosurgery is associated with favorable survival in patients with melanoma brain metastasis. *Immunotherapy* (2019) 11(4):297–309. doi: 10.2217/imt-2018-0149

40. Gabani P, Fischer-Valuck BW, Johanns TM, Hernandez-Aya LF, Keller JW, Rich KM, et al. Stereotactic radiosurgery and immunotherapy in melanoma brain metastases: Patterns of care and treatment outcomes. *Radiotherapy Oncol* (2018) 128(2):266–73. doi: 10.1016/j.radonc.2018.06.017

41. Kotecha R, Miller JA, Venur VA, Mohammadi AM, Chao ST, Suh JH, et al. Melanoma brain metastasis: The impact of stereotactic radiosurgery, BRAF mutational status, and targeted and/or immune-based therapies on treatment outcome. *J Neurosurgery* (2018) 129(1):50–9. doi: 10.3171/2017.1.JNS162797

42. Martins F, Schiappacasse L, Levivier M, Tuleasca C, Cuendet MA, Aedo-Lopez V, et al. The combination of stereotactic radiosurgery with immune checkpoint inhibition or targeted therapy in melanoma patients with brain metastases: A retrospective study. *J Neuro-Oncol* (2020) 146(1):181–93. doi: 10.1007/s11060-019-03363-0

43. Wattson DA, Sullivan RJ, Niemierko A, Merritt RM, Lawrence DP, Oh KS, et al. Survival patterns following brain metastases for patients with melanoma in the MAP-kinase inhibitor era. *J Neuro-Oncol* (2015) 123(1):75–84. doi: 10.1007/s11060-015-1761-x

44. Stokes WA, Binder DC, Jones BL, Oweida AJ, Liu AK, Rusthoven CG, et al. Impact of immunotherapy among patients with melanoma brain metastases managed with radiotherapy. *J Neuroimmunol* (2017) 313:118–22. doi: 10.1016/j.jneuroim.2017.10.006

45. Tio M, Wang X, Carlino M, Shivalingam B, Fogarty G, Guminski A, et al. Survival and prognostic factors for patients with melanoma brain metastases in the era of modern systemic therapy. *Pigment Cell Melanoma Res* (2018) 31(4):509–15. doi: 10.1111/pcmr.12682

46. Alvarez-Breckenridge C, Giobbie-Hurder A, Gill CM, Bertalan M, Stocking J, Kaplan A, et al. Upfront surgical resection of melanoma brain metastases provides a bridge toward immunotherapy-mediated systemic control. *Oncologist* (2019) 24(5):671–9. doi: 10.1634/theoncologist.2018-0306

47. Amaral T, Kiecker F, Schaefer S, Stege H, Kaehler K, Terheyden P, et al. Combined immunotherapy with nivolumab and ipilimumab with and without local therapy in patients with melanoma brain metastasis: A DeCOG* study in 380 patients. *J ImmunoTherapy Cancer* (2020) 8(1)e000333. doi: 10.1136/jitc-2019-000333

48. Cohen-Inbar O, Shih HH, Xu Z, Schlesinger D, Sheehan JP. The effect of timing of stereotactic radiosurgery treatment of melanoma brain metastases treated with ipilimumab. *J Neurosurgery* (2017) 127(5):1007–14. doi: 10.3171/2016.9.JNS161585

49. White RJ, Abel S, Horne ZD, Lee J, Edington H, Greenberg L, et al. Melanoma brain metastases: is it time to eliminate radiotherapy? *J Neuro-Oncol* (2020) 149(1):27–33. doi: 10.1007/s11060-020-03485-w

50. Sloot S, Chen YA, Zhao X, Weber JL, Benedict JJ, Mulé JJ, et al. Improved survival of patients with melanoma brain metastases in the era of targeted BRAF and immune checkpoint therapies. *Cancer* (2018) 124(2):297–305. doi: 10.1002/cncr.30946

51. Robin TP, Breeze RE, Smith DE, Rusthoven CG, Lewis KD, Gonzalez R, et al. Immune checkpoint inhibitors and radiosurgery for newly diagnosed melanoma brain metastases. *J Neuro-Oncol* (2018) 140(1):55–62. doi: 10.1007/s11060-018-2930-5

52. Davies MA, Saiag P, Robert C, Grob JJ, Flaherty KT, Arance A, et al. Dabrafenib plus trametinib in patients with BRAFV600-mutant melanoma brain metastases (COMBI-MB): A multicentre, multicohort, open-label, phase 2 trial. *Lancet Oncol* (2017) 18(7):863–73. doi: 10.1016/S1470-2045(17)30429-1

53. Goldberg SB, Gettinger SN, Mahajan A, Chiang AC, Herbst RS, Sznol M, et al. Pembrolizumab for patients with melanoma or non-small-cell lung cancer and untreated brain metastases: early analysis of a non-randomised, open-label, phase 2 trial. *Lancet Oncol* (2016) 17(7):976–83. doi: 10.1016/S1470-2045(16)30053-5

54. Gupta A, Roberts C, Tysoe F, Goff M, Nobes J, Lester J, et al. RADVAN: A randomised phase 2 trial of WBRT plus vandetanib for melanoma brain metastases-results and lessons learnt. *Br J Cancer* (2016) 115(10):1193–200. doi: 10.1038/bjc.2016.318

55. Hauswald H, Bernhardt D, Krug D, Katayama S, Habl G, Bermejo JL, et al. Whole-brain helical tomotherapy with integrated boost for brain metastases in patients with malignant melanoma - final results of the BRAINRT trial. *Cancer Manage Res* (2019) 11:4669–76. doi: 10.2147/CMAR.S204729

56. Hong AM, Fogarty GB, Dolven-Jacobsen K, Burmeister BH, Lo SN, Haydu LE, et al. Adjuvant whole-brain radiation therapy compared with observation after local treatment of melanoma brain metastases: A multicenter, randomized phase III trial. *J Clin Oncol* (2019) 37(33):3132–41. doi: 10.1200/JCO.19.01414

57. Roche H-L. A study of vemurafenib in metastatic melanoma participants with brain metastases. (2016). Available at: https://clinicaltrials.gov/ct2/show/NCT01378975.

58. Long GV, Atkinson V, Lo S, Hu S, Guminski AD, Brown MP, et al. Combination nivolumab and ipilimumab or nivolumab alone in melanoma brain metastases: a multicentre randomised phase 2 study. *Lancet Oncol* (2018) 19(5):672–81. doi: 10.1016/S1470-2045(18)30139-6

59. Kluger HM, Chiang V, Mahajan A, Zito CR, Sznol M, Tran T, et al. Long-term survival of patients with melanoma with active brain metastases treated with pembrolizumab on a phase II trial. *J Clin Oncol* (2019) 37(1):52–60. doi: 10.1200/JCO.18.00204

60. McArthur GA, Maio M, Arance A, Nathan P, Blank C, Avril MF, et al. Vemurafenib in metastatic melanoma patients with brain metastases: An open-label, single-arm, phase 2, multicentre study. *Ann Oncol* (2017) 28(3):634–41. doi: 10.1093/annonc/mdw641

61. McQuade JL, Posada LP, Lecagoonporn S, Cain S, Bassett RL, Patel SP, et al. A phase I study of TPI 287 in combination with temozolomide for patients with

metastatic melanoma. *Melanoma Res* (2016) 26(6):604–8. doi: 10.1097/CMR.0000000000000296

62. Tawbi HA, Forsyth PA, Algazi A, Hamid O, Hodi FS, Moschos SJ, et al. Combined nivolumab and ipilimumab in melanoma metastatic to the brain. *New Engl J Med* (2018) 379(8):722–30. doi: 10.1056/NEJMoa1805453

63. Squibb. *A multi-center phase II study to evaluate tumor response to ipilimumab (BMS-734016) monotherapy in subjects with melanoma brain metastases*. Available at: https://clinicaltrials.gov/ct2/show/NCT00623766.

64. Kano H, Morales-Restrepo A, Iyer A, Weiner GM, Mousavi SH, Kirkwood JM, et al. Comparison of prognostic indices in patients who undergo melanoma brain metastasis radiosurgery. *J Neurosurg* (2018) 128(1):14–22. doi: 10.3171/2016.9.JNS161011

65. Zubatkina I, Ivanov P. Early imaging radioresponsiveness of melanoma brain metastases as a predictor of patient prognosis. *J Neurosurgery* (2018) 129 (2):354–65. doi: 10.3171/2017.1.JNS162075

66. Bian SX, Routman D, Liu J, Yang D, Groshen S, Zada G, et al. Prognostic factors for melanoma brain metastases treated with stereotactic radiosurgery. *J Neurosurg* (2016) 125:31–9. doi: 10.3171/2016.8.GKS161359

67. Badakhshi H, Engeling F, Budach V, Ghadjar P, Zschaeck S, Kaul D. Are prognostic indices for brain metastases of melanoma still valid in the stereotactic era? *Radiat Oncol* (2018) 13(1):3. doi: 10.1186/s13014-017-0951-4

68. Wilkins A, W Corbett R, Bloomfield A, Porta N, Morris S, Ali Z, et al. The melanoma-specific graded prognostic assessment does not adequately discriminate prognosis in a modern population with brain metastases from malignant melanoma. *Br J Cancer* (2015) 113(9):1275–81. doi: 10.1038/bjc.2015.357

69. Gummadi T, Valpione S, Kim C, Kottschade LA, Mittapalli RK, Chiarion-Sileni V, et al. Impact of BRAF mutation and BRAF inhibition on melanoma brain metastases. *Melanoma Res* (2015) 25(1):75–9. doi: 10.1097/CMR.0000000000000133

70. Partl R, Kaiser J, Kronhuber E, Cetin-Strohmer K, Steffal C, Böhmer-Breitfelder B, et al. KPS/LDH index: a simple tool for identifying patients with metastatic melanoma who are unlikely to benefit from palliative whole brain radiotherapy. *Supportive Care Cancer* (2016) 24(2):523–8. doi: 10.1007/s00520-015-2793-7

71. Chowdhury IH, McMillan MT, Miller D, Kolker JD, Kurtz G, Dorsey JF, et al. Alonso-basanta, m. novel risk scores for survival and intracranial failure in patients treated with radiosurgery alone to melanoma brain metastases. *Radiat Oncol* (2015) 10:248. doi: 10.1186/s13014-015-0553-y

72. Rodenburg RJ, Hanssens PE, Ho VKY, Beerepoot LV. Validation of the chowdhury overall survival score in patients with melanoma brain metastasis treated with gamma knife radiosurgery. *J Neuro-Oncol* (2018) 138(2):391–9. doi: 10.1007/s11060-018-2808-6

73. Ramos RI, Wu J, Jones P, Chang SC, Kiyohara E, Tran K, et al. Upregulation of cell surface GD3 ganglioside phenotype is associated with human melanoma brain metastasis. *Mol Oncol* (2020) 14(8):1760–78. doi: 10.1002/1878-0261.12702

74. Marzese DM, Liu M, Huynh JL, Hirose H, Donovan NC, Huynh KT, et al. Brain metastasis is predetermined in early stages of cutaneous melanoma by CD44v6 expression through epigenetic regulation of the spliceosome. *Pigment Cell Melanoma Res* (2015) 28(1):82–93. doi: 10.1111/pcmr.12307

75. Farris M, McTyre ER, Cramer CK, Hughes R, olph DM, Ayala-Peacock DN, et al. Brain metastasis velocity: A novel prognostic metric predictive of overall survival and freedom from whole-brain radiation therapy after distant brain failure following upfront radiosurgery alone. *Int J Radiat Oncol Biol Physics* (2017) 98 (1):131–41. doi: 10.1016/j.ijrobp.2017.01.201

76. Mastorakos P, Xu Z, Yu J, Hess J, Qian J, Chatrath A, et al. BRAF V600 mutation and BRAF kinase inhibitors in conjunction with stereotactic radiosurgery for intracranial melanoma metastases: A multicenter retrospective study. *Neurosurgery* (2019) 84(4):872–80. doi: 10.1093/neuros/nyy203

77. Liu H, Xu YB, Guo CC, Li MX, Ji JL, Dong RR, et al. Predictive value of a nomogram for melanomas with brain metastases at initial diagnosis. *Cancer Med* (2019) 8(18):7577–85. doi: 10.1002/cam4.2644

78. Ferrel EA, Roehrig AT, Kaya EA, Carlson JD, Carlson JD, Wagner A, et al. Retrospective study of metastatic melanoma and renal cell carcinoma to the brain with multivariate analysis of prognostic pre-treatment clinical factors. *Int J Mol Sci* (2016) 17(3):400. doi: 10.3390/ijms17030400

79. Rades D, Sehmisch L, Janssen S, Schild SE. Prognostic factors after whole-brain radiotherapy alone for brain metastases from malignant melanoma. *Anticancer Res* (2016) 36(12):6637–40. doi: 10.21873/anticanres.11271

80. Schaule J, Kroeze SGC, Blanck O, Blanck O, Stera S, Kahl KH, et al. Predicting survival in melanoma patients treated with concurrent targeted- or immunotherapy and stereotactic radiotherapy. *Radiat Oncol* (2020) 15(1):135. doi: 10.1186/s13014-020-01708-y

81. Sehmisch L, Schild S, Rades D. Development of a survival score for patients with cerebral metastases from melanoma. *Anticancer Res* (2017) 37(1):249–52. doi: 10.21873/anticanres.11314

82. Gallaher IS, Watanabe Y, DeFor TE, Dusenbery KE, Lee CK, Hunt MA, et al. BRAF mutation is associated with improved local control of melanoma brain metastases treated with gamma knife radiosurgery. *Front Oncol* (2016) 6. doi: 10.3389/fonc.2016.00107

83. Sperduto PW, Jiang W, Brown PD, Braunstein S, Sneed P, Wattson DA, et al. The prognostic value of BRAF, c-KIT, and NRAS mutations in melanoma patients with brain metastases. *Int J Radiat Oncol Biol Phys* (2017) 98(5):1069–77. doi: 10.1016/j.ijrobp.2017.03.030

84. Xu Z, Lee CC, Ramesh A, Mueller AC, Schlesinger D, Cohen-Inbar O, et al. BRAF V600E mutation and BRAF kinase inhibitors in conjunction with stereotactic radiosurgery for intracranial melanoma metastases. *J Neurosurgery* (2017) 126(3):726–34. doi: 10.3171/2016.2.JNS1633

85. Frinton E, Tong D, Tan J, Read G, Kumar V, Kennedy S, et al. Metastatic melanoma: prognostic factors and survival in patients with brain metastases. *J Neuro-Oncol* (2017) 135(3):507–12. doi: 10.1007/s11060-017-2591-9

86. Zhang M, Rodrigues AJ, Bhambhvani HP, Fatemi P, Pollom EL, Gibbs IC, et al. Intracranial tumor control after immune-related adverse events and discontinuation of immunotherapy for melanoma. *World Neurosurg* (2020) 144: e316–e325. doi: 10.1016/j.wneu.2020.08.124

87. Maxwell R, Garzon-Muvdi T, Lipson EJ, Sharfman WH, Bettegowda C, Redmond KJ, et al. BRAF-V600 mutational status affects recurrence patterns of melanoma brain metastasis. *Int J Cancer* (2017) 140(12):2716–27. doi: 10.1002/ijc.30241

88. Hirshman BR, Wilson BR, Ali MA, Schupper AJ, Proudfoot JA, Goetsch SJ, et al. Cumulative intracranial tumor volume augments the prognostic value of diagnosis-specific graded prognostic assessment model for survival in patients with melanoma cerebral metastases. *Neurosurgery* (2018) 83(2):237–44. doi: 10.1093/neuros/nyx380

89. Bates JE, Youn P, Usuki KY, Walter KA, Huggins CF. Okunieff, p.; milano, m. t. brain metastasis from melanoma: The prognostic value of varying sites of extracranial disease. *J Neuro-Oncol* (2015) 125(2):411–8. doi: 10.1007/s11060-015-1932-9

90. Tawbi HA-H, Long GV, Meyer N, Breznen B, Vyas C, Leung L, et al. Treatment outcomes in patients (pts) with melanoma brain metastases (MBM) treated with systemic therapy: A systematic literature review (SLR) and meta-analysis. *J Clin Oncol* (2021) 39(15_suppl):9561. doi: 10.1200/JCO.2021.39.15_suppl.9561

91. Ludmir EB, Mainwaring W, Lin TA, Miller AB, Jethanandani A, Espinoza AF, et al. Factors associated with age disparities among cancer clinical trial participants. *JAMA Oncol* (2019) 5(12):1769–73. doi: 10.1001/jamaoncol.2019.2055

frontiers | Frontiers in Oncology

TYPE Original Research
PUBLISHED 20 December 2022
DOI 10.3389/fonc.2022.1014711

OPEN ACCESS

EDITED BY
David Kaul,
Charité Universitätsmedizin Berlin,
Germany

REVIEWED BY
Peter Truckenmüller,
Charité University Medicine Berlin,
Germany
Carolin Weiss Lucas,
University Hospital of Cologne,
Germany

*CORRESPONDENCE
Niklas Thon
niklas.thon@med.uni-muenchen.de

†These authors have contributed equally to this work

SPECIALTY SECTION
This article was submitted to Neuro-Oncology and Neurosurgical Oncology, a section of the journal Frontiers in Oncology

RECEIVED 08 August 2022
ACCEPTED 30 November 2022
PUBLISHED 20 December 2022

CITATION
Katzendobler S, Do A, Weller J, Rejeski K, Dorostkar MM, Albert NL, Forbrig R, Niyazi M, Egensperger R, Tonn J-C, von Baumgarten L, Quach S and Thon N (2022) The value of stereotactic biopsy of primary and recurrent brain metastases in the era of precision medicine.
Front. Oncol. 12:1014711.
doi: 10.3389/fonc.2022.1014711

The value of stereotactic biopsy of primary and recurrent brain metastases in the era of precision medicine

Sophie Katzendobler[1†], Anna Do[1†], Jonathan Weller[1], Kai Rejeski[2,3], Mario M. Dorostkar[4], Nathalie L. Albert[3,5], Robert Forbrig[6], Maximilian Niyazi[3,7], Rupert Egensperger[4], Joerg-Christian Tonn[1,3], Louisa von Baumgarten[1,3], Stefanie Quach[1†] and Niklas Thon[1,3*]

[1]Department of Neurosurgery, University Hospital, Ludwig-Maximilians-Universität (LMU) Munich, Munich, Germany, [2]Department of Medicine III, Hematology and Oncology, University Hospital, Ludwig-Maximilians-Universität (LMU) Munich, Munich, Germany, [3]German Cancer Consortium (DKTK), Partner Site Munich, German Cancer Research Center (DKFZ), Heidelberg, Germany, [4]Center for Neuropathology and Prion Research, Ludwig-Maximilians-Universität (LMU) Munich, Munich, Germany, [5]Department of Nuclear Medicine, University Hospital, Ludwig-Maximilians-Universität (LMU) Munich, Munich, Germany, [6]Institute of Neuroradiology, University Hospital, Ludwig-Maximilians-Universität (LMU) Munich, Munich, Germany, [7]Department of Radiation Oncology, University Hospital, Ludwig-Maximilians-Universität (LMU) Munich, Munich, Germany

Background: Brain metastases (BM) represent the most frequent intracranial tumors with increasing incidence. Many primary tumors are currently treated in protocols that incorporate targeted therapies either upfront or for progressive metastatic disease. Hence, molecular markers are gaining increasing importance in the diagnostic framework of BM. In cases with diagnostic uncertainty, both in newly diagnosed or recurrent BM, stereotactic biopsy serves as an alternative to microsurgical resection particularly whenever resection is not deemed to be safe or feasible. This retrospective study aimed to analyze both diagnostic yield and safety of an image-guided frame based stereotactic biopsy technique (STX).

Material and methods: Our institutional neurosurgical data base was searched for any surgical procedure for suspected brain metastases between January 2016 and March 2021. Of these, only patients with STX were included. Clinical parameters, procedural complications, and tissue histology and concomitant molecular signature were assessed.

Results: Overall, 467 patients were identified including 234 (50%) with STX. Median age at biopsy was 64 years (range 29 – 87 years). MRI was used for frame-based trajectory planning in every case with additional PET-guidance in 38 cases (16%). In total, serial tumor probes provided a definite diagnosis in 230 procedures (98%). In 4 cases (1.7%), the pathological tissue did not allow a definitive neuropathological diagnosis. 24 cases had to be excluded due to non-metastatic histology, leaving 206 cases for further analyses. 114 patients (49%) exhibited newly diagnosed BM, while 46 patients (20%) displayed progressive BM. Pseudoprogression was seen in

46 patients, a median of 12 months after prior therapy. Pseudoprogression was always confirmed by clinical course. Metastatic tissue was found most frequently from lung cancer (40%), followed by breast cancer (9%), and malignant melanoma (7%). Other entities included gastrointestinal cancer, squamous cell cancer, renal cell carcinoma, and thyroid cancer, respectively. In 9 cases (4%), the tumor origin could not be identified (cancer of unknown primary). Molecular genetic analyses were successful in 137 out of 144 analyzed cases (95%). Additional next-generation sequencing revealed conclusive results in 12/18 (67%) cases. Relevant peri-procedural complications were observed in 5 cases (2.4%), which were all transient. No permanent morbidity or mortality was noted.

Conclusion: In patients with BM, frame-based stereotactic biopsy constitutes a safe procedure with a high diagnostic yield. Importantly, this extended to discerning pseudoprogression from tumor relapse after prior therapy. Thus, comprehensive molecular characterization based on minimal-invasive stereotactic biopsies lays the foundation for precision medicine approaches in the treatment of primary and recurrent BM.

KEYWORDS

stereotactic biopsy, brain metastases, recurrent brain metastases, pseudoprogression, precision medicine, molecular diagnostics, image guided procedures, targeted therapy

Introduction

Brain metastases (BM) occur in up to 40% of all patients with solid tumors over the course of disease (1, 2). Patients suffering from lung carcinoma, both non-small cell lung cancer (NSCLC) and small cell lung cancer (SCLC), as well as breast cancer and malignant melanoma are most commonly affected (1–3). Due to a short median survival time of less than 12 months across nearly all primary sites and the often-limited efficacy of systemic therapy, clinical management of BMs can be exhausting and requires multidisciplinary expertise (1, 2). According to the 2021 joint European Association of Neuro-Oncology (EANO) and European Society for Medical Oncology (ESMO) guidelines for diagnosis, treatment and follow-up of patients with brain metastasis from solid tumors, any new neurological deficit in a cancer patient should always be suggestive of BM (4). Suspicious brain lesions may also appear on routine check-up magnetic resonance imaging (MRI)-scans of cancer patients, incidentally or during the recommended work-up (2). Singular lesions amenable to safe surgical resection should be operated upon, space-occupying lesions may even require urgent decompression (4, 5). Microsurgical tumor resection serves both therapeutic and diagnostic purposes, but at the risk of potential surgical complications particularly in frail patients (6).

Versatile histopathological and molecular-genetic analyses, however, should also be available in all unclear cases with multiple or highly eloquent lesions, particularly in patients with a history of more than one primary tumor, and those with unclear tumor status after therapy (7–9). Novel high-throughput sequencing methods have improved our understanding of individual cellular and molecular tumor targets. As a result, multiple novel personalized treatment strategies have been identified to treat cancer patients, thus opening novel treatment options for BMs. For example, in patients with Her2-positive breast cancer BMs (10, 11), those with ALK-rearranged (12, 13) or EGFR-mutated (14, 15) NSCLC BMs, and for BRAF V600 E mutated melanoma BMs (16), targeted therapies with significant intracranial activity are available. Still, there may be discrepancies between the actionable mutations of the primary tumor and their respective BM (17) and thus tissue-based analyses of BM can be necessary to guide therapy.

Due to the high recurrence rate of BM, follow-up imaging with short intervals is pivotal to monitor the course of disease and to potentially re-adjust therapy in case of tumor progression. However, suspicious lesions on MRI-scans can also be a manifestation of post-therapeutic changes, e.g., tissue necrosis after a radiation procedure or inflammatory reactions during immunotherapies, also termed pseudoprogression (18, 19).

Due to similar visual characteristics, correct differentiation from tumor recurrence can be a diagnostic challenge. The response assessment in neuro-oncology (RANO) working group recommends O-(2-^{18}Fluorethyl)-L-tyrosine ([^{18}F] FET PET) to discriminate true tumor progression from pseudoprogression (20–22). Nevertheless, in unclear cases tissue acquisition remains the gold standard to resolve this diagnostic quandary and to select the appropriate treatment modality (18, 23).

Consequently, minimally invasive biopsy techniques are of high importance in the field of brain metastases (4, 5). Even though stereotactic frame-based biopsy represents a well-established procedure, general analyses of BM biopsy cases and their respective histopathologic results have only been performed in a few studies to date. Importantly, these studies have mostly lacked in-depth molecular data and concomitant analyses of the associated risk profile. With the present study, we aim to delineate diagnostic accuracy, intervention-related risks and the diagnostic benefit of stereotactic biopsy for suspected BM.

Materials and methods

Study population

Our neurosurgical database was retrospectively searched for all patients undergoing any surgical procedure for suspected brain metastases between January 2016 and March 2021. Of these, only patients undergoing stereotactic biopsy were included. Ethical approval for this analysis was obtained from the ethics committee of the Ludwigs-Maximilians University Hospital (project number 22-0476). Patients provided informed written consent to allow for anonymous or pseudonymous data handling.

A standardized set of demographic, radiological, neuropathological, and clinical data was obtained. This included information on any known primary tumor as well as results of histological and, whenever conducted, molecular diagnosis. Complications were evaluated according to the Common Terminology Criteria for Adverse Events (CTCAE 5.0) classification system (24).

Stereotactic biopsy technique

A highly standardized, frame-based, imaging-guided stereotactic biopsy technique was applied in all patients (23, 25).

Preoperative workup comprised a 1.5 or 3T MRI scan (with T2 and T1 sequences before and after application of a Gadolinium-based contrast agent and MR-angiography sequences) that was acquired one day prior to surgery and fused with an intraoperative, contrast-enhanced computed tomography (CT) angiography scan with the patients' head fixed in the frame. If available, PET imaging data based on [^{18}F] FET was included in the triplanar trajectory planning (Brainlab® Elements Stereotactic Planning). At our center, [^{18}F] FET-PET is used as an additional diagnostic examination method for BMs, primarily during the course of the disease in cases of suspected local recurrence after (radiation) therapy and to identify reactive changes (26, 27). The indication for [^{18}F] FET-PET is consented for each individual patient within the interdisciplinary neuro-oncological tumor board.

Each trajectory was meticulously planned to harvest maximal active tumor tissue (no necrosis) and to avoid any risk of vascular damage, contact to sulci or cerebrospinal fluid (CSF) drainage, which may lead to intraoperative brain-shift with subsequent mismatch between planning MRI and real anatomy. A phantom frame was used to confirm correct 3-dimensional angulation prior to surgery in all patients. A skin incision of 4-6 millimeters (mm) was made and followed by a frame-guided burr hole trepanation with a diameter of 3 mm. After perforation of the dura through advancing a sharp trocar, a blunt trocar is used to reach the lesion. Subsequently, after inserting a rigid tube, multiple small tissue samples of 1 mm^3 each were taken by utilizing a designated biopsy forceps inserted in the tube. An experienced neuropathologist was on site in the operating room (OR) during the procedure to examine whether the material obtained was sufficient in terms of quantity and quality for gaining a diagnosis. In our routine protocol, the first tissue samples are already used for smear preparation in order to limit the number of tissue samples taken that are necessary for a comprehensive neuropathologic diagnosis. Thereafter, the skin was closed with a suture. A routine control CT was performed within 24 hours to exclude hemorrhage and to confirm the correct site of tissue sampling in case of an inconclusive neuropathological finding.

Neuropathological diagnosis and molecular genetic analyses

Histopathological and molecular diagnosis including next-generation sequencing was performed according to EANO guidelines at the Center for Neuropathology and Prion Research of the University Hospital Munich (28). To determine the origin of the respective BM, basic morphology is investigated in a first step to differentiate between carcinomas, lymphomas and melanomas. Immunohistochemical profiles of BM may be indicative of the site and lineage of the primary tumor. In case of a cerebral adenocarcinoma of unknown primary, TTF-1 status was investigated, as positive results are strongly associated with lung cancer and thyroid cancer. CK7 negativity and CK20 positivity were studied for potential

evidence of colorectal cancer. Neuro-endocrine differentiation was tested using chromogranin, synaptophysin antibodies directed against specific hormones (e.g. insulin, gastrin, and glucagon). When sarcoma or other related mesenchymal primary malignancies were suspected, immunohistochemical panels for mesenchymal tumors were utilized (vimentin, desmin, S100) (28). In the absence of clear neuropathologic diagnostic criteria, when predominantly reactive changes were detected after tumor therapy without unequivocal tumor cell evidence, the neuropathologic presumption of a pseudoprogression was made, but this was always interpreted in light of the clinical course and imaging findings. This also includes the distinction from radiation necrosis, which was expressed if in particular necrosis zones and vascular proliferates were detected.

Statistics

Patient-related, clinical and molecular information was collected and anonymized. Data analysis and descriptive statistics were performed using IBM SPSS Statistic software v25.0 (IBM, Armonk, New York, USA). When normal distribution of data sets was to be assumed, median and range were calculated. For comparison of absolute numbers, percentages were calculated. Subgroups were compared according to categorical and continuous variables. The level of significance was set at 0.05. The time between treatment and re-biopsy was compared between patients with true tumor progression or pseudoprogression using Log-rank test. Hazard Ratios (HR) were calculated and Confidence Intervals (CI) were given.

Results

Patients, procedure and tumor characteristics

Between January 2016 and March 2021, 467 patients underwent neurosurgical procedures for suspected BM with 234 (50%) stereotactic biopsies. Of the latter, 24 (12%) were excluded due to non-metastatic tissue (mainly cerebral lymphomas and inflammatory reactions). In 4 cases, histopathology and molecular analyses of lesional tissue samples was inconclusive, leaving a total number of 206 biopsied BM patients for further analyses (see Figure 1). In this study population, median age was 64 years, ranging from 29 to 87 years. 106 patients (52%) were female.

Out of 159 (77%) lesions with lobar location, 78 were left sided and 18 were located bilaterally. 39 BM (19%) were deep seated (insula, thalamus, pineal region, cerebellum) and 8 (3.9%) lesions involved the brainstem (Table 1).

Table 2 lists all primary tumor entities of the BM. Most frequent was lung cancer (39.8%), followed by breast cancer (9.2%) and malignant melanoma (7.3%).

In 114 out of 206 (55%) patients, BM were newly diagnosed. This included 45 cases with new-onset neurological symptoms and a first diagnosis of metastatic disease. In 64 patients, BM from known cancer diagnosis was confirmed. In 5 exceptional cases, the histologic examination revealed a metastatic origin different from the prior established cancer diagnosis.

In 92 (45% of) cases, STX was performed because of suspected tumor recurrence. As recommended by the interdisciplinary tumor board, additional [^{18}F]-FET-PET imaging was available in 38 of these patients to rule out

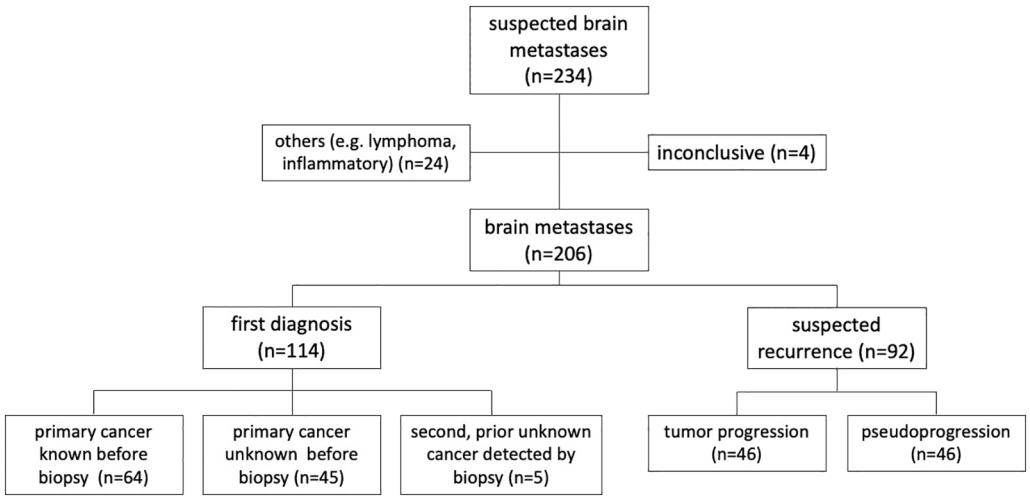

FIGURE 1
Study population.

TABLE 1 Biopsy locations in primary and recurrent disease.

Location		first diagnosis n (%)	recurrence n (%)	total n (%)
lobar	*frontal*	35 (17.0)	35 (17.0)	70 (34.0)
	temporal	13 (6.3)	8 (3.9)	21 (10.2)
	parietal	17 (8.3)	15 (7.3)	32 (15.5)
	occipital	3 (1.5)	9 (4.4)	12 (5.8)
	central	11 (5.4)	13 (6.3)	24 (11.7)
deep seated	*insular*	1 (0.5)	6 (2.9)	7 (3.4)
	thalamic	1 (0.5)	0 (0.0)	1 (0.5)
	pineal	3 (1.5)	0 (0.0)	3 (1.5)
	cerebellar	24 (11.7)	4 (1.9)	28 (13.6)
brainstem	*mesencephalon*	2 (1.0)	0 (0.0)	2 (1.0)
	pons	4 (1.9)	2 (1.0)	6 (2.9)
total		**114 (55.3)**	**92 (44.7)**	**206 (100)**

pseudoprogression/radionecrosis (Table 3). In this patient population, [^{18}F] FET PET was indicative of tumor recurrence in 28 cases (subsequently confirmed histologically in 14 patients), while pseudoprogression/radionecrosis was noted in 10 cases (2 with histology showing tumor recurrence). This resulted in a sensitivity of 88% and specificity of 36% for [^{18}F] FET PET to detect malignant progression, as well as a sensitivity of 80% and a specificity 88% of [^{18}F] FET PET to determine cerebral reactive changes.

Overall, neuropathological evaluation confirmed recurrent BM in 46 patients. These patients underwent additional treatment. In the other 46 patients, the biopsies showed only

TABLE 2 Listing of systemic tumor diseases.

Primary tumor entity	n (%)
Lung cancer	82 (39.8)
Breast cancer	19 (9.2)
Malignant melanoma	15 (7.3)
Cancer of unknown primary (CUP)	9 (4.4)
Gastrointestinal cancer	9 (4.4)
Squamous cell carcinoma	6 (2.9)
Thyroid cancer	5 (2.4)
Renal cell carcinoma	5 (2.4)
Other primary tumors	4 (1.9)
Gynecological tumor	3 (1.5)
Prostate cancer	3 (1.5)
Pseudoprogression	46 (22.3)
	Lung cancer 22 (47.8) Malignant melanoma 11 (23.9) Breast cancer 6 (13.0) Squamous cell carcinoma 3 (0.7) Other primary tumors 3 (0.7) Renal cell carcinoma 1 (0.2)
Total	**206 (100)**

TABLE 3 Results of [^{18}F] FET PET and stereotactic biopsy in suspected recurrences.

Histology of biopsy specimen	Tumor	Reactive Changes	Total
[^{18}F]FET PET suggestive of tumor	14	14	16
[^{18}F]FET PET suggestive of reactive changes	2	8	22
Total	28	10	38

reactive changes consistent with pseudoprogression/radionecrosis. These latter patients were last pretreated with radiosurgery (n=19), fractionated stereotactic irradiation (N=8), interstitial brachytherapy (N=4) or systemic treatment (N=15), respectively. The median time between last treatment and occurrence of pseudoprogression/radionecrosis was 12 months (range, 3-112 months) and differed significantly from patients with proven tumor progression (median 7 months; Log-rank: HR 2.61; 95% CI of ratio 1.6-4.24; p<0.0001). Patients with pseudoprogression underwent close clinical and imaging follow-up, which ultimately confirmed reactive changes without active tumor activity in all these patients.

Molecular analyses

Depending on the type of cancer confirmed histologically, certain biomarkers (all listed in Table 4) were requested by the interdisciplinary tumor board to establish the diagnosis and guide further therapeutic decisions.

For lung cancer metastases, ALK-protein and EGF-receptor (EGFR) were analyzed most frequently, with 31 conclusive cases out of 32 analyzed (97%). Furthermore, the PD-L1 surface protein was conclusively evaluated in 20/20 (100%) and the ROS1-protein in 13/15 cases (87%). In the 19 cases with breast cancer metastases, the estrogen-receptor (ER) was conclusively analyzed in 14/14 cases (100%), the progesteron-receptor in 7/7 cases (100%), and Her2/neu in 10/11 cases (91%). For patients with a malignant melanoma, molecular analysis was requested for the BRAF-gen in 13 cases and conclusive in 11 (85%). In total, the specific molecular genetic analysis was conclusive in 137 out of 144 cases (95%). Next-generation sequencing revealed 12 (67%) conclusive results in a small subgroup of 18 analyzed cases.

In addition, the molecular genetic signature of BM could be compared with the original tumor signature of 9 breast cancer patients regarding Her2/neu, ER and PR expression. From this group, 4 patients had an identical molecular signature, 3 had a partially matched signature, while in 2 cases a molecular signature different from the primary site was identified.

Periprocedural complications

In 136 out of 206 cases (66%), a regular postoperative CT was performed. Minimal, clinically asymptomatic hemorrhages

TABLE 4 Molecular markers analysed among different tumor entities.

Primary tumor	Molecular marker	Positive n (%)	Negative n (%)	Inconclusive n (%)	Examinedn (%) Examined/Total (%)
Breast cancer	Her2/neu	8 (72.7)	2 (18.2)	1 (9.1)	11 (100.0) 11/19 (57.9)
	Estrogen receptor (ER)	13 (92.9)	1 (7.1)	0 (0.0)	14 (100.0) 14/19 (73.7)
	Progesteron receptor (PR)	6 (85.7)	1 (14.3)	0 (0.0)	7 (100.0) 7/19 (36.8)
Lung cancer	ALK	2 (6.3)	29 (90.6)	1 (3.1)	32 (100.0) 32/82 (39.0)
	ROS1	0 (0.0)	13 (86.7)	2 (13.3)	15 (100.0) 15/82 (18.3)
	EGFR	10 (31.3)	21 (65.6)	1 (3.1)	32 (100.0) 32/82 (39.0)
	PD-L1	9 (45.0)	11 (55.0)	0 (0.0)	20 (100.0) 20/82 (24.4)
Malignant melanoma	BRAF	7 (53.8)	4 (30.8)	2 (15.4)	13 (100.0) 13/15 (86.7)

were visible in 59 postoperative CT scans (29%). Local hemorrhages with mild clinical symptoms occurred in 10 cases (4.9%). A space-occupying bleeding event was observed in one patient, which was successfully managed conservatively (Table 5). Overall, eloquent/deep-seated tumor location was not associated with an increased risk of bleeding.

A summary of complications according the CTCAE classification is provided in Table 6. Five (2.4%) patients reported mild symptoms (CTCAE grade 1) such as headaches, nausea, dizziness and rashes caused by perioperative antibiotics. CTCAE grade 2 complications were noted in two cases (1.0%), including one case of higher blood loss in need of transfusion most likely due to puncture of an intraosseous vein, and one case of perioperative atrial fibrillation. Severe symptoms (CTCAE grade 3) developed in 6 cases (2.9%): a paresis occurred in 3 cases after the intervention, one patient additionally presented with aphasia, and one with a fall due to this deficit. Two cases presented with a decreased level of consciousness immediately after the procedure, which resolved without further intervention. In all cases, CT scans were unremarkable. One patient without a prior history of epilepsy experienced a new focal tonic-clonic seizure. Overall, no life-threatening complications (CTCAE grade 4) or mortalities (CTCAE grade 5) emerge across the entire cohort. All complications were transient and resolved during the inpatient stay.

Discussion

In this retrospective analysis from a high-volume comprehensive cancer center, we addressed the diagnostic value and peri-procedural risk of a highly standardized, advanced imaging-based stereotactic biopsy technique. Furthermore, we performed extended molecular-genetic analyses in a sub-cohort. Overall, the diagnostic accuracy of representative tissue samples was found to be high and the associated risk was low, even in highly eloquent locations such as the brain stem. The high diagnostic certainty of >98% definite neuropathological diagnoses (only 4 inconlusive cases among 234 biopsies for suspected metastases) and low peri-procedural risk of 2.6% for clinically relevant transient morbidity is in line with our previous results on the value of stereotactic biopsy in a large cohort of primary brain tumors (23), and differs from retrospective analyses by other groups studying the respective diagnostic yield (up to 11% inconclusive results) (29).

The low procedural risk and high diagnostic yield of the collected tumor tissue is realized due to the combination of two relevant factors. First, a spatially precise fusion of advanced high-resolution imaging data (including MR-angiography and PET) to the frame-based CT-scan. Second, a versatile, small-sample size optimized neuropathological evaluation integrating intraoperative smear-preparation for representative tissue selection. Because of the low bleeding rate, we have largely eliminated postoperative cranial CT scans from our clinical routine and limit it to the rare cases with diagnostic uncertainty to rule out a missed biopsy.

No comparison was made to frameless biopsy procedures. At our institution, the latter technique is usually applied only for superficial primarily dural lesions without significant involvement of adjacent brain tissue and for extended cortical-subcortical tissue cubes when vasculitis is suspected. There are

TABLE 5 Complications according postoperative imaging.

CT (post-operative)	First diagnosis n (%)	Recurrence n (%)	Total n (%)
no visible blood	77 (37.4)	59 (28.6)	136 (66.0)
Minimal hemorrhage	30 (14.6)	29 (14.1)	59 (28.6)
Local hemorrhage	6 (2.9)	4 (1.9)	10 (4.9)
Space-occupying hemorrhage	1 (0.5)	0 (0.0)	1 (0.5)
Total	**114 (55.3)**	**92 (44.7)**	**206 (100.0)**

TABLE 6 Clinical complications according severity.

CTCAE	First diagnosis n (%)	Recurrence n (%)	Total n (%)
0	110 (53.4)	83 (40.3)	193 (93.7)
1	1 (0.5)	4 (1.9)	5 (2.4)
2	0 (0.0)	2 (1.0)	2 (1.0)
3	3 (1.5)	3 (1.5)	6 (2.9)
Total	**114 (55.3)**	**92 (44.7)**	**206 (100.0)**

no prospective studies addressing the different biopsy techniques in terms of diagnostic yield and associated risk profiles. However, retrospective studies have demonstrated that frameless biopsy also provides good diagnostic value with low procedural risk (30). Whether this is also the case for highly eloquently located lesions in the midbrain or brainstem has not been clearly shown. Indeed, eloquent location was associated with in increased risk of periprocedural morbidity in 284 cases undergoing frameless biopsy (31). In our clinical experience, this subgroup of patients is often referred to us for further evaluation from other university and/or tertiary centers. In our hands there is no obvious disadvantage in terms of time of operating theater occupancy and staff retention compared to frameless procedures (30): Our stereotaxy system (Brainlab® Elements Stereotactic Planning) already enables target-point-accurate trajectory planning the day before, which is merely supplemented by the information from the intraoperative CT. The actual operating time is usually 20 minutes. A major advantage of frameless systems, however, lies in the prevention of intraoperative radiation exposure.

The intraoperative presence of the neuropathologist certainly contributed to the high quality of our result. Although the results of the smear preparations did not result in a second trajectory being performed, the neuropathologist can help to minimize the total number of serial biopsies needed by providing early feedback, thereby reducing the overall risk of the procedure (32). This could be of particular benefit in highly vascularized tumors and in the case of highly eloquent tumor localizations such as the brainstem.

The study population reflects the current challenges in patients with BM. In this large cohort of over 450 patients in 5 years, we demonstrate that approximately 50% were not amenable for surgical resection, but were referred for biopsy as part of a risk-adapted interdisciplinary treatment regimen. Of note, only BM patients referred to our neuro-oncology center due to diagnostic uncertainty were included in this study. In clinical routine, many BM patients with a limited number of small BMs in known primary tumors as well as those with miliary seeding are usually scheduled for radiosurgery, stereotactic fractionated protocols, or whole-brain irradiation without being discussed in an interdisciplinary tumor board. The majority of our study patients underwent stereotactic biopsy in the setting of newly diagnosed brain metastasis. In 40% of these patients, BM biopsy was recommended to diagnose the systemic tumor because systemic biopsy was deemed either technically impossible or too risky. Remarkably, in a small subset of patients with newly diagnosed suspected brain metastasis (5/114, 4.4%), a previously unknown second tumor was detected.

After BM treatment, routine follow-up imaging is recommended in short intervals to readily detect tumor progression and to re-adjust treatment recommendations accordingly. However, the differentiation of tumor relapse from pseudoprogression/radionecrosis still represents a major challenge in BM. Standardized MRI as well as [^{18}F] FET PET is routinely performed at our institution according to current RANO guidelines (20, 21). However, the diagnostic certainty of [^{18}F] FET PET outlined in this study (sensitivity 87.5%, specificity 36.4% to detect malignant progression) is not sufficient to guide therapy decisions, so that the indication for tissue diagnosis has to be confirmed. In fact, reactive alterations without significant tumor cell content were observed in a striking 50% of patients and pseudoprogression could be confirmed due to the subsequent clinical course of disease in all these cases. The rate of reactive alterations may further increase if treatment approaches combining radiotherapy and immunotherapy are applied. However, this combination was rarely administered in this series, and as a result no such analysis could be performed. In our neuropathological diagnosis, the transition from reactive changes in the sense of a pseudoprogress to (symptomatic) radiation necrosis appears to be fluid. In the absence of clear neuropathological differentiation criteria, the interpretation often depends additionally on the clinical appearance and the image morphological findings and remains an individual decision. High numbers of radionecrosis, however, were reported in a case series of 2,200 BM patients treated with radiosurgery (33). Follow-up investigation confirmed a recurrence in 203 cases (46%), radionecrosis in 118 cases (27%), both recurrence and radionecrosis in 30 cases (6.8%), and 90 patients (20%) displayed inconclusive results. An even higher number of 69% histologically confirmed cases of radionecrosis were reported in 35 BM after radiosurgery (34). Therefore, STX as a minimal-invasive tissue sampling procedure for accurate tissue diagnosis will certainly gain increasing relevance in the era of precision medicine for BM (35–37).

The evolving landscape of effective targeted therapies has significantly altered the management paradigm of BMs (7, 38, 39). For example, targeted therapies have established intracranial activity in patients with Her2-positive breast cancer BM (10, 11), ALK-rearranged (12, 13) or EGFR-mutated NSCLC BM (40) and for BRAF V600E mutated melanoma BM (41). For subgroups of asymptomatic patients, targeted systemic therapy as monotherapy even represents a first-line consideration (41–43). Notably, tumor-dependent discrepancies can arise between the actionable mutational profile of the primary tumor and the respective BM (17). Strikingly, approximately 50% of brain metastases can harbor clinically relevant mutations that are not present in the primary tumor, indicating significant clonal heterogeneity across the various geographic regions of the tumor (44). Therefore, tissue-based analyses of BM are not only important to understand the pathogenesis of tumorigenesis, but are essential in guiding therapeutic concepts. Discordance in regards to EGFR status between brain metastases and matched NSCLC samples has been reported in 0–33% of cases, whereas the discordance rate for ALK rearrangements lies in the range of 0–13% (8). For breast cancer BM, a discordance rate of

14% for Her2 and 29% for ER/PR has been reported (45). Discordant molecular profiles were also observed in a small subgroup of breast cancer patients in this case series. Such discrepancies indicate a dynamic, clonal evolution of the spreading disease and has important implications for combinatorial treatment approaches (46). In this context, a safe and simple way to diagnose and longitudinally evaluate BM is of increasing clinical relevance.

In summary, the high diagnostic yield and low complication rate supports an important role for minimal-invasive biopsy procedures in risk-adapted management algorithms for BM. Since it is still an invasive intervention, a reasonable and cautious assessment of the individual indication and risk-benefit profile is clearly demanded. However, due to increasingly specialized teams and interdisciplinary cooperation, a high-quality standard of this procedure can be maintained. While other diagnostic methods, such as liquid biopsy, represent a less invasive examination method, they are less-researched, still of experimental nature in most cases, and do not have the same informational value as stereotactic biopsy (47, 48).

Our study has several important limitations. Due to the retrospective study design, several relevant questions such as the significance of [18F] FET-PET, timing of biopsy, and longitudinal treatment data, remain unanswered and warrant future systematic study. Important information concerning the intraoperative interaction between the stereotactic neurosurgeon and treating neuropathologist regarding the number and use (for smear preparation vs. final neuropathologic assessment or molecular genetic analysis) of serial tissue samples cannot be objectively recorded. In addition, no qualitative comparison can be made with other biopsy techniques, such as frameless procedures. In our study, the result of neuropathologic examination was the gold standard and the basis for any management decision in individual cases. Although in all cases the further clinical course supported a correct assessment, clinical misjudgment based on neuropathologic diagnosis cannot be excluded with absolute certainty.

In conclusion, image-guided stereotactic biopsy represents a valid and safe tool for diagnosis and even molecular characterization of BM. The precise identification of the molecular signatures of BM can guide the appropriate choice of targeted therapies, heralding a new era of precision medicine in the treatment of primary and recurrent brain metastases.

Data availability statement

The datasets presented in this article are not readily available because of national and institutional laws to protect patient confidentiality. Requests to access the datasets should be directed to the Center for Neuropathology and Prion Research of the University Hospital of Munich.

Ethics statement

Ethical approval for this analysis was obtained from the ethics committee of the Ludwigs-Maximilians University Hospital (project number 22-0476). Patients provided informed written consent to allow for anonymous or pseudonymous data handling.

Author contributions

J-CT, SQ, LB and NT contributed to conception and design of the study. AD, SK, SQ, and NT organized the database, evaluated the clinical courses and performed image analyses. AD and SK carried out the statistical analyses. AD, SQ, SK, JW, J-CT, LB, and NT wrote the manuscript. MD, NA, RF, MN, and RE edited the manuscript. All authors contributed to manuscript revision, read and approved the submitted version.

Conflict of interest

The authors declare that the research was conducted in the absence of any commercial or financial relationships that could be construed as a potential conflict of interest.

Publisher's note

All claims expressed in this article are solely those of the authors and do not necessarily represent those of their affiliated organizations, or those of the publisher, the editors and the reviewers. Any product that may be evaluated in this article, or claim that may be made by its manufacturer, is not guaranteed or endorsed by the publisher.

References

1. Cagney DN, Martin AM, Catalano PJ, Redig AJ, Lin NU, Lee EQ, et al. Incidence and prognosis of patients with brain metastases at diagnosis of systemic malignancy: a population-based study. *Neuro Oncol* (2017) 19(11):1511–21. doi: 10.1093/neuonc/nox077

2. Lamba N, Wen PY, Aizer AA. Epidemiology of brain metastases and leptomeningeal disease. *Neuro Oncol* (2021) 23(9):1447–56. doi: 10.1093/neuonc/noab101

3. Ostrom QT, Wright CH, Barnholtz-Sloan JS. Brain metastases: epidemiology. *Handb Clin Neurol* (2018) 149:27–42. doi: 10.1016/B978-0-12-811161-1.00002-5

4. Le Rhun E, Guckenberger M, Smits M, Dummer R, Bachelot T, Sahm F, et al. EANO-ESMO clinical practice guidelines for diagnosis, treatment and follow-up of patients with brain metastasis from solid tumours. *Ann Oncol* (2021) 32(11):1332–47. doi: 10.1016/j.annonc.2021.07.016

5. Vogelbaum MA, Brown PD, Messersmith H, Brastianos PK, Burri S, Cahill D, et al. Treatment for brain metastases: ASCO-SNO-ASTRO guideline. *J Clin Oncol* (2022) 40(5):492–516. doi: 10.1200/JCO.21.02314

6. Karschnia P, Le Rhun É, Vogelbaum MA, van den Bent MJ, Grau SJ, Preusser M, et al. The evolving role of neurosurgery for central nervous system metastases in the era of personalized cancer therapy. *Eur J cancer.* (2021) 156:93–108. doi: 10.1016/j.ejca.2021.07.032

7. Tan AC, Bagley SJ, Wen PY, Lim M, Platten M, Colman H, et al. Systematic review of combinations of targeted or immunotherapy in advanced solid tumors. *J Immunother Cancer* (2021) 9(7). doi: 10.1136/jitc-2021-002459

8. Berghoff AS, Bartsch R, Wohrer A, Streubel B, Birner P, Kros JM, et al. Predictive molecular markers in metastases to the central nervous system: recent advances and future avenues. *Acta Neuropathol.* (2014) 128(6):879–91. doi: 10.1007/s00401-014-1350-7

9. Brastianos PK, Carter SL, Santagata S, Cahill DP, Taylor-Weiner A, Jones RT, et al. Genomic characterization of brain metastases reveals branched evolution and potential therapeutic targets. *Cancer Discovery* (2015) 5(11):1164–77. doi: 10.1158/2159-8290.CD-15-0369

10. Murthy RK, Loi S, Okines A, Paplomata E, Hamilton E, Hurvitz SA, et al. Tucatinib, trastuzumab, and capecitabine for HER2-positive metastatic breast cancer. *N Engl J Med* (2020) 382(7):597–609. doi: 10.1056/NEJMoa1914609

11. Lin NU, Borges V, Anders C, Murthy RK, Paplomata E, Hamilton E, et al. Intracranial efficacy and survival with tucatinib plus trastuzumab and capecitabine for previously treated HER2-positive breast cancer with brain metastases in the HER2CLIMB trial. *J Clin Oncol* (2020) 38(23):2610–9. doi: 10.1200/JCO.20.00775

12. Cadranel J, Cortot AB, Lena H, Mennecier B, Do P, Dansin E, et al. Real-life experience of ceritinib in crizotinib-pretreated ALK(+) advanced non-small cell lung cancer patients. *ERJ Open Res* (2018) 4(1). doi: 10.1183/23120541.00058-2017

13. Rybarczyk-Kasiuchnicz A, Ramlau R, Stencel K. Treatment of brain metastases of non-small cell lung carcinoma. *Int J Mol Sci* (2021) 22(2). doi: 10.3390/ijms22020593

14. Hsu WH, Yang JC, Mok TS, Loong HH. Overview of current systemic management of EGFR-mutant NSCLC. *Ann Oncol* (2018) 29(suppl_1):i3–9. doi: 10.1093/annonc/mdx702

15. Costa C, Molina MA, Drozdowskyj A, Gimenez-Capitan A, Bertran-Alamillo J, Karachaliou N, et al. The impact of EGFR T790M mutations and BIM mRNA expression on outcome in patients with EGFR-mutant NSCLC treated with erlotinib or chemotherapy in the randomized phase III EURTAC trial. *Clin Cancer Res* (2014) 20(7):2001–10. doi: 10.1158/1078-0432.CCR-13-2233

16. Long GV, Weber JS, Infante JR, Kim KB, Daud A, Gonzalez R, et al. Overall survival and durable responses in patients with BRAF V600-mutant metastatic melanoma receiving dabrafenib combined with trametinib. *J Clin Oncol* (2016) 34 (8):871–8. doi: 10.1200/JCO.2015.62.9345

17. Cacho-Diaz B, Garcia-Botello DR, Wegman-Ostrosky T, Reyes-Soto G, Ortiz-Sanchez E, Herrera-Montalvo LA. Tumor microenvironment differences between primary tumor and brain metastases. *J Transl Med* (2020) 18(1):1. doi: 10.1186/s12967-019-02189-8

18. Lee D, Riestenberg RA, Haskell-Mendoza A, Bloch O. Brain metastasis recurrence versus radiation necrosis: Evaluation and treatment. *Neurosurg Clin N Am* (2020) 31(4):575–87. doi: 10.1016/j.nec.2020.06.007

19. Le Rhun E, Wolpert F, Fialek M, Devos P, Andratschke N, Reyns N, et al. Response assessment and outcome of combining immunotherapy and radiosurgery for brain metastasis from malignant melanoma. *ESMO Open* (2020) 5(4). doi: 10.1136/esmoopen-2020-000763

20. Galldiks N, Kocher M, Ceccon G, Werner JM, Brunn A, Deckert M, et al. Imaging challenges of immunotherapy and targeted therapy in patients with brain metastases: response, progression, and pseudoprogression. *Neuro Oncol* (2020) 22 (1):17–30. doi: 10.1093/neuonc/noz147

21. Okada H, Weller M, Huang R, Finocchiaro G, Gilbert MR, Wick W, et al. Immunotherapy response assessment in neuro-oncology: a report of the RANO working group. *Lancet Oncol* (2015) 16(15):e534–e42. doi: 10.1016/S1470-2045(15)00088-1

22. Bodensohn R, Forbrig R, Quach S, Reis J, Boulesteix AL, Mansmann U, et al. MRI-Based contrast clearance analysis shows high differentiation accuracy between radiation-induced reactions and progressive disease after cranial radiotherapy. *ESMO Open* (2022) 7(2):100424. doi: 10.1016/j.esmoop.2022.100424

23. Katzendobler S, Do A, Weller J, Dorostkar MM, Albert NL, Forbrig R, et al. Diagnostic yield and complication rate of stereotactic biopsies in precision medicine of gliomas. *Front Neurol* (2022) 13:822362. doi: 10.3389/fneur.2022.822362

24. National Institutes of Health NCI. Common terminology criteria for adverse events (CTCAE) version. (2017) 5. doi: 10.1177/1740774517698645

25. Weller J, Katzendobler S, Karschnia P, Lietke S, Egensperger R, Thon N, et al. PCV chemotherapy alone for WHO grade 2 oligodendroglioma: prolonged disease control with low risk of malignant progression. *J Neurooncol.* (2021) 153 (2):283–91. doi: 10.1007/s11060-021-03765-z

26. Galldiks N, Abdulla DSY, Scheffler M, Wolpert F, Werner JM, Hullner M, et al. Treatment monitoring of immunotherapy and targeted therapy using (18)F-FET PET in patients with melanoma and lung cancer brain metastases: Initial experiences. *J Nucl Med* (2021) 62(4):464–70. doi: 10.2967/jnumed.120.248278

27. Galldiks N, Langen KJ, Albert NL, Chamberlain M, Soffietti R, Kim MM, et al. PET imaging in patients with brain metastasis-report of the RANO/PET group. *Neuro Oncol* (2019) 21(5):585–95. doi: 10.1093/neuonc/noz003

28. Soffietti R, Abacioglu U, Baumert B, Combs SE, Kinhult S, Kros JM, et al. Diagnosis and treatment of brain metastases from solid tumors: Guidelines from the European association of neuro-oncology (EANO). *Neuro Oncol* (2017) 19 (2):162–74. doi: 10.1093/neuonc/now241

29. Georgiopoulos M, Ellul J, Chroni E, Constantoyannis C. Efficacy, safety, and duration of a frameless fiducial-less brain biopsy versus frame-based stereotactic biopsy: A prospective randomized study. *J Neurol Surg A Cent Eur Neurosurg* (2018) 79(1):31–8. doi: 10.1055/s-0037-1602697

30. Dorward NL, Paleologos TS, Alberti O, Thomas DG. The advantages of frameless stereotactic biopsy over frame-based biopsy. *Br J Neurosurg* (2002) 16 (2):110–8. doi: 10.1080/02688690220131705

31. Air EL, Leach JL, Warnick RE, McPherson CM. Comparing the risks of frameless stereotactic biopsy in eloquent and noneloquent regions of the brain: a retrospective review of 284 cases. *J Neurosurg* (2009) 111(4):820–4. doi: 10.3171/2009.3.JNS081695

32. Dhawan S, Venteicher AS, Butler WE, Carter BS, Chen CC. Clinical outcomes as a function of the number of samples taken during stereotactic needle biopsies: a meta-analysis. *J Neurooncol.* (2021) 154(1):1–11. doi: 10.1007/s11060-021-03785-9

33. Sneed PK, Mendez J, Vemer-van den Hoek JG, Seymour ZA, Ma L, Molinaro AM, et al. Adverse radiation effect after stereotactic radiosurgery for brain metastases: incidence, time course, and risk factors. *J Neurosurg* (2015) 123 (2):373–86. doi: 10.3171/2014.10.JNS141610

34. Narloch JL, Farber SH, Sammons S, McSherry F, Herndon JE, Hoang JK, et al. Biopsy of enlarging lesions after stereotactic radiosurgery for brain metastases frequently reveals radiation necrosis. *Neuro Oncol* (2017) 19(10):1391–7. doi: 10.1093/neuonc/nox090

35. Lazaro T, Brastianos PK. Immunotherapy and targeted therapy in brain metastases: emerging options in precision medicine. *CNS Oncol* (2017) 6(2):139–51. doi: 10.2217/cns-2016-0038

36. Tan XL, Le A, Lam FC, Scherrer E, Kerr RG, Lau AC, et al. Current treatment approaches and global consensus guidelines for brain metastases in melanoma. *Front Oncol* (2022) 12:885472. doi: 10.3389/fonc.2022.885472

37. De Carlo E, Bertoli E, Del Conte A, Stanzione B, Berto E, Revelant A, et al. Brain metastases management in oncogene-addicted non-small cell lung cancer in the targeted therapies era. *Int J Mol Sci* (2022) 23(12). doi: 10.3390/ijms23126477

38. Chukwueke UN, Brastianos PK. Sequencing brain metastases and opportunities for targeted therapies. *Pharmacogenomics.* (2017) 18(6):585–94. doi: 10.2217/pgs-2016-0170

39. Churilla TM, Weiss SE. Emerging trends in the management of brain metastases from non-small cell lung cancer. *Curr Oncol Rep* (2018) 20(7):54. doi: 10.1007/s11912-018-0695-9

40. Ramalingam SS, Vansteenkiste J, Planchard D, Cho BC, Gray JE, Ohe Y, et al. Overall survival with osimertinib in untreated, EGFR-mutated advanced NSCLC. *N Engl J Med* (2020) 382(1):41–50. doi: 10.1056/NEJMoa1913662

41. Tawbi HA, Forsyth PA, Algazi A, Hamid O, Hodi FS, Moschos SJ, et al. Combined nivolumab and ipilimumab in melanoma metastatic to the brain. *N Engl J Med* (2018) 379(8):722–30. doi: 10.1056/NEJMoa1805453

42. Soria JC, Ohe Y, Vansteenkiste J, Reungwetwattana T, Chewaskulyong B, Lee KH, et al. Osimertinib in untreated EGFR-mutated advanced non-Small-Cell lung cancer. *N Engl J Med* (2018) 378(2):113–25. doi: 10.1056/NEJMoa1713137

43. Aizer AA, Lamba N, Ahluwalia MS, Aldape K, Boire A, Brastianos PK, et al. Brain metastases: A society for neuro-oncology (SNO) consensus review on current management and future directions. *Neuro Oncol* (2022). doi: 10.1093/neuonc/noac118

44. Brastianos PK, Cahill DP. Management of brain metastases in the era of targeted and immunomodulatory therapies. *Oncol (Williston Park).* (2015) 29 (4):261–3.

45. Duchnowska R, Dziadziuszko R, Trojanowski T, Mandat T, Och W, Czartoryska-Arłukowicz B, et al. Conversion of epidermal growth factor receptor 2 and hormone receptor expression in breast cancer metastases to the brain. *Breast Cancer Res BCR.* (2012) 14(4):R119. doi: 10.1186/bcr3244

46. Valiente M, Ahluwalia MS, Boire A, Brastianos PK, Goldberg SB, Lee EQ, et al. The evolving landscape of brain metastasis. *Trends Cancer.* (2018) 4(3):176–96. doi: 10.1016/j.trecan.2018.01.003

47. Boire A, Brandsma D, Brastianos PK, Le Rhun E, Ahluwalia M, Junck L, et al. Liquid biopsy in central nervous system metastases: a RANO review and proposals for clinical applications. *Neuro Oncol* (2019) 21(5):571–84. doi: 10.1093/neuonc/noz012

48. Soler DC, Kerstetter-Fogle A, Elder T, Raghavan A, Barnholtz-Sloan JS, Cooper KD, et al. A liquid biopsy to assess brain tumor recurrence: Presence of circulating Mo-MDSC and CD14+ VNN2+ myeloid cells as biomarkers that distinguish brain metastasis from radiation necrosis following stereotactic radiosurgery. *Neurosurgery.* (2020) 88(1):E67–e72. doi: 10.1093/neuros/nyaa334

frontiers | Frontiers in Oncology

TYPE Original Research
PUBLISHED 16 March 2023
DOI 10.3389/fonc.2023.1056330

OPEN ACCESS

EDITED BY
Constantin Tuleasca,
Centre Hospitalier Universitaire Vaudois (CHUV), Switzerland

REVIEWED BY
Georges Sinclair,
University Hospital Southampton NHS Foundation Trust, United Kingdom
Mirza Pojskic,
University Hospital of Giessen and Marburg, Germany
Susanne Rogers,
Aarau Cantonal Hospital, Switzerland

*CORRESPONDENCE
Gueliz Acker
gueliz.acker@charite.de

SPECIALTY SECTION
This article was submitted to Neuro-Oncology and Neurosurgical Oncology, a section of the journal Frontiers in Oncology

RECEIVED 28 September 2022
ACCEPTED 20 February 2023
PUBLISHED 16 March 2023

CITATION
Acker G, Nachbar M, Soffried N, Bodnar B, Janas A, Krantchev K, Kalinauskaite G, Kluge A, Shultz D, Conti A, Kaul D, Zips D, Vajkoczy P and Senger C (2023) What if: A retrospective reconstruction of resection cavity stereotactic radiosurgery to mimic neoadjuvant stereotactic radiosurgery. *Front. Oncol.* 13:1056330. doi: 10.3389/fonc.2023.1056330

What if: A retrospective reconstruction of resection cavity stereotactic radiosurgery to mimic neoadjuvant stereotactic radiosurgery

Gueliz Acker[1,2,3]*, Marcel Nachbar[3], Nina Soffried[3], Bohdan Bodnar[3], Anastasia Janas[1], Kiril Krantchev[1], Goda Kalinauskaite[3], Anne Kluge[3], David Shultz[4], Alfredo Conti[5], David Kaul[3,6], Daniel Zips[3], Peter Vajkoczy[1] and Carolin Senger[3]

[1]Department of Neurosurgery, Charité-Universitätsmedizin Berlin (Corporate Member of Freie Universität Berlin, Humboldt-Universität zu Berlin, and Berlin Institute of Health), Berlin, Germany, [2]Berlin Institute of Health at Charité - Universitätsmedizin Berlin, BIH Academy, Clinician Scientist Program, Berlin, Germany, [3]Department of Radiation Oncology and Radiotherapy, Charité-Universitätsmedizin Berlin (Corporate Member of Freie Universität Berlin, Humboldt-Universität zu Berlin, and Berlin Institute of Health), Berlin, Germany, [4]Department of Radiation Oncology, University of Toronto, Toronto, ON, Canada, [5]Department of Biomedical and Neuromotor Sciences, Alma Mater Studiorum - Università di Bologna, Bologna, Italy, [6]German Cancer Consortium (DKTK), Partner Site Berlin, German Cancer Research Center (DKFZ), Heidelberg, Germany

Introduction: Neoadjuvant stereotactic radiosurgery (NaSRS) of brain metastases has gained importance, but it is not routinely performed. While awaiting the results of prospective studies, we aimed to analyze the changes in the volume of brain metastases irradiated pre- and postoperatively and the resulting dosimetric effects on normal brain tissue (NBT).

Methods: We identified patients treated with SRS at our institution to compare hypothetical preoperative gross tumor and planning target volumes (pre-GTV and pre-PTV) with original postoperative resection cavity volumes (post-GTV and post-PTV) as well as with a standardized-hypothetical PTV with 2.0 mm margin. We used Pearson correlation to assess the association between the GTV and PTV changes with the pre-GTV. A multiple linear regression analysis was established to predict the GTV change. Hypothetical planning for the selected cases was created to assess the volume effect on the NBT exposure. We performed a literature review on NaSRS and searched for ongoing prospective trials.

Results: We included 30 patients in the analysis. The pre-/post-GTV and pre-/post-PTV did not differ significantly. We observed a negative correlation between pre-GTV and GTV-change, which was also a predictor of volume change in the regression analysis, in terms of a larger volume change for a smaller pre-GTV. In total, 62.5% of cases with an enlargement greater than 5.0 cm^3 were smaller tumors (pre-GTV < 15.0 cm^3), whereas larger tumors greater than 25.0 cm^3 showed only a decrease in post-GTV. Hypothetical planning for the selected cases to evaluate the volume effect resulted in a median NBT exposure of only

67.6% (range: 33.2–84.5%) relative to the dose received by the NBT in the postoperative SRS setting. Nine published studies and twenty ongoing studies are listed as an overview.

Conclusion: Patients with smaller brain metastases may have a higher risk of volume increase when irradiated postoperatively. Target volume delineation is of great importance because the PTV directly affects the exposure of NBT, but it is a challenge when contouring resection cavities. Further studies should identify patients at risk of relevant volume increase to be preferably treated with NaSRS in routine practice. Ongoing clinical trials will evaluate additional benefits of NaSRS.

KEYWORDS

neoadjuvant, stereotactic radiosurgery (SRS), CyberKnife®, brain metastases (BM), preoperative

1 Introduction

The incidence of brain metastases in patients with solid tumors is estimated to be as high as 20.0% to 30.0% and is increasing due to improvements in systemic treatments and diagnostic imaging (1, 2). Consequently, and due to better control of the primary tumor and extracranial metastases, the treatment of brain metastases is gaining importance. Surgical resection of large or symptomatic tumors is most often the first treatment step followed by irradiation, as several randomized trials have demonstrated better local control with postoperative whole brain radiation therapy (post-WBRT) or postoperative stereotactic radiosurgery (post-SRS) compared to surgery alone (3–5). With increasing life expectancy due to individualized treatment approaches, there is a need to prevent cognitive impairment, which is why SRS is coming to the fore as a replacement for WBRT. Subsequently, Brown et al. compared post-WBRT with post-SRS in a randomized phase III study showing a better cognition-deterioration-free survival in post-SRS cohort with comparable overall survival in both groups. However, local control rates were worse after post-SRS (6). However, this could be due to the wide dose range, which in this study design was as low as 12 Gy in a single fraction, reflecting the need for improvement in this treatment regimen. In this context, El Safie et al. performed a comparison that also included hypofractionated SRS (HF-SRS) and found a 12-month local control rate of 94.9% for SRS/HF-SRS versus 81.7% for WBRT (7). A previous study from Patel et al. also presented 1-year local control (LC) 83% for SRS including single and HF-SRS vs. 74% for WBRT (8). Kepka et al. performed a randomized trial on this, but failed to demonstrate the non-inferiority of SRS to WBRT in terms of local control most likely due to underpowering (9). Taken together, further randomized trials are warranted including HF-SRS instead of using too low single doses.

In addition to the dose scheme issue that has to be further optimized, one further important limitation of post-SRS is probably the uncertainty of target delineation, as evidenced by the wide range of contours for ill-defined resection cavities in the contouring guidelines (10). This was also reflected in the comparative simulation study of Vellayappan et al. with high interobserver variability in resection cavity target delineation (11). Therefore, the usual practice to expand the margins, in addition to the resection cavity and to cover the surgical tracts and meninges along the bone flap, may result in larger volumes than the metastases themselves, exposing more normal brain tissue (NBT) to radiation (10, 12). Another potential pitfall of post-SRS is leptomeningeal disease (LMD), which has been reported to account for up to 35% (13, 14). Reported risk factors for LMD include primary tumor entities of the intracranial metastasis (15–18), number of intracranial lesions (13, 16, 17, 19), prior resection of an intracranial lesion (18–20), no additional immunotherapy (20, 21) and hemorrhagic or cystic features of the lesion (17), although the results of univariate and multivariate analysis vary amongst these papers. Importantly, Foreman et al. reported that they found no significant differences in LMD rates after SRS and HF-SRS (13). If we look at the above-mentioned comparative studies, Patel et al. reported WBRT to be associated with a significantly lower rate of LMD occurrence compared to SRS alone (18-month LMD 13% vs. 31%, log-rank P = 0.045); however, they did not assess the influence of SRS and HF-SRS (8).

In view of the disadvantages presented and with the aim of improving local control, neoadjuvant radiosurgical treatment (NaSRS) of intact brain metastases is currently attracting increasing attention. To date, there are nine published studies that have evaluated the efficacy of NaSRS with encouraging results, however, they are mainly retrospective in design (Table 1) (19, 22–27, 29, 30). Although a possible reduction in target volume and better sparing of healthy brain tissue have been frequently proposed as potential advantages of NaSRS, no detailed analysis of these benefits has been published. For instance, Udovicich et al. demonstrated a larger target volume after resection in a representative case (29), whereas Vellayappan et al. could not confirm a smaller volume preoperatively in a small cohort of ten patients after simulation of a NaSRS treatment (11). Atalar et al. reported that resection cavities were smaller than the target volume before resection in most cases, but without considering the recommended margin of 2 to 3 mm for planning target volume (PTV) (31, 32). In this regard, a very recent study by Bugarini et al.

TABLE 1 Published studies on neoadjuvant SRS.

Reference	Design	Patients	Patient characteristics	Intervention	Outcome	Limitations
(22)	Combined prospective and retrospective study of preoperative SRS	47	47 patients with 51 lesions; 23 patients from database and 24 patients on prospective trial	SRS within 24 h of surgery; 80% isodose; radiation dose 14 Gy; no additional margin expansion (GTV = CTV = PTV); median follow-up time 12 months	6-, 12- and 24-month LC 97.8%, 85.6%, and 71.8%, respectively; LR more likely with lesions >10 cm^3 (P = 0.01) and with largest unidimensional measurement >3.4 cm (P = 0.014); DBR 38.2%; 6-, 12- and 24-month OS 7.8%, 60% and 26.9%, respectively	Retrospective character, selection bias due to lack of randomization, small patient cohort
(19)	Multicenter retrospective study to compare preoperative and postoperative SRS	180	180 patients with 189 lesions; 66 patients with 71 BM treated with preoperative SRS, 114 patients with 118 RC treated with postoperative SRS	Preoperative SRS within 48 h of surgery; postoperative SRS 2-3 weeks after surgery; 80% isodose; preoperative radiation dose 14.5 Gy and postoperative radiation dose 18 Gy; PTV of BM without additional margin expansion (GTV = CTV = PTV); margin expansion of RC defined as CTV = GTV + 1 cm and PTV = GTV + 2 cm; median follow-up time 24.6 months	No difference between groups for 1-year LR (P = 0.24), 1-year DBR (P = 0.75), and 1-year OS (P = 0.1); 2-year LMD 3.2% for preoperative SRS vs. 16.6% for postoperative SRS (P = 0.01); 2-year RN 4.9% for preoperative SRS vs. 16.4 for postoperative SRS (P = 0.01)	Retrospective study, selection bias due to lack of randomization, differences between institutions in radiographic diagnosis of RN or LMD, and criteria for recommendation of surgical intervention
(23)	Multicenter retrospective study to compare preoperative SRS and postoperative WBRT	102	102 patients with 113 lesions; 66 patients with 71 BM treated with preoperative SRS, 36 patients with 42 RC treated with postoperative WBRT	SRS within 48 h of surgery; WBRT 2-3 weeks after surgery; 80% isodose; preoperative radiation dose 14.8 Gy and postoperative WBRT with 30-37.5 Gy over 10–15 treatments; PTV of BM without additional margin expansion (GTV = PTV); median follow-up time 22.4 months	No difference between groups for 2-year-LR (P = 0.81), 2-year DBR (P = 0.66), 2-year LMD (P = 0.66) and 1-year OS (P = 0.43); crude rate of symptomatic RN 5.6% for preoperative SRS vs. 0% for postoperative WBRT (P = 0.29)	Retrospective study, selection bias due to lack of randomization, difference in duration of study arm treatments, lack of neurocognitive data
(24)	Combined prospective and retrospective study of preoperative SRS	117	117 patients with 125 lesions; 93 patients from database and 24 patients on prospective trial	SRS within 48 h of surgery; 80% isodose; radiation dose 15 Gy; PTV of BM without additional margin expansion (GTV = PTV); median follow-up time 18.7 months	2-year LR 25.1%; 2-year DBR 60.2%; 2-year LMD 4.3%; 2-year RN 4.8%; 1- and 2-year OS 60.6% and 36.7%, respectively	Retrospective study, selection bias due to lack of randomization, lack of neurocognitive, neurological death, and quality-of-life information
(25)	Retrospective study of preoperative SRS	12	12 patients	SRS within 24 h of surgery; radiation dose 16 Gy; median follow-up time 13 months	6- and 12-month LC 81.8% and 49.1%, respectively; LR 33%; DBR 67%; LMD 17%; RN 0%; 6- and 12-month OS 83.3% and 74.1%, respectively	Retrospective study, selection bias due to lack of randomization, small patient cohort, large percentage of female patients with breast cancer, therefore, results might not be generalizable
(26)	Retrospective study of preoperative SRS	19	19 patients with 22 lesions; 8 patients with previously treated recurrent lesions (previous treatment of 5 patients with SRT and 3 patients with surgical resection)	SRC within 24 h to 48 h of surgery; 80% isodose; radiation dose 18 Gy; median follow-up time 6.3 months	LR in two cases 5.5 and 17.4 months after treatment (10.5%); DBR in four cases (21.1%); LMD in one case (5.3%) 1.5 months after treatment; RN in one case (5.3%) 4.6 months after treatment; OS 89.5%	Retrospective study, selection bias due to lack of randomization, small patient cohort, short follow-up time
(27)	Retrospective study of	242	242 patients with 253 lesions	SRS within 24 h of surgery; 80% isodose; radiation dose 15 Gy;	2-year LR 17.9%; 2-year DBR 45.9%; 2-year LMD	Retrospective study, selection bias due to

(Continued)

TABLE 1 Continued

Reference	Design	Patients	Patient characteristics	Intervention	Outcome	Limitations
	preoperative SRS			PTV of 166 BM without additional margin expansion (GTV = PTV); 81 lesions with PTV = GTV + 0.5 mm or PTV = GTV + 1 mm; unknown PTV in 6 lesions; median follow-up time 24.9 months	7.6%; symptomatic adverse radiation effects 3.5%; 1- and 2-year OS 57.7% and 38.4%, respectively; subtotal resection as the primary risk factor for LR	lack of randomization, lack of neurocognitive and quality-of-life information, potential confounding for OS endpoints
(28)	Prospective phase II dose escalation study of preoperative SRS	27	27 patients with brain metastases >2 cm in maximal dimension	Dose escalation at 3 Gy increments from currently accepted RTOG dosing; cohorts of 2–6 patients treated at each dose; SRS within 2 weeks of surgery; median follow-up time 7.4 months	No DLT; 6- and 12-month LC 93.8% and 72.3%, respectively; 6- and 12-month with DC 38.6% and 25.8%, respectively; LMD in one patient 5 months after SRS; symptomatic adverse radiation effects 15%; 6- and 12-month OS 80.8% and 53.5%, respectively	NR
(29)	Retrospective study of preoperative SRS	28	28 patients with 29 lesions after exclusion of nonmetastatic pathology; hypofractionated SRS used in 18 lesions and single-fraction SRS in 11 lesions; 12 patients from database and 17 patients on prospective trial	SRS within 24 h of surgery; hypofractionated SRS with 24 Gy in 3 fractions and single-fraction SRS with 20 Gy; PTV of BM defined as PTV = GTV + 1 mm; median follow-up time 12.8 months	1-year LC 91.3%; 1-year DC 51.5%; 1-year LMD 4%; 1-year RN 5%; 1-year OS 60.1%;	Case series, selection bias due to lack of randomization, small and heterogeneous patient cohort

BM, brain metastasis; CTV, clinical target volume; DBR, distant brain recurrence; DC, distant control; DLT, dose-limiting toxicity; GTV, gross tumor volume; LC, local control; LMD, leptomeningeal disease; LR, local recurrence; NR, not reported; OS, overall survival; PTV, planning target volume; RC, resection cavity; RN, radio necrosis; SRS, stereotactic radiosurgery; SRT, stereotactic radiotherapy; WBRT, whole brain radiotherapy.

observed a tendency for larger postoperative PTV compared to preoperative PTV in their cohort (33). Given the partly inconsistent results, the benefit of NaSRS in terms of volume reduction and consequent better protection of normal brain tissue requires further investigation. The aim of this study is to 1) compare the gross tumor volume and planning target volume of preoperative metastasis with the postoperative cavity volumes in adjuvant SRS patients, 2) identify the patient cohort with a potential volume benefit in NaSRS, and finally, 3) investigate the impact of NaSRS on NBT sparing for cases where a volume reduction is observed.

2 Methods

2.1 Patient cohort

This retrospective analysis of patient data and the registry of prospective patient data collection were approved by the local ethics committee, as this cohort contains both data sets (EA1/037/20). Patients in the prospective cohort signed a consent. We identified all patients with post-SRS treatment of resection cavities from brain metastases (index lesion) between July 2011 and August 2021 at our institution. We then checked whether adequate preoperative magnetic resonance imaging (MRI) was available and set a maximum diameter of 5.0 cm as the limit for the index lesion to be suitable for NaSRS simulation (34). We excluded patients with previous SRS to the index lesion or WBRT (Figure 1).

We collected data on patient characteristics regarding the primary disease, tumor location, morphology, operation technique (en bloc vs. piecemeal), and local and distant tumor control. Tumors were described as superficial or deep based on their location and classified as cystic or non-cystic depending on their morphology, as described previously (11, 35). The extent of resection was assessed when a postoperative MRI performed within 30 days after surgery was available, since an early MRI was not a routine neurosurgical procedure in the past years. Data on systemic treatments were also collected, but we limited the report to "yes" or "no" and, if yes, only the timing of treatment, as this was outside the scope of this project.

2.2 Cyberknife SRS of the resection cavities: Retrospective treatment description

The indication for post-SRS/HF-SRS treatment was decided by a multidisciplinary neuro-oncology board team including a radiation oncologist and a neurosurgeon. The Cyberknife radiosurgery treatment preparation and planning were similar to the already published algorithm of our clinic (36). Briefly, a thermoplastic mask was individually produced for each patient for treatment immobilization

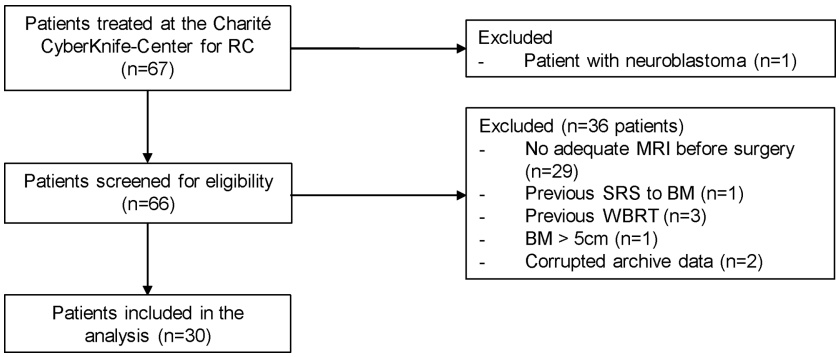

FIGURE 1
Patients with surgically resected brain metastases who underwent postoperative stereotactic radiosurgery to the resection cavity in our department were included. One pediatric patient with neuroblastoma was excluded from the cohort. Additional exclusion criteria included: no adequate intracranial MRI before surgery, previous SRS at the index lesion or WBRT as well as a diameter of the preoperative lesion greater than 5 cm. Two patients had to be additionally excluded because their data could not be extracted from the Accuray archive. RC, resection cavity; BM, brain metastasis; SRS, stereotactic radiosurgery.

before contrast enhanced high-resolution thin-slice (0.75 mm) computed tomography (CT). This reference CT was co-registered to T1-weighted magnetic resonance images (MRI). Since the visible tumor in the preoperative contrast enhanced T1-weighted MRI imaging is referred to as gross tumor volume (GTV), we referred to the contour of the resection cavity as post-GTV despite the absence of tumor volume to allow for better comparability in further analyses. In case of cystic lesions, the tumor-associated cyst was included in the GTV. The post-GTV was defined as the resection cavity volume based on postoperative contrast enhanced planning CT and a co-registered T1-weighted MRI, considering the surgical pathway and meninges near the craniotomy. The post-GTV was extended by 0 to 3.0 mm at the discretion of the treating radiosurgeon to create the postoperative planning target volume (post-PTV) in this retrospective cohort (Table 2). In 9 out of 30 postoperative cavities no margin was added to post-GTV, therefore, in these cases post-GTV and post-PTV do not differ. The doses were mostly prescribed to the 80% isodose line covering the PTV (Table 2). Depending on the vicinity to the organs at risk (e.g., optic nerves, chiasm, and brainstem) and the size of the resection cavity, different dose schedules were applied. If a brain metastasis was eloquently located (e.g. in the brainstem or along the optic pathway), either a reduction of the single fraction dose or hypofractionation was performed, depending on how the dose constraints were met. Briefly, doses in the range of 15–19 Gy, 21–24 Gy, and 25–30 Gy have been applied for one, three, and five fractions, respectively (Tables 2, 3).

The isodose volume of the normal brain tissue (NTB, excluding the PTV), circumscribed with 10.0 Gy (V10 < 10 cm^3) for single fraction, 18.0 Gy (V18 < 10 cm^3) for three fractions, and 28.8 Gy (V28.8 < 7 cm^3) for five fractions, which were defined based on the published data on this topic, was measured and recorded in each patient as clinical routine to determine the risk of adverse effects on the surrounding healthy brain (37–39). However, if the parameters defined in the internal guidelines were not applicable, i.e., due to a dose reduction to 25 Gy in 5 fractions, the evaluated parameter was adjusted individually (Table 2: Pt. number 27, Table 4: case 7, the evaluated parameter adjusted to V22.5 Gy < 10 cm^3 accordingly). To protect the other organs at risk, we applied the recommended threshold doses published by Benedict et al. for SRS/HF-SRS in particular (40).

The equivalent dose for 2 Gy per fraction was calculated according to the LQ-model assuming an α/β ratio 10 for tumor ($EQD2_{10}$) for the comparison to conventional irradiation treatment. The calculated $EQD2_{10}$ encompassing the PTV was 31.2–45.9 Gy for a single fraction, 29.8–36.0 Gy for three-fraction treatment, and 31.2–40.0 Gy for five-fraction SRS.

2.3 Follow-up

Radiological imaging by contrast-enhanced MRI and clinical assessment were performed every 3 months as follow-up. The latest available follow-up was included in this analysis. MRI scans were interpreted by both a radiology specialist and the radiosurgery physician to determine response to treatment. We first examined local and distant brain control. Local recurrence was defined as a new progressive nodular contrast enhancing lesion involving the resection cavity as performed in other studies (27, 29) or when a progressive residual lesion with a diameter increase by at least 20.0% was observed (41). Distant failure was defined as new brain metastasis elsewhere or as LMD on the follow-up MRI. LMD is also reported separately to differentiate these cases from the patients with only new solid lesions. The complications were recorded based on Common Terminology Criteria of Adverse Events CTCAE Version 5.0.

2.4 Simulation contouring and planning study

After co-registration of the preoperative MRI with the planning reference CT, the unresected metastasis was countered first as pre-GTV based on the contrast enhanced T1 weighted thin-sliced MRI. Clinical target volume was equal to pre-GTV. When creating the pre-PTV, a standardized margin of 1 mm was added to all metastases in accordance with hospital guidelines, which is commonly used to

TABLE 2 Treatment characteristics of the performed resection cavity irradiation as well as gross tumor- and planning target volumes in the hypothetical planning.

Pat. Nr.	Pre-GTV (cm^3)	Pre-PTV (cm^3)	Post-GTV (cm^3)	Post-PTV (cm^3)	Post-Margin* (mm)	Std. Post-PTV (cm^3)	Min Dose (Gy)	Max Dose (Gy)	Mean Dose (Gy)	Prescribed Dose (Gy)	Fx	nCI **	Coverage (%)	Isodose
1	2.6	3.6	6.0	6.0	0	10.2	17.0	22.5	20.5	18.0	1.0	1.1	98.9	80.0
2	2.9	3.9	6.5	9.7	1.5-2.5^{+}	10.8	16.1	22.5	20.5	18.0	1.0	1.0	97.5	80.0
3	3.0	3.9	3.2	5.5	1.5	6.3	17.7	24.9	22.2	19.0	1.0	1.1	99.5	80.0
4	3.1	4.1	1.3	1.3	0	3.1	22.8	30.0	26.4	24.0	3.0	1.3	98.9	80.0
5	3.8	5.0	3.3	5.7	2.0	6.0	19.6	26.3	23.5	21.0	3.0	1.2	98.2	70.0
6	4.5	5.9	9.7	14.4	2.0	14.4	14.2	18.7	16.9	15.0	1.0		97.7	80.0
7	5.5	7.0	8.3	15.3	2.8	12.9	20.9	30.0	27.3	24.0	3.0	1.1	97.7	80.0
8	5.9	7.9	11.1	16.6	1.5-3.5^{+}	17.2	23.2	30.0	27.4	24.0	3.0	1.1	99.7	80.0
9	6.7	8.0	9.6	13.0	1.5	15.8	26.4	37.5	34.1	30.0	5.0	1.1	99.1	80.0
10	7.2	11.7	6.5	6.5	0	10.7	17.1	22.6	20.7	18.0	1.0	1.2	99.3	80.0
11	8.2	10.4	26.7	31.6	1	38.3	26.3	37.5	34.0	30.0	5.0	1.0	95.1	80.0
12	8.2	10.7	7.1	7.1	0	11.3	22.6	30.0	27.6	24.0	3.0	1.1	98.6	80.0
13	8.6	9.9	5.2	7.4	1.5	9.1	20.0	26.1	23.8	21.0	3.0		98.1	80.0
14	8.9	10.2	4.0	5.8	1.5	7.4	22.9	30.1	27.6	24.0	3.0	1.1	99.7	80.0
15	9.9	12.1	8.7	14.4	2	14.1	21.2	30.0	27.0	24.0	3.0	1.1	97.2	80.0
16	10.0	12.6	7.7	12.2	2	12.4	19.9	24.7	23.2	21.0	3.0	1.1	99.9	80.0
17	10.4	12.6	21.8	28.7	1.5-2.5^{+}	30.6	21.6	26.9	24.9	22.5	3.0		99.3	85.0
18	11.6	13.3	13.4	17.4	1.5	20.7	22.8	30.0	27.5	24.0	3.0	1.1	99.7	80.0
19	11.6	17.3	8.9	15.3	2.1	14.7	6.8	18.0	14.4	14.4$^{\#}$	1.0	1.1	60.8$^{\#}$	80.0
20	12.2	15.4	14.5	14.5	0	21.4	22.1	30.0	27.3	24.0	3.0	1.1	97.5	80.0
21	13.3	21.8	15.1	15.1	0	24.3	14.4	20.0	17.8	16.0	1.0	1.1	95.2	80.0
22	13.4	16.5	13.5	13.5	0	19.8	21.2	30.0	27.0	24.0	3.0	1.1	97.4	80.0
23	16.0	19.0	21.5	21.5	0	30.1	11.9	20.7	17.7	15.0	1.0	2.0	95.1	70.0
24	20.6	25.0	30.9	36.0	1	42.9	24.1	37.5	33.9	30.0	5.0	1.0	93.8	70.0
25	20.6	24.2	13.4	18.6	1.5	20.5	30.0	40.6	37.1	32.5	5.0	1.0	97.7	80.0
26	21.0	30.2	16.8	22.8	1.8	25.0	21.8	30.3	27.7	24.0	3.0	1.1	98.5	80.0

(Continued)

10.3389/fonc.2023.1056330

10.3389/fonc.2023.1056330

TABLE 2 Continued

Pat. Nr.	Pre-GTV (cm^3)	Pre-PTV (cm^3)	Post-GTV (cm^3)	Post-PTV (cm^3)	Post-Margin* (mm)	Std. Post-PTV (cm^3)	Min Dose (Gy)	Max Dose (Gy)	Mean Dose (Gy)	Prescribed Dose (Gy)	Fx	nCI **	Coverage (%)	Isodose
27	21.4	25.6	33.9	45.7	2	45.9	23.2	35.7	30.3	25.0	5.0	1.1	99.73	70.0
28	24.4	28.5	9.2	9.2	0	14.8	21.7	30.0	27.4	24.0	3.0	1.1	98.1	80.0
29	32.8	35.9	17.1	22.2	1.5	26.0	19.5	26.3	23.6	21.0	3.0	1.1	98.5	80.0
30	34.5	40.1	9.1	14.4	2	14.6	22.9	30.0	27.6	24.0	3.0	1.1	99.6	80.0

*As the exact margins were not documented separately, a retrospective approximation was performed based on the GTV and PTV volumes. + The actual margin was too irregular to be determined retrospectively., **In cases where other brain metastases were irradiated at the same session as the resection cavity the conformity index for the resection cavity was not documented separately., #This plan was interrupted so that the prescribed dose could not be administered and ended at 14.4 Gy, so this coverage was not included into the results.,
Fx, fractions; GTV, gross tumor volume; pre, preoperative; nCI, new conformality index; PTV, planning target volume std, standardized.
The margin added to the pre-GTV was set to 1 mm, while this was 2 mm for the standardized post-PTV.

compensate for uncertainties (42). The post-PTV was taken from the original plans. The hypothetical preoperative volumes (pre-GTV and pre-PTV, respectively) were subsequently compared with the real postoperative irradiation volumes (post-GTV and post-PTV, respectively; Table 2). In addition, a standardized post-PTV (std. post-PTV) volume was generated with a 2 mm margin, as the latest practice guidelines from international stereotactic radiosurgery society recommend a margin of 2 to 3 mm (32), while the retrospective cohort was heterogenous in this regard. The volume changes were assessed in absolute values (cm^3) and also in percentage of volume difference as described by Atalar et al. (31).

For the cases with a GTV volume increase greater or equal to 5 cm^3 from the pre-GTV to the post-GTV, a retrospective simulation study was performed, identifying the potential dose sparing for normal brain tissue. One patient had to be excluded due additional multiple lesions in the treated clinical treatment plan, which strongly influence the exposure of NTB. Within this simulation, first all clinical existing patient plans on the post-PTV were newly optimized within the current available treatment planning system (Precision 3.1 software, Accuray Inc., Sunnyvale, CA, USA). In the second step, the identical plan templates were used for a new optimization on the pre-PTV with 1 mm margin to GTV, therefore, simulating the equivalent dose prescription to the pre-PTV as employed for the clinical used post-PTV treatment plan. Subsequently, to guarantee equivalent sparing of the organs at risk, the weights of conformity ensuring margins around the targets were tightened until differences in PTV coverage were within 0.2%. For the evaluation of dose distribution for both existing plans a healthy brain tissue (brain minus pre-PTV/brain minus post-PTV) was generated and the clinically employed dose-volume histogram (DVH) parameter evaluated. The relative effect of the NaSRS was evaluated in terms of the dose-specific DVH parameter ratio between simulated NaSRS and postoperative original irradiation (pre/post), whereas a value below 100% depicts a relative decrease and above 100% a relative increase of the evaluated DVH parameter.

2.5 Statistics

The data are presented as mean, standard deviation, median, and range depending on the context. As the volumes before and after GTV and PTV were not normally distributed in the Kolmogorov-Smirnov test, we performed the Wilcoxon test to compare paired data and the Mann-Whitney-U-test for unpaired data. A correlation was established between pre-GTV and changes in GTV as well as PTV volumes and a correlation analysis was also performed between the time from surgical resection to post-GTV MRI acquisition in days and GTV volume change (Pearson correlation). Progression-free survival was investigated using Kaplan-Meier analysis for local and distant control as well as LMD-free survival. Furthermore, overall survival was also calculated using Kaplan-Meier analysis based on information from the Berlin-Brandenburg tumor registry. Patients are censored when follow-up is terminated prior to an event. To identify possible predictors of post-GTV volume change, we performed a multiple linear regression analysis. We defined the dependent factor as GTV change (normally distributed) and

10.3389/fonc.2023.1056330

TABLE 3 Patient, tumor and treatment characteristics.

Number of patients	30
Number of resection cavity treated lesions	30
Sex, n (%)	
Female	14 (46.6%)
Male	16 (53.3%)
Age	
Average (SD)	63.1 (13.3)
Median (Range)	66.9 (32.1-85.7)
Primary tumor, n (%)	
NSCLC	17 (56.7%)
Breast cancer	4 (13.3%)
Malignant melanoma	2 (6.7%)
RCC	2 (6.7%)
Rest	5 (16.7%)
Localization of brain metastases, n (%)	
Occipital	7 (23.3%)
Frontal	7 (23.3%)
Cerebellar	5 (16.7%)
Temporal	6 (20%)
Parietal	4 (13.3%)
Intraventricular	1 (3.3%)
Dose and fractionation, n (%)	
14.4 Gy in 1 fraction*	1 (3.3%)
15 Gy in 1 fraction	2 (6.7%)
16 Gy in 1 fraction	1 (3.3%)
18 Gy in 1 fraction	3 (10%)
19 Gy in 1 fraction	1 (3.3%)
21 Gy in 3 fractions	4 (13.3%)
22.5 Gy in 3 fractions	1 (3.3%)
24 Gy in 3 fractions	12 (40%)
25 Gy in 5 fractions	1 (3.3%)
30 Gy in 5 fractions	3 (10%)
32.5 Gy in 5 fractions	1 (3.3%)
Fractionation regime, n (%)	
HF-SRS	22 (73.3%)
S-SRS	8 (26.6%)
Extent of resection, n (%)	
Gross total	22 (84.6%**)
Subtotal	4 (15.4%**)
n.a.	4 (13.3%)
Method of resection, n (%)	
En bloc	6 (20%)
Piecemeal	14 (46.7%)
n.a.	10 (33.3%)
Time interval between resection date and irradiation	
Average (SD)	36.7 days (10.4)
Median (Range)	37.5 days (17-57)

HF-SRS, hypofractionated SRS; NSCLC, non-small cell lung cancer; RCC; renal cell carcinoma; Rest = gastrointestinal, ovarian cancer, cervical cancer, base of tongue, cancer of unknown origin; s-SRS, single-fraction SRS. *This plan was interrupted so the prescribed dose could not be applied and ended at 14.4 Gy. **calculated as % of 26 patients with the available information.

assessed the morphologic characteristics of the tumor such as cystic/non-cystic, superficial/deep, and supratentorial/infratentorial (categorical), as well as pre-GTV volume as variables. IBM SPSS Statistic Program (Version 25.0. Armonk, NY: IBM Corp.) was used, and $P \leq 0.05$ was considered as statistically significant. Prism 9 was used for the graphical representation of the collected data. Since this was only an exploratory study, no correction for multiple testing was performed.

2.6 Literature review

Since the latest reviews were not up to date, we have created an overview of published and ongoing NaSRS studies (24, 43). For the literature review the electronic database "PubMed" was consulted on the 27th of July 2022 according to PRISMA guidelines. The search included the following terms: "((neoadjuvant [MeSH Terms]) AND (radiosurgery [MeSH Terms]) AND (brain metastases [MeSH Terms])". After excluding studies due to unrelated title/abstract and including publications from other sources, a total of 14 full-text studies were assessed for eligibility (Figure 2). We summarized 9 studies in Table 1. For the ongoing studies on NaSRS, the U.S. National Library of Medicine (clinicaltrials.gov) and the WHO Clinical Trials Registry Platform (trialsearch.who.int) databases were searched on 18th August 2022. For the U.S. National Library of Medicine, the advanced search mode was used. The following entries were applied: Condition: Brain Metastases; Intervention: (Neoadjuvant OR Preoperative) AND Radiosurgery. For the WHO Registry, the following term was used: Radiosurgery AND Brain Metastasis AND (Neoadjuvant OR preoperative). A total of 21 results were found in both databases. After accessing the results, one study was excluded because it did not include SRS as a neoadjuvant treatment (Supplementary Table 1).

3 Results

3.1 Patient cohort

We identified 30 resection cavity patients fulfilling the criteria in our retrospective cohort (Figure 1). Demographic and clinical characteristics are summarized in Table 3. Briefly, gender was evenly distributed (males 53.3%, females 46.6%), mean age was 63.1 years with a range of 32.1 to 85.7 years. The most frequent primary tumor type was lung cancer (56.7%) followed by breast cancer (13.3%), malignant melanoma, and renal cell carcinoma (RCC) with 6.7% each. Only 16.7% were infratentorial. The superficial localization was more frequent with 73.0%, while 60.0% were cystic tumors. Gross total resection was achieved in 84.6% of cases, and the piecemeal technique was most frequently used (Table 3). In 9 patients a postoperative MRI within 48 hours was available. In the cases with presumably subtotal resection the median time interval between the first MRI after resection was 26 days (range: 20-27 days).

3.2 Resection cavity SRS details and treatment response

The median time interval between surgery and SRS/HF-SRS was 37.5 days with a range of 17-57 days. In 26.6% of the cases, the treatment was performed in a single fraction as SRS with a median prescribed dose of 18.0 Gy (Tables 2, 3). In more than half (56.9%), a multi-session treatment as HF-SRS with 3 fractions was preferred, while 5 fractions were less frequent with 16.6%. For one patient the clinical treated dose was reduced to 25 Gy in 5 fractions due to additional sequentially irradiated lesions. Coverage ranged between 93.8% to 99.8%. Further

10.3389/fonc.2023.1056330

TABLE 4 Simulation planning details.

CASE	Fx	Dose	Pre-GTV (cm^3)	Post-GTV (cm^3)	Change in GTV (post-GTV - pre-GTV) (cm^3)	Brain PTV Volume Parameter (Vxx)	Volume of the defined DVH parameter (pre) (cm^3)	Volume of the defined DVH parameter (post) (cm^3)	Percentual difference of the dose defined DVH parameter (pre/post)
1	1	18	4.5	9.7	5.2	10.0	24.6	36.4	68%
2	3	24	5.5	12.9	7.4	18.0	5.8	11.0	52%
3	3	24	5.9	11.1	5.1	18.0	9.0	12.5	72%
4	5	30	8.2	26.7	18.6	28.8	1.0	2.0	47%
5	3	22.5	10.4	21.8	11.4	18.0	15.1	22.1	68%
6	5	30	20.6	30.9	10.3	28.8	2.4	7.1	33%
7*	5	25	21.4	33.9	12.6	22.5	12.0	14.3	84%

DVH, dose volume histogram; Fx, fractions; GTV, gross target volume; pre, preoperative; PTV, planning target volume. *Due to the dose reduction to 25 Gy in 5 fractions, the DVH parameter was defined as V22.5.

treatment details are listed in Table 2. Information on systemic treatments was present in 29 patients. Additional systemic treatment with chemotherapy and/or immunotherapy and/or targeted therapies was performed in a total of 26 patients. In each 27.6% of these patients, this treatment took place before or during irradiation, in 24.1% before and after treatment. Only in three cases did the systemic treatment take place exclusively after irradiation.

A total of 27 patients were re-examined with a median follow-up time of 14.2 months (range: 2.8 to 72.7 months). Within this period, local progression occurred in five patients (18.5%), whereas distant intracranial progression occurred in 51.8% (n = 14). LMD occurred in 6 cases (22.2%), and all six patients also had lesional distant recurrences. In three cases, SRS treatment was administered, and the other three cases occurred after HF-SRS (two received three fractions and one received five fractions). The estimated rates for local progression-free survival at 6.0, 12.0, and 24.0 months were 92.7%, 88.0%, and 88.0%, respectively (Figure 3D), while the rates for distant progression-free survival at 6.0, 12.0, and 24.0 months were 67.9%, 54.3%, and 47.5%, respectively. The estimated LMD-free survival rates were accordingly 100.0%, 81.4%, and 72.4% (Figures 3A–C). The estimated median overall survival was 23.4 months (95% CI: 11.3 – 35.6). The overall survival rates at 12.0, 24.0 and 36.0 months were 69.0%, 49.3%, and 44.1%, respectively (Figure 3D). Imaging-based suspected radionecrosis was observed in two cases (7.4%). A total of five adverse effects were recorded, a local alopecia and mild headache as CTCAE grade I and moderate dizziness, aphasia, and severe headache as grade II.

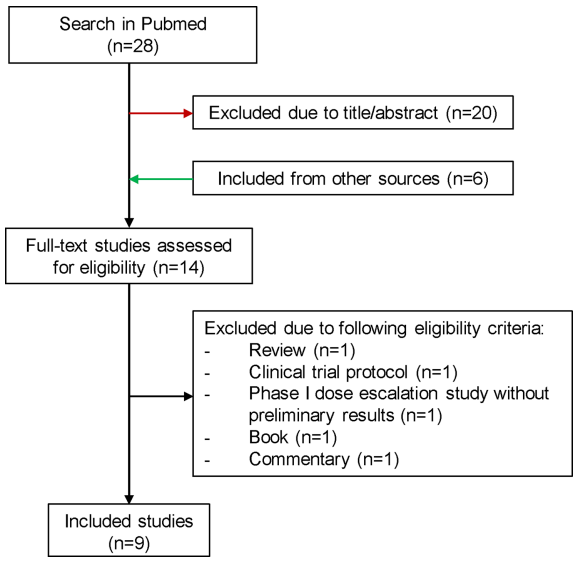

FIGURE 2
Flowchart for the selection process of published studies for preoperative SRS. SRS, stereotactic radiosurgery.

3.3 Comparison of volumes

The pre-GTV and pre-PTV are shown in Figures 4A–F and in Table 2 in comparison to the postoperative values. Here, we could not find any significant differences between pre- and postoperative volumes when looking at the median values (Figure 4A, P = 0.551 and B, P = 0.781), while the median of std. post-PTV tended to be higher than pre-PTV (P = 0.051). The volume change in binarized pre-GTV volumes depending on size with a cut-off at 15.0 cm^3 highlighted the wider range in larger tumors, while the smaller tumors tended to have greater GTV after resection, but this did not reach significance (Figure 4C, P = 0.205). We also present the distribution of postoperative volume changes as an absolute value in cm^3 compared to the original tumor size (pre-GTV) (Figures 5A, B). Remarkably, the majority of cases with enlargement greater than 5.0 cm^3 were smaller tumors with pre-GTV < 15.0 cm^3 (62.5% of all cases with > 5 cm^3), whereas larger tumors greater than 25 cm^3 showed only a decrease in post-GTV and post-PTV. For the hypothetical standardized PTV with the fixed margin of 2 mm, the difference from pre-PTV was greater for the few cases with no or less margin in the original post-PTV (Figure 5C). The correlation assessment revealed a significant negative correlation between pre-GTV volume and all three volume changes (GTV change: r: -0.558, P = 0.001, PTV change: r = -0.507, P = 0.004, hypothetical PTV

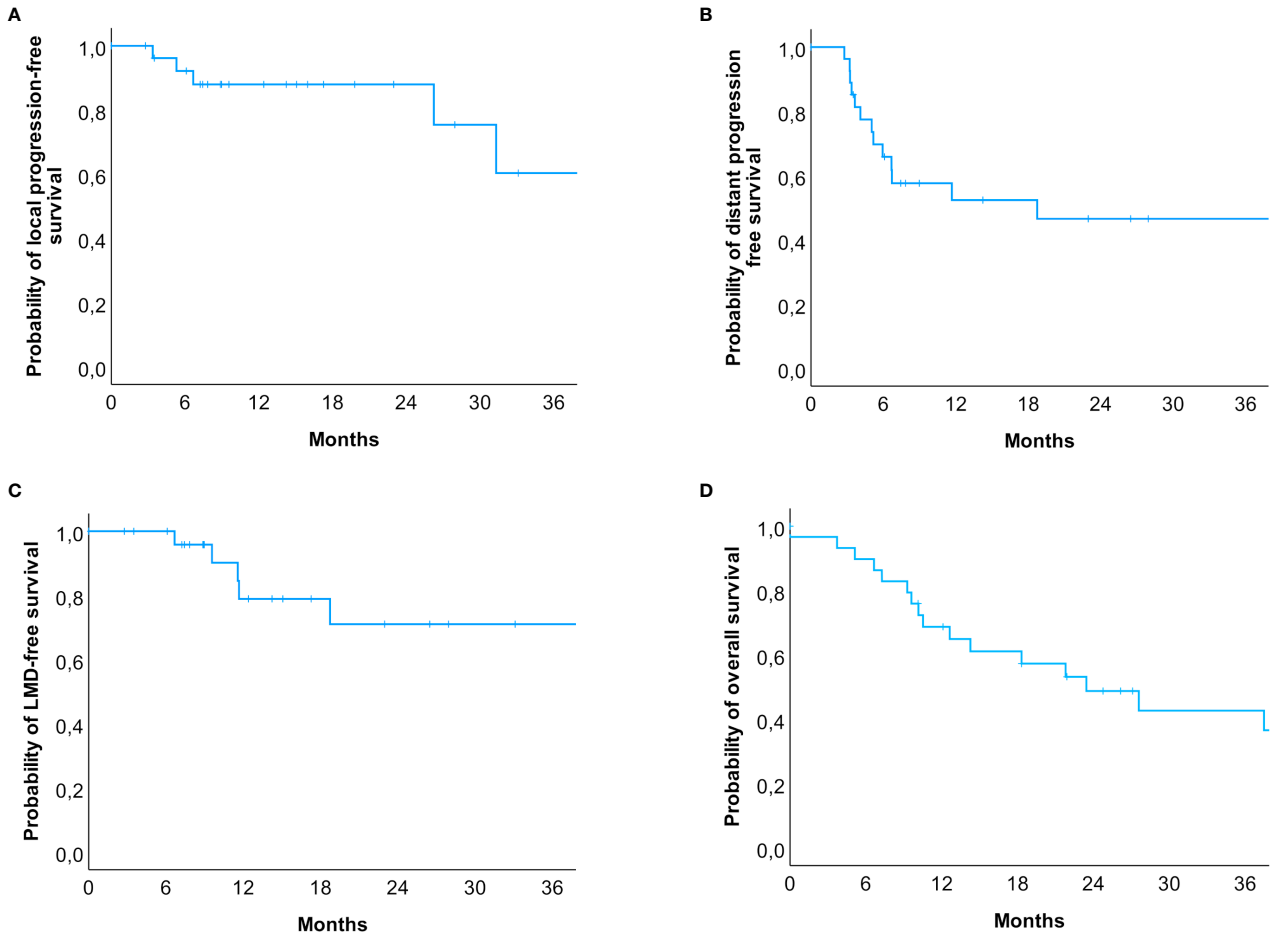

FIGURE 3
Kaplan-Meier-Curves for **(A)** local progression-free, **(B)** distant progression-free, **(C)** leptomeningeal disease-free survival and **(D)** overall survival. **(A)** Patients at risk were n = 30 (0 months), n = 23 (6 months), n = 15 (12 months), n = 7 (24 months), and n = 3 (36 months). **(B)** Patients at risk were n = 30 (0 months), n = 17 (6 months), n = 10 (12 months), n = 6 (24 months), and n = 4 (36 months). **(C)** Patients at risk were n = 30 (0 months), n = 25 (6 months), n = 14 (12 months), n = 7 (24 months), and n = 4 (36 months). **(D)** The estimated median survival of our patients was 23.4 months (95% CI: 11.3 – 35.6). Patients at risk were n = 30 (0 months), n = 19 (12 months), n = 11 (24 months), n = 7 (36 months). In total, 14 events occurred within 24 months after the radiosurgical treatment, but only 4 events in the subsequent years were reported.

change: r = -0.451, P = 0.012). As it was shown that the time after surgery may influence the size of the resection cavity (44), we analysed the volume change in GTV in relation to the time interval between surgery and MRI in our cohort. However, we could not identify a significant correlation (r: -0.091, P = 0.634, Figure 5D).

3.4 Predictors for GTV change

A multiple linear regression was calculated to predict a volume change of GTV after resection. A significant regression equation was found (F (4, 25) = 3.060, P = 0.035) with an adjusted R^2 = 0.221 (unadjusted R^2 = 0.329). The pre-GTV size was the only significant predictor for volume change of GTV (Table 5).

3.5 Simulation planning study

We identified a total of 16 patients with post-GTV greater than pre-GTV, however, the range for the GTV change was wide, from 0.11 to 18.57 cm^3; thus, we set the cut-off at 5 cm^3 based on the median GTV increase of 4.3 cm^3. Within the planning study for both treatment scenarios clinically applicable treatment plans could be generated for 7 identified patient cases with an increase of GTV from the pre-GTV to the post-GTV of over 5 cm^3. The median annotated GTV of the primary metastasis was 8.2 cm^3 with a range of 4.5–21.4 cm^3. The median increase of GTV was 5.5 cm^3 with a range of 5.1–18.6 cm^3. In this cohort, margins for post-PTV were heterogeneous 0 to 3 mm, as in the entire cohort, however, all but one had margins of 1 to 3 mm. In the hypothetical planning NBT exposure was less in NaSRS group with a median of only 67.6% (range: 33.2–84.5%) of NBT calculated with post-PTV receiving the fractionation-specific evaluated dose. The relative NBT exposure in relation to the change in GTV volume is shown in Figure 6. Accordingly, the evaluated DVH parameter showed a median relative decrease for the analyzed brain minus PTV parameter of 32.4% with a range of 15.5–66.9% (Table 4). The analyzed Pearson correlation coefficient for the changes in volume in relation to the relative decrease of the evaluated DVH parameter presented no significant correlation (r = -0.16; P = 0.73).

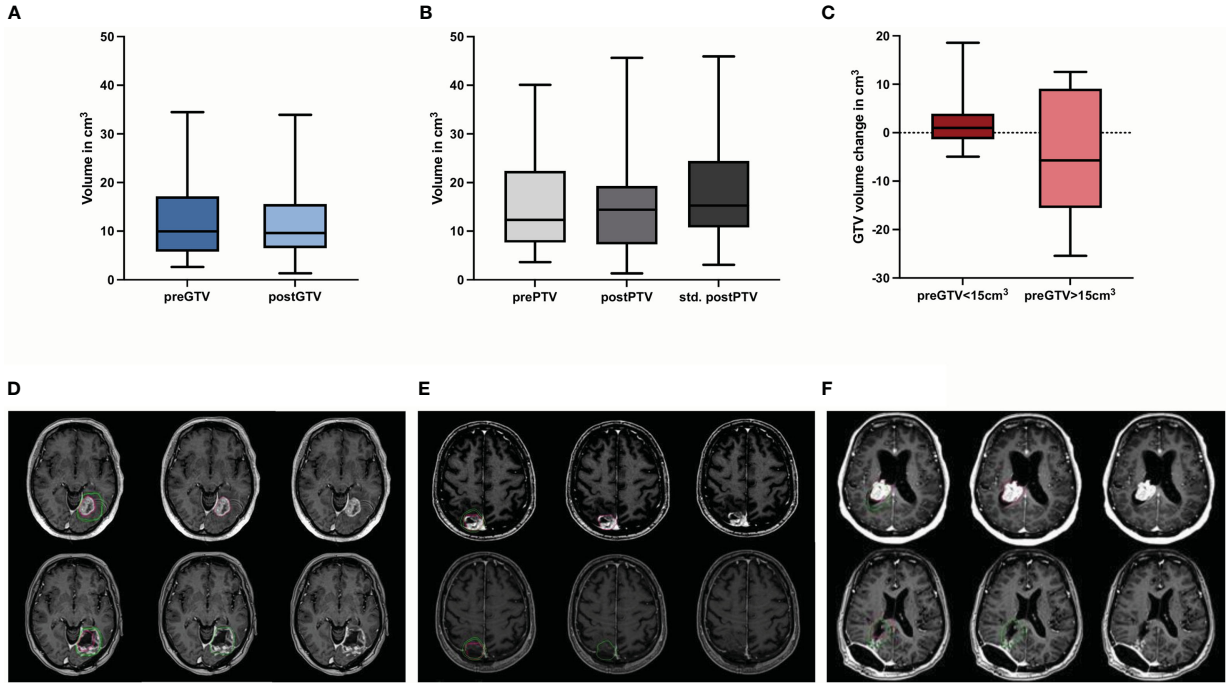

FIGURE 4
Quantification of the preoperative (pre) and postoperative (post) **(A)** gross tumor volume (GTV) and **(B)** planning target volume (PTV) including hypothetical standardized PTV with a 2 mm margin to post-GTV (n = 30; no significant differences, Wilcoxon test), **(C)** shows the volume change of binarized pre-GTV volumes depending on size with a cut-off of 15 cm^3, (n = 22 for pre-GTV < 15.0 cm^3 and n = 8 for pre-GTV > 15.0 cm^3; no significant differences, Mann-Whitney-U-test.) Boxplots represent the interquartile range, the thicker line inside the boxes the median, and the whiskers indicate the range from minimum to maximum. Representative case presentations with one deep **(D)** one superficial **(E)** and one intraventricular **(F)** metastasis from non-small cell lung carcinoma shown in axial MRI images with contrast demonstrating comparison of GTV in red for preoperative metastases and in green for the resection cavity. In these cases, an increase in post-GTV compared with pre-GTV can be seen, which was 227.3% in **(D)**, 86.6% in **(E)**, and 19.3% in **(F)**.

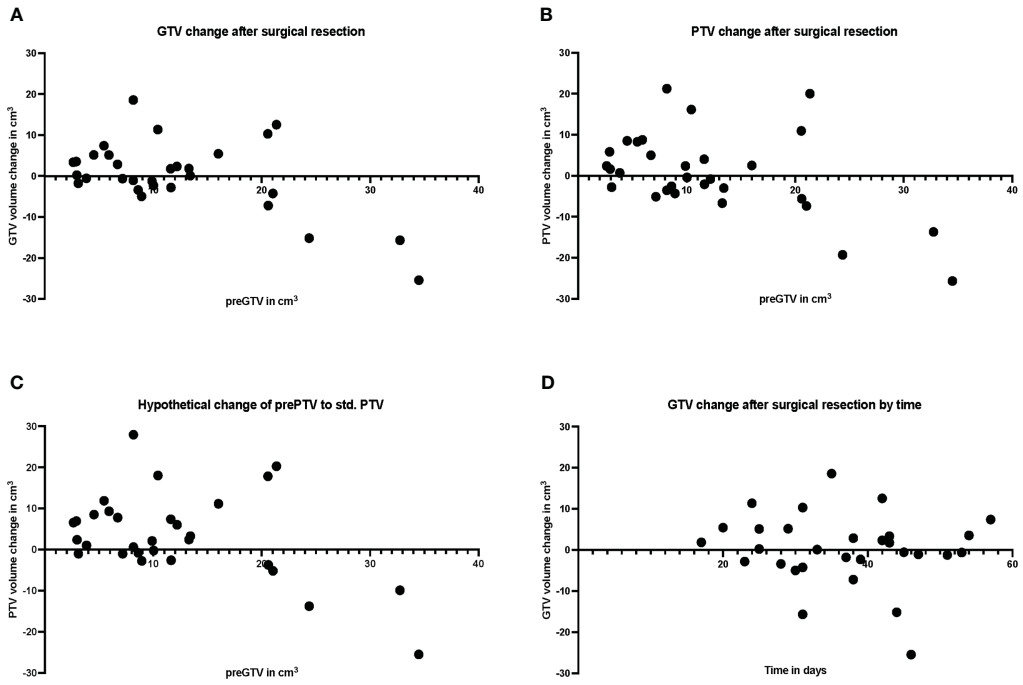

FIGURE 5
Plot of individual patient data (n = 30) for resection cavity volume changes compared with preoperative volumes, **(A)** for gross tumor volume (GTV), **(B)** for planning target volume (PTV), and **(C)** for standardized PTV, shown relative to preoperative (pre) GTV. **(D)** shows the volume change of the resection cavity after surgical resection in relation to the days between surgery and MRI.

TABLE 5 Multiple linear regression analysis for prediction of GTV change.

Variables	B	95% CI	Beta	t	P
superficial vs. deep	2.2	-4.4 - 8.8	0.1	0.7	0.490
cystic vs. not cystic	-1.2	-7.3 – 4.9	-0.1	-0.4	0.694
supra- vs. infratentorial	-0.6	-8.8 - 7.3	0.02	-0.2	0.878
pre-GTV in cm	-0.6	-0.9 - -0.2	-0.6	-3.2	0.004

Dependent Variable: GTV change (pre-GTV to post-GTV). R^2 adjusted: 0.221 (n = 30, P = 0.035). CI, confidence interval for B; GTV, gross tumor volume; post-GTV, postoperative GTV; pre-GTV, preoperative GTV.

4 Discussion

In this study, we show an increase in the volume of the resection cavity dependent on the initial tumor size, which may lead to higher dose exposure of the NBT in selected cases. In addition, we provide an update on published and ongoing NaSRS studies as a comprehensive overview and discuss crucial aspects for the further use of NaSRS.

Neoadjuvant SRS or so-called preoperative SRS has become a hot topic in the treatment of brain metastases requiring surgery with potential benefits such as better local control, less LMD, and more convenient target delineation. NaSRS was included in the most recent American Society of Radiation Oncology (ASTRO) 2022 guidelines with a conditional recommendation as a potential alternative to post-SRS, but the level of evidence was rated low by the endorsement panel, warranting further study on this topic (45). Table 1 lists 9 studies that have been published on NaSRS, including the most recent studies following the latest reviews (24, 43). Although the existing data are mainly from retrospective studies, they have led to the initiation of several prospective studies that are currently underway (Supplementary Table 1). Our department also takes part in a Phase II bicentric study with the University of Toronto (NCT03368625) (34). Per protocol, the diameter of the index lesion is set between 2.0 to 5.0 cm, and NaSRS administered at a single dose of 14.0 to 20.0 Gy depending on tumor volume. In example, 14 Gy was the dose regimen for tumors with a volume of ≥ 20 to < 50 cc.

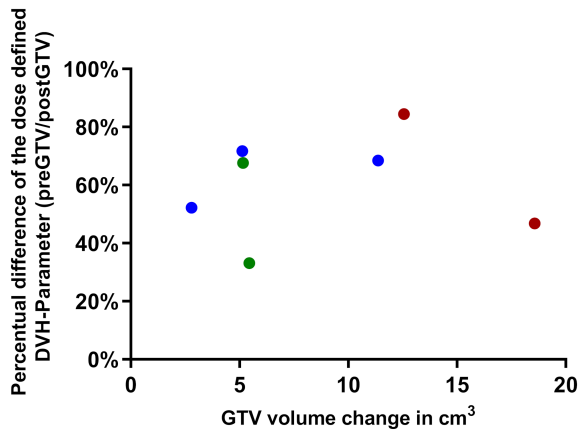

FIGURE 6
Graphical representation for the seven simulated plannings, visualizing the dose-defined dose-volume histogram (DVH) parameter ratio between simulated NaSRS and postoperative original irradiation (pre/post) against the absolute difference in GTV volume. Fractionations are color coded: Single fraction in green, 3-fractions in blue, and 5-fractions in red. GTV, gross tumor volume.

However, the protocols of ongoing studies differ in terms of dosing; in particular, a dose-escalation study aims to determine the maximum tolerated dose of SRS administered before neurosurgical treatment, whereas a dose de-escalation study compares 12.0 to 15.0 Gy. In addition, there are several studies testing HF-SRS (Supplementary Table 1). Because the results of several prospective studies are still outstanding to clarify the role of NaSRS in routine clinical practice, we sought to determine its potential benefits in a matched analysis based on hypothetical planning of preoperative lesions treated after surgery in real-world settings. There are several studies that have investigated resection cavity dynamics independent of association with NaSRS, which are summarized in the review by Yuan et al. (44). Here, the authors reported that on average the resection cavities were smaller than the preoperative tumors. The most postulated predictor of greater volume depletion after surgery was larger tumor size (31, 46, 47), whereas Scharl et al. made an inverse observation (48). In our study, we found a negative correlation between pre-GTV size and resection cavity volume change, with smaller tumors leading to more changes, often an increase in post-GTV like Atalar et al. (31). Our data suggested 15.0 cm^3 as a possible cut-off volume to predict a volume increase, however, this must be assessed in larger cohorts. In comparison, Atalar et al. reported that for pre-resection tumors greater than 4.2 cm^3 the cavity volume was smaller than the tumor itself (31). In this context, one may ask why surgery is necessary at all for small lesions. Surgery for smaller lesions that can be treated directly with SRS is still warranted in selected cases due to severe edema, neurologic symptoms, and histologic tissue demands. Steindl et al. published recently a large series including 1608 patients with NSCLC brain metastases. Although they did not include tumor volumes in the investigation, it is of importance to note that 740 of 1107 (68.8%) patients with tumors less than 3 cm in diameter suffered from neurologic symptoms (49). In addition, the potential discordance between primary tumor and CNS metastases, as demonstrated in several publications, necessitates in selected cases a surgical tissue sampling to optimize systemic treatment (50–52). Another inconsistent aspect is the resection cavity dynamics over time as shown in the above-mentioned review with different observations amongst seven studies (44). In our series, we could not find any correlation between the time interval from surgery to postoperative planning MRI and volume change consistent with Atalar et al. (31). Importantly, to exclude residual tumor after resection an early MRI must be performed within 48 hours (53).

However, given that the resection cavity is a dynamic process, optimal SRS/HF-SRS planning requires the timeliest MRI possible (48, 54). However, there are no guidelines either on the optimal time interval between surgery and SRS/HF-SRS. In the latest ISRS guidelines the authors did not comment on these points (32). Yuan et al. focused on the aspect of the timing of post-SRS/HF-SRS and resection and came to the conclusion that as the initial tumor size influences cavity size, and smaller metastases may profit from a longer time interval until the postoperative radiosurgery without a particular time proposal (44). Importantly, the patients mostly need a recovery period after resection that is also needed for wound healing. A time interval of at least two weeks is reasonable to our point of view and should be limited to 6 weeks postoperatively to avoid tumor recurrence. In the consensus paper by Soliman et al., 9 of 10 participants favored post-SRS within the first 4 weeks that we also favor in the routine (10). Starting radiosurgery within 30 days was also the setting in the randomized trial by Majaharan et al. (3). This is clearly one of the treatment algorithms steps that need to be standardized in the radiosurgical society in the future.

Since we focused on the NaSRS aspect, we compared the PTVs. For post-PTV we used real world data including some older cases without an additional margin, but in our recent routine clinical practice a 2.0 mm margin is now standard, as it was in the randomized phase III trial (6). The recent proposed guidelines also recommend a margin of 2.0 to 3.0 mm for the resection cavity (32). For SRS in brain metastases GTV = CTV = PTV is suggested by the German Society for Radiooncology [*Deutsche Gesselschaft für Radioonologie – DEGRO*], especially with regard to frame-based SRS treatments, with the possibility of a margin of up to 2.0 mm (55). A margin of 1.0 mm should be added in view of possible infiltrative growth of brain metastases according to Baumert et al., which is our routine practice (56). In the comparative studies for pre- and postoperative tumor volumes, only a few ones included PTVs. For instance, after a 2.0 mm margin was added to pre-GTV, the volume decrease of the originally larger tumors after resection disappeared in Atalar et al. (31). El Shafie et al. compared the PTVs of a hypothetical pre-PTV with 1.0 mm margin to different postoperative scenarios with a margin up to 3.0 mm. However, the authors did not compare the original PTV of the resection cavity treated with Cyberknife SRS with the hypothetical plans using Elekta VERSA HD linear accelerator (57). In a very recent similar comparative study by Bugarini et al. PTVs were also not significantly different between pre- and post-scenarios as in our study. In our case, based on the apparent trend, there seems to be a difference between the preoperative and standardized postoperative PTV, in the sense of greater PTV postoperatively. However, our study did not have the power to determine this conclusively. Further studies with larger case series are warranted to assess this. These authors did not present a detailed volume change dependency as in our study (33).

The amount of normal brain tissue volume receiving a relevant dose is the primary important factor regarding side effects, especially radionecrosis, but with some differences in practice for reporting that require specific guidelines to standardize data in the future. The brain volume that receives 10.0 Gy and 12.0 Gy (V10 and V12) was shown to predict the radionecrosis risk (58). For example, in SRS of brain metastases, volumes greater than or equal to 10.0 cm^3 irradiated with 12.0 Gy (V12) were associated with a 15.0% risk of symptomatic radionecrosis (37). In the same study, three-fraction V18 < 30.0 cm^3 and V23 < 7.0 cm^3 were associated with less than 10.0% risk of radionecrosis in normal brain tissue (37). Another common method of assessing NBT exposure in SRS is brain minus PTV (57, 59). Zindler et al. reported for single-, three-, and five-fraction dose–volume constraints for brain minus GTV V12 = 10.0 cm^3, V19.2 = 10.0 cm^3, and a V20 = 20.0 cm^3, respectively (60). Brain-GTV receiving 30 Gy was identified as a significant predictor for adverse effects in the HF-SRS series of Faruqi et al. (61) In routine clinical practice for NBT we use the following constrains regarding brain minus PTV in single session SRS V10 < 10.0 cm^3 and for three-fraction V18 < 10.0 cm^3 to maintain a low risk of radionecrosis (37–39). We investigated the potential benefit of NaSRS to reduce NBT exposure in a selected cohort. Because PTV margins were not standardized in this retrospective cohort, we selected cases with a 5.0 cm^3 increase in post-GTV for further analysis to examine the effects of such volume increase on NBT exposure. In this preselected small cohort, we demonstrated less normal brain tissue receiving the evaluated DVH parameter for NaSRS (pre-PTV) with median 67.6% of the current standard (post-PTV), resulting in an advantage in normal-tissue preservation in NaSRS scenario. Since we kept the dosing regimen completely identical and based our hypothetical optimization on the clinical used constraints, this effect can clearly be attributed to a lower volume of the preoperative tumors. A similar advantage for normal tissue exposure was also presented in the above mentioned study favoring preoperative SRS, however, in this study the authors also changed the dose regimen for preoperative scenario (33). Because we wanted to evaluate only the volume effect on NBT exposure, we kept the SRS schedule completely identical and ensured with a robust template-based workflow in a stepwise procedure and equivalent coverage, an unbiased comparison between pre- and postoperative radiosurgery in the simulation.

We are aware of the bias within this planning study due to potential changes between pre-op and post-op conditions affecting optimal dose regimens and consecutively the planning constraints. However, as the optimization template was created for the clinical post-PTV scenario, a better set of planning parameters might have been possible within the hypothetical planning study, potentially further increasing NBT sparing. Additionally, as the volume increase was not present in all cases after resection, the different possible dose regimens in NaSRS should also be further compared to dose regimens in post-SRS. The comparability of our results with the study by Bugarini et al, in which the dosing regimen was adjusted for preoperative simulation, is very encouraging for NaSRS.

An important issue is the unintended residual tumor after surgical resection of brain metastases, which reached 15.8% in a recent study of 150 patients (53). Comparably, we observed 15.4% residual tumor in our series, however, with the caveat that we did not include only MRIs within 48 hours as this was a retrospective cohort that was not investigated by early MRI regularly. Since the dose regimens in the ongoing studies vary and are sometimes far below routinely applied doses such as 12.0 Gy, it is of great

importance to select patients well for NaSRS. For *in situ* brain metastases a single dose of at least 18.0 Gy is recommended by DEGRO (55). Rosenstock et al. found that subcortical metastases located ≥ 5.0 mm from the cortex with diffuse contrast enhancement had the highest incidence of unintended subtotal resection. The proposed MRI-based assessment allows estimation of individual risk for subtotal resection and may help identify patients who are not suitable for NaSRS with regard to the risk of residual tumor (53). However, if the dose used in NaSRS was as effective as the routine doses, then the remaining tumor would not be a limitation for NaSRS. Therefore, hypofractionated NaSRS should be considered rather than dose reduction for larger tumors, which is also a topic of ongoing studies (Supplementary Table 1) and has already been shown to be eligible recently (2).

Although analysis of the efficacy of post-SRS was not the primary objective of this study, we examined it to demonstrate the representativeness of the cohort in comparison to other published post-SRS studies. The sole purpose of this analysis was to demonstrate the efficacy of the treatment used in this cohort to support the evaluation of tissue exposure in this setting. With only 30 patients with heterogeneous characteristics in terms of histology, location, volume, and systemic treatments, as well as nonstandard target margin, our data on this are less valuable than previously reported prospective studies. Because of the small total number of patients, we also did not perform subgroup analyses. Nevertheless, we evaluated the local progression-free survival, which was 88.0%, slightly better than the 12-month local control of 72.0% in Majahan et al. and 61.8% in the series by Brown et al. (3, 6). The distant progression-free survival in our cohort was also within the reported range of these studies (3, 6). At 12.0 months LMD control was reported 92.8% in Brown et al., which was lower in our series with an estimated LMD-free survival of 81.0% at 12.0 months (6). This may be due to inconsistent margins applied in this cohort or target delineation differences (11). In comparison, the review article by Redmond et al. reported a median leptomeningeal failure of 14.0%, with a range of up to 22.8%, comparable to our series also highlighting the need for NaSRS concepts in the future to reduce LMD risk (32). We do not elaborate on overall survival data because systemic treatment data are underreported, and we did not analyze additional extracranial metastases in this retrospective cohort.

The major limitation of our study is the small number of patients, which makes it difficult to establish a reliable threshold for GTV volume increase and to identify additional predictors. Nevertheless, this is the first matched Cyberknife SRS treated cohort with simulation of a theoretical plan to test irradiation exposure of NBT. The purpose of this study was to facilitate further studies and to simulate discussions in clinical routine as NaSRS is already mentioned in ASTRO guidelines as a possible intervention. Our study provides insights and awakens thoughts for NaSRS concepts. For further studies, we would recommend placing more emphasis on the aspect of sparing irradiation exposure of normal brain tissue and reevaluating dose regimens to achieve sufficient doses instead of single doses as low as 12.0 Gy. This is particularly crucial regarding radioresistant tumor histologies such as renal cell carcinoma.

In conclusion, the volume change of the resection cavity seems to be dependent on the preoperative lesion size. Dosimetric analysis favored NaSRS for normal brain tissue preservation in selected cases. Since the target volume directly affects the exposure of NBT, this should be considered when making treatment recommendations for NaSRS in smaller lesions. A reliable cut-off value for the preoperative lesion size to estimate volume benefit should be determined in a larger multicenter cohort. Ongoing studies will lead the way for further benefits of NaSRS independent of the volume effect.

Ethics statement

The studies involving human participants were reviewed and approved by Charités Ethics Committee, Berlin, Germany. The patients/participants from the prospective registery provided their written informed consent to participate in this study.

Author contributions

Conceptualization: CS and GA. Investigation, data curation: NS, BB, GK, KK, and GA. Formal analysis: AJ, NS and BB. Statistics: GA and MN. Writing—original draft preparation: CS, GA, KK, and MN. Writing—review and editing: all authors. Visualization: AK, NS, AJ. Supervision: DS, AC, DZ, PV. Project administration: GA. Revision process. All authors contributed to the article and approved the submitted version.

Acknowledgments

GA is a participant of the BIH-Charité Clinician Scientist Program funded by the Charité—Universitätsmedizin Berlin and the Berlin Institute of Health. We thank Amir Alaeddini for his support in data management. We also thank Miss M. Sc Kerstin Rubarth from the Institute of Biometry and Clinical Epidemiology for her advisory support in the statistical analyses.

Conflict of interest

The authors declare that the research was conducted in the absence of any commercial or financial relationships that could be construed as a potential conflict of interest.

Publisher's note

All claims expressed in this article are solely those of the authors and do not necessarily represent those

of their affiliated organizations, or those of the publisher, the editors and the reviewers. Any product that may be evaluated in this article, or claim that may be made by its manufacturer, is not guaranteed or endorsed by the publisher.

Supplementary material

The Supplementary Material for this article can be found online at: https://www.frontiersin.org/articles/10.3389/fonc.2023.1056330/full#supplementary-material

References

1. Nayak L, Lee EQ, Wen PY. Epidemiology of brain metastases. *Curr Oncol Rep* (2012) 14(1):48–54. doi: 10.1007/s11912-011-0203-y

2. Vogelbaum MA, Brown PD, Messersmith H, Brastianos PK, Burri S, Cahill D, et al. Treatment for brain metastases: ASCO-SNO-ASTRO guideline. *J Clin Oncol* (2022) 40(5):492–516. doi: 10.1200/JCO.21.02314

3. Mahajan A, Ahmed S, McAleer MF, Weinberg JS, Li J, Brown P, et al. Post-operative stereotactic radiosurgery versus observation for completely resected brain metastases: A single-centre, randomised, controlled, phase 3 trial. *Lancet Oncol* (2017) 18(8):1040–8. doi: 10.1016/S1470-2045(17)30414-X

4. Kocher M, Soffietti R, Abacioglu U, Villà S, Fauchon F, Baumert BG, et al. Adjuvant whole-brain radiotherapy versus observation after radiosurgery or surgical resection of one to three cerebral metastases: Results of the EORTC 22952-26001 study. *J Clin Oncol* (2011) 29(2):134–41. doi: 10.1200/JCO.2010.30.1655

5. Patchell RA, Tibbs PA, Regine WF, Dempsey RJ, Mohiuddin M, Kryscio RJ, et al. Postoperative radiotherapy in the treatment of single metastases to the brain: a randomized trial. *JAMA* (1998) 280(17):1485–9. doi: 10.1001/jama.280.17.1485

6. Brown PD, Ballman KV, Cerhan JH, Anderson SK, Carrero XW, Whitton AC, et al. Postoperative stereotactic radiosurgery compared with whole brain radiotherapy for resected metastatic brain disease (NCCTG N107C/CEC.3): A multicentre, randomised, controlled, phase 3 trial. *Lancet Oncol* (2017) 18(8):1049–60. doi: 10.1016/S1470-2045(17)30441-2

7. El Shafie RA, Dresel T, Weber D, Schmitt D, Lang K, Konig L, et al. Stereotactic cavity irradiation or whole-brain radiotherapy following brain metastases resection-outcome, prognostic factors, and recurrence patterns. *Front Oncol* (2020) 10:693. doi: 10.3389/fonc.2020.00693

8. Patel KR, Prabhu RS, Kandula S, Oliver DE, Kim S, Hadjipanayis C, et al. Intracranial control and radiographic changes with adjuvant radiation therapy for resected brain metastases: Whole brain radiotherapy versus stereotactic radiosurgery alone. *J Neurooncol* (2014) 120(3):657–63. doi: 10.1007/s11060-014-1601-4

9. Kepka L, Tyc-Szczepaniak D, Bujko K, Olszyna-Serementa M, Michalski W, Sprawka A, et al. Stereotactic radiotherapy of the tumor bed compared to whole brain radiotherapy after surgery of single brain metastasis: Results from a randomized trial. *Radiother Oncol* (2016) 121(2):217–24. doi: 10.1016/j.radonc.2016.10.005

10. Soliman H, Ruschin M, Angelov L, Brown PD, Chiang VLS, Kirkpatrick JP, et al. Consensus contouring guidelines for postoperative completely resected cavity stereotactic radiosurgery for brain metastases. *Int J Radiat Oncol Biol Phys* (2018) 100(2):436–42. doi: 10.1016/j.ijrobp.2017.09.047

11. Vellayappan BA, Doody J, Vandervoort E, Szanto J, Sinclair J, Caudrelier JM, et al. Pre-operative versus post-operative radiosurgery for brain metastasis: Effects on treatment volume and inter-observer variability. *J Radiosurg SBRT* (2018) 5(2):89–97.

12. Choi CY, Chang SD, Gibbs IC, Adler JR, Harsh GRT, Lieberson RE, et al. Stereotactic radiosurgery of the postoperative resection cavity for brain metastases: prospective evaluation of target margin on tumor control. *Int J Radiat Oncol Biol Phys* (2012) 84(2):336–42. doi: 10.1016/j.ijrobp.2011.12.009

13. Foreman PM, Jackson BE, Singh KP, Romeo AK, Guthrie BL, Fisher WS, et al. Postoperative radiosurgery for the treatment of metastatic brain tumor: Evaluation of local failure and leptomeningeal disease. *J Clin Neurosci* (2018) 49:48–55. doi: 10.1016/j.jocn.2017.12.009

14. Shi S, Sandhu N, Jin MC, Wang E, Jaoude JA, Schofield K, et al. Stereotactic radiosurgery for resected brain metastases: Single-institutional experience of over 500 cavities. *Int J Radiat Oncol Biol Phys* (2020) 106(4):764–71. doi: 10.1016/j.ijrobp.2019.11.022

15. Brown DA, Lu VM, Himes BT, Burns TC, Quiñones-Hinojosa A, Chaichana KL, et al. Breast brain metastases are associated with increased risk of leptomeningeal disease after stereotactic radiosurgery: A systematic review and meta-analysis. *Clin Exp Metastasis* (2020) 37(2):341–52. doi: 10.1007/s10585-020-10019-1

16. Huang AJ, Huang KE, Page BR, Ayala-Peacock DN, Lucas JT Jr, Lesser GJ, et al. Risk factors for leptomeningeal carcinomatosis in patients with brain metastases who have previously undergone stereotactic radiosurgery. *J Neurooncol* (2014) 120(1):163–9. doi: 10.1007/s11060-014-1539-6

17. Press RH, Zhang C, Chowdhary M, Prabhu RS, Ferris MJ, Xu KM, et al. Hemorrhagic and cystic brain metastases are associated with an increased risk of leptomeningeal dissemination after surgical resection and adjuvant stereotactic radiosurgery. *Neurosurgery* (2019) 85(5):632–41. doi: 10.1093/neuros/nyy436

18. Johnson MD, Avkshtol V, Baschnagel AM, Meyer K, Ye H, Grills IS, et al. Surgical resection of brain metastases and the risk of leptomeningeal recurrence in patients treated with stereotactic radiosurgery. *Int J Radiat Oncol Biol Phys* (2016) 94(3):537–43. doi: 10.1016/j.ijrobp.2015.11.022

19. Patel KR, Burri SH, Asher AL, Crocker IR, Fraser RW, Zhang C, et al. Comparing preoperative with postoperative stereotactic radiosurgery for resectable brain metastases: A multi-institutional analysis. *Neurosurgery* (2016) 79(2):279–85. doi: 10.1227/NEU.0000000000001096

20. Nguyen TK, Sahgal A, Detsky J, Atenafu EG, Myrehaug S, Tseng CL, et al. Predictors of leptomeningeal disease following hypofractionated stereotactic radiotherapy for intact and resected brain metastases. *Neuro Oncol* (2020) 22(1):84–93. doi: 10.1093/neuonc/noz144

21. Minniti G, Lanzetta G, Capone L, Giraffa M, Russo I, Cicone F, et al. Leptomeningeal disease and brain control after postoperative stereotactic radiosurgery with or without immunotherapy for resected brain metastases. *J Immunother Cancer* (2021) 9(12):e003730. doi: 10.1136/jitc-2021-003730

22. Asher AL, Burri SH, Wiggins WF, Kelly RP, Boltes MO, Mehrlich M, et al. A new treatment paradigm: Neoadjuvant radiosurgery before surgical resection of brain metastases with analysis of local tumor recurrence. *Int J Radiat Oncol Biol Phys* (2014) 88(4):899–906. doi: 10.1016/j.ijrobp.2013.12.013

23. Patel KR, Burri SH, Boselli D, Symanowski JT, Asher AL, Sumrall A, et al. Comparing pre-operative stereotactic radiosurgery (SRS) to post-operative whole brain radiation therapy (WBRT) for resectable brain metastases: A multi-institutional analysis. *J Neurooncol* (2017) 131(3):611–8. doi: 10.1007/s11060-016-2334-3

24. Prabhu RS, Miller KR, Asher AL, Heinzerling JH, Moeller BJ, Lankford SP, et al. Preoperative stereotactic radiosurgery before planned resection of brain metastases: Updated analysis of efficacy and toxicity of a novel treatment paradigm. *J Neurosurg* (2018), 131(5):1–8. doi: 10.3171/2018.7.JNS181293

25. Patel AR, Nedzi L, Lau S, Barnett SL, Mickey BE, Moore W, et al. Neoadjuvant stereotactic radiosurgery before surgical resection of cerebral metastases. *World Neurosurg* (2018) 120:e480–7. doi: 10.1016/j.wneu.2018.08.107

26. Vetlova E, Golbin DA, Golanov AV, Potapov AA, Banov SM, Antipina N, et al. Preoperative stereotactic radiosurgery of brain metastases: Preliminary results. *Cureus* (2017) 9(12):e1987. doi: 10.7759/cureus.1987

27. Prabhu RS, Dhakal R, Vaslow ZK, Dan T, Mishra MV, Murphy ES, et al. Preoperative radiosurgery for resected brain metastases: The PROPS-BM multicenter cohort study. *Int J Radiat Oncol Biol Phys* (2021) 111(3):764–72. doi: 10.1016/j.ijrobp.2021.05.124

28. Murphy ES, Yang K, Suh J, Yu J, Schilero C, Mohammadi A, et al. Early results from a prospective phase II dose escalation study for neoadjuvant radiosurgery for brain metastases. *Int J Radiat Oncol Biol Phys* (2019) 103(5):E5. doi: 10.1016/S0360-3016(19)30411-0

29. Udovicich C, Ng SP, Tange D, Bailey N, Haghighi N. From postoperative to preoperative: A case series of hypofractionated and single-fraction neoadjuvant stereotactic radiosurgery for brain metastases. *Oper Neurosurg (Hagerstown)* (2022) 22(4):208–14. doi: 10.1227/ONS.0000000000000101

30. Murphy E, Yang K, Suh J, Yu J, Schilero C, Mohammadi A, et al. Trls-05. early results from a prospective phase I/Ii dose escalation study of neoadjuvant radiosurgery for brain metastases. *Neurooncol Adv* (2019) 1(Suppl 1):i9. doi: 10.1093/noajnl/vdz014.038

31. Atalar B, Choi CY, Harsh Chang GRt SD, Gibbs IC, Adler JR. Cavity volume dynamics after resection of brain metastases and timing of postresection cavity stereotactic radiosurgery. *Neurosurgery* (2013) 72(2):180–5; discussion 185. doi: 10.1227/NEU.0b013e31827b99f3

32. Redmond KJ, De Salles AAF, Fariselli L, Levivier M, Ma L, Paddick I, et al. Stereotactic radiosurgery for postoperative metastatic surgical cavities: A critical review and international stereotactic radiosurgery society (ISRS) practice guidelines. *Int J Radiat Oncol Biol Phys* (2021) 111(1):68–80. doi: 10.1016/j.ijrobp.2021.04.016

33. Bugarini A, Meekins E, Salazar J, Berger AL, Lacroix M, Monaco EA 3rd, et al. Pre-operative stereotactic radiosurgery for cerebral metastatic disease: A retrospective dose-volume study. *Radiother Oncol* (2022). doi: 10.1016/j.radonc.2022.07.019

34. Takami H, Nassiri F, Moraes FY, Zadeh G, Bernstein M, Conrad T, et al. A phase II study of neoadjuvant stereotactic radiosurgery for Large brain metastases: Clinical trial protocol. *Neurosurgery* (2020) 87(2):403–7. doi: 10.1093/neuros/nyz442

35. Sun B, Huang Z, Wu S, Ding L, Shen G, Cha L, et al. Cystic brain metastasis is associated with poor prognosis in patients with advanced breast cancer. *Oncotarget* (2016) 7(45):74006–14. doi: 10.18632/oncotarget.12176

36. Acker G, Hashemi SM, Fuellhase J, Kluge A, Conti A, Kufeld M, et al. Efficacy and safety of CyberKnife radiosurgery in elderly patients with brain metastases: a retrospective clinical evaluation. *Radiat Oncol* (2020) 15(1):225. doi: 10.1186/s13014-020-01655-8

37. Milano MT, Grimm J, Niemierko A, Soltys SG, Moiseenko V, Redmond KJ, et al. Single- and multifraction stereotactic radiosurgery Dose/Volume tolerances of the brain. *Int J Radiat Oncol Biol Phys* (2021) 110(1):68–86. doi: 10.1016/j.ijrobp.2020.08.013

38. Milano MT, Usuki KY, Walter KA, Clark D, Schell MC. Stereotactic radiosurgery and hypofractionated stereotactic radiotherapy: Normal tissue dose constraints of the central nervous system. *Cancer Treat Rev* (2011) 37(7):567–78. doi: 10.1016/j.ctrv.2011.04.004

39. Minniti G, Scaringi C, Paolini S, Lanzetta G, Romano A, Cicone F, et al. Single-fraction versus multifraction (3 × 9 gy) stereotactic radiosurgery for Large (>2 cm) brain metastases: A comparative analysis of local control and risk of radiation-induced brain necrosis. *Int J Radiat Oncol Biol Phys* (2016) 95(4):1142–8. doi: 10.1016/j.ijrobp.2016.03.013

40. Benedict SH, Yenice KM, Followill D, Galvin JM, Hinson W, Kavanagh B, et al. Stereotactic body radiation therapy: Tthe report of AAPM task group 101. *Med Phys* (2010) 37(8):4078–101. doi: 10.1118/1.3438081

41. Lin NU, Lee EQ, Aoyama H, Barani IJ, Barboriak DP, Baumert BG, et al. Response assessment criteria for brain metastases: Proposal from the RANO group. *Lancet Oncol* (2015) 16(6):e270–8. doi: 10.1016/S1470-2045(15)70057-4

42. Raza GH, Capone L, Tini P, Giraffa M, Gentile P, Minniti G. Single-isocenter multiple-target stereotactic radiosurgery for multiple brain metastases: dosimetric evaluation of two automated treatment planning systems. *Radiat Oncol* (2022) 17 (1):116. doi: 10.1186/s13014-022-02086-3

43. Routman DM, Yan E, Vora S, Peterson J, Mahajan A, Chaichana KL, et al. Preoperative stereotactic radiosurgery for brain metastases. *Front Neurol* (2018) 9:959. doi: 10.3389/fneur.2018.00959

44. Yuan M, Behrami E, Pannullo S, Schwartz TH, Wernicke AG. The relationship between tumor volume and timing of post-resection stereotactic radiosurgery to maximize local control: A critical review. *Cureus* (2019) 11(9):e5762. doi: 10.7759/cureus.5762

45. Schiff D, Messersmith H, Brastianos PK, Brown PD, Burri S, Dunn IF, et al. Radiation therapy for brain metastases: ASCO guideline endorsement of ASTRO guideline. *J Clin Oncol* (2022) 40(20):2271–6. doi: 10.1200/JCO.22.00333

46. Alghamdi M, Hasan Y, Ruschin M, Atenafu EG, Myrehaug S, Tseng CL, et al. Stereotactic radiosurgery for resected brain metastasis: Cavity dynamics and factors affecting its evolution. *J Radiosurg SBRT* (2018) 5(3):191–200.

47. Jarvis LA, Simmons NE, Bellerive M, Erkmen K, Eskey CJ, Gladstone DJ, et al. Tumor bed dynamics after surgical resection of brain metastases: Implications for postoperative radiosurgery. *Int J Radiat Oncol Biol Phys* (2012) 84(4):943–8. doi: 10.1016/j.ijrobp.2012.01.067

48. Scharl S, Kirstein A, Kessel KA, Duma MN, Oechsner M, Straube C, et al. Cavity volume changes after surgery of a brain metastasis-consequences for stereotactic radiation therapy. *Strahlenther Onkol* (2019) 195(3):207–17. doi: 10.1007/s00066-018-1387-y

49. Steindl A, Yadavalli S, Gruber KA, Seiwald M, Gatterbauer B, Dieckmann K, et al. Neurological symptom burden impacts survival prognosis in patients with newly diagnosed non-small cell lung cancer brain metastases. *Cancer* (2020) 126(19):4341–52. doi: 10.1002/cncr.33085

50. Hulsbergen AFC, Claes A, Kavouridis VK, Ansaripour A, Nogarede C, Hughes ME, et al. Subtype switching in breast cancer brain metastases: A multicenter analysis. *Neuro Oncol* (2020) 22(8):1173–81. doi: 10.1093/neuonc/noaa013

51. Duchnowska R, Dziadziuszko R, Trojanowski T, Mandat T, Och W, Czartoryska-Arłukowicz B, et al. Conversion of epidermal growth factor receptor 2 and hormone receptor expression in breast cancer metastases to the brain. *Breast Cancer Res* (2012) 14(4):R119. doi: 10.1186/bcr3244

52. Tonse R, Rubens M, Appel H, Tom MC, Hall MD, Odia Y, et al. Systematic review and meta-analysis of lung cancer brain metastasis and primary tumor receptor expression discordance. *Discovery Oncol* (2021) 12(1):48. doi: 10.1007/s12672-021-00445-2

53. Rosenstock T, Pöser P, Wasilewski D, Bauknecht HC, Grittner U, Picht T, et al. MRI-Based risk assessment for incomplete resection of brain metastases. *Front Oncol* (2022) 12:873175. doi: 10.3389/fonc.2022.873175

54. Shah JK, Potts MB, Sneed PK, Aghi MK, McDermott MW. Surgical cavity constriction and local progression between resection and adjuvant radiosurgery for brain metastases. *Cureus* (2016) 8(4):e575. doi: 10.7759/cureus.575

55. Kocher M, Wittig A, Piroth MD, Treuer H, Seegenschmiedt H, Ruge M, et al. Stereotactic radiosurgery for treatment of brain metastases. a report of the DEGRO working group on stereotactic radiotherapy. *Strahlenther Onkol* (2014) 190(6):521–32. doi: 10.1007/s00066-014-0648-7

56. Baumert BG, Rutten I, Dehing-Oberije C, Twijnstra A, Dirx MJ, Debougnoux-Huppertz RM, et al. A pathology-based substrate for target definition in radiosurgery of brain metastases. *Int J Radiat Oncol Biol Phys* (2006) 66(1):187–94. doi: 10.1016/j.ijrobp.2006.03.050

57. El Shafie RA, Tonndorf-Martini E, Schmitt D, Weber D, Celik A, Dresel T, et al. Pre-operative versus post-operative radiosurgery of brain metastases-volumetric and dosimetric impact of treatment sequence and margin concept. *Cancers (Basel)* (2019) 11(3):294. doi: 10.3390/cancers11030294

58. Minniti G, Clarke E, Lanzetta G, Osti MF, Trasimeni G, Bozzao A, et al. Stereotactic radiosurgery for brain metastases: Analysis of outcome and risk of brain radionecrosis. *Radiat Oncol* (2011) 6:48. doi: 10.1186/1748-717X-6-48

59. Bohoudi O, Bruynzeel AM, Lagerwaard FJ, Cuijpers JP, Slotman BJ, Palacios MA. Isotoxic radiosurgery planning for brain metastases. *Radiother Oncol* (2016) 120 (2):253–7. doi: 10.1016/j.radonc.2016.05.001

60. Zindler JD, Schiffelers J, Lambin P, Hoffmann AL. Improved effectiveness of stereotactic radiosurgery in large brain metastases by individualized isotoxic dose prescription: An in silico study. *Strahlenther Onkol* (2018) 194(6):560–9. doi: 10.1007/s00066-018-1262-x

61. Faruqi S, Ruschin M, Soliman H, Myrehaug S, Zeng KL, Husain Z, et al. Adverse radiation effect after hypofractionated stereotactic radiosurgery in 5 daily fractions for surgical cavities and intact brain metastases. *Int J Radiat Oncol Biol Phys* (2020) 106 (4):772–9. doi: 10.1016/j.ijrobp.2019.12.002

Frontiers in Oncology

Advances knowledge of carcinogenesis and tumor progression for better treatment and management

The third most-cited oncology journal, which highlights research in carcinogenesis and tumor progression, bridging the gap between basic research and applications to imrpove diagnosis, therapeutics and management strategies.

Discover the latest Research Topics

See more →

Frontiers

Avenue du Tribunal-Fédéral 34
1005 Lausanne, Switzerland
frontiersin.org

Contact us

+41 (0)21 510 17 00
frontiersin.org/about/contact